UiT The Arctic University of Norway

Faculty of Biosciences, Fisheries and Economics

Department of Arctic and Marine Biology

Response and resilience of the microbial methane filter to ecosystem changes in Arctic peatlands

Edda Marie Rainer

A dissertation for the degree of Philosophiae Doctor [April 2022]

Table of contents

List of Figures

Front Page: Lake Solvatn, Ny-Ålesund and the surrounding peatland June 2016. Photographer: Edda M. Rainer

The photographs shown in **Figure 3** to **Figure 7** were taken by Edda M. Rainer and Mette M. Svenning.

Acknowledgments

First and foremost, I would like to thank my team of supervisors; without you there would have been no project and no opportunity for me to pursue a PhD at the University of Tromsø.

Mette Svenning, my main supervisor: You both supported and challenged me throughout the project and gave me the opportunity to grow as a scientist. You always reminded me how important it is to have a red thread throughout ideas and projects, and when writing up the thesis I truly realized how important it was to have someone who always checked that there was a continuous flow connecting all the different parts. I am also grateful to you for having such confidence in my goal to complete this project even when I had to take on a new position, and that you supported me until the end. **Alexander Tveit**, my first co-supervisor: Your vast expertise was inspiring, and you were a great help in designing the experiments. You taught me the importance of being meticulous both when analyzing the data and when writing the papers. I believe you and Mette complemented each other well as a team and I am thankful for how you guided me throughout the project. **Svetlana Dedysh**, my second co-supervisor: Unfortunately, our fieldwork plans did not work out as initially thought and I missed the opportunity to visit you in Russia. However, you were essential in designing the project with Mette and I was grateful that you were such a strong collaborator in methanotroph ecology.

Apart from my supervisors there were several other people that were closely involved in my life, either scientifically or personally. **Christophe Seppey**, you were the bioinformatics and statistics brain in two of my papers. You helped me to get my head around the analyses and you were a great person to discuss all kinds of things - from the peculiarities of statistics to life in general. **Yvonne Piotrowski**, you provided me with steady support and became a scientific mentor for me after I transferred to biochemistry. There were times where I was thinking of giving up, but you were always encouraging me to believe in myself and to keep going. You also helped me to grow my scientific interests outside the field of microbial ecology and I am looking forward to many future collaborations. **Atle Larsen**, you were also a steady source of support and you provided me with the freedom to finish my PhD while working on several of our biochemistry projects. I truly appreciate your continuous full trust in me, and I am looking forward to focusing my attention on our future ideas.

Working at two different departments I met a lot of fantastic people and experienced two very welcoming work environments. I would love to write a bit about every one of you, but this would go beyond the scope of this thesis. I hope that all the people I met both at the biology (**microorganisms and plants group**) and the chemistry (**biomolecular and structural chemistry group**) departments know that you did an outstanding job in creating a wonderful atmosphere before, during and after work. I would also like to thank **all my friends**, both those close by as well as those that are far away. All these friendships were essential in finding my life's balance and I would not miss a minute of the time we spent outside playing in the mountains or meeting up for a cup of coffee. A big thanks goes also to **my family** and especially to my mom, her partner, and my uncle. You always supported me in my ideas even when it meant living far away. I never felt anything but positive encouragement in pursuing the life I have envisioned for myself and could not be more grateful for these opportunities.

To conclude I would like to thank **Philipp**, my partner in crime and the most important person in my life. It would not have been possible without you! Starting with food deliveries when working long hours to being a steady rock beside me. You were a never-ending source of support and care, you always believed in me and cheered me up and you dealt with my frustration and the paralyzing feeling of not being or doing enough. I don't think I can ever thank you enough for this, but I hope I can show you my gratitude in our life post PhD.

Photo taken by Edda M. Rainer in June 2016 during the Spring sampling campaign.

Abstract

Climate change is a major concern in the Arctic region, as large amounts of organic carbon (C) are stored in permafrost soils and sediments. Increasing average temperatures have the potential to release that C and making it available to biologic activity. Carbon-rich, anoxic soils such as peatlands are inhabited by methanogenic archaea that can metabolize by-products of microbial C decomposition and consequently release methane (CH_4). Methane oxidizing bacteria (MOB) comprise a major biological filter for CH_4 in terrestrial and aquatic ecosystems and thereby regulate CH_4 emissions to the atmosphere. The genus *Methylobacter* has been detected in many CH_4 rich ecosystems and several circumpolar locations. Climate change in the Arctic includes changes in both temperature and precipitation as well as ecosystem changes related to plant cover and herbivory. All of these changes have the potential to influence soil structure and soil biological processes. Thus, they are important factors controlling the soil C cycle and eventually the activity of MOB. The aim of this thesis was to investigate the ability of the Arctic biological CH_4 filter to adapt to changes in vegetation, CH_4 concentrations and temperature. Further, to gain insights in the resilience and resistance of the MOB community to environmental changes.

We have shown that herbivory by geese changes the soil structure and thus the vertical distribution of CH_4 and oxygen (O_2) concentrations in a high Arctic peatland. These differences are accompanied by changes in the potential rates of CH_4 oxidation. The highest activity was detected in shallower parts of the peatland in grazed sites compared to sites protected from grazing. Different MOB communities are responsible for the CH_4 oxidation, depending on the above ground grazing and these communities are composed of closely related *Methylobacter* OTUs. Exposing peat soils from both grazed and protected sites to increased CH_4 concentrations and temperature revealed that MOB respond strongly to changing CH_4 concentrations, but apparently not to temperature. The response to changing CH_4 concentrations involved different members of the *Methylobacter* community depending on the CH_4 concentration and their previous exposure to herbivory. Temperature had minor effects on the CH_4 oxidation activity and the MOB community *pmoA* transcription in the soils. However, temperature clearly influences growth, CH_4 oxidation and CO_2 production in the native peat soil isolate *Methylobacter tundripaludum* SV96. The temperature adaptation of *M. tundripaludum* SV96 is modulated by fine tuning transcription and translation to

achieve the optimal balance between substrate availability, growth, and energy generation at different temperatures. These findings show that identical CH_4 oxidation rates can be produced from very different physiological states. This also explains how the apparent lack of temperature responses in soil MOB communities is a result of physiological acclimation.

Our results show that MOB in high Arctic peatlands and particular the genus *Methylobacter* is both physiologically and ecologically flexible in adapting to changes in plant cover, O_2 distribution, CH_4 concentrations and temperature. Thus, the MOB community comprises an efficient and resilient CH_4 filter in high Arctic peat soils.

List of papers

Paper I

Rainer EM, Seppey CVW, Tveit AT, Svenning MM. Methanotroph populations and CH_4 oxidation potentials in high-Arctic peat are altered by herbivory induced vegetation change. FEMS Microbiol Ecol. 2020;96(10):fiaa140. doi:10.1093/femsec/fiaa140

Paper II

Rainer EM, Seppey CVW, Hammer C, Svenning MM, Tveit AT. The Influence of Above-Ground Herbivory on the Response of Arctic Soil Methanotrophs to Increasing CH_4 Concentrations and Temperatures. Microorganisms. 2021; 9(10):2080. https://doi.org/10.3390/microorganisms9102080

Paper III

Tveit AT, Söllinger A, **Rainer EM**, Didriksen A, Hestnes AG, Motleleng L, Hellinger HJ, Rattei T, Svenning MM. Glycogen storage and ribosome regulation controls methanotroph temperature acclimation. Manuscript (in preparation)

List of Abbreviations

C	Carbon
CAP	Cold adapted protein
CH_4	Methane
CO_2	Carbon dioxide
CSP	Cold shock protein
DNA	Deoxyribonucleic acid
GC-FID	Gas-Chromatograph with a flame ionization detector
GHG	Greenhouse gases
HGT	Horizontal gene transfer
HSP	Heat shock protein
LGT	Lateral gene transfer
MMO	Methane monooxygenase
mmoX	Methane monooxygenase component A alpha chain
MOB	Methane-oxidizing bacteria
mRNA	messenger RNA
N_2O	Nitrous oxide
O_2	Oxygen
OM	Organic matter
OTU	Operational taxonomic unit
pMMO	Particulate MMO
pmoA	Particulate methane monooxygenase subunit A
RNA	Ribonucleic acid
RNAse	Ribonuclease
rRNA	Ribosomal RNA
RuMP	Ribulose monophosphate
sMMO	Soluble MMO
USC	Upland soil cluster

1 Introduction

1.1 Climate change in the Arctic

During the last centuries, our planets climate and biosphere has changed and is still changing related to anthropogenic activities. While the earth's climate has changed before, it has never been shown to have changed as rapidly. One element of climate change is the warming of our atmosphere which is caused by radiative forcing and influenced by the presence and concentration of greenhouse gases (GHG). While water vapor is the most abundant GHG in our atmosphere, CO_2 is the biggest driver of the observed temperature increase. However, while present at much lower concentrations, methane (CH_4) is an even more powerful greenhouse gas as CH_4 is up to 23 times more potent than CO_2. [1]. Nitrous oxide (N_2O) is another important GHG, and while its levels are lower than for both CH_4 and CO_2, it is the most potent compared to the other GHGs.

Northern latitudes are especially threatened and have experienced an increase in temperature that is double compared to the global average [2]. Indeed models predict a 3.3 - 10 °C temperature increase in the Arctic at the end of the 21st century [3]. The northern hemisphere is at present still a major carbon (C) sink [4] and its overall CO_2 uptake capacity has increased in the course of recent centuries [5]. To what extent this increase can make up for the loss of C from melting permafrost is uncertain [6,7] as permafrost stores significant amounts of organic C.

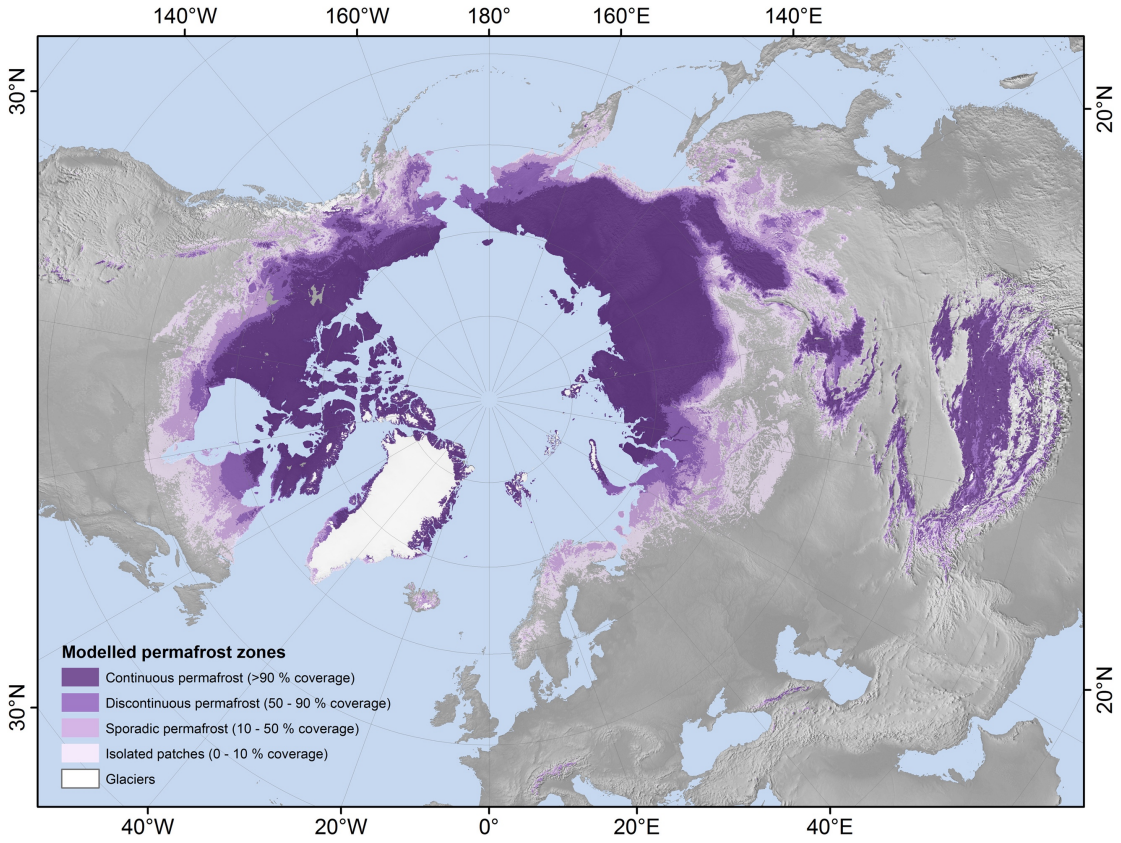

Figure 1 Distribution of terrestrial permafrost in the Northern hemisphere. The figure was published in 2019 by Obu et al [8].

About 22% of the land in the northern hemisphere is covered by permafrost [9,10]. For ground (soil, sediment or rocks) to be defined as permafrost it has to remain frozen for at least two consecutive years [10]. Permafrost is divided into continuous permafrost (90-100 % of the area is frozen), discontinuous (90-50 %), sporadic (50-10 %) and isolated patches (10-0 %) (Figure 1 [8]). The active layer is the part of permafrost soils that thaws temporarily, and its thickness varies depending on spatial and seasonal patterns as well as the type of permafrost soil. Permafrost is considered one of the major uncertainties and concerns in future climate change predictions as thawing of permafrost potentially releases much of that stored, and presently unavailable, C to microbial degradation.

1.2 Peatlands and carbon cycling

Around 19% of permafrost soils in the Northern hemisphere are peatlands which store most organic C of all permafrost soils [11]. A peatland is a type of wetland that accumulates peat which is the accumulation of partially degraded animal and plant biomass [12]. Peatlands can further be classified into bogs and fens. Bogs are

hydrologically isolated, acidic and oligotrophic whereas fens are connected with a water source, vary from acidic to neutral and from oligo- to eutrophic [12].

As long as Northern peatlands remain frozen, they release small amounts of C and are at present considered a C sink [13]. With increased annual thawing and the active layer remaining unfrozen for longer periods, microbial C degradation of can continue for longer time periods and with increasing temperatures also at higher rates [14]. Peatlands are therefore considered a potential future C source rather than a C sink. Research targeting physical and biological processes that influence the C balance of peatlands is therefore of the utmost importance [15].

The organic C is stored in the form of partially degraded organic matter (OM). The decomposition of OM fuels microbes which incorporate part of the organic C into their own biomass and release both CO_2 and CH_4 from their metabolism [16]. Microorganisms that produce CH_4 belong to the archaea, and they comprise a large group of different microorganisms that are collectively referred to as methanogens. CH_4 is produced under anaerobic conditions and in environments that are poor in other electron acceptors such as nitrite (NO_3^-), iron (Fe^{3+}) or sulfate (SO_4^{2-}) [17]. Methanogens use intermediates and end products from the degradation of biopolymers and depend on the presence and activity of anaerobic microorganisms (bacteria, fungi and protozoa) and syntrophic as well as acetogenic bacteria [18]. These substrates for methanogens are H_2/CO_2, formate, acetate and different methyl-compounds [17]. Methanogens are commonly found in environments, such as peat – and wetland soils [19,20] that account for a large portion of biologically produced CH_4.

How much CH_4 is eventually released into the atmosphere depends not only on the metabolic activity of the methanogens, but also on the consumption of CH_4 by methane oxidizing bacteria (MOB) [21]. The MOB comprise a biological filter and their presence and activity is decisive for the final amount of CH_4 that is released from a CH_4 emitting environment. Their resilience to changing environmental conditions is therefore highly important for the C budget and future climate predictions.

1.3 Ecology and Biochemistry of Methane Oxidizing Bacteria

1.3.1 Taxonomy and Environmental distribution of MOB

While MOB are widely distributed and their habitats range from soils to aquatic environments [22,23], they all possess the unique ability to live on CH_4 as their sole C and energy source [21]. Most MOB are found within the *Gammaproteobacteria* (previously referred to as Type-I and Type-X) and the *Alphaproteobacteria* (previously referred to as Type-II), with some exceptions found within the *Verrucomicrobia* [23,24]. Many MOB isolates and sequences were retrieved from environments that are rich in CH_4, such as wetlands, methane seeps, landfill soils etc. There are also distinct groups of MOB that originate from environments that have small to no detectable CH_4. These MOB survive on CH_4 from the atmosphere alone and are found in habitats such as forest soils, deserts or grasslands. The MOB belonging to this group are referred to as the upland soil cluster (USC) and depending on if they belong to the *Alpha*- or *Gammaprotebacteria* they are further classified by the nominator USC-alpha or USC-gamma [23,25]. There is also a completely different group of Archaea that oxidize CH_4 anaerobically in soils, waters and sediments and which rely on a completely different enzymatic mechanisms for oxidation [26]. As anaerobic oxidation of CH_4 was not investigated in this thesis, they will not be discussed further.

1.3.2 Biochemistry of methane oxidation

The aerobic oxidation of CH_4 is catalyzed by several enzymes and results in C assimilation or CO_2 formation to generate energy for the cells. The first step is catalyzed by the enzyme methane monooxygenase (MMO), which oxidizes CH_4 to methanol and is unique to MOB. There are two different types of the MMO – a membrane bound enzyme (particulate MMO, pMMO) and a cytoplasmatic, soluble enzyme (soluble MMO, sMMO) [21]. MOB can either have the pMMO, the sMMO or both enzymes. In those MOB that contain both types of the MMO the ratio of copper to biomass regulates which of the two enzymes is active as pMMO is depending on the presence of copper [27,28]. Methanol is further oxidized to formaldehyde by the enzyme methanol dehydrogenase. Formaldehyde is oxidized to formic acid and CO_2 by a formaldehyde dehydrogenase and a formate dehydrogenase, respectively [21,29]. Formaldehyde can also be incorporated into biomass and MOB use different C

assimilation pathways. *Gammaproteobacteria* use the ribulose mono phosphate (RuMP) pathway and *Alphaproteobacteria* use the serine pathway whereas *Verrucomicrobia* seem to use CH_4 as an energy source only and rely on CO_2 fixation for C assimiliation [29].

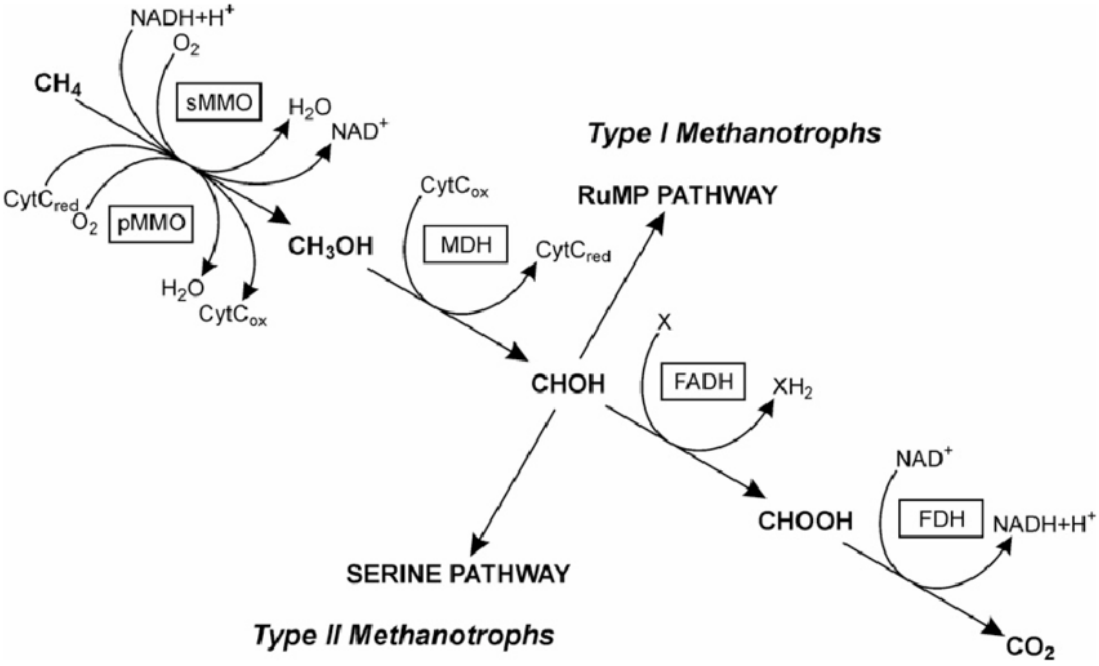

Figure 2 CH_4 oxidation pathway for Type I (*Gammaproteobacteria*) and Type II (*Alphaproteobacteria*) MOB, published by Hanson & Hanson et al in 1996 [21].

Both pMMO and sMMO consist of several subunits and are encoded by the gene cluster *pmoCAB* and *mmoXYBZDC*, respectively. The genes *pmoA* and *mmoX* are widely used to detect and taxonomically classify the different types of MOB [30,31].

1.3.3 *Methylobacter* – an important contributor to the high Arctic methane filter

The genus *Methylobacter* is found within the *Gammaproteobacteria*, more precisely in the family of the *Methyloccocales* [23,32]. MOB belonging to the genus *Methylobacter* are cosmopolitans [33] and have been detected in many different ecosystems [23]. In lakes and other freshwater ecosystems such as wetlands *Methylobacter* is frequently found to be the most dominant CH_4 oxidizer [33–35]. *Methylobacter* is also found in rice paddy soils [36] and landfill cover soils [37]. The genus *Methylobacter* seems to thrive when CH_4 concentrations are high and copes well with low O_2 concentrations compared to other MOB [38–41].

In Arctic peatlands *M. tundripaludum* is found to be a key CH_4 oxidizer [42–44] . *M. tundripaludum* or closely related species have been detected in permafrost soils [45,46] and polar lake and river sediments [47–50]. *M. tundripaludum* has also been shown to be responsible for CH_4 oxidation beneath both the Greenlandic and the Antarctic ice sheet and is thought to be crucial to reducing CH_4 emissions from these subglacial ecosystems [51–53]. All these habitats experience changes in climatic conditions and the flexibility of *M. tundripaludum* could be important for future emissions from Arctic ecosystems.

1.3.4 Ecological significance of closely related bacterial strains

Genetic variation in populations is driven by endogenic processes (mutations and DNA rearrangements within the cells) and external processes (acquisition of DNA via horizontal gene transfer (HGT, also known as lateral gene transfer (LGT)) [54,55]. Of these processes, HGT is the most important driver of evolution in prokaryotes as it provides the exchange of genetic material between cells, in contrast to eukaryotes that can exchange genetic material by sexual reproduction (also known as vertical gene transfer) [55,56]. HGT can cause extensive evolutionary changes. It has been proposed that the ability of MOB to utilize CH_4 was acquired by HGT of genes encoding several co-enzymes and co-factors from methanogenic archaea [57]. HGT also plays a role in the diversification of close relatives with several examples reviewed in [58]. Modelling species dynamics in a heterogenic environment has shown that a high diversity of species inhibits evolution when they are experiencing change [59]. The researchers showed in this study that there is a strong possibility that pre-adapted species are present and that these can potentially outcompete others. Thus there is no need for new species to specifically adapt to those changes [59]. The high diversity of *Methylobacter* in lakes [60] and wetlands [33] may explain the success of this MOB genus as it allows for successful niche adaptation across chemical gradients of, for example, O_2 and CH_4 concentrations. This high *Methylobacter* diversity may also facilitate a faster adaptation to changes associated with climate change and provide higher ecosystem stability.

1.4 Environmental conditions controlling methane oxidation and MOB communities

Soils can either act as a CH_4 source or a CH_4 sink which will often depend on the soil moisture regime and the presence and O_2. Water content and O_2 concentrations are therefore key environmental variables when investigating both CH_4 producing and CH_4 oxidizing microorganisms. Temperature, CH_4 concentration, pH and the availability of other nutrients can also influence MOB activity. In the following sections some of these variables are explored with emphasis on those variables that are most relevant for the studies in this thesis.

1.4.1 Hydrology / Soil moisture

Soil moisture can have varying effects on MOB and their CH_4 oxidation activity depends on the type of soil. Forest upland soils, which are dry soils and hotspots for atmospheric CH_4 oxidation, are sensitive to changes in soil moisture both when the soil moisture level is decreasing or increasing [61,62]. The optimal soil moisture for CH_4 oxidation in dry soils is relatively high based on their maximum water holding capacity [63]. Wet soils are much less sensitive to changes in soil moisture and high CH_4 oxidation is maintained under a wide range of soil moisture contents [61,63]. Interestingly, the optimal soil moisture for CH_4 oxidation based on the maximum water holding capacity in wet soils is relatively low [63]. The dependency of CH_4 oxidation on soil moisture is similar for net CH_4 emissions in different soil types. In wet soils, soil moisture content was not found to be a controlling factor for high net CH_4 emissions whereas drier soils are more sensitive to changes in water table [64]. It has also been shown that changes in soil moisture act as an on/off switch for CH_4 emissions [65] instead of a linear relationship between an increase in water content and CH_4 emissions.

Rice paddy soils were shown to have a rather complex response to changes in soil moisture content: Drainage moved the zone of highest CH_4 oxidation from the rhizosphere and surface soil to the bulk of the soil. These changes were associated with an increase in the activity of MOB belonging to the G*ammaproteobacteria* and a decrease of MOB belonging to the *Alphaproteobacteria* [66,67]. The bulk portion of the soil is usually deprived of O_2 and drainage may have activated those MOB that normally survive better under O_2 limited conditions, while the re-wetting of the soil led

to a faster recovery of the CH_4 oxidation activity of MOB belonging to the *Alphaproteobacteria* [66]. Similar observations were also made in natural vs. drained peatlands, where the natural state was associated with *Methylocystis*-like MOB (belonging to the *Alphaproteobacteria*) and the drained peat was dominated by *Methylobacter* [68].

All these results from different soil ecosystems highlight the dependency of MOB and their CH_4 oxidation activity on a certain soil moisture regime and changes in water content can lead to shifts in the MOB community. However, changes in hydrology and precipitation will affect ecosystems differently.

1.4.2 Oxygen availability

Aerobic MOB are dependent on the presence of O_2 to oxidize CH_4 to methanol. Some MOB survive under anaerobic conditions, but they are not able to grow and multiply under complete O_2 depletion. In soils the availability of O_2 is often linked to the soil's moisture regime. The solubility of O_2 in water is small and O_2 diffusion from the atmosphere into water-logged soils is very slow. Thus, the availability of O_2 normally decreases rapidly in peatlands and often determines the depth range at which MOB actively oxidize CH_4. There are MOB that can oxidize CH_4 efficiently at microaerophilic conditions, i.e., at O_2 concentrations that are well below 21% and some species even seem to be facultative microaerophilic [69] .The survival under low O_2 conditions is crucial not only in wetlands but many aquatic environments [39,40] and rice paddy soils [36,70]. Low O_2 concentrations even seem to sometimes increase MOB activity [39,40]. *Methylobacter* is often detected in freshwater lakes and their dominance may be linked to their ability to oxidize efficiently under micro-oxic conditions [40]. Experiments with *Methylomonas* have coupled nitrate reduction to the oxidation of CH_4 when O_2 is limited and this could be a strategy used by MOB in anoxic peatland soils [20,71]. Plant roots also play a role when it comes to the supply of O_2 in soils. In both wetland and rice paddy soils high CH_4 oxidation activity has been measured in the rhizosphere of the plants present [72–74] with some plant species being more suitable for MOB activity than others [75]. To summarize, MOB activity at different O_2 concentrations will vary depending on the MOB community, i.e., if the community is adapted to micro-oxic conditions or how well they can survive periods of O_2 depletion. In addition, as O_2 concentrations are closely linked to the type of

vegetation and the soil moisture, these three variables will together influence MOB activity and community composition in a soil ecosystem.

1.4.3 Methane and nitrogen concentrations

While there are some MOB that can use other C sources than CH_4, so called methylotrophs, the majority of MOB are strictly methanotrophs and are dependent on the availability of CH_4. Methane oxidation follows Michaelis-Menten kinetics and the rate of CH_4 oxidation can be calculated based on the consumption of CH_4 over time [76]. Measuring CH_4 oxidation rates in soils revealed that MOB display biphasic activity and that CH_4 oxidation kinetics are influenced both by enzymatic activity and cell growth [77,78]. Steenbergh et al [77] showed that CH_4 oxidation is highly influenced by MOB growth especially in the later phase of oxidation and *Gammaproteobacteria* responded with increased growth.

MOB are often found to reside close to the CH_4 rich part of their habitat. While it has been shown that the interface between oxic and anoxic areas in rice paddies harbors highest MOB activity [36], in peat bogs there is surprising evidence that MOB are located more towards the anaerobic parts of the soil which contain the highest CH_4 concentrations [79]. The availability of higher amounts of CH_4, even if only temporary, seems to stimulate MOB to survive periods of low CH_4 concentrations, or even atmospheric concentrations [41,80]. *Methylobacter* with its ability to cope with micro-oxic conditions may have certain advantages in surviving close to the zone that is richest in CH_4 and to use CH_4 directly at its biological source [81]. Thus, CH_4 concentrations can directly influence the MOB biodiversity and their activity.

The presence of nitrogen has also been shown to affect MOB and CH_4 oxidation and studies have shown both stimulation and inhibition of CH_4 oxidation activity. In lake sediments and soils, ammonia was shown to positively stimulate *Gammaproteobacteria,* and *Methylobacter* in particular [82–84]. Contrarily, in the water column ammonia was shown to inhibit CH_4 oxidation [85]. In rice paddy soils fertilization with nitrogen compounds was also shown to have a stimulating effect on the *Gammaproteobacteria* [86]. Ammonia and CH_4 have very similar structures and competition between ammonia oxidizing bacteria and MOB for O_2 could explain decreases in both CH_4 and ammonia oxidation activity if O_2 is a limiting factor. [87] Whether nitrogen has a negative or positive effect on the MOB is ultimately dependent

on the habitat and its underlying conditions [88]. Some MOB were also shown to fix their own nitrogen [89,90] which is an advantage when nitrogen is limited in an environment. A study in sphagnum dominated wetlands has shown that nitrogen fixation by MOB is of lesser importance in that environment [91].

1.4.4 Temperature

Different microorganisms are adapted to the temperature regime of their natural habitat and can be classified in cold-adapted (psychrophilic, up to 20 °C), temperate (mesophilic, 20 to 45 °C) and heat-adapted (thermophilic, higher than 45 °C). In addition, there are many microorganisms that are "in between" these classifications; for example, they can be psychrotolerant and able to grow at low temperatures but have an optimal growth temperature that is above 20 °C. Landfill soils are CH_4 rich habitats in which temperatures can fluctuate a lot within one season and several studies have addressed CH_4 oxidation activity in response to temperature in these soils. A study that monitored both CH_4 oxidation activity and changes in the MOB community in landfill soils incubated between 6 to 70 °C showed that OTUs belonging to *Methylobacter* were clearly dominant at temperatures lower than 40 °C [37]. In addition, in the soils incubated at the lowest temperatures a clear dominance of *M. tundripaludum* OTUs was observed and those OTUs decreased significantly at higher temperatures [37]. Psychrotolerant MOB have been previously identified in landfill cover soils [92] and CH_4 oxidation activity was measured also at low temperatures [93]. Reddy and colleagues also observed a clear shift at temperatures higher than 40 °C where thermotolerant *Methylocaldum* OTUs started to dominate the soil microcosms [37,94].

Studies in permafrost and landfill soils have also seen even more drastic shifts in MOB communities in response to temperature, where communities dominated by *Gammaproteobacteria* changed to communities dominated by *Alphaproteobacteria* ([95–97]). Forest soils were shown to be less sensitive to increases in temperature [98]. In another study investigating CH_4 oxidation activity in response to temperature in permafrost soils, the response varied depending on the type of soil [99]. As such the MOB community response to increases in temperature can vary and may depend on the habitat and natural temperature range. In isolates, responses to increased temperature are more predictable and both growth and CH_4 oxidation rates responded positively to temperature until optimum growth temperature was reached [98,100]. However,

physiological temperature responses and acclimation strategies in MOB is generally understudied, and a proper understanding of what physiological phenomena produce the CH_4 oxidation rates observed in nature is still not available.

1.4.5 pH

pH is an important variable in determining microbial biodiversity and activity. Soil pH is influenced by the type of underlying bedrock, however it is also influenced by climate, vegetation, weathering and time [101]. Alkaline soils are more common in arid environments, whereas acidic soils are more common in humid environments (such as peatlands) and neutral soils are generally less common as they may be poorly buffered [102]. Bogs are poor in nutrients and strongly acidic as they are only supplied with precipitation from the atmosphere, whereas fens can be acidic to neutral as they are connected to the ground water or another source of water [12]. Vegetation cover is a good indicator of peatland types as well as an indicator of the pH range [12]. Both vegetation and soil pH influence the presence of microbes in general [103] and of MOB in particular. Acidic peatlands are often dominated by MOB belonging to the *Alphaproteobacteria* [104,105], whereas more neutral peatlands are dominated by MOB belonging to the *Gammaproteobacteria* [20,42,43]. Studies investigating neutral and acidic rice paddy soils have shown that *Gammaproteobacteria* dominate in neutral rice paddy soils [36,106] and *Alphaproteobacteria* in acidic rice paddy soils [107].

1.5 The adaptation to temperature change and cold temperatures in bacteria

Prokaryotes have adapted to a wide range of temperatures and are found in habitats with temperatures ranging from well below zero to higher than plus seventy centigrade. All biochemical reactions are temperature dependent and adaptations in the enzymatic machinery are necessary to function efficiently at either low or high temperatures. High temperatures have a denaturing effect on proteins. Adaptations in the amino acid sequence resulting in a tightly packed hydrophobic core, more disulfides bonds and salt brides to make the protein more rigid and a higher surface charge can ensure the proteins are less likely to denature [108]. At low temperatures enzymatic reactions slow down because of the lower kinetic energy available in addition to a higher barrier in

enzyme activation energy. To counterbalance these energy deficits, cold-adapted proteins display higher structural flexibility and increased specific activity at the cost of a lower thermal stability – i.e., they unfold at much lower temperatures than mesophilic proteins [108]. Another strategy to overcome the energy deficits in the cell at low temperature is the increased production of ATP to keep the enzymatic machinery going [109,110]. To keep growth rates high the cells need higher substrate concentrations [111] as substrate affinity decreases at low temperatures [112,113]. For MOB this relationship would mean that more CH_4 needs to be consumed per cell to achieve the same growth rate as at the optimum temperature. In addition, an energy increase would be necessary to satisfy the demands at lower temperature, manifesting itself in an increase in CO_2 production.

Besides having to deal with low energy availability at low temperatures, bacterial cells also need to regulate their membrane fluidity to be able to transport molecules in and out of the cell. The lipid composition of the cell wall changes when growing at different temperatures to maintain membrane fluidity and to ensure membrane permeability also at cold temperatures and the composition can differ in species that are adapted to different temperature ranges [114–116].

Fast adaptation of the cellular machinery is important when temperatures fluctuate, and bacteria use both heat shock proteins (HSPs) and cold shock proteins (CSPs) to cope with a sudden change in temperature. The main function of HSPs is to help other proteins to get properly folded and protect them from aggregation as well as to degrade misfolded or aggregated proteins [117]. Cold shock proteins regulate transcription and translation by preventing mRNA from forming secondary structures in combination with a ribonuclease (RNAse) that degrades defective mRNA molecules [118,119]. After the acclimation to the new temperature the bacterial cells resume growth, but at a slower rate [119]. The proteins upregulated for long-term growth at cold temperature are not the same as the CSPs upregulated directly after cold shock [119]. Adaptations to temperatures that are within the “normal” range for a bacterium is different from the response to a temperature shock. Psychrophilic microorganisms synthesize cold-adapted proteins (CAPs) which are similar to CSPs in their mesophilic counterparts, but CAPs are synthesized continuously to maintain growth at low temperature [120,121]. These CAPs are thought to both help regulating the membrane fluidity, but can also replace other proteins that were damaged by the colder temperature [120]. Growing at lower temperatures is also accompanied by a decrease

in the bacterial translation machinery which results in lower growth rates [122]. To handle this decrease coupled to the need for cold-specific proteins bacterial cells have to tightly control protein expression related to temperature and to allocate resources efficiently [123–125]. While most of the processes described in the section above were investigated in *Escherichia coli*, similar regulative mechanisms must be available in MOB especially in soil habitats that can experience frequent temperature fluctuations. *M. tundripaludum* SV96 has been shown to cope well over a relatively broad range of temperatures [44] and efficient use of CH_4 is probably necessary to allow for growth at all of these temperatures.

1.6 Vegetation changes and herbivory in the Arctic

Warmer temperatures in summer and over a longer time will lead directly to changes in vegetation and a longer growing season, especially in the Arctic [1]. Plants affect the structure of the soil, which itself influences properties such as pore space, moisture regime, nutrient cycling, gas transport and other processes in the soil [126]. As discussed in the previous section, many of these properties affect MOB and their activity. Thus, Arctic peatlands and their C cycle will potentially be altered by vegetation-driven changes. Changes in the vegetation composition can act both on the strength of the CO_2 sink as well as on CH_4 emissions [127]. For example, an increase in shrubs and trees at higher latitudes increases the uptake of CO_2 and higher C storage in plant biomass [128]. This can however, be outweighed by an increase in overall C loss when considering plant-soil interactions [129].

In peatlands, climate and land-use changes can lead to drying and it has been shown that drying has a negative effect on the net CO_2 uptake [130]. Warming can also increase soil moisture due to more frequent and intense rain events or the thawing of permafrost in the northern hemisphere which can lead to the expansion of peat- and wetlands. While some plant species might thrive in wetter and warmer conditions which can result in increased CO_2 fixation [131], it was also shown that warmer temperatures can lead to increasing CH_4 emissions from anaerobic microorganisms [14]. Considering that CH_4 has higher radiative forcing, the overall strength as a C sink decreases in a warmer, wetter peatland and these ecosystems can therefore contribute significantly to future GHG emissions [131].

While these changes in vegetation are happening directly because of warming, other changes are more indirectly linked to the changing climate. Increased grazing by herbivores in high latitude ecosystems comprises an additional pressure and has the potential to change C dynamics. Again, grazing can have a positive or negative effect on C emissions. Grazing in shrub dominated ecosystems by large herbivores on Greenland favors the growth of lower plants such as grasses and mosses, thus leading to an increase in C uptake by respiration [132]. In a study from Greenland, it was shown that muskoxen grazing in mires that are dominated by vascular plants leads to higher CH_4 emissions [133]. Different species of geese have had a tremendous impact on the vegetation in large parts of the Arctic and peatlands that were dominated by vascular plants are now outcompeted by mosses [134]. Mosses are generally quite temperature sensitive and drying [135] and the general prediction for northern peatlands is that with increasing temperature grasses will dominate over mosses [135,136]. Thus, in peatlands that are now dominated by mosses as a result of geese grazing, increases in temperature will potentially lead to the loss of much of the moss cover and reduced ecosystem productivity [134,137].

Grazing does not only directly affect the plant cover by removing certain plant species, but also changes the structure and thus the physical properties of the soil. Large herbivores are known to compact the upper layers of the soil, particularly when the soil is wet and especially when the grazers are present in large numbers [138,139]. Compaction of the soil leads to changes in soil hydrology and the reduction of pore space makes it more difficult for roots to penetrate the soil, thus affecting the growth of the plants [138]. Interestingly, similar effects have been recorded by the presence of small herbivores that reduce the plant biomass by trophic interactions, i.e., grazing, but small herbivores can also compact and change the physical parameters of the soil [140]. Geese on the other hand remove not only the plant biomass above the soil, but are known to eat the roots of bryophytes and vascular plants – a process called grubbing which is especially common in wet tundra and grubbing in combination with soil erosion will probably lead to a significant loss of C from these ecosystems [137,141].

In addition, nutrient availability in soils is influenced by the type of plant cover and its abundance. Plant roots excrete high and low molecular weight molecules into the soil that vary with the age and physiological state of the plant, the type of soil type and the nutrient availability in that soil [142,143]. These excreted molecules can be used by the soil microbiota and by other plants in symbiosis or inhibit the growth of

competing plants or pests [142]. Thus, it is apparent that extensive grazing also influences the nutrient availability in the soil. Indeed, higher amounts of polysaccharides were found in the Solvatn peatland sites protected from grazing which are probably linked to the presence of vascular plants and were shown to directly influence the soil microbiota [144].

1.7 A warming Arctic

As already described, herbivores influence both plant cover and soil structure, thus they have an impact on the overall ecosystem processes taking place in the soil. Hence, the presence and increasing abundance of herbivores is detrimental to the fate of the Arctic vegetation. Arctic plant species are generally slow growing and plant species that are least resistant to grazing will disappear quickly when herbivore activity increases [145]. The exclusion of herbivores has a much smaller effect and will not necessarily lead to the return of the original plant cover as the least resistant species have already disappeared. The "new" vegetation is now dominated by plants that were more resistant to grazing from the beginning [145]. Warming will allow Arctic plants to grow longer and faster and it is predicted that more thermophilic plant species will invade Arctic ecosystems in addition to the shrub cover increasing [145–147]. Both shrubs and thermophilic plants are expected to be favored by herbivores, thus herbivores will have a regulating effect [148,149]. Stable populations of herbivores are important to balance those effects that warming has on the plant cover in Arctic ecosystems and their presence and absence will influence the magnitude of changes in vegetation. Animals are slow in adapting to the changes happening in the Arctic due to warming. Since the plant composition and the growing season is changing, processes like calving are not synchronized optimally with the growing season anymore and can lead to a reduction in numbers [150]. Rain in winter renders the snowpack impenetrable and makes it harder for wild reindeers as well as rodents to find food [151]. While one single winter with rain can cause a drastic population reduction in that particular year, perennial events seem to affect the population less [152].

While herbivores such as reindeer and rodents are only able to migrate on land, geese breeding in the Arctic are affected both by changes in their breeding grounds and in their overwintering grounds. Geese populations have doubled in the last century due to the protection from hunting and an increase in food sources [153]. The impact of this

increase on the vegetation has been extensive [154–156]. Warmer temperatures in their Arctic breeding grounds also leads to increased egg production and hatching, which further leads to an increase in the population [157]. Predators such as Arctic foxes and polar bears will likely respond positively to this and can potentially regulate population increases [157].

The Arctic is a closely knit network of herbivores, predators, plants and microorganisms influenced by climate change and above and below ground interactions. Thus, the overall magnitude of changes will depend on responses of each of these groups and their interactions and eventually decide if the Arctic will become a major C source or remain an overall C sink. At the same time few studies have targeted the response of CH_4 oxidizing bacteria to climate change related variables, both in the field and in laboratory studies. Therefore, we think that the results of this thesis are valuable for future climate predictions and the understanding of the Arctic CH_4 filter. Also, microbial soil processes and activities are vital information for integrated Arctic climate models.

2 Objectives

The overall objective of this thesis was to investigate the effect of climate change associated variables on the MOB community and their CH_4 oxidation activity in Arctic peatlands. We wanted to better understand which factors shape the MOB community and how changes from the present state to a warmer Arctic might affect different MOB community members and their activity. Within this complex of numerous changes and interactions the emphasis of this work has been on the specific objectives addressed in the three different papers:

1. How do herbivory induced vegetation changes affect the activity and community composition of Arctic MOB?
2. What effects have increasing temperatures and CH_4 concentrations on the response of Arctic MOB?
3. Which temperature acclimation strategies are used by *M. tundripaludum* SV96?

3 Summary of the papers

3.1 Paper I

Increased herbivory has modified the vegetation of high Arctic peatlands and reduced the amount of vascular plants compared to mosses [134,154]. Master student Vaïk Küpfer measured CH_4 oxidation in mosses collected from peatland sites exposed to herbivory (grazed peat soils). He could not measure CH_4 oxidation in mosses from sites that are protected from grazing (exclosed peat soils) [158]. However, he did detect CH_4 in pore water samples from exclosed peat soils. The CH_4 concentrations in exclosed peat soils were smaller than in grazed peat soils. Sjögersten et al 2011 did not measure any difference in CH_4 net emissions from the same peatland when comparing exclosed peat soils to grazed peat soils [134]. These findings indicated that herbivory influences MOB and we hypothesized that the location, the activity, and the community composition of peatland MOB depend on their exposure to herbivory.

We used microcosms to measure CH_4 oxidation activity along a vertical soil gradient and measured environmental parameters that influence CH_4 oxidation in both peat soils (O_2, pore water CH_4 and water content). In addition, we sequenced 16S rRNA and *pmoA* amplicons to identify the MOB communities responsible for the observed CH_4 oxidation rates.

We could show that herbivory changed the soil structure and chemistry of the soils with higher water contents, lower O_2 concentrations and higher CH_4 concentrations in grazed peat soils. Along with these changes we could detect higher rates of CH_4 oxidation in grazed peat soils and the depth with the highest CH_4 activity was located just below the vegetation (0-2 cm peat soil depth). Exclosed peat soils were characterized by lower water contents, higher O_2 concentrations and lower CH_4 concentrations. Highest CH_4 oxidation was detected at an increased depth (4-8 cm peat soil depth) and CH_4 oxidation rates were lower than in grazed peat soils. The MOB communities in both peat soils were dominated by the genus *Methylobacter*. There was a higher relative abundance of MOB OTUs in the grazed peat soils that was responsible for the higher CH_4 oxidation rates measured in these soils. The MOB communities of grazed and exclosed peat soils were composed of different *Methylobacter* OTUs and both peat soils had unique OTUs that were identified as bioindicators for either grazed or exclosed peat soils.

3.2 Paper II

High Arctic peatlands will be exposed to a larger temperature increase than peatlands further south due to Arctic amplification [1]. Increasing temperatures lead to higher rates of permafrost thaw and increases the availability of organic C. In addition, increases in temperature change important pathways in the peat microbial community and leads to an increase in CH_4 production [14]. Peatland microbes are also influenced by the vegetation and increases in herbivory can affect the C balance in Arctic peatlands [144,159,160]. But how much C is emitted as CH_4 from these peatlands depends eventually on the presence and the activity of MOB. We hypothesized that MOB will be affected both by increases in temperature and CH_4 concentrations and that their response may be affected by herbivory. To test this, we used peat soil microcosms to investigate the combined effect of temperature and CH_4 concentrations on soils that are exposed to herbivory (grazed peat soils) compared to soils protected from herbivory (exclosed peat soils). We targeted peat soils depths which were identified to accommodate the majority of MOB and thus contained the highest CH_4 oxidation activity (**Paper I**). We quantified and sequenced *pmoA* transcripts to relate changes in the abundance and the composition of the MOB community to the responses in CH_4 oxidation activity.

The microcosms experiments revealed that the MOB community of both peat soils responded positively to higher CH_4 concentrations by increasing their CH_4 oxidation activity. This increase was especially pronounced in grazed peat soils which are naturally exposed to higher CH_4 concentrations. The response to the different CH_4 concentrations was modulated by changes in the composition of OTUs belonging to the genus *Methylobacter*. On the transcriptional level this response was however depending on their exposure to herbivory: We observed a larger transcriptional response to low CH_4 concentrations in grazed peat soils and a larger response to high CH_4 concentrations in exclosed peat soils. This suggests that the MOB community will change more drastically when exposed to conditions that are different from what the community experiences at the present state.

We could only detect a minor effect of temperature both on the CH_4 oxidation activity and the MOB community composition in both peat soils. Comparing the response of the soil MOB communities to *M. tundripaludum* SV96, a peat soil isolate

originating from the same peatland, revealed that an increase in temperature has a positive effect on CH_4 oxidation in a pure culture.

3.3 Paper III

Methylobacter is an important CH_4 oxidizer in soils, sediments and freshwater ecosystems [33–37] . MOB are often found close to the surface of their habitat and temperatures can therefore fluctuate considerably during one season, within days and even diurnally. The species *M. tundripaludum* was detected in several low temperature habitats and is a relevant representative of an important genus with close relatives being detected in Arctic, subarctic and temperate environments [33,45,46,48–53,161]. Few studies have investigated temperature responses of MOB isolates [100] and there is a large gap in our understanding how MOB regulate their metabolism at different temperatures to efficiently grow and oxidize CH_4. To grow efficiently at different temperatures, an adjustment of the enzymatic machinery is necessary, but it is unknown which pathways need to be regulated to achieve optimal growth and CH_4 oxidation in response to different temperatures. To investigate *M. tundripaludum* SV96's acclimation to different temperatures we monitored growth, CH_4 oxidation and gene transcription at 8, 15, 21 and 27 °C using pure cultures of the isolate. To map the transcriptional and translational responses, we extracted RNA from *M. tundripaludum* SV96 at all temperatures and sequenced the transcriptomes. We also compared the temperature acclimation profile of *M. tundripaludum* SV96 to another Arctic *Methylobacter* species and a mesophilic *Methylobacter* species.

Our results show that *M. tundripaludum* SV96 grows fastest at 15 °C and 21 °C when CH_4 is saturated, whereas with decreasing CH_4 concentrations growth increased most at 8°C. Highest rates of CH_4 oxidation were also measured at 15 °C. What was interesting however was that more CH_4 was oxidized to achieve the same growth at the lower temperatures; 15°C compared to 21°C or at 8 °C compared to 27°C. Thus, these results indicated more inefficient growth at 8 and 15 °C when exposed to high CH_4 concentrations. Growth efficiency increased for all temperatures but especially at 8 and 15 °C when CH_4 concentrations were decreasing. These observations indicated a physiological response involving resource allocation due to temperature and CH_4 concentration. The increased use of CH_4 at low temperatures was related to an increase in C assimilation towards glycogen storage at both 8 and 15 °C. At 15 °C we could also

detect an upregulation of the entire protein biosynthesis machinery which corresponded with high concentrations of cellular RNA whereas protein concentrations remained stable. This was a demonstration of catalytic compensation through regulatory adjustments of protein biosynthesis. The experiments with the other two *Methylobacter* species also confirmed the large influence of physiological adjustments to temperature and substrate concentrations on growth and CH_4 oxidation rates.

4 Methods

4.1 Field site and in situ measurements

The Solvatn peatland (N78°55.550, E11°56.611) is near the research settlement of Ny-Ålesund, Svalbard (Figure 1). The peatland is situated on a marine terrace on top of continuous permafrost. The water table varies between seasons, but also within one single sampling season. The active layer depth layer is approximately 40 cm [20]. Methane emissions from the peatland range from 25 - 2800 µg $CH_4/m^2.h^2$ depending on the sampling time point and the year and are below or within the average emissions of Northern peatlands [134,162,163]. The Solvatn peatland is heavily grazed by barnacle geese (*Branta leucopsis*) which have changed the vegetation significantly. Exclosures were set up in 1998 to protect parts of the peatland from grazing and the original vegetation was restored. The grazed peatland is dominated by mosses (mostly brown but also green mosses, Figure 3), whereas in exclosed plots grasses, vascular plants and herbs are found alongside the mosses [134,144].

For this thesis, two exclosures that are situated in wet parts of the peatland where CH_4 is produced in anoxic layers of the soil were studied (Figure 4). Samples from the grazed peat soils were taken in the vicinity of these two exclosures. As the Solvatn peatland is near the research station and the laboratory (Figure 4), time between sampling and controlled experimental work could be reduced to a minimum. Its proximity to the research station also allowed us to set up microcosm experiments on site for **Paper I**. The Solvatn peatland is representative of similar peatlands on the peninsula called Brøggerhalvøya with regards to its microbial community [20].

Figure 3 Close-up of lake Solvatn and the surrounding peatland. The field sites SV1 and SV2 are located on the opposite shore of the lake.

Figure 4 Aerial Picture of the Eastern part of Ny Ålesund, lake Solvatn and the surrounding peatland. SV1 and SV2 indicate the sampling sites used for Paper I and II. The isolate *M. tundripaludum* SV96 (**Paper III**) has its origin from this peatland. The laboratory building used for the microcosm experiments of **Paper I** and the preparation of samples is indicated in the picture.

To measure dissolved O_2 in the peat soil, we used the Fibox 4 (Presens, Germany), a portable O_2 probe (PSt-3) and a Pt-100 temperature sensor to correct for dissolved O_2

concentration at in situ temperature. To determine CH_4 concentrations in the peat soils, porewater samples were extracted using brass rods with a syringe connector and holes that could be inserted at the desired depth. A detailed protocol for the extraction and the preparation of the porewater samples can be found in Liebner et al 2012 [164]. Headspace CH_4 concentrations were measured using a gas chromatograph with a flame-ionization detector (GC-FID, SRI Instruments, CA, USA) and the dissolved CH_4 concentrations were calculated from these measurements. Soil water content was determined gravimetrically by drying peat soil samples at 150 °C over-night.

4.2 Microcosms to measure potential methane consumption

Microcosms allow us to study bacterial community responses in environmental samples such as soils, sediments, or water samples and incubate them under defined laboratory conditions. While the experiment is considered as controlled, there are still variables that cannot be accounted for. These arise from within the sample ecosystem such as total nutrient-composition, minerals or by products from microbic metabolism. External conditions such as light, nutrients, temperature, pH etc. can be manipulated and monitored. Microcosms are therefore valuable tools to study the ecosystem effects caused by changing environmental conditions and can serve as a bridge between field studies and laboratory experiments with pure cultures.

In this thesis, microcosms were core experiments both in **Paper I** and **Paper II**. Detailed description of the experimental microcosm setup and the calculation of the CH_4 oxidation rates for each of the two studies are provided in the respective method sections of **Paper I** and **Paper II**.

Figure 5 Microcosm preparation for Paper I. To the left is the intact peat profile. The picture in the middle shows the seven sections cut for the CH_4 oxidation potential along vertical peat soil gradients. To the right are the soils microcosms while being measured using a GC-FID.

For **Paper I**, we wanted to mimic the present conditions in the field as closley as possible to identify the depth with the highest CH_4 oxidation in spring and summer. The microcosm experiments were conducted in the laboratory facilities in Ny-Ålesund (Figure 4), where we installed the portable GC-FID (SRI instruments, CA, USA). The microcosms were incubated outside the laboratory while shaded from direct sunlight. Temperature was monitored regularly. The temperature recorded during experiments was 7 - 8.5 °C (Summer 2015), 3.5 - 5.5 °C (Spring 2016) and 6.5 - 8.0 °C (Summer 2018).

For **Paper II**, the set-up was slightly more complex as we wanted to control for both temperature and CH_4 concentrations. The argument to include temperature in this experiment was that increases in CH_4 concentrations are tightly coupled to temperature and are of relevance for a warming Artic [14]. Soil samples were transported to the university laboratories in Tromsø to set-up the experiment. Soil samples could have been transported cold or frozen. We decided to freeze them at -20 °C to reduce bacterial activity within the soil until the start of the experiment. Storing them cold (around 4 °C) could have led to changes in the soil microbial community as this is comparable to in situ soil temperatures. Freezing occurs in winter every year and temporarily during spring and autumn, thus, the soil microbial communities are used to the shift between freezing and thawing. MOB communities were immediately active after thawing as confirmed by measuring CH_4 oxidation directly after microcosm preparation.

The rapid consumption of CH_4 within the incubation period where CH_4 concentrations were held constant had to be considered. We needed to define a threshold concentration below which concentrations never dropped. The microcosms were then fed according to the CH_4 consumed. As the activity was different for the different microcosms depending on the origin (grazed or closed) and the temperature (8 and 15 °C), all individual microcosms were monitored regularly using our GC-FID and supplied with CH_4 accordingly.

4.3 *pmoA* amplicon sequencing to elucidate the MOB community

Amplicon sequencing allows targeting of specific regions in the genome and the identification of variations in these regions. 16S rRNA gene amplicon sequencing is the most used form of amplicon sequencing in microbial ecology as it allows us to study variations in the 16S rRNA gene of different bacteria and thus the classification of those bacteria. There is a limit in the resolution when sequencing the 16S rRNA gene in microbial ecology and there are uncertainties regarding the placement of certain species in the phylogenetic tree. The marker gene *pmoA* has been widely used to identify MOB and for taxonomic classification. More recently, it has been used for diversity studies based on amplicon sequencing [165,166]. The pipeline used in our study incorporated a frameshift correction step as proposed in other studies and the OTU assignation was based on the published database from Wen et al 2016 [165]. OTU clustering was not based on cut offs, but used the iterative approach employed by Swarm [167]. Considering the aim of our study and the number of samples sequenced, *pmoA* amplicons provided us with MOB community data which we could relate to the CH_4 oxidation activity and the field data.

4.4 MOB enrichments

To study the metabolism of microorganisms that have important ecosystem functions, enrichment and isolation are needed. The cultivation and isolation of MOB is also of interest for various biotechnological applications as pMMO, their key enzyme, has yet not been expressed recombinantly while fully functioning [168]. Thus, there is a need for new MOB isolates that potentially could be used in fermentation applications [169]. Several isolation techniques exist for MOB, using a CH_4 atmosphere

as the sole C source. MOB can be cultivated on solid medium (i.e., agar plates), on surfaces (e.g., filter-cultivation) or directly in liquid cultures.

Both from our field campaign in 2015 and the two campaigns in 2016 we collected soil samples for the enrichment of peat soil MOB. Some enrichments were set up directly from microcosm samples, while some were set up directly from in-situ samples (pore water samples). The enrichment preparation was the same for all types of samples: approximately 2-4 g soil or the pore water from the same amount of soil was transferred in to 125 ml glass bottles and 20 ml NMS medium [170]. The bottles were closed with butyl rubber stoppers (Wheaton, USA) and aluminum crimp caps [171]. A headspace concentration of 20 % CH_4 was set by adding 25 ml of 100 % CH_4. The bottles were incubated at 15 °C for summer samples (August) in 2015 and at 8 °C for spring/summer samples (June and August) in 2016. Enrichments from June 2016 were maintained and analyzed by master student Caroline Hammer. After approximately four weeks the bottles were inspected for bacterial growth using light microscopy. Several rounds of sub-culturing started by inoculating 5 mL fresh NMS medium with 0.5 ml of enrichment culture and 10 ml 95% CH_4/5% CO_2. For the sub cultivation, 50 ml bottles with glass beads providing an increased surface to stimulate MOB growth, were used. When a sufficient density of one bacterial morphology was observed in the light microscope, cells were spun down in a microcentrifuge and identified using the *pmoA* primer pair A189F/mb661R combined with sequencing.

The majority of the sequences were identified as either *M. tundripaludum* SV96 or *Methylobacter* sp. CMS7, both isolates from Arctic habitats [44,49]. The results from the enrichments were used together with the bioindicator OTUs from **Paper I** and **Paper II** to construct a phylogenetic tree (Figure 8). The tree shows the need to obtain new *Methylobacter* isolates to resolve the phylogeny at a higher taxonomic level in combination with physiological insights. The enrichment data presented in this thesis has so far not been published. One of the enrichments resulted in a pure culture and its genome was sequenced. These data will be used for genome comparison studies of *Methylobacter* isolates from cold environments in collaboration with our Russian partners, Svetlana N. Dedysh and Igor Oshkin.

4.5 Methane oxidation, growth, and carbon dioxide production in pure MOB cultures

An important asset for this thesis was the in-house collection of MOB isolates that allowed for detailed studies of temperature acclimation. We conducted experiments with two Arctic *Methylobacter* isolates. One was *M. tundripaludum* SV96, isolated from the same peatland we used for the field and microcosms studies of **Paper I and II** – thus being a relevant MOB that was identified to be active in situ [43]. The other was an unpublished *Methylobacter* isolate, retrieved from a biofilm in an Arctic coal mine and named *Methylobacter* sp. G7. In contrast to *M. tundripaludum* SV96 it is exposed to a constant in situ temperature of 10 °C. We also compared these two isolates to the temperate isolate *Methylobacter luteus* (MV-B-3098). Some physiological data (CH_4 oxidation and growth) for *M. tundripaludum* SV96 were used in **Paper II**, but most of the data was used in combination with transcriptome analysis in **Paper III**.

We cultivated MOB isolates under controlled conditions and monitored growth, CH_4 oxidation activity and CO_2 production at selected temperatures. These rates indicate changes in growth and CH_4 oxidation efficiency, and metabolic adjustments as responses to the conditions applied. To study temperature acclimation, the isolates were preincubated for at least ten generations prior to the experiments at their respective experimental temperatures. Details for the experimental designs are presented in the methods section of **Paper II and III**.

5 Results and Discussion

5.1 Grazing changes the soil structure and the soil environment

The different vegetation cover and the lack of vascular plants (Figure 6) influences the structure of the soil and creates different soil habitats in the grazed and the exclosed peat soils (Figure 7). Grazed peat soils were sponge-like and consisted of degraded mosses and thin, fragmented roots. When excising soil blocks from the grazed peatland sites, we had to be careful as the blocks could disintegrate relatively easily and would have fallen apart if treated without care. Peat soil from the exclosed sites was coarser and the peat soil blocks were held together by a web of roots. The network of roots spanned from the vegetation to a depth of approximately ten centimeters and kept the

peat block more tightly packed together. Sjögersten and colleagues (2012) documented that the root biomass in the exclosed peat soil is higher than in the grazed peat soil [134].

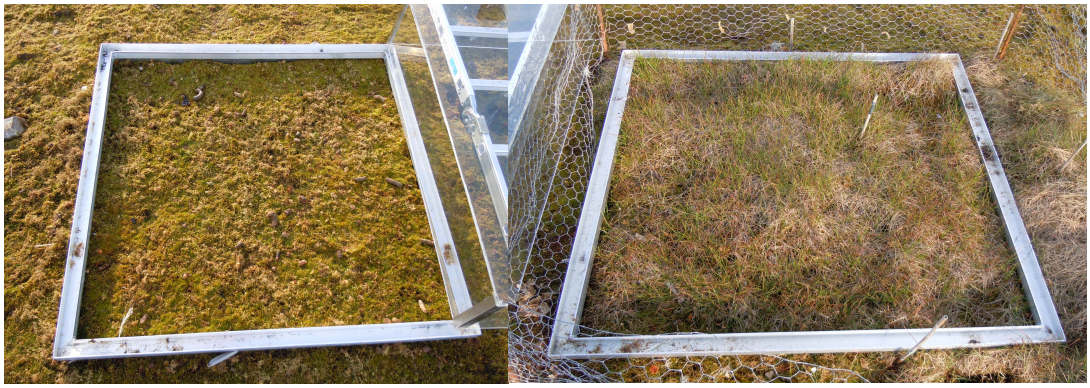

Figure 6 Vegetation from a grazed site (left) and vegetation that is protected from grazing by exclosures (right).

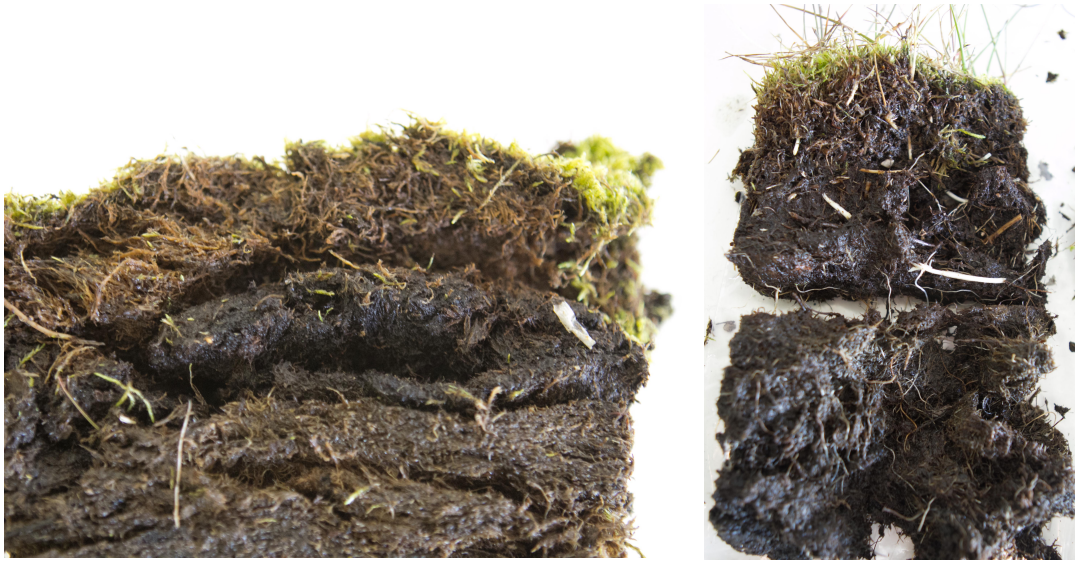

Figure 7 Peat soil from grazed (left) and exclosed (right) peat soil sites.

We measured similar O_2 concentrations in the vegetation and the top five centimeters of the exclosed peat soils and a decrease in O_2 concentrations from a depth of five centimeters. In grazed peat soils, O_2 concentrations decreased instantly and the O_2 decline was steeper than for exclosed peat soils. It has been shown previously that the presence of certain vascular plants can increase O_2 concentrations and create aerobic conditions around the plant roots [75]. Thus, we could show that the presence or absence of vascular plants influenced O_2 availability and that the anaerobic zone of the peat soil was larger in grazed peat than in exclosed peat.

We measured higher porewater CH_4 concentrations at a shallower depth in grazed peat soils compared to exclosed peat soils. Porewater CH_4 concentrations are an indicator at which depth most CH_4 is produced by anaerobic microorganisms and indicates the highest substrate availability for MOB. Highest MOB activity is often found directly at the aerobic/anaerobic interface where CH_4 is available and enough O_2 is present for the oxidation [36]. In addition to the difference in depth, the CH_4 concentrations measured in grazed peat soils were higher than in exclosed peat soils. This suggests that grazed peat soils favor CH_4 production compared to exclosed peat soils. It was shown that grazing leads to increased CH_4 emissions [133,159] and is linked to increased abundances of CH_4 producing archaea [172]. This confirms that the higher CH_4 concentrations measured in the grazed peat soils indicate increased CH_4 production because of herbivory.

The soil water content was lower in the top centimeters of the exclosed peat soils, especially in summer. The differences were less pronounced in spring, probably due to the more recent snowmelt. The structure of the soil could be one explanation for the lower water content in the top part of the exclosed peat soils as water probably drains more easily in the coarser peat soil structure. While we did measure a lower water content, exclosed peat soils are still water-logged with an average water content above 90 %. CH_4 emissions do not increase in a linear way as the water content of a peat soil increases and the water table rather acts as a on and off switch for CH_4 emissions [173]. The lower water table observed in the exclosed peat soils was not low enough to switch off CH_4 production. However, the water table indicated at which depth CH_4 production and oxidation was expected to be located.

5.2 Methane oxidation activity and the MOB community are strongly influenced by herbivory and methane concentrations

We found that the highest potential for CH_4 oxidation was vertically shifted equally to the shift in soil properties described in the previous paragraph hence the highest MOB activity was detected at a shallower depth in the grazed peat soils compared to the exclosed peat soils. Also, the highest MOB activity was measured just above the highest CH_4 pore water concentrations recorded in both peat soils. We measured higher CH_4 oxidation activity in grazed peat soils compared to exclosed peat soils. Increased CH_4 oxidation as a result of grazing has been shown before in Alpine meadows [174] and

higher rates of CH_4 oxidation have the potential to compensate for the overall larger amounts of CH_4 produced in grazed peat soils. Indeed, previous measurements from the Solvatn peatland did not show significant differences in the CH_4 emissions from grazed and exclosed peat soils [134]. These results highlight the importance of MOB and how they can regulate CH_4 emissions.

In line with the increased CH_4 oxidation activity, we found a larger active MOB community in grazed soils (higher transcription of MOB OTUs) which indicated a larger active community compared to exclosed soils.

The Solvatn MOB community was different in both grazed and exclosed soils but consisted mostly of *Methylobacter* OTUs. While there were several environmental differences that could cause these differences, CH_4 concentrations were probably one important driver in shaping the MOB community and their oxidation activity. High CH_4 concentrations are usually favored by MOB belonging to the *Gammaproteobacteria,* while *Alphaproteobacteria* are more resistant to environmental stress and changing conditions [175,176]. *Methylocystis* has been isolated from the Solvatn peatland [177] which suggest that alphaprotoebacterial MOB are present in the soil, but was not identified in the soil layers investigated in these studies. The predominance of *Methylobacter* OTUs is probably caused by an ample supply of CH_4 in both soils but could also be caused by the *Methylobacter's* to cope with low O_2 concentrations.

To investigate more closely how the Arctic peatland MOB community responds to different CH_4 concentrations, we designed a microcosm experiment in which we simultaneously increased CH_4 concentrations as well as temperatures in both soil ecosystems. CH_4 concentrations had a significant impact on CH_4 oxidation activity and higher CH_4 concentrations lead to increased CH_4 oxidation and different MOB OTUs responded to low and high CH_4 concentrations. Most of the responding OTUs were assigned to *Methylobacter*. When comparing the MOB community in the microcosms incubated at low and high CH_4, *Methylobacter* always increased at high CH_4 at the expense of other genera (see Figure 6, **Paper II**).

When comparing the in situ bioindicator OTUS for grazed or exclosed peat soils (**Paper I**) to the bioindicator OTUs responding to either high or low CH_4 concentrations in the microcosm experiment (**Paper II**), no match was found. To explain this more in more detail, the bioindicator OTUs responding to 1% CH_4 in the microcosm experiment were not found to be bioindicator OTUs for grazed peat soils in situ. Similarly, those bioindicators OTUs responding to 0.1% CH_4 in the microcosms experiment were not

found to be bioindicators for exclosed peat soils in situ. On the contrary, the 0.1% CH_4 bioindicator OTUs M3, M35 and A3 were found to be bioindicator OTUs for grazed sites in situ. An explanation could be that in the microcosm experiment from **Paper II** a response in the MOB community was measured which was caused by experimental disturbance over a relative short time and the bioindicator OTUs responding were most flexible in adapting to such a change. The grazing treatment that was chosen for the discrimination in **Paper I** selected for bioindicator OTUS in MOB communities that have established themselves over a longer time. This suggests that CH_4 concentrations were only one of the parameters different in grazed and exclosed soils that selected for different MOB communities. This implies that the explanation for the presence of certain *Methylobacter* OTUs is probably more complex and influenced by several other parameters than CH_4 concentrations alone. Both studies showed the ability of the Solvatn MOB communities to respond to different environmental conditions by the presence of a large consortium of different *Methylobacter* OTUs.

5.3 The importance of *M. tundripaludum* and close relatives in high Arctic peat soils

Most enrichments were identified as either *M. tundripaludum* SV96 or *Methylobacter sp*. CMS7 and cluster with the *pmoA* sequence of those two isolates in the phylogenetic tree (Figure 8). This was true for both enrichments from the most active zone of CH_4 oxidation and from other depths with smaller rates of CH_4 oxidation. *Methylobacter* was also enriched from depths that were considered anaerobic, highlighting *Methylobacter*'s ability to survive at low O2 concentrations.

The 1% bioindicators from **Paper II**, M29 and M20, belong to the same clusters. OTU M29 was identified as *M. tundripaludum* SV96 whereas M20 was identified as *Methylobacter* sp. CMS7. This highlights the selection of some *Methylobacter* species at high CH_4 concentrations. We could not find any herbivory induced difference in the peat soil enrichments, i.e., that one MOB species is more prevalent in grazed or exclosed peat soils. These findings contradicted the different in situ MOB communities in grazed and closed peat soils (Figure 5, **Paper I**). The lack of herbivory induced differences in the enrichments might be caused by the identical cultivation conditions (i.e., high CH_4 headspace concentrations were used for both peat soils), selecting *Methylobacter* species that thrive under high CH_4 concentrations.

We could not find any seasonal patterns in the enrichments or in the in situ MOB community (**Paper I**). Only one enrichment was specific to the Spring 2016 sampling campaign, which did not cluster with *Methylobacter* but with *Methylovulum* and OTU M7, an "unconditional bioindicator OTU" for 1% CH_4. We did vary temperature and used lower temperatures for the 2016 enrichments. Considering the microcosms experiment from **Paper II**, the observation that temperature did not yield more diversity in the enrichments fits well with the observation that temperature plays a lesser role than CH_4 concentrations in determining which MOB are active.

Lower CH_4 concentrations during enrichment and cultivation could result in novel MOB isolates from the Solvatn peatland. Other MOB species that are more adapted to low CH_4 concentrations could then potentially outcompete *Methylobacter tundripaludum* SV96 and *Methylobacter* sp. CMS7. Considering the in situ conditions in the Solvatn peat soils (i.e., high CH_4 concentrations available), the importance of the two *Methylobacter* species identified in most of the enrichments is however well represented. This makes them also good candidates for MOB physiology studies.

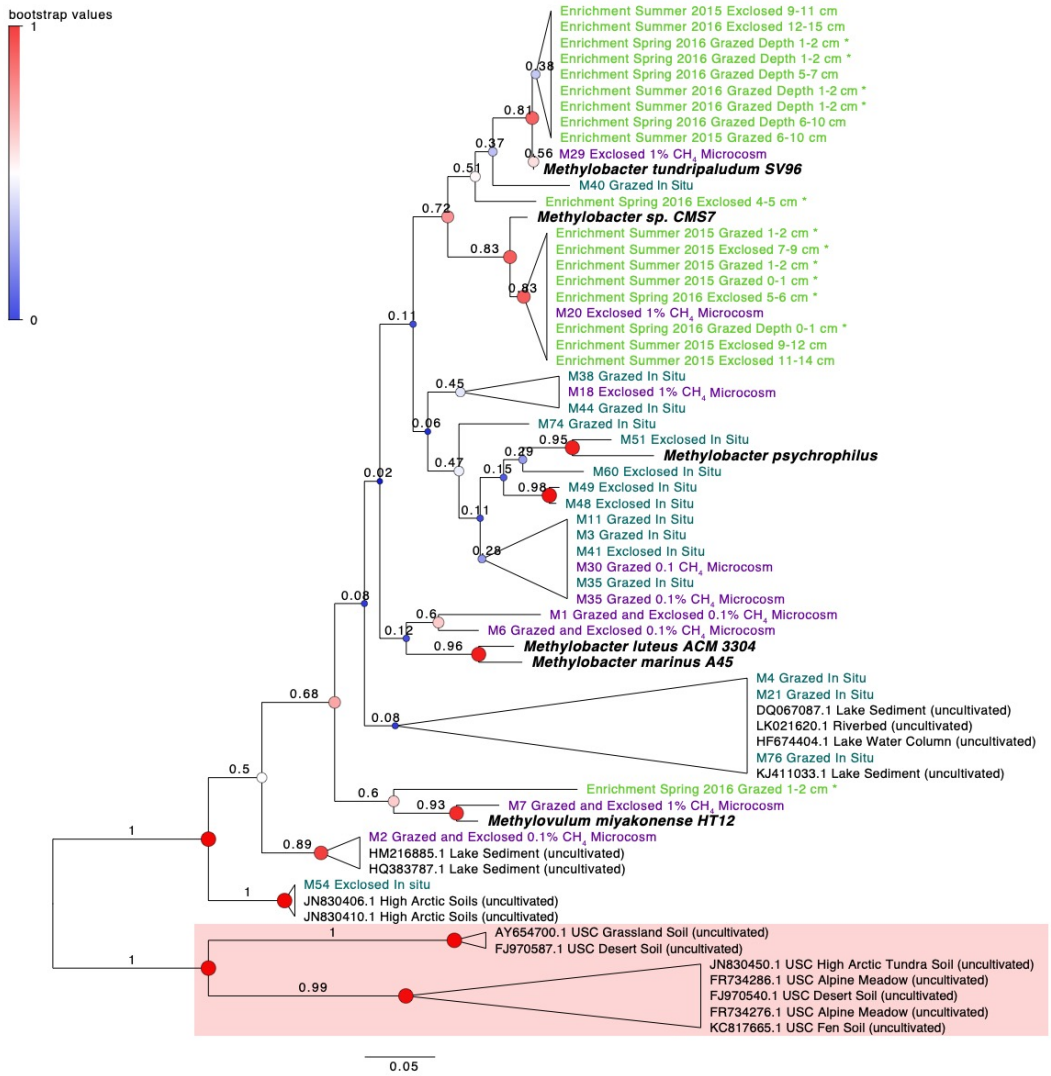

Figure 8 Phylogenetic tree combining the MOB enrichments (light green) and the bioindicator OTUs from Paper I (petrol blue) and Paper II (violet). MOB enrichments that were chosen from layers with the highest CH_4 oxidation activity in grazed (0-2 cm) and exclosed (4-8 cm) peat soil are marked with an *. The other MOB enrichments were from layers outside the most active CH_4 oxidation zone. The tree is based on a 414 nt alignment using MUSCLE. The tree is constructed using the maximum likelihood method with the jukes-cantor model. Alignment and tree construction was executed in MEGA-X, whereas modifications were made in FigTree. Red indicates high, white indicates medium and blue indicates low bootstrap values.

5.4 Temperature responses in peat soil MOB communities compared to MOB isolates

Temperature is critical in controlling biochemical processes in all microorganisms and our hypothesis for the microcosm experiments from **Paper II** was that an increase in temperature can potentially increase CH_4 oxidation activity. Nonetheless, we could not show a significant effect on either the CH_4 oxidation activity or on the MOB community composition in the soil microcosms after the incubations at 8 and 15 °C. These results suggest that the present MOB community from both exclosed and grazed peat soils are already adapted to cope with both experimental temperatures and that their acclimation does not involve higher CH_4 oxidation rates at higher temperatures. This was interesting, as MOB isolates show an increase in growth with increasing temperature until an optimum was reached [44,100] and we assumed that CH_4 oxidation would follow the same pattern.

To understand more in more detail why we could not detect any temperature effect on CH_4 oxidation rates in the soil communities, we conducted experiments with two Arctic *Methylobacter* isolates in comparison to a temperate *Methylobacter* isolate for **Paper III**. The two Arctic isolates *M. tundripaludum* SV96 and *Methylobacter* sp. G7 showed that both species grow best at low temperatures and are most efficient at low CH_4 concentrations. Under saturated CH_4 concentrations, *Methylobacter* sp. G7 and *M. tundripaludum* SV96 grew best at 8 °C and 15 °C, respectively. *Methylobacter* sp. G7 was isolated from an Arctic coal mine with a constant temperature of 10 °C, which is reflected by favoring temperatures of 8 °C and lower relative to *M. tundripaludum* SV96. *M. tundripaludum* SV96 has its origin from Arctic peat soils that experiences both warmer temperatures and larger temperature fluctuations. This is also reflected in a broader optimum for growth, with more similar growth rates measured at 15 and 21 °C. This broader optimum for growth has also been shown previously in Wartiainen et al 2006 [44]. The temperature profiles for *M. luteus* (MV-B-3098) revealed that the isolate is adapted to warmer temperatures than the two Arctic isolates, with best growth and high CH_4 oxidation at higher temperatures. Common for all the three strains were the relatively large shifts in CH_4 uptake relative to their growth rate at different CH_4 concentrations and temperature. This indicated that resources in the cell are allocated differently depending on the temperature and that this controls CH_4 uptake in *Methylobacter* and probably also in other MOB.

5.5 Temperature acclimation in *M. tundripaludum* SV96

Considering that *M. tundripaludum* SV96 was isolated from a cold, CH_4 rich environment, it was interesting that the isolate showed more inefficient growth at low temperatures under saturated CH_4 conditions. This inefficient growth is indicated by the higher amounts of CH_4 that are oxidized at 8 °C and at 15 °C to achieve the same growth rate as observed at 21 °C. To understand why growth is more inefficient at low temperatures, we extracted total RNA from *M. tundripaludum* SV96 cultures incubated under saturated CH_4 conditions at the different temperatures and sequenced the transcriptomes.

The highest amounts of RNA were extracted at 15 °C, closely followed by 21 °C. Most of the cellular RNA is rRNA [178] which suggests that the highest concentration of ribosomes was found in cells growing at 15 and 21 °C. Bacteria can maximize growth by increasing their concentration of ribosomes and therefore growth rates and ribosome concentrations often have a linear relationship [124,125]. We could not find a good correlation between total RNA and growth rates in our experiments as the cells grew faster at 21 °C than at 15 °C with similar RNA concentrations. It has been shown previously that the correlation between ribosomes and growth rate disappears when the changes in the growth rate depend on changes in temperature [124]. However, this does not exclude a link between growth and CH_4 oxidation rates and ribosome concentrations.

The transcriptomes showed that several pathways were upregulated at 15 °C compared to 21 °C. These pathways included increased transcription of tetrahydromethanopterin and several genes of the RuMP pathway leading from CH_4 oxidation towards nucleotide biosynthesis. Overall, the upregulated pathways and gene expressions indicated an increased investment in transcription, translation, amino acid synthesis and protein folding as a result of temperature and matched previous studies in *E.coli* [179,180]. This upregulation of the protein biosynthesis machinery in *M. tundripaludum* SV96 at 15 °C compared to 21 °C comes at a cost for the cell and helps to explain how the cell acclimates. It is also possible that the high CH_4 oxidation activity and the decrease in growth efficiency is due to this increased investment into protein biosynthesis.

We could not detect the same increased investment in the protein biosynthesis machinery at 8 °C. At 8 °C we detected that the desaturation of fatty acids was significantly upregulated but was also increased at 15 °C when compared to the higher temperatures. Desaturated fatty acids are commonly found in cold adapted microorganisms and bacteria exposed to low temperatures respond by upregulation their production [114,116]. Also, the observed upregulation of fatty acid desaturation at both 8 and 15 °C could not explain the seemingly inefficient use of C. To see if the missing C had been used mainly to generate energy, we measured CO_2 production at 8, 15 and 21 °C. CO_2 is the last product of the CH_4 oxidation cascade when the C is not assimilated and increases in CO_2 indicate energy generation over biomass assimilation. Highest CO_2 production was measured at 21 °C, followed by 8 °C and then 15 °C. Therefore, energy generation could not explain the lost C. Some bacteria use molecules like glycogen to store C. Pathways for glycogen synthesis were upregulated, indicating an increased investment in storage as a response to the lower temperature. The glycogen content of the cells was quantified and confirmed that the highest accumulation of glycogen was detected in the cultures at 27 °C, followed by 8 °C, 15 °C and 21 °C when the cells were harvested in early stationary phase and at 21 °C, followed by 27 °C, 15 °C and 8 °C in mid-exponential-phase. Thus, it seems *M. tundripaludum* SV96 uses C to balance metabolism relative to growth, affecting how much CH_4 is consumed relative to cell division at different temperatures and growth phases. An important question is why CH_4 uptake is not downregulated when less substrates are needed for growth. We could hypothesize that the ecological conditions that these organisms are exposed to have through evolution acclimated them towards adjusting C and energy storage relative to growth to maximize survival.

To conclude, our results suggest that *M. tundripaludum* SV96 is directly influenced by temperature and adopts different strategies depending on temperature. These temperature adaptation strategies allow the isolate to finetune its metabolism either by adjusting C storage or its protein biosynthesis machinery to different temperatures. This in turn strongly influences the CH_4 oxidation rates which from our findings is confirmed not to be a simple product of temperature and CH_4 concentrations, but rather precisely regulated thorough a complex physiological acclimation to allow the highest chance of survival for the organism.

6 Conclusions and future perspectives

Arctic peatlands are exposed to higher temperatures and to increased herbivory, both having the potential to increase CH_4 emissions from these ecosystems. At the same time MOB display a high flexibility and resilience in their response to environmental changes.

MOB colonize sections in the peat soil that contain sufficient O_2 for CH_4 oxidation. The depths of these sections depend on the presence of herbivory and are vertically shifted when comparing grazed peat soil to peat soil that is protected from grazing. Grazed peat soils also contain higher amounts of CH_4 compared to the protected peat, but we could show that the microbial CH_4 filter can compensate for the higher concentrations by increasing CH_4 oxidation. The extent of herbivory in the Arctic has the potential to increase if not other factors which regulate geese populations take over [157] and this may lead to higher losses of plant biomass and soil erosion. MOB in grazed peat soils are already confided to a very narrow part of the peat soil and an increase in herbivore activity might affect the efficiency of the biological CH_4 filter activity negatively.

MOB respond to increases in CH_4 concentrations by increased CH_4 oxidation activity, both when exposed to higher in situ CH_4 concentrations and when incubated at increased CH_4 concentrations. It seems plausible from our studies that peat soil MOB can compensate for increased CH_4 production, at least to the extend tested in our studies. Future changes in climate and herbivory can however limit the MOB activity and result in higher CH_4 emissions from the Solvatn peatland or similar Arctic peatlands. In addition, increased permafrost thaw and precipitation has the potential to raise the soil water table, confining peat MOB to even narrower zones for CH_4 oxidation. As such the moisture regime of peat soil could be included in experiments testing the limit of CH_4 oxidation capacity. Anaerobic CH_4 oxidation – which has been reported to also occur in peatlands [181] while so far not detected in the Solvatn peatland [20]– may become a significant sink for CH_4 and could help regulating CH_4 emissions.

We observed that responses in the CH_4 oxidation activity are modulated by a consortium of *Methylobacter* OTUs. The genus *Methylobacter* is known as an efficient CH_4 sink in soils and aquatic ecosystems [20,33–37,42,43]. The co-existence of closely related MOB allows for efficient responses to changes within an ecosystem [59]. We

assume this is the case for the *Methylobacter* OTUs detected in the Solvatn peatland with different members adapted to slightly different conditions and activated depending on the present environmental condition. Also, this closely related network of *Methylobacter* OTUs provides the peat soil ecosystem with the necessary resilience when exposed to environmental changes.

An important member of the peat soil community is *M. tundripaludum* SV96 We could show that the strain regulates its metabolism to optimize growth and the use of substrate depending on temperature. This metabolic fine tuning allows the MOB isolate to control growth, energy generation and substrate storage depending on the conditions it is exposed to, which can be advantageous in a changing Arctic. These findings also highlight the need to better understand the response of environmental isolates which are important for the C balance in soils affected by climate change.

To conclude this thesis, we could show that both the regulation on community level modulated by a network of closely related species and the fine tuning of the individual species' metabolism are crucial for the response and the resilience of the CH_4 filter in high Arctic peatlands when exposed to changing environmental conditions.

7 References

1. IPCC 2021: Climate Change 2021: The Physical Science Basis. Contribution of Working Group I to the Sixth Assessment Report of the Intergovernmental Panel on Climate Change. *Cambride Univ. Press (In Press.* **2021**.
2. Cohen, J.; Zhang, X.; Francis, J.; Jung, T.; Kwok, R.; Overland, J.; Ballinger, T.J.; Bhatt, U.S.; Chen, H.W.; Coumou, D.; et al. Divergent consensuses on Arctic amplification influence on midlatitude severe winter weather. *Nat. Clim. Chang.* **2020**, *10*, 20–29, doi:10.1038/s41558-019-0662-y.
3. AMAP, 2021. Arctic Climate Change Update 2021: Key Trends and Impacts. Summary for Policy-makers. *Arct. Monit. Assess. Program. (AMAP), Tromsø, Norw.* **2021**, 16.
4. Ciais, P.; Tan, J.; Wang, X.; Roedenbeck, C.; Chevallier, F.; Piao, S.L.; Moriarty, R.; Broquet, G.; Le Quéré, C.; Canadell, J.G.; et al. Five decades of northern land carbon uptake revealed by the interhemispheric CO_2 gradient. *Nature* **2019**, *568*, 221–225, doi:10.1038/s41586-019-1078-6.
5. Graven, H.D.; Keeling, R.F.; Piper, S.C.; Patra, P.K.; Stephens, B.B.; Wofsy, S.C.; Welp, L.R.; Sweeney, C.; Tans, P.P.; Kelley, J.J.; et al. Enhanced seasonal exchange of CO_2 by Northern ecosystems since 1960. *Science (80-.).* **2013**, *341*, 1085–1089, doi:10.1126/science.1239207.
6. Turetsky, M.R.; Abbott, B.W.; Jones, M.C.; Walter Anthony, K.; Olefeldt, D.; Schuur, E.A.G.; Koven, C.; McGuire, A.D.; Grosse, G.; Kuhry, P.; et al. Permafrost collapse is accelerating carbon release. *Nature* **2019**, 32–34, doi:10.1038/d41586-019-01313-4.
7. McGuire, A.D.; Lawrence, D.M.; Koven, C.; Clein, J.S.; Burke, E.; Chen, G.; Jafarov, E.; MacDougall, A.H.; Marchenko, S.; Nicolsky, D.; et al. Dependence of the evolution of carbon dynamics in the northern permafrost region on the trajectory of climate change. *Proc. Natl. Acad. Sci. U. S. A.* **2018**, *115*, 3882–3887, doi:10.1073/pnas.1719903115.
8. Obu, J.; Westermann, S.; Bartsch, A.; Berdnikov, N.; Christiansen, H.H.; Dashtseren, A.; Delaloye, R.; Elberling, B.; Etzelmüller, B.; Kholodov, A.; et al. Northern Hemisphere permafrost map based on TTOP modelling for 2000–2016 at 1 km^2 scale. *Earth-Science Rev.* **2019**, *193*, 299–316, doi:10.1016/j.earscirev.2019.04.023.
9. Schuur, E.A.G.; Bockheim, J.; Canadell, J.G.; Euskirchen, E.; Field, C.B.; Goryachkin, S. V.; Hagemann, S.; Kuhry, P.; Lafleur, P.M.; Lee, H.; et al. Vulnerability of permafrost carbon to climate change: Implications for the global carbon cycle. *Bioscience* **2008**, *58*, 701–714, doi:10.1641/B580807.
10. Zhang, T.; Barry, R.G.; Knowles, K.; Heginbottom, J.A.; Brown, J. Statistics and characteristics of permafrost and ground-ice distribution in the Northern Hemisphere. *Polar Geogr.* **1999**, *23*, 132–154, doi:10.1080/10889379909377670.
11. Tarnocai, C.; Canadell, J.G.; Schuur, E.A.G.; Kuhry, P.; Mazhitova, G.; Zimov, S. Soil organic carbon pools in the northern circumpolar permafrost region. *Global Biogeochem. Cycles* **2009**, *23*, 1–11, doi:10.1029/2008GB003327.
12. Jeglum, J.K. Peatland habitats. In *Biology of Peatlands*; Oxford University Press, 2006; pp. 1–20.
13. Gallego-Sala, A. V.; Charman, D.J.; Brewer, S.; Page, S.E.; Prentice, I.C.; Friedlingstein, P.; Moreton, S.; Amesbury, M.J.; Beilman, D.W.; Björck, S.; et al. Latitudinal limits to the predicted increase of the peatland carbon sink with warming. *Nat. Clim. Chang.* **2018**, *8*, 907–913, doi:10.1038/s41558-018-0271-1.
14. Tveit, A.T.; Urich, T.; Frenzel, P.; Svenning, M.M. Metabolic and trophic interactions modulate methane production by Arctic peat microbiota in response to warming. *Proc. Natl. Acad. Sci.* **2015**, *112*, E2507–E2516, doi:10.1073/pnas.1420797112.
15. Loisel, J.; Gallego-Sala, A. V.; Amesbury, M.J.; Magnan, G.; Anshari, G.; Beilman, D.W.; Benavides, J.C.; Blewett, J.; Camill, P.; Charman, D.J.; et al. Expert assessment of future vulnerability of the global peatland carbon sink. *Nat. Clim. Chang.* **2021**, *11*, 70–77, doi:10.1038/s41558-020-00944-0.
16. Abatenh, E.; Gizaw, B.; Tsegaye, Z.; Tefera, G. Microbial Function on Climate Change - A Review. *Environ. Pollut. Clim. Chang.* **2018**, *02*, 1–6, doi:10.4172/2573-458x.1000147.

17. Lyu, Z.; Shao, N.; Akinyemi, T.; Whitman, W.B. Methanogenesis. *Curr. Biol.* **2018**, *28*, R727–R732, doi:10.1016/j.cub.2018.05.021.
18. Thauer, R.K.; Kaster, A.K.; Seedorf, H.; Buckel, W.; Hedderich, R. Methanogenic archaea: Ecologically relevant differences in energy conservation. *Nat. Rev. Microbiol.* **2008**, *6*, 579–591, doi:10.1038/nrmicro1931.
19. Metje, M.; Frenzel, P. Methanogenesis and methanogenic pathways in a peat from subarctic permafrost. *Environ. Microbiol.* **2007**, *9*, 954–964, doi:10.1111/j.1462-2920.2006.01217.x.
20. Tveit, A.; Schwacke, R.; Svenning, M.M.; Urich, T. Organic carbon transformations in high-Arctic peat soils: key functions and microorganisms. *ISME J.* **2013**, *7*, 299–311, doi:10.1038/ismej.2012.99.
21. Hanson, R.S.; Hanson, T.E. Methanotrophic bacteria. *Microbiol. Rev.* **1996**, *60*, 439–471, doi:10.1128/mr.60.2.439-471.1996.
22. Nazaries, L.; Murrell, J.C.; Millard, P.; Baggs, L.; Singh, B.K. Methane, microbes and models: Fundamental understanding of the soil methane cycle for future predictions. *Environ. Microbiol.* **2013**, *15*, 2395–2417, doi:10.1111/1462-2920.12149.
23. Knief, C. Diversity and habitat preferences of cultivated and uncultivated aerobic methanotrophic bacteria evaluated based on *pmoA* as molecular marker. *Front. Microbiol.* **2015**, *6*, doi:10.3389/fmicb.2015.01346.
24. Op den Camp, H.J.M.; Islam, T.; Stott, M.B.; Harhangi, H.R.; Hynes, A.; Schouten, S.; Jetten, M.S.M.; Birkeland, N.K.; Pol, A.; Dunfield, P.F. Environmental, genomic and taxonomic perspectives on methanotrophic *Verrucomicrobia*. *Environ. Microbiol. Rep.* **2009**, *1*, 293–306, doi:10.1111/j.1758-2229.2009.00022.x.
25. Knief, C.; Lipski, A.; Dunfield, P.F. Diversity and Activity of Methanotrophic Bacteria in Different Upland Soils. *Appl. Environ. Microbiol.* **2003**, *69*, 6703–6714, doi:10.1128/AEM.69.11.6703-6714.2003.
26. Cui, M.; Ma, A.; Qi, H.; Zhuang, X.; Zhuang, G. Anaerobic oxidation of methane: An "active" microbial process. *Microbiologyopen* **2015**, *4*, 1–11, doi:10.1002/mbo3.232.
27. Stanley, S.H.; Prior, S.D.; Leak, D.J.; Dalton, H. Copper stress underlies the fundamental change in intracellular location of methane mono-oxygenase in methane-oxidizing organisms: Studies in batch and continuous culture. *Biotechnol. Lett.* **1983**, *5*, 487–492, doi:https://doi.org/10.1007/BF00132233.
28. Semrau, J.D.; DiSpirito, A.A.; Yoon, S. Methanotrophs and copper. *FEMS Microbiol. Rev.* **2010**, *34*, 496–531, doi:10.1111/j.1574-6976.2010.00212.x.
29. Khmelenina, V.N.; Murrell, J.C.; Smith, T.J.; Trotsenko, Y.A. Physiology and Biochemistry of the Aerobic Methanotrophs. In *Aerobic Utilization of Hydrocarbons, Oils, and Lipids*; Spring, Cham, 2019 ISBN 9783319397825.
30. Liebner, S.; Svenning, M.M. Environmental Transcription of *mmoX* by Methane-Oxidizing *Proteobacteria* in a Subarctic Palsa Peatland. *Appl. Environ. Microbiol.* **2013**, *79*, 701–706, doi:10.1128/AEM.02292-12.
31. Degelmann, D.M.; Borken, W.; Drake, H.L.; Kolb, S. Different atmospheric methane-oxidizing communities in european beech and norway spruce soils. *Appl. Environ. Microbiol.* **2010**, *76*, 3228–3235, doi:10.1128/AEM.02730-09.
32. Orata, F.D.; Meier-Kolthoff, J.P.; Sauvageau, D.; Stein, L.Y. Phylogenomic analysis of the gammaproteobacterial Methanotrophs (order *Methylococcales*) calls for the reclassification of members at the genus and species evels. *Front. Microbiol.* **2018**, *9*, 1–17, doi:10.3389/fmicb.2018.03162.
33. Smith, G.J.; Angle, J.C.; Solden, L.M.; Borton, M.A.; Morin, T.H.; Daly, R.A.; Johnston, M.D.; Stefanik, K.C.; Wolfe, R.; Gil, B.; et al. Members of the genus *Methylobacter* are inferred to account for the majority of aerobic methane oxidation in oxic soils from a freshwater eetland. *MBio* **2018**, *9*, e00815-18, doi:10.1128/mBio.00815-18.
34. Chistoserdova, L. Methylotrophy in a lake: From metagenomics to single-organism physiology. *Appl. Environ. Microbiol.* **2011**, *77*, 4705–4711, doi:10.1128/AEM.00314-11.
35. Kalyuzhnaya, M.G.; Lamb, A.E.; McTaggart, T.L.; Oshkin, I.Y.; Shapiro, N.; Woyke, T.; Chistoserdova, L. Draft genome sequences of gammaproteobacterial methanotrophs isolated from Lake Washington sediment. *Genome Announc.* **2015**, *3*, e00103-15, doi:10.1128/genomeA.00103-15.
36. Reim, A.; Lüke, C.; Krause, S.; Pratscher, J.; Frenzel, P. One millimetre makes the

difference: High-resolution analysis of methane-oxidizing bacteria and their specific activity at the oxic-anoxic interface in a flooded paddy soil. *ISME J.* **2012**, *6*, 2128–2139, doi:10.1038/ismej.2012.57.
37. Reddy, K.R.; Rai, R.K.; Green, S.J.; Chetri, J.K. Effect of temperature on methane oxidation and community composition in landfill cover soil. *J. Ind. Microbiol. Biotechnol.* **2019**, *46*, 1283–1295, doi:10.1007/s10295-019-02217-y.
38. Hernandez, M.E.; Beck, D.A.C.; Lidstrom, M.E.; Chistoserdova, L. Oxygen availability is a major factor in determining the composition of microbial communities involved in methane oxidation. *PeerJ* **2015**, *3*, e801, doi:10.7717/peerj.801.
39. Steinle, L.; Maltby, J.; Treude, T.; Kock, A.; Bange, H.W.; Engbersen, N.; Zopfi, J.; Lehmann, M.F.; Niemann, H. Effects of low oxygen concentrations on aerobic methane oxidation in seasonally hypoxic coastal waters. *Biogeosciences* **2017**, *14*, 1631–1645, doi:10.5194/bg-14-1631-2017.
40. Blees, J.; Niemann, H.; Wenk, C.B.; Zopfi, J.; Schubert, C.J.; Kirf, M.K.; Veronesi, M.L.; Hitz, C.; Lehmann, M.F. Micro-aerobic bacterial methane oxidation in the chemocline and anoxic water column of deep south-alpine Lake Lugano (Switzerland). *Limnol. Oceanogr.* **2014**, *59*, 311–324, doi:10.4319/lo.2014.59.2.0311.
41. Mayr, M.J.; Zimmermann, M.; Dey, J.; Brand, A.; Wehrli, B.; Bürgmann, H. Growth and rapid succession of methanotrophs effectively limit methane release during lake overturn. *Commun. Biol.* **2020**, *3*, 1–9, doi:10.1038/s42003-020-0838-z.
42. Wartiainen, I.; Hestnes, A.G.; Svenning, M.M. Methanotrophic diversity in high arctic wetlands on the islands of Svalbard (Norway)-denaturing gradient gel electrophoresis analysis of soil DNA and enrichment cultures. *Can. J. Microbiol.* **2003**, *49*, 602–12, doi:10.1139/w03-080.
43. Graef, C.; Hestnes, A.G.; Svenning, M.M.; Frenzel, P. The active methanotrophic community in a wetland from the High Arctic. *Environ. Microbiol. Rep.* **2011**, *3*, 466–472, doi:10.1111/j.1758-2229.2010.00237.x.
44. Wartiainen, I.; Hestnes, A.G.; McDonald, I.R.; Svenning, M.M. *Methylobacter tundripaludum* sp. nov., a methane-oxidizing bacterium from Arctic wetland soil on the Svalbard islands, Norway (78° N). *Int. J. Syst. Evol. Microbiol.* **2006**, *56*, 109–113, doi:10.1099/ijs.0.63728-0.
45. Martineau, C.; Whyte, L.G.; Greer, C.W. Stable isotope probing analysis of the diversity and activity of Methanotrophic bacteria in soils from the Canadian high Arctic. *Appl. Environ. Microbiol.* **2010**, *76*, 5773–5784, doi:10.1128/AEM.03094-09.
46. Liebner, S.; Rublack, K.; Stuehrmann, T.; Wagner, D. Diversity of aerobic methanotrophic bacteria in a permafrost active layer soil of the Lena Delta, Siberia. *Microb. Ecol.* **2009**, *57*, 25–35, doi:10.1007/s00248-008-9411-x.
47. He, R.; Wooller, M.J.; Pohlman, J.W.; Catranis, C.; Quensen, J.; Tiedje, J.M.; Leigh, M.B. Identification of functionally active aerobic methanotrophs in sediments from an Arctic lake using stable isotope probing. *Environ. Microbiol.* **2012**, *14*, 1403–1419, doi:10.1111/j.1462-2920.2012.02725.x.
48. He, R.; Wooller, M.J.; Pohlman, J.W.; Quensen, J.; Tiedje, J.M.; Leigh, M.B. Shifts in identity and activity of methanotrophs in Arctic Lake sediments in response to temperature changes. *Appl. Environ. Microbiol.* **2012**, *78*, 4715–4723, doi:10.1128/AEM.00853-12.
49. Belova, S.E.; Oshkin, I.Y.; Glagolev, M. V.; Lapshina, E.D.; Maksyutov, S.S.; Dedysh, S.N. Methanotrophic bacteria in cold seeps of the floodplains of northern rivers. *Microbiology* **2013**, *82*, 743–750, doi:10.1134/s0026261713060040.
50. Roldán, D.M.; Carrizo, D.; Sánchez-García, L.; Menes, R.J. Diversity and Effect of Increasing Temperature on the Activity of Methanotrophs in Sediments of Fildes Peninsula Freshwater Lakes, King George Island, Antarctica. *Front. Microbiol.* **2022**, *13*, 1–16, doi:10.3389/fmicb.2022.822552.
51. Lamarche-Gagnon, G.; Anesio, A.M.; Wadham, J.L.; Zarsky, J.D.; Kohler, T.J.; Bagshaw, E.A.; Telling, J.; Hawkings, J.R.; Stibal, M. Meltwater runoff from the greenland ice sheet reveals microbial consortia from contrasting subglacial drainage systems. *bioRxiv* **2020**, doi:10.1101/2020.05.26.116566.
52. Dieser, M.; Broemsen, E.L.J.E.; Cameron, K.A.; King, G.M.; Achberger, A.; Choquette, K.; Hagedorn, B.; Sletten, R.; Junge, K.; Christner, B.C. Molecular and biogeochemical

evidence for methane cycling beneath the western margin of the Greenland Ice Sheet. *ISME J.* **2014**, *8*, 2305–2316, doi:10.1038/ismej.2014.59.
53. Michaud, A.B.; Dore, J.E.; Achberger, A.M.; Christner, B.C.; Mitchell, A.C.; Skidmore, M.L.; Vick-Majors, T.J.; Priscu, J.C. Microbial oxidation as a methane sink beneath the West Antarctic Ice Sheet. *Nat. Geosci.* **2017**, *10*, 582–586, doi:10.1038/NGEO2992.
54. Arber, W. Genetic variation: Molecular mechanisms and impact on microbial evolution. *FEMS Microbiol. Rev.* **2000**, *24*, 1–7, doi:10.1111/j.1574-6976.2000.tb00529.x.
55. Palmer, M.; Venter, S.N.; Coetzee, M.P.A.; Steenkamp, E.T. Prokaryotic species are *sui generis* evolutionary units. *Syst. Appl. Microbiol.* **2019**, *42*, 145–158, doi:10.1016/j.syapm.2018.10.002.
56. Bapteste, E.; Burian, R.M. On the need for integrative phylogenomics, and some steps toward its creation. *Biol. Philos.* **2010**, *25*, 711–736, doi:10.1007/s10539-010-9218-2.
57. Chistoserdova, L.; Vorholt, J.A.; Thauer, R.K.; Lidstrom, M.E. C1 Transfer Enzymes and Coenzymes Linking Methylotrophic Bacteria and Methanogenic Archaea. *Science (80-.).* **1998**, *281*, 99–102, doi:10.1126/science.281.5373.99.
58. Wiedenbeck, J.; Cohan, F.M. Origins of bacterial diversity through horizontal genetic transfer and adaptation to new ecological niches. *FEMS Microbiol. Rev.* **2011**, *35*, 957–976, doi:10.1111/j.1574-6976.2011.00292.x.
59. De Mazancourt, C.; Johnson, E.; Barraclough, T.G. Biodiversity inhibits species' evolutionary responses to changing environments. *Ecol. Lett.* **2008**, *11*, 380–388, doi:10.1111/j.1461-0248.2008.01152.x.
60. Mayr, M.J.; Zimmermann, M.; Guggenheim, C.; Brand, A.; Bürgmann, H. Niche partitioning of methane-oxidizing bacteria along the oxygen-methane counter gradient of stratified lakes. *ISME J.* **2020**, *14*, 274–287, doi:10.1038/s41396-019-0515-8.
61. Gulledge, J.; Schimel, J.P. Moisture control over atmospheric CH_4 consumption and CO_2 production in diverse Alaskan soils. *Soil Biol. Biochem.* **1998**, *30*, 1127–1132, doi:10.1111/j.1574-6941.2001.tb00778.x.
62. Christiansen, J.R.; Gundersen, P.; Frederiksen, P.; Vesterdal, L. Influence of hydromorphic soil conditions on greenhouse gas emissions and soil carbon stocks in a Danish temperate forest. *For. Ecol. Manage.* **2012**, *284*, 185–195, doi:10.1016/j.foreco.2012.07.048.
63. Christiansen, J.R.; Levy-Booth, D.; Prescott, C.E.; Grayston, S.J. Different soil moisture control of net methane oxidation and production in organic upland and wet forest soils of the Pacific coastal rainforest in Canada. *Can. J. For. Res.* **2017**, *47*, 628–635, doi:10.1139/cjfr-2016-0390.
64. Olefeldt, D.; Turetsky, M.R.; Crill, P.M.; Mcguire, A.D. Environmental and physical controls on northern terrestrial methane emissions across permafrost zones. *Glob. Chang. Biol.* **2013**, *19*, 589–603, doi:10.1111/gcb.12071.
65. Mastepanov, M.; Sigsgaard, C.; Tagesson, T.; Ström, L.; Tamstorf, M.P.; Lund, M.; Christensen, T.R. Revisiting factors controlling methane emissions from high-Arctic tundra. *Biogeosciences* **2013**, *10*, 5139–5158, doi:10.5194/bg-10-5139-2013.
66. Ma, K.; Conrad, R.; Lu, Y. Dry/wet cycles change the activity and population dynamics of methanotrophs in rice field soil. *Appl. Environ. Microbiol.* **2013**, *79*, 4932–4939, doi:10.1128/AEM.00850-13.
67. Henckel, T.; Jäckel, U.; Conrad, R. Vertical distribution of the methanotrophic community after drainage of rice field soil. *FEMS Microbiol. Ecol.* **2001**, *34*, 279–291, doi:10.1016/S0168-6496(00)00105-7.
68. Kravchenko, I.; Kizilova, A.; Menko, E.; Sirin, A. Methane Cycling Microbial Communities in Natural and Drained Sites of Taldom Peatland, Moscow Region, Russia. *Annu. Res. Rev. Biol.* **2015**, *6*, 121–132, doi:10.9734/arrb/2015/14978.
69. Danilova, O. V.; Suzina, N.E.; Van De Kamp, J.; Svenning, M.M.; Bodrossy, L.; Dedysh, S.N. A new cell morphotype among methane oxidizers: A spiral-shaped obligately microaerophilic methanotroph from northern low-oxygen environments. *ISME J.* **2016**, *10*, 2734–2743, doi:10.1038/ismej.2016.48.
70. Van Bodegom, P.; Stams, F.; Mollema, L.; Boeke, S.; Leffelaar, P. Methane Oxidation and the Competition for Oxygen in the Rice Rhizosphere. *Appl. Environ. Microbiol.* **2001**, *67*, 3586–3597, doi:10.1128/AEM.67.8.3586-3597.2001.
71. Kits, K.D.; Klotz, M.G.; Stein, L.Y. Methane oxidation coupled to nitrate reduction under

hypoxia by the Gammaproteobacterium *Methylomonas denitrificans*, sp. nov. type strain FJG1. *Environ. Microbiol.* **2015**, *17*, 3219–3232, doi:10.1111/1462-2920.12772.
72. Segers, R. Methane production and methane consumption: A review of processes underlying wetland methane fluxes. *Biogeochemistry* **1998**, *41*, 23–51, doi:10.1023/A:1005929032764.
73. Raghoebarsing, A.A.; Smolders, A.J.P.; Schmid, M.C.; Rijpstra, W.I.C.; Wolters-Arts, M.; Derksen, J.; Jetten, M.S.M.; Schouten, S.; Damsté, J.S.S.; Lamers, L.P.M.; et al. Methanotrophic symbionts provide carbon for photosynthesis in peat bogs. *Nature* **2005**, *436*, 1153–1156, doi:10.1038/nature03802.
74. Denier Van Der Gon, H.A.C.; Neue, H.U. Oxidation of methane in the rhizosphere of rice plants. *Biol. Fertil. Soils* **1996**, *22*, 359–366, doi:10.1007/BF00334584.
75. Fritz, C.; Pancotto, V.A.; Elzenga, J.T.M.; Visser, E.J.W.; Grootjans, A.P.; Pol, A.; Iturraspe, R.; Roelofs, J.G.M.; Smolders, A.J.P. Zero methane emission bogs: Extreme rhizosphere oxygenation by cushion plants in Patagonia. *New Phytol.* **2011**, *190*, 398–408, doi:10.1111/j.1469-8137.2010.03604.x.
76. Baani, M.; Liesack, W. Two isozymes of particulate methane monooxygenase with different methane oxidation kinetics are found in *Methylocystis* sp. strain SC2. *Proc. Natl. Acad. Sci. U. S. A.* **2008**, *105*, 10203–10208, doi:10.1073/pnas.0702643105.
77. Steenbergh, A.K.; Meima, M.M.; Kamst, M.; Bodelier, P.L.E. Biphasic kinetics of a methanotrophic community is a combination of growth and increased activity per cell. *FEMS Microbiol. Ecol.* **2010**, *71*, 12–22, doi:10.1111/j.1574-6941.2009.00782.x.
78. Cai, Z.; Yan, X. Kinetic model for methane oxidation by paddy soil as affected by temperature, moisture and N addition.pdf. **1999**, *31*, 715–725, doi:10.1016/S0038-0717(98)00170-9.
79. Singleton, C.M.; McCalley, C.K.; Woodcroft, B.J.; Boyd, J.A.; Evans, P.N.; Hodgkins, S.B.; Chanton, J.P.; Frolking, S.; Crill, P.M.; Saleska, S.R.; et al. Methanotrophy across a natural permafrost thaw environment. *ISME J.* **2018**, *12*, 2544–2558, doi:10.1038/s41396-018-0065-5.
80. Cai, Y.; Zheng, Y.; Bodelier, P.L.E.; Conrad, R.; Jia, Z. Conventional methanotrophs are responsible for atmospheric methane oxidation in paddy soils. *Nat. Commun.* **2016**, *7*, 1–10, doi:10.1038/ncomms11728.
81. Biderre-Petit, C.; Jézéquel, D.; Dugat-Bony, E.; Lopes, F.; Kuever, J.; Borrel, G.; Viollier, E.; Fonty, G.; Peyret, P. Identification of microbial communities involved in the methane cycle of a freshwater meromictic lake. *FEMS Microbiol. Ecol.* **2011**, *77*, 533–545, doi:10.1111/j.1574-6941.2011.01134.x.
82. Yang, Y.; Tong, T.; Chen, J.; Liu, Y.; Xie, S. Ammonium Impacts Methane Oxidation and Methanotrophic Community in Freshwater Sediment. *Front. Bioeng. Biotechnol.* **2020**, *8*, 1–11, doi:10.3389/fbioe.2020.00250.
83. Yang, Y.; Zhao, Q.; Cui, Y.; Wang, Y.; Xie, S.; Liu, Y. Spatio-temporal Variation of Sediment Methanotrophic Microorganisms in a Large Eutrophic Lake. *Microb. Ecol.* **2016**, *71*, 9–17, doi:10.1007/s00248-015-0667-7.
84. Zhang, X.; Kong, J.Y.; Xia, F.F.; Su, Y.; He, R. Effects of ammonium on the activity and community of methanotrophs in landfill biocover soils. *Syst. Appl. Microbiol.* **2014**, *37*, 296–304, doi:10.1016/j.syapm.2014.03.003.
85. Murase, J.; Sugimoto, A. Inhibitory effect of light on methane oxidation in the pelagic water column of a mesotrophic lake (Lake Biwa, Japan). *Limnol. Oceanogr.* **2005**, *50*, 1339–1343, doi:10.4319/lo.2005.50.4.1339.
86. Shrestha, M.; Shrestha, P.M.; Frenzel, P.; Conrad, R. Effect of nitrogen fertilization on methane oxidation, abundance, community structure, and gene expression of methanotrophs in the rice rhizosphere. *ISME J.* **2010**, *4*, 1545–1556, doi:10.1038/ismej.2010.89.
87. Bedard, C.; Knowles, R. Physiology, Biochemistry, and Specific Inhibitors of CH_4, NH_4, and CO Oxidation by Methanotrophs and Nitrifiers. *Microbiol. Rev.* **1989**, *53*, 68–84, doi:10.1128/mr.53.1.68-84.1989.
88. Bodelier, P.L.E.; Laanbroek, H.J. Nitrogen as a regulatory factor of methane oxidation in soils and sediments. *FEMS Microbiol. Ecol.* **2004**, *47*, 265–277, doi:10.1016/S0168-6496(03)00304-0.
89. Auman, A.J.; Speake, C.C.; Lidstrom, M.E. *nifH* Sequences and Nitrogen Fixation in Type I and Type II Methanotrophs. *Appl. Environ. Microbiol.* **2001**, *67*, 4009–4016,

doi:10.1128/AEM.67.9.4009-4016.2001.
90. Mäkipää, R.; Leppänen, S.M.; Sanz Munoz, S.; Smolander, A.; Tiirola, M.; Tuomivirta, T.; Fritze, H. Methanotrophs are core members of the diazotroph community in decaying Norway spruce logs. *Soil Biol. Biochem.* **2018**, *120*, 230–232, doi:10.1016/j.soilbio.2018.02.012.
91. Kox, M.A.R.; Aalto, S.L.; Penttilä, T.; Ettwig, K.F.; Jetten, M.S.M.; van Kessel, M.A.H.J. The influence of oxygen and methane on nitrogen fixation in subarctic *Sphagnum* mosses. *AMB Express* **2018**, *8*, doi:10.1186/s13568-018-0607-2.
92. Kallistova, A.Y.; Montonen, L.; Jurgens, G.; Münster, U.; Kevbrina, M. V.; Nozhevnikova, A.N. Culturable psychrotolerant methanotrophic bacteria in landfill cover soil. *Microbiology* **2013**, *82*, 847–855, doi:10.1134/S0026261714010044.
93. Einola, J.K.M.; Kettunen, R.H.; Rintala, J.A. Responses of methane oxidation to temperature and water content in cover soil of a boreal landfill. *Soil Biol. Biochem.* **2007**, *39*, 1156–1164, doi:10.1016/j.soilbio.2006.12.022.
94. Takeuchi, M.; Kamagata, Y.; Oshima, K.; Hanada, S.; Tamaki, H.; Marumo, K.; Maeda, H.; Nedachi, M.; Hattori, M.; Iwasaki, W.; et al. *Methylocaldum marinum* sp. nov., A thermotolerant, Methane-oxidizing bacterium isolated from marine sediments, And emended description of the genus *Methylocaldum*. *Int. J. Syst. Evol. Microbiol.* **2014**, *64*, 3240–3246, doi:10.1099/ijs.0.063503-0.
95. Börjesson, G.; Sundh, I.; Svensson, B. Microbial oxidation of CH_4 at different temperatures in landfill cover soils. *FEMS Microbiol. Ecol.* **2004**, *48*, 305–312, doi:10.1016/j.femsec.2004.02.006.
96. Ho, A.; Frenzel, P. Heat stress and methane-oxidizing bacteria: Effects on activity and population dynamics. *Soil Biol. Biochem.* **2012**, *50*, 22–25, doi:10.1016/j.soilbio.2012.02.023.
97. Knoblauch, C.; Zimmermann, U.; Blumenberg, M.; Michaelis, W.; Pfeiffer, E.M. Methane turnover and temperature response of methane-oxidizing bacteria in permafrost-affected soils of northeast Siberia. *Soil Biol. Biochem.* **2008**, *40*, 3004–3013, doi:10.1016/j.soilbio.2008.08.020.
98. King, G.M.; Adamsen, A.P.S. Effects of temperature on methane consumption in a forest soil and in pure cultures of the methanotroph *Methylomonas rubra*. *Appl. Environ. Microbiol.* **1992**, *58*, 2758–2763, doi:10.1128/aem.58.9.2758-2763.1992.
99. Zheng, J.; RoyChowdhury, T.; Yang, Z.; Gu, B.; Wullschleger, S.D.; Graham, D.E. Impacts of temperature and soil characteristics on methane production and oxidation in Arctic tundra. *Biogeosciences* **2018**, *15*, 6621–6635, doi:10.5194/bg-15-6621-2018.
100. Kevbrina, M. V.; Okhapkina, A.A.; Akhlynin, D.S.; Kravchenko, I.K.; Nozhevnikova, A.N.; Gal'chenko, V.F. Growth of mesophilic methanotrophs at low temperatures. *Microbiology* **2001**, *70*, 384–391, doi:10.1023/A:1010417724037.
101. van Breemen, N.; Mulder, J.; Driscoll, C.T. Acidification and alkalinization of soils. *Plant Soil* **1983**, *75*, 283–308, doi:10.1007/BF02369968.
102. Slessarev, E.W.; Lin, Y.; Bingham, N.L.; Johnson, J.E.; Dai, Y.; Schimel, J.P.; Chadwick, O.A. Water balance creates a threshold in soil pH at the global scale. *Nature* **2016**, *540*, 567–569, doi:10.1038/nature20139.
103. Tveit, A.T.; Kiss, A.; Winkel, M.; Horn, F.; Hájek, T.; Svenning, M.M.; Wagner, D.; Liebner, S. Environmental patterns of brown moss- and *Sphagnum*-associated microbial communities. *Sci. Rep.* **2020**, *10*, 1–16, doi:10.1038/s41598-020-79773-2.
104. Dedysh, S.N. Exploring methanotroph diversity in acidic northern wetlands: Molecular and cultivation-based studies. *Microbiology* **2009**, *78*, 655–669, doi:10.1134/S0026261709060010.
105. Gupta, V.; Smemo, K.A.; Yavitt, J.B.; Basiliko, N. Active Methanotrophs in Two Contrasting North American Peatland Ecosystems Revealed Using DNA-SIP. *Microb. Ecol.* **2012**, *63*, 438–445, doi:10.1007/s00248-011-9902-z.
106. Qiu, Q.; Noll, M.; Abraham, W.R.; Lu, Y.; Conrad, R. Applying stable isotope probing of phospholipid fatty acids and rRNA in a Chinese rice field to study activity and composition of the methanotrophic bacterial communities *in situ*. *ISME J.* **2008**, *2*, 602–614, doi:10.1038/ismej.2008.34.
107. Zhao, J.; Cai, Y.; Jia, Z. The pH-based ecological coherence of active canonical

methanotrophs in paddy soils. *Biogeosciences* **2020**, *17*, 1451–1462, doi:10.5194/bg-17-1451-2020.
108. Reed, C.J.; Lewis, H.; Trejo, E.; Winston, V.; Evilia, C. Protein adaptations in archaeal extremophiles. *Archaea* **2013**, *2013*, 1–14, doi:10.1155/2013/373275.
109. Napolitano, M.J.; Shain, D.H. Distinctions in adenylate metabolism among organisms inhabiting temperature extremes. *Extremophiles* **2005**, *9*, 93–98, doi:10.1007/s00792-004-0424-1.
110. Amato, P.; Christner, B.C. Energy metabolism response to low-temperature and frozen conditions in *Psychrobacter cryohalolentis*. *Appl. Environ. Microbiol.* **2009**, *75*, 711–718, doi:10.1128/AEM.02193-08.
111. Wiebe, W.J.; Sheldon, W.M.; Pomeroy, L.R. Bacterial growth in the cold: Evidence for an enhanced substrate requirement. *Appl. Environ. Microbiol.* **1992**, *58*, 359–364, doi:10.1128/aem.58.1.359-364.1992.
112. Nedwell, D.B. Effect of low temperature on microbial growth: Lowered affinity for substrates limits growth at low temperature. *FEMS Microbiol. Ecol.* **1999**, *30*, 101–111, doi:10.1111/j.1574-6941.1999.tb00639.x.
113. Struvay, C.; Feller, G. Optimization to low temperature activity in psychrophilic enzymes. *Int. J. Mol. Sci.* **2012**, *13*, 11643–11665, doi:10.3390/ijms130911643.
114. Bajerski, F.; Wagner, D.; Mangelsdorf, K. Cell membrane fatty acid composition of Chryseobacterium frigidisoli PB4^{T}, isolated from antarctic glacier forefield soils, in response to changing temperature and pH conditions. *Front. Microbiol.* **2017**, *8*, 1–11, doi:10.3389/fmicb.2017.00677.
115. Suutari, M.; Laakso, S. Microbial fatty acids and thermal adaptation. *Crit. Rev. Microbiol.* **1994**, *20*, 285–328, doi:10.3109/10408419409113560.
116. Hassan, N.; Anesio, A.M.; Rafiq, M.; Holtvoeth, J.; Bull, I.; Haleem, A.; Shah, A.A.; Hasan, F. Temperature Driven Membrane Lipid Adaptation in Glacial Psychrophilic Bacteria. *Front. Microbiol.* **2020**, *11*, 1–10, doi:10.3389/fmicb.2020.00824.
117. Roncarati, D.; Scarlato, V. Regulation of heat-shock genes in bacteria: from signal sensing to gene expression output. *FEMS Microbiol. Rev.* **2017**, *41*, 549–574, doi:10.1093/femsre/fux015.
118. Zhang, Y.; Burkhardt, D.H.; Rouskin, S.; Li, G.W.; Weissman, J.S.; Gross, C.A. A Stress Response that Monitors and Regulates mRNA Structure Is Central to Cold Shock Adaptation. *Mol. Cell* **2018**, *70*, 274–286, doi:10.1016/j.molcel.2018.02.035.
119. Cairrão, F.; Cruz, A.; Mori, H.; Arraiano, C.M. Cold shock induction of RNase R and its role in the maturation of the quality control mediator SsrA/tmRNA. *Mol. Microbiol.* **2003**, *50*, 1349–1360, doi:10.1046/j.1365-2958.2003.03766.x.
120. Hébraud, M.; Potier, P. Cold shock response and low temperature adaptation in psychrotrophic bacteria. *J. Mol. Microbiol. Biotechnol.* **1999**, *1*, 211–219.
121. D'Amico, S.; Collins, T.; Marx, J.C.; Feller, G.; Gerday, C. Psychrophilic microorganisms: Challenges for life. *EMBO Rep.* **2006**, *7*, 385–389, doi:10.1038/sj.embor.7400662.
122. Thieringer, H.A.; Jones, P.G.; Inouye, M. Cold shock and adaptation. *BioEssays* **1998**, *20*, 49–57, doi:10.1002/(SICI)1521-1878(199801)20:1<49::AID-BIES8>3.0.CO;2-N.
123. Hu, X.P.; Dourado, H.; Schubert, P.; Lercher, M.J. The protein translation machinery is expressed for maximal efficiency in *Escherichia coli*. *Nat. Commun.* **2020**, *11*, 1–10, doi:10.1038/s41467-020-18948-x.
124. Mairet, F.; Gouzé, J.L.; de Jong, H. Optimal proteome allocation and the temperature dependence of microbial growth laws. *NPJ Syst. Biol. Appl.* **2021**, *7*, 14, doi:10.1038/s41540-021-00172-y.
125. Bosdriesz, E.; Molenaar, D.; Teusink, B.; Bruggeman, F.J. How fast-growing bacteria robustly tune their ribosome concentration to approximate growth-rate maximization. *FEBS J.* **2015**, *282*, 2029–2044, doi:10.1111/febs.13258.
126. Angers, D.; Caron, J. Plant-Induced Changes in Soil Structure: Processes and Feedbacks. *Biogeochemistry* **1998**, *42*, 55–72, doi:10.1023/A:1005944025343.
127. Ward, S.E.; Ostle, N.J.; Oakley, S.; Quirk, H.; Henrys, P.A.; Bardgett, R.D. Warming effects on greenhouse gas fluxes in peatlands are modulated by vegetation composition. *Ecol. Lett.* **2013**, *16*, 1285–1293, doi:10.1111/ele.12167.
128. Epstein, H.E.; Raynolds, M.K.; Walker, D.A.; Bhatt, U.S.; Tucker, C.J.; Pinzon, J.E.

Dynamics of aboveground phytomass of the circumpolar Arctic tundra during the past three decades. *Environ. Res. Lett.* **2012**, *7*, doi:10.1088/1748-9326/7/1/015506.
129. Parker, T.C.; Thurston, A.M.; Raundrup, K.; Subke, J.A.; Wookey, P.A.; Hartley, I.P. Shrub expansion in the Arctic may induce large-scale carbon losses due to changes in plant-soil interactions. *Plant Soil* **2021**, *463*, 643–651, doi:10.1007/s11104-021-04919-8.
130. Huang, Y.; Ciais, P.; Luo, Y.; Zhu, D.; Wang, Y.; Qiu, C.; Goll, D.S.; Guenet, B.; Makowski, D.; De Graaf, I.; et al. Tradeoff of CO_2 and CH_4 emissions from global peatlands under water-table drawdown. *Nat. Clim. Chang.* **2021**, *11*, 618–622, doi:10.1038/s41558-021-01059-w.
131. Johansson, T.; Malmer, N.; Crill, P.M.; Friborg, T.; Åkerman, J.H.; Mastepanov, M.; Christensen, T.R. Decadal vegetation changes in a northern peatland, greenhouse gas fluxes and net radiative forcing. *Glob. Chang. Biol.* **2006**, *12*, 2352–2369, doi:10.1111/j.1365-2486.2006.01267.x.
132. Cahoon, S.M.P.; Sullivan, P.F.; Post, E.; Welker, J.M. Large herbivores limit CO_2 uptake and suppress carbon cycle responses to warming in West Greenland. *Glob. Chang. Biol.* **2012**, *18*, 469–479, doi:10.1111/j.1365-2486.2011.02528.x.
133. Falk, J.M.; Schmidt, N.M.; Christensen, T.R.; Ström, L. Large herbivore grazing affects the vegetation structure and greenhouse gas balance in a high Arctic mire. *Environ. Res. Lett.* **2015**, *10*, 045001, doi:10.1088/1748-9326/10/4/045001.
134. Sjögersten, S.; van der Wal, R.; Loonen, M.J.J.E.; Woodin, S.J. Recovery of ecosystem carbon fluxes and storage from herbivory. *Biogeochemistry* **2011**, *106*, 357–370, doi:10.1007/s10533-010-9516-4.
135. Gallego-Sala, A. V.; Colin Prentice, I. Blanket peat biome endangered by climate change. *Nat. Clim. Chang.* **2013**, *3*, 152–155, doi:10.1038/nclimate1672.
136. Walker, M.D.; Wahren, C.H.; Hollister, R.D.; Henry, G.H.R.; Ahlquist, L.E.; Alatalo, J.M.; Bret-Harte, M.S.; Calef, M.P.; Callaghan, T. V.; Carroll, A.B.; et al. Plant community responses to experimental warming across the tundra biome. *Proc. Natl. Acad. Sci. U. S. A.* **2006**, *103*, 1342–1346, doi:10.1073/pnas.0503198103.
137. van Der Wal, R.; Sjögersten, S.; Woodin, S.J.; Cooper, E.J.; Jónsdóttir, I.S.; Kuijper, D.; Fox, T.A.D.; Huiskes, A.D. Spring feeding by pink-footed geese reduces carbon stocks and sink strength in tundra ecosystems. *Glob. Chang. Biol.* **2007**, *13*, 539–545, doi:10.1111/j.1365-2486.2006.01310.x.
138. Roesch, A.; Weisskopf, P.; Oberholzer, H.; Valsangiacomo, A.; Nemecek, T. An approach for describing the effects of grazing on soil quality in life-cycle assessment. *Sustain.* **2019**, *11*, doi:10.3390/su11184870.
139. Drewry, J.J.; Cameron, K.C.; Buchan, G.D. Pasture yield and soil physical property responses to soil compaction from treading and grazing - A review. *Aust. J. Soil Res.* **2008**, *46*, 237–256, doi:10.1071/SR07125.
140. Pascual, J.; Alberti, J.; Daleo, P.; Iribarne, O. Herbivory and trampling by small mammals modify soil properties and plant assemblages. *J. Veg. Sci.* **2017**, *28*, 1028–1035, doi:10.1111/ivs.12562.
141. Speed, J.D.M.; Woodin, S.J.; Tømmervik, H.; van der Wal, R. Extrapolating herbivore-induced carbon loss across an arctic landscape. *Polar Biol.* **2010**, *33*, 789–797, doi:10.1007/s00300-009-0756-5.
142. Bertin, C.; Yang, X.; Weston, L.A. The role of root exudates and allelochemicals in the rhizosphere. *Plant Soil* **2003**, *256*, 67–83, doi:10.1023/A:1026290508166.
143. Bais, H.P.; Weir, T.L.; Perry, L.G.; Gilroy, S.; Vivanco, J.M. The role of root exudates in rhizosphere interactions with plants and other organisms. *Annu. Rev. Plant Biol.* **2006**, *57*, 233–266, doi:10.1146/annurev.arplant.57.032905.105159.
144. Bender, K.M.; Svenning, M.M.; Hu, Y.; Richter, A.; Schückel, J.; Jørgensen, B.; Liebner, S.; Tveit, A.T. Microbial responses to herbivory-induced vegetation changes in a high-Arctic peatland. *Polar Biol.* **2021**, *44*, 899–911, doi:10.1007/s00300-021-02846-z.
145. Olofsson, J.; Post, E. Effects of large herbivores on tundra vegetation in a changing climate, and implications for rewilding. *Philos. Trans. R. Soc. B Biol. Sci.* **2018**, *373*, doi:10.1098/rstb.2017.0437.
146. Myers-Smith, I.H.; Elmendorf, S.C.; Beck, P.S.A.; Wilmking, M.; Hallinger, M.; Blok, D.; Tape, K.D.; Rayback, S.A.; Macias-Fauria, M.; Forbes, B.C.; et al. Climate sensitivity of

shrub growth across the tundra biome. *Nat. Clim. Chang.* **2015**, *5*, 887–891, doi:10.1038/nclimate2697.
147. Jia, G.J.; Epstein, H.E.; Walker, D.A. Vegetation greening in the canadian arctic related to decadal warming. *J. Environ. Monit.* **2009**, *11*, 2231–2238, doi:10.1039/b911677j.
148. Olofsson, J.; Oksanen, L.; Callaghan, T.; Hulme, P.E.; Oksanen, T.; Suominen, O. Herbivores inhibit climate-driven shrub expansion on the tundra. *Glob. Chang. Biol.* **2009**, *15*, 2681–2693, doi:10.1111/j.1365-2486.2009.01935.x.
149. Christie, K.S.; Bryant, J.P.; Gough, L.; Ravolainen, V.T.; Ruess, R.W.; Tape, K.D. The Role of Vertebrate Herbivores in Regulating Shrub Expansion in the Arctic: A Synthesis. *Bioscience* **2015**, *65*, 1123–1133, doi:10.1093/biosci/biv137.
150. Post, E.; Forchhammer, M.C. Climate change reduces reproductive success of an Arctic herbivore through trophic mismatch. *Philos. Trans. R. Soc. B Biol. Sci.* **2008**, *363*, 2369–2375, doi:10.1098/rstb.2007.2207.
151. Stien, A.; Ims, R.A.; Albon, S.D.; Fuglei, E.; Irvine, R.J.; Ropstad, E.; Halvorsen, O.; Langvatn, R.; Loe, L.E.; Veiberg, V.; et al. Congruent responses to weather variability in high Arctic herbivores. *Biol. Lett.* **2012**, *8*, 1002–1005, doi:10.1098/rsbl.2012.0764.
152. Hansen, B.B.; Gamelon, M.; Albon, S.D.; Lee, A.M.; Stien, A.; Irvine, R.J.; Sæther, B.E.; Loe, L.E.; Ropstad, E.; Veiberg, V.; et al. More frequent extreme climate events stabilize reindeer population dynamics. *Nat. Commun.* **2019**, *10*, 1–8, doi:10.1038/s41467-019-09332-5.
153. Hessen, D.O.; Tombre, I.M.; van Geest, G.; Alfsnes, K. Global change and ecosystem connectivity: How geese link fields of central Europe to eutrophication of Arctic freshwaters. *Ambio* **2017**, *46*, 40–47, doi:10.1007/s13280-016-0802-9.
154. Kuijper, D.P.J.; Bakker, J.P.; Cooper, E.J.; Ubels, R.; Jónsdóttir, I.S.; Loonen, M.J.J.E. Intensive grazing by Barnacle geese depletes High Arctic seed bank. *Can. J. Bot.* **2006**, *84*, 995–1004, doi:10.1139/B06-052.
155. Jefferies, R.L.; Rockwell, R.F. Foraging geese, vegetation loss and soil degradation in an Arctic salt marsh. *Appl. Veg. Sci.* **2002**, *5*, 7–16, doi:10.1111/j.1654-109X.2002.tb00531.x.
156. Handa, I.T.; Harmsen, R.; Jefferies, R.L. Patterns of vegetation change and the recovery potential of degraded areas in a coastal marsh system of the Hudson Bay lowlands. *J. Ecol.* **2002**, *90*, 86–99, doi:10.1046/j.0022-0477.2001.00635.x.
157. Layton-Matthews, K.; Hansen, B.B.; Grøtan, V.; Fuglei, E.; Loonen, M.J.J.E. Contrasting consequences of climate change for migratory geese: Predation, density dependence and carryover effects offset benefits of high-arctic warming. *Glob. Chang. Biol.* **2020**, *26*, 642–657, doi:10.1111/gcb.14773.
158. Küpfer, V. Biodiversity and activity of methane oxidizing bacteria associated with Arctic plants, Master's Thesis, UiT - The Arctic University of Norway, 2014.
159. Kelsey, K.C.; Leffler, A.J.; Beard, K.H.; Schmutz, J.A.; Choi, R.T.; Welker, J.M. Interactions among vegetation, climate, and herbivory control greenhouse gas fluxes in a subarctic coastal wetland. *J. Geophys. Res. Biogeosciences* **2016**, *121*, 2960–2975, doi:10.1002/2016JG003546.
160. Sjögersten, S.; Van Der Wal, R.; Woodin, S.J. Habitat type determines herbivory controls over CO_2 fluxes in a warmer Arctic. *Ecology* **2008**, *89*, 2103–2116, doi:10.1890/07-1601.1.
161. van Grinsven, S.; Sinninghe Damsté, J.S.; Harrison, J.; Polerecky, L.; Villanueva, L. Nitrate promotes the transfer of methane-derived carbon from the methanotroph *Methylobacter* sp. to the methylotroph *Methylotenera* sp. in eutrophic lake water. *Limnol. Oceanogr.* **2020**, *66*, 1–14, doi:10.1002/lno.11648.
162. Abdalla, M.; Hastings, A.; Truu, J.; Espenberg, M.; Mander, Ü.; Smith, P. Emissions of methane from northern peatlands: a review of management impacts and implications for future management options. *Ecol. Evol.* **2016**, *6*, 7080–7102, doi:10.1002/ece3.2469.
163. Høj, L.; Olsen, R.A.; Torsvik, V.L. Archaeal communities in High Arctic wetlands at Spitsbergen, Norway (78°N) as characterized by 16S rRNA gene fingerprinting. *FEMS Microbiol. Ecol.* **2005**, *53*, 89–101, doi:10.1016/j.femsec.2005.01.004.
164. Liebner, S.; Schwarzenbach, S.P.; Zeyer, J. Methane emissions from an alpine fen in central Switzerland. *Biogeochemistry* **2012**, *109*, 287–299, doi:10.1007/s10533-011-9629-4.
165. Wen, X.; Yang, S.; Liebner, S. Evaluation and update of cutoff values for methanotrophic *pmoA* gene sequences. *Arch. Microbiol.* **2016**, *198*, 629–636, doi:10.1007/s00203-016-

1222-8.
166. Lüke, C.; Frenzel, P. Potential of *pmoA* Amplicon Pyrosequencing for Methanotroph Diversity Studies. **2011**, *77*, 6305–6309, doi:10.1128/AEM.05355-11.
167. Mahé, F.; Rognes, T.; Quince, C.; de Vargas, C.; Dunthorn, M. Swarm: robust and fast clustering method for amplicon-based studies. *PeerJ* **2014**, *2*, e593, doi:10.7717/peerj.593.
168. Oshkin, I.Y.; Beck, D.A.C.; Lamb, A.E.; Tchesnokova, V.; Benuska, G.; McTaggart, T.L.; Kalyuzhnaya, M.G.; Dedysh, S.N.; Lidstrom, M.E.; Chistoserdova, L. Methane-fed microbial microcosms show differential community dynamics and pinpoint taxa involved in communal response. *ISME J.* **2015**, *9*, 1119–1129, doi:10.1038/ismej.2014.203.
169. Kwon, M.; Ho, A.; Yoon, S. Novel approaches and reasons to isolate methanotrophic bacteria with biotechnological potentials: recent achievements and perspectives. *Appl. Microbiol. Biotechnol.* **2019**, *103*, 1–8, doi:10.1007/s00253-018-9435-1.
170. Whittenbury, R.; Philipps, K.C.; Wilkinson, J.F. Enrichment , Isolation and Some Properties of Methane-utilizing Bacteria. *J. Gen. Microbiol.* **1970**, *61*, 205–218, doi:10.1099/00221287-61-2-205.
171. Niemann, H.; Steinle, L.; Blees, J.; Bussmann, I.; Treude, T.; Krause, S.; Elvert, M.; Lehmann, M.F. Toxic effects of lab-grade butyl rubber stoppers on aerobic methane oxidation. *Limnol. Oceanogr. Methods* **2015**, *13*, 40–52, doi:10.1002/lom3.10005.
172. Aggerbeck, M.R.; Nielsen, T.K.; Mosbacher, J.B.; Schmidt, N.M.; Hansen, L.H. Muskoxen homogenise soil microbial communities and affect the abundance of methanogens and methanotrophs. *Sci. Total Environ.* **2022**, *827*, 153877, doi:10.1016/j.scitotenv.2022.153877.
173. Christensen, T.R.; Ekberg, A.; Ström, L.; Mastepanov, M.; Panikov, N.; Öquist, M.; Svensson, B.H.; Nykänen, H.; Martikainen, P.J.; Oskarsson, H. Factors controlling large scale variations in methane emissions from wetlands. *Geophys. Res. Lett.* **2003**, *30*, 1414, doi:10.1029/2002GL016848.
174. Abell, G.C.J.; Stralis-Pavese, N.; Sessitsch, A.; Bodrossy, L. Grazing affects methanotroph activity and diversity in an alpine meadow soil. *Environ. Microbiol. Rep.* **2009**, *1*, 457–465, doi:10.1111/j.1758-2229.2009.00078.x.
175. Ho, A.; Kerckhof, F.-M.; Lüke, C.; Reim, A.; Krause, S.; Boon, N.; Bodelier, P.L.E. Conceptualizing functional traits and ecological characteristics of methane-oxidizing bacteria as life strategies. *Environ. Microbiol. Rep.* **2013**, *5*, 335–345, doi:10.1111/j.1758-2229.2012.00370.x.
176. Siljanen, H.M.P.; Saari, A.; Bodrossy, L.; Martikainen, P.J. Seasonal variation in the function and diversity of methanotrophs in the littoral wetland of a boreal eutrophic lake. *FEMS Microbiol. Ecol.* **2012**, *80*, 548–555, doi:10.1111/j.1574-6941.2012.01321.x.
177. Wartiainen, I.; Hestnes, A.G.; McDonald, I.R.; Svenning, M.M. *Methylocystis rosea* sp. nov., a novel methanotrophic bacterium from Arctic wetland soil, Svalbard, Norway (78° N). *Int. J. Syst. Evol. Microbiol.* **2006**, *56*, 541–547, doi:10.1099/ijs.0.63912-0.
178. Blazewicz, S.J.; Barnard, R.L.; Daly, R.A.; Firestone, M.K. Evaluating rRNA as an indicator of microbial activity in environmental communities: Limitations and uses. *ISME J.* **2013**, *7*, 2061–2068, doi:10.1038/ismej.2013.102.
179. Matsumoto, Y.; Murakami, Y.; Tsuru, S.; Ying, B.W.; Yomo, T. Growth rate-coordinated transcriptome reorganization in bacteria. *BMC Genomics* **2013**, *14*, doi:10.1186/1471-2164-14-808.
180. Gadgil, M.; Kapur, V.; Hu, W.-S. Transcriptional response of *Escherichia coli* to Temperature. *Biotechnoloy Prog.* **2005**, *21*, 689–699, doi:10.1021/bp049630l.
181. Segarra, K.E.A.; Schubotz, F.; Samarkin, V.; Yoshinaga, M.Y.; Hinrichs, K.U.; Joye, S.B. High rates of anaerobic methane oxidation in freshwater wetlands reduce potential atmospheric methane emissions. *Nat. Commun.* **2015**, *6*, 1–8, doi:10.1038/ncomms8477.

Paper I

FEMS Microbiology Ecology, 96, 2020, fiaa140

doi: 10.1093/femsec/fiaa140
Advance Access Publication Date: 8 July 2020
Research Article

RESEARCH ARTICLE

Methanotroph populations and CH_4 oxidation potentials in high-Arctic peat are altered by herbivory induced vegetation change

Edda M. Rainer*, Christophe V. W. Seppey, Alexander T. Tveit and Mette M. Svenning

Department of Arctic and Marine Biology, UiT – The Arctic University of Norway, Tromsø, Norway

*Corresponding author: Biologibygget, Framstredet 39, 9019 Tromsø, Norway. Tel: +47 77623287/+47 90879768; E-mail: edda.m.rainer@uit.no

One sentence summary: Grazing in high-Arctic peatlands leads to soil ecosystem changes selecting for niche-adapted methanotrophs.

Editor: Max Haggblom

ABSTRACT

Methane oxidizing bacteria (methanotrophs) within the genus *Methylobacter* constitute the biological filter for methane (CH_4) in many Arctic soils. Multiple *Methylobacter* strains have been identified in these environments but we seldom know the ecological significance of the different strains. High-Arctic peatlands in Svalbard are heavily influenced by herbivory, leading to reduced vascular plant and root biomass. Here, we have measured potential CH_4 oxidation rates and identified the active methantrophs in grazed peat and peat protected from grazing by fencing (exclosures) for 18 years. Grazed peat sustained a higher water table, higher CH_4 concentrations and lower oxygen (O_2) concentrations than exclosed peat. Correspondingly, the highest CH_4 oxidation potentials were closer to the O_2 rich surface in the grazed than in the protected peat. A comparison of 16S rRNA genes showed that the majority of methanotrophs in both sites belong to the genus *Methylobacter*. Further analyses of *pmoA* transcripts revealed that several *Methylobacter* OTUs were active in the peat but that different OTUs dominated the grazed peat than the exclosed peat. We conclude that grazing influences soil conditions, the active CH_4 filter and that different *Methylobacter* populations are responsible for CH_4 oxidation depending on the environmental conditions.

Keywords: methane oxidation; *Methylobacter*; high-Arctic peatland soils; grazing pressure; active MOB community

INTRODUCTION

High-Arctic peatlands store large amounts of organic carbon that is a source for microbial production of the greenhouse gas methane (CH_4). As a result of climate change, these peatlands are exposed to increased temperatures, changes in precipitation, herbivory and vegetation composition that might lead to increased CH_4 production rates (Parish *et al.* 2008; Sjögersten *et al.* 2011). Methane oxidizing bacteria (MOB), or methanotrophs, act as the dominant biological CH_4 filter in peat soils, consuming CH_4 produced in deeper anaerobic peat before it is released to the atmosphere (Reay, Smith and Hewitt 2007). MOB are a diverse group of bacteria, found within the classes *Gammaproteobacteria, Alphaproteobacteria* and *Verrucomicrobia* (Hanson and Hanson 1996; Knief 2015). The abundances and distribution of most MOB can be assessed by quantification and analysis of the *pmoA* gene which encodes the β-subunit of the particulate CH_4 monooxygenase (McDonald *et al.* 2008; Knief 2015). A broad diversity of MOB has been identified using *pmoA*, making it possible to evaluate the habitat preferences of different MOB (Knief 2015). Many cold ecosystems with a neutral pH are found to be dominated by MOB within *Gammaproteobacteria* (Wartiainen, Hestnes and Svenning 2003; Börjesson, Sundh

Received: 23 March 2020; Accepted: 7 July 2020

and Svensson 2004; Wartiainen *et al.* 2006; Martineau, Whyte and Greer 2010; Graef *et al.* 2011). Among these, MOB within the genus *Methylobacter* are identified as the main CH_4 oxidizers in many freshwater wetlands (Yun *et al.* 2010; Tveit *et al.* 2013; Singleton *et al.* 2018; Smith *et al.* 2018; Zhang *et al.* 2019). Members of this group and other gammaproteobacterial MOB were also found in association with *Sphagnum sp.* mosses and vascular plants in a temperate peatland with their composition and activities being directly related to the plant biodiversity (Stępniewska *et al.* 2018). Methanotroph communities and their activities are known to be influenced by CH_4 concentration, pH, O_2 concentration, temperature, nitrogen concentration and copper availability (Amaral and Knowles 1995; Semrau, DiSpirito and Yoon 2010; Ho *et al.* 2013). It has been suggested that O_2 distribution plays a crucial role and may explain niche-adaptation in freshwater lakes (Biderre-Petit *et al.* 2011; Blees *et al.* 2014; Oshkin *et al.* 2015; Mayr *et al.* 2020) and flooded paddy soils (Reim *et al.* 2012). However, the ecology of large OTU numbers within e.g. *Methylobacter* and other gammaproteobacterial MOB (Tsutsumi *et al.* 2011; He *et al.* 2012; Beck *et al.* 2013; Oshkin *et al.* 2014; Knief 2015; Oswald *et al.* 2015; Bornemann *et al.* 2016), is mostly unknown. As a result, it is still difficult to explain the co-existence of many closely related OTUs within a defined ecosystem.

Grazing by geese and reindeer reduces the biomass of grasses and herbs. Warmer winters in temperate regions, increased food availability due to changes in agriculture and protection from hunting has led to an increase in the total geese population (Hessen *et al.* 2017). In Solvatn (Ny Ålesund, Svalbard, Northern Norway) experimental peat plots protected from geese herbivory by fences doubled the vegetation over the course of nine years, leading to increased peatland carbon uptake (Sjögersten *et al.* 2011). During peat formation, the plant cover and its roots influence the physical properties of the soil such as porosity and pore direction (Kruse, Lennartz and Leinweber 2008). In addition, root exudates stimulate microbial communities within the soil and the exudates from different plant types (Bardgett *et al.* 2013), potentially create niches for different microorganisms. Thus, herbivory or its absence, may have a substantial effect on the soil structure, biology and chemistry.

Solvatn and adjacent peatlands close to Ny-Ålesund have been studied thoroughly during the last 15 years with emphasis on the CH_4 cycle, showing that substantial potentials for CH_4 production and oxidation exist in these soils (Høj, Olsen and Torsvik 2005; Graef *et al.* 2011; Tveit *et al.* 2013, 2015). However, the effect of changes in herbivory on the CH_4 cycles were not studied. Here, in a comparison of 18-year old exclosures (Sjögersten *et al.* 2011) and nearby grazed sites, we have addressed how the microbial CH_4 filter is affected by intensive herbivore grazing over years. Specifically, we investigated the relationship between altered soil properties, potential CH_4 oxidation rates and the active methanotroph communities by 16S rRNA gene and *pmoA* transcript amplicon analyses.

MATERIALS AND METHODS

Field site and sampling

The Solvatn peatland (N78°55.550, E11°56.611) is located close to Ny Ålesund, Svalbard. It is heavily grazed by Barnacle geese (*Branta leucopsis*) and is dominated by brown mosses, primarily *Calliergon richardsonii* (Solheim, Endal and Vigstad 1996). Exclosures established in 1998 protect parts of the peatland vegetation from geese grazing (Sjögersten *et al.* 2011) allowing growth of vascular plants that are otherwise suppressed by grazing (Fig. 1). Two sampling sites from the Solvatn peatland were selected (SV1 and SV2), both of which were used by Sjögersten *et al.* (2011). Each site includes an exclosed plot and an adjacent grazed plot. Two field campaigns were conducted in summer, during the active growing season (August 2015 and 2016), while one field campaign was conducted immediately after snowmelt (June 2016). Below, we refer to these time points as summer 2015, spring 2016 and summer 2016.

In each plot, two blocks (approx. 30 × 30 × 20 cm) were cut from the peat soil and kept cool throughout transportation to the on-site laboratory, approximately 600 m away from the field site. Each block was separated in three vertical sections designated A, B and C (approx. 30 × 10 × 20 cm).

Section A was frozen at −20 °C and transported to the laboratory at UiT, The Arctic University of Norway, where it was used for the determination of water content and soil organic matter (SOM).

Section B and C were then divided in seven horizontal layers (0.5–8 cm for the upper six layers, 8–12 cm for the lowest layer), which served as material for the further analyses. The top layers (soil surface) of all plots were composed only of plants, whereas the layers two to seven were composed of partly decomposed peat. In the exclosed plots, the top 2–3 cm below the vegetation was a mixture of roots and peat soil. In the grazed plots, few or no living roots were observed.

Section B layers were used to measure CH_4 oxidation potentials *ex situ* (see next section). At the end of these measurements, peat samples from each microcosm were collected in 15 ml plastic tubes (VWR High-Performance polypropylene centrifuge tubes), flash frozen in liquid nitrogen (N_2) and stored at −80 °C.

Section C layers were transferred to sterile 15 ml plastic tubes (VWR High-Performance polypropylene centrifuge tubes), flash frozen in liquid N_2 immediately after arrival on the on-site laboratory and stored at −80 °C.

All soil samples from section B and C were shipped to the laboratory at UiT, the Arctic University of Norway, and stored at −80 °C until further processing. An overview of the sampling design and the respective analyses for each sampling is provided in Table S1 (Supporting Information).

Environmental characterization

Prior to soil water content and SOM analysis, section A from each sampling campaign was thawed in a cold room (8 °C) and separated into horizontal layers as described for sections B and C. Soil water content was determined gravimetrically by drying 10 g of peat at 150 °C over night. The dried peat soil was then incinerated at 450 °C and the amount of burnt peat matter was determined gravimetrically to deduce the amount of SOM.

O_2 concentration and temperature were measured *in situ*, using an optical O_2 sensor and thermometer (Fibox 4 Optode, Presens, Germany). Measurements were taken at the soil surface and at 5 cm intervals down to 20 cm depth.

To measure *in situ* CH_4 concentrations, pore water samples were extracted at 5, 10, 15 and 20 cm depth below the vegetation as described in Liebner *et al.* (2012). Briefly, we extracted 5 ml pore water using perforated brass rods and injected the pore water into 20 ml serum vials, which had been added 0.1 ml 1 M HCl and flushed with N_2. Headspace CH_4 concentrations in these vials were measured using a GC-FID (SRI Instruments, CA, USA). Gas samples were retrieved using a pressure tight syringe (Vici Precision Sampling, LA, USA) and injected directly onto a GC-FID with a HayeSep D packed column (SRI Instruments, CA, USA). The instrument sensitivity was set to its maximum and the elution time for CH_4 was 1.8 min.

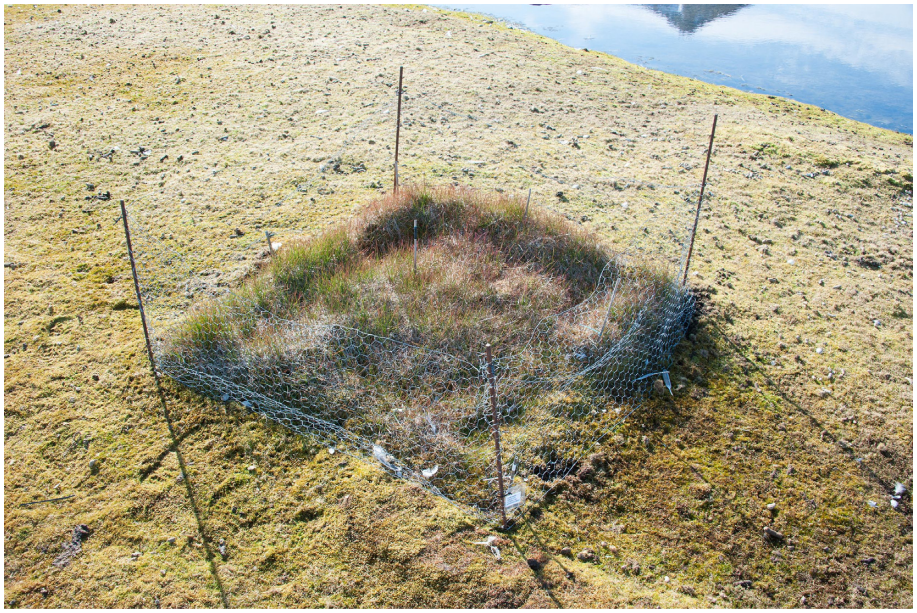

Figure 1. Exclosure at site SV1, Solvatn peatland, Ny Ålesund, Svalbard. Exclosure size is 1 × 1 m. It has been protected from grazing by a wire fence for 18 years.

From the headspace concentrations we could estimate the mass of headspace CH_4 by the ideal gas law. Further, when accounting for the dissolved CH_4 at room temperature (21 °C) and serum vial pressure using Henrys law constant for solubility of CH_4 in water, the headspace CH_4 content inside the serum vials equals the pore water CH_4 content.

Microcosm experiment for potential CH_4 oxidation *ex situ* along soil gradients

To measure potential CH_4 oxidation, approximately 15 g of each peat soil layer from section B were transferred to sterile 175 ml serum bottles and closed using Butyl rubber stoppers (Wheaton, Niemann *et al.* 2015) and aluminium crimp caps. CH_4 was added to obtain headspace concentrations of 0.5%–0.6% CH_4 (injection of 1 ml CH_4, 100 v/v %). Such high concentrations were chosen to ensure CH_4 availability for the MOB during the incubation. We acknowledge a potential selective pressure towards low affinity MOB but we considered this bias as preferable to several perturbations caused by a large number of CH_4 injections or periods of CH_4 starvation. A volume of 34 ml air was added to obtain overpressure in the microcosms to enable easier sampling. Gas measurements were conducted from the headspace of the incubation bottles immediately after CH_4 injection followed by four subsequent time-points at regular intervals during a maximum of 45 h of incubation at 8 °C using a GC-FID (SRI Instruments, CA, USA). Details for the headspace sampling and the GC program are described in the section 'Environmental characterization' above. From the headspace CH_4 concentrations measured at each time point we calculated the CH_4 oxidation rate.

Nucleic acid extraction/16S rRNA gene and *pmoA* amplicon sequencing

Nucleic acids were extracted from the *in situ* peat soil layers (section C, spring and summer 2016). For extraction, we selected the layers with maximum CH_4 oxidation activity (0–2 cm depth in grazed plots, 4–8 cm depth in exclosed plots). From these extracts, we purified both DNA and RNA to identify the *in situ* bacterial community and active MOB community by 16S rRNA gene and *pmoA* transcript sequencing, respectively.

Additionally, nucleic acids were extracted from the samples collected and frozen at the end of the 45-hours incubation period (section B from summer 2015). In correspondence with the *in situ* peat soil samples, we selected layers with maximal CH_4 oxidation activity. From these extracts, RNA was purified and used for sequencing of *pmoA* transcripts. This was done to identify the active MOB community responsible for CH_4 oxidation during the microcosm experiment.

All samples were ground with mortar and pestle in liquid N_2. Total nucleic acids were purified in duplicates from 0.2 g of each ground peat soil sample using a phenol/chloroform extraction protocol (Urich *et al.* 2008; Tveit *et al.* 2013). The duplicates of nucleic acids were mixed and then split in two samples, one for DNA purification and one for RNA purification.

DNA was purified by removing RNA with RNase A/T1 (Thermo Fisher Scientific, Waltham, MA/USA), followed by phenol/chloroform extraction and ethanol precipitation. Quality of DNA was assessed by Nanodrop and gel electrophoresis. DNA amplification was confirmed for the 16S rRNA gene using the 27F/1492R primer pair (Lane 1991). For 16S rRNA gene sequencing the V3-V4 region was targeted (Klindworth *et al.* 2013) using the Illumina MiSeq platform at IMGM Laboratories, Germany. The 16S rRNA gene amplicons were generated by a 2-step target-specific (TS)-PCR using 1 ng DNA as template for 25 cycles followed by an 8-cycle index PCR using 1 μL TS PCR product as template. The Q5® High Fidelity polymerase from NEB (Ipswich, MA, USA) was used for both PCRs and a negative control as well as a Mock community were amplified and sequenced in parallel to ensure sufficient quality.

To purify RNA, DNA was removed (RQ1 DNase, Promega), followed by RNA clean-up (MegaClear, Ambion) and ethanol precipitation. The RNA quality was assessed by Nanodrop and gel electrophoresis. RNA was reverse-transcribed (Superscript IV, Thermo Fisher) and the cDNA template was verified for the *pmoA* gene using the A189F/mb661R primer pair (Costello and Lidstrom 1999). The cDNA samples were sequenced using Illumina MiSeq and the two *pmoA* targeting primer pairs,

A189F/mb661R and A189F/A682R (Holmes *et al.* 1995; Costello and Lidstrom 1999) at IMGM Laboratories, Germany. The *pmoA* gene amplicons were generated by a 2-step TS-PCR using 10 ng cDNA as template for 25 cycles followed by a 12-cycle index PCR using 1 μL from the TS PCR products. The polymerase used was the Q5® High-Fidelity polymerase from NEB (Ipswich, MA, USA). Both a negative control and a Mock Community were amplified and sequenced in parallel to the samples to ensure sufficient quality.

Bioinformatics

Databases

Taxonomic assignment of OTUs for each of the three sequenced communities was done with a de-replicated database with sequences trimmed according to the primers used in this study. The sequences used for the *pmoA* database were retrieved from a published collection of *pmoA* sequences (Wen, Yang and Liebner 2016) and complemented with three Arctic *Methylobacter* sequences originating from Svalbard (GenBank id = AJ414658.1, KC878619.1, G7 Arctic mine isolate (genome not published)). The V3-V4 16S rRNA gene database was built from fragments of the SILVA 128 SSU database (Quast *et al.* 2013) (downloaded the 1st of October 2017). Both databases were trimmed according to the corresponding primers and de-replicated with a custom Perl script (https://github.com/cseppey/bin_src_my_prog/tree/master/perl/sel_db.pl).

Sequence data analyses

For each of the environmental sequence datasets, reads were merged using the program Flash (v. 1.2.8; (Magoč and Salzberg 2011)). Good quality sequences were filtered using a custom script (https://github.com/cseppey/bin_src_my_prog/tree/master/cpp/qualCheck.cpp) by keeping only sequences without any window of 50 nucleotides with an average phred score below 20 prior to trimming the primers (https://github.com/cseppey/bin_src_my_prog/tree/master/perl/trim_primer.pl). Chimeras were removed using the program Vsearch (v. 2.4.4; (Rognes *et al.* 2016)) comparing the environmental sequences between them (de novo approach), as well as by comparing the sequences against the corresponding database (for *pmoA* primers: (Wen, Yang and Liebner 2016); for V3-V4 primer: SILVA 128). After trimming the primers the *pmoA* sequences were expected to start with the nucleotides 188–190 (TCG: serine) and finish with the nucleotides 658–660 (TAT: tyrosine) for the reversed primer mb661 or nucleotides 679–681 (TCG: serine) for the reversed primer A682R (Semrau *et al.* 1995). To avoid sequences containing frameshift mutations, thus incorrect open reading frames, sequences with a number of nucleotides not divisible by three and sequences containing a stop codon were removed.

OTUs were clustered from the processed environmental sequences using the program Swarm (v. 2.1.13; (Mahé *et al.* 2014)), and taxonomically assigned by using the best alignment between the dominant sequence of each OTU and the database using the program Ggsearch36 (v. 36.3.8f; (Pearson 2000)). The OTUs were finally selected according to their length (mb661: [465–474 basepairs (bp)], A682: [492–495 bp], V3-V4: [370–435 bp]) in order to remove obvious sequencing errors as well as to their taxonomic affiliation by discarding OTUs assigned to Archaea, chloroplast or mitochondria.

Statistical analyses

To reduce the noise caused by low relative abundances, we consider an OTU as absent of a sample if its relative abundance was < 0.001 in that sample. Prior to analyses, the three relative abundance community matrices were log normalized as previously described in (Anderson, Ellingsen and McArdle 2006) (function decostand, package vegan v. 2.5–2; (Oksanen *et al.* 2018)). The effect of factor (treatment i.e. grazing and sampling date), interaction between the factors and CH_4 rate, while removing the effect of sites, were assessed through redundancy analysis (RDA) (function capscale, package vegan v.2.5–2; (Oksanen et al 2018)). The significance of the factors, factors interaction and CH_4 rate, as well as the significance of the RDA axes were tested by a permutation test (10 000 permutations, function anova.cca, package vegan v. 2.5–2; (Oksanen *et al.* 2018)). To disentangle the effect of the interaction between grazing and sampling date, two other RDAs were calculated for each treatment. For each new RDA, the effects of sampling date, CH_4 oxidation rate as well as the RDA axes were tested as for the RDA performed on the two treatments together.

The most representative OTUs of each treatment (bioindicators) were assessed using an indicator species analysis (indval; function indval, package labdsv v. 1.8–0; (Roberts 2016)) on the relative abundance community matrices. For each OTU in each treatment, a score is calculated, which is maximized if (i) the OTU is mostly found in the given treatment (high specificity) and (ii) is found in all samples of the given treatment (high fidelity). An OTU was selected as a bioindicator if the probability of a higher indicator value was < 0.001 on 10 000 permutations. All statistical analyses were performed in R (R Core Team 2018) and an overview of the sequence/OTU number at each step of the pipeline is found in the Table S2 (Supporting Information).

A phylogenetic tree was built from the bioindicator OTU sequences as well as closely related sequences retrieved from NCBI GenBank in order to better assess their taxonomy. The closely related sequences were retrieved by aligning (BLASTn) the bioindicator sequences against the NCBI nucleotide database and choosing the two highest scoring matches. In addition, a set of cultivated gammaproteobacterial MOB sequences was retrieved in addition to a set of *pmoA* sequences belonging to upland-soil cluster (USC)-gamma that served as an outgroup. Sequences were aligned in MEGA7 (Kumar, Stecher and Tamura 2016) using MUSCLE, choosing the UPGMB clustering (Edgar 2004). The length of the alignment was inspected visually for an overlap for all sequences and a section of 440 bp was chosen for phylogenetic analysis. A phylogenetic tree was constructed in MEGA7 using the neighbor-joining method with the Jukes-Cantor correction and 500 bootstraps (Kumar, Stecher and Tamura 2016). The tree was visualized using FigTree v1.4.4 (Rambaut 2018).

RESULTS

Soil parameters

Soil temperatures decreased with depth in both grazed and exclosed plots, and higher temperatures were measured in the summer seasons than in the spring season (Table S3, Supporting Information). At the soil surface, temperatures up to 16 °C were observed but temperatures varied substantially depending on air temperature and cloud cover (Fig. S1, Supporting Information). Below the surface, temperatures rarely exceeded 8 °C throughout the peat profile. Slightly warmer temperatures were recorded in grazed plots in the top 10 cm of the peat soil.

The decrease in O_2 concentration with depth was similar in grazed (-0.51 ± 0.18 mg/L per cm depth) and exclosed plots (-0.35 ± 0.25 mg/L per cm depth). However, O_2 concentrations in

grazed plots dropped from 9.8–11.5 mg/L O_2 at the surface to 1.7–9.5 mg/L O_2 at 5 cm depth. No drop was observed in exclosed plots when comparing surface concentrations (10.4–11.6 mg/L O_2) to 5 cm depth (9.6–12.1 mg/L O_2) and a more gradual decrease in O_2 concentration was observed (Fig. S2, Supporting Information).

Comparing the vegetation and the top 2 cm of peat soil, the water content was lower in exclosed plots (73.4–89.6 wt% H_2O) than in grazed plots (88.7–94.7 wt% H_2O) (Fig. 2), whereas between 2 and 10 cm below vegetation the water content was more similar for both environments. Overall, the soil water content measured in exclosed plots was 2%–15% lower than in grazed plots. SOM was slightly higher in exclosed peat (11.5 ± 3.2%) compared to grazed peat (8.3% ± 1.5%).

The *in situ* pore water CH_4 concentrations were higher at 10 cm depth than 5 cm depth in the grazed plots. Similarly, the CH_4 concentrations were higher at 20 cm depth than 15 cm depth in exclosed plots. Moreover, *in situ* CH_4 pore water concentrations were consistently higher in grazed plots than exclosed plots (Fig. S3, Supporting Information).

Potential CH_4 oxidation

Microcosm experiments were conducted *ex situ* to estimate the potential soil CH_4 oxidation rates at different depths in grazed and exclosed plots, for different seasons (spring and summer) and years. The highest CH_4 oxidation rates were measured at 0.5–2.5 cm depth in the grazed plots (115.0–319.6 μg CH_4 oxidized per g dry soil and day, Fig. 3). The exclosed plots had highest CH_4 oxidation rates at 3–8 cm depth (21.8–105.7 μg CH_4 oxidized per g dry soil and day, Fig. 3). This shift in potential CH_4 oxidation rates between the grazed and exclosed plots coincided with the shifts in O_2 concentrations, water content and CH_4 pore water concentrations. Overall higher CH_4 oxidation rates were measured in grazed plots, exceeding 50 μg CH_4 oxidized per g dry soil and day at most depths. In exclosed plots, CH_4 oxidation rates higher than 50 μg per g dry soil and day were almost exclusively observed in the zones of maximal CH_4 oxidation between 3 to 8 cm. The differences between grazed and exclosed plots, and different depths were true for both summer seasons (2015 and 2016) and the spring season. However, the potential CH_4 oxidation rates in spring were overall lower than in summer for the grazed plots, while for the exclosed plots spring and summer CH_4 oxidation rates were similar.

Bacterial and MOB community structure

We then wanted to identify the main MOB taxa within the bacterial communities to specifically target the MOB responsible for the CH_4 oxidation activity.

Larger amounts of DNA and RNA per gram dry soil were extracted from grazed plots compared to exclosed plots, suggesting a larger bacterial biomass in grazed soils (Fig. S4, Supporting Information). Sequencing of 16S rRNA gene libraries from these soils provided us with 10 816 sequences per library on average after quality filtering, the smallest library containing 2383 and the largest 19 608 sequences.

The results of the RDA showed that the bacterial communities in grazed plots differed significantly from the communities in the exclosed plots ($P < 0.001$, Fig. 4). The RDA showed that the sampling date had an impact on the communities in the grazed plots ($P = 0.004$), which was less pronounced for exclosed plots ($P = 0.124$), similar as observed for the measured CH_4 oxidation potentials.

The separation between grazed and exclosed plots correlated with *ex situ* CH_4 oxidation rates and the communities in the grazed plots were associated with high CH_4 oxidation rates while communities in the exclosed plots were associated with low rates (Fig. 4). However, CH_4 oxidation rates did not have a significant impact on the community structure ($P = 0.300$ grazed plots, $P = 0.673$ exclosed plots, $P = 0.613$ both treatments). All p-values for the variables and variables' interaction tested in the RDA analyses are listed in Table S4 (Supporting Information).

The 16S rRNA gene sequences assigned to the order Methylococcales were relatively more abundant (Kruskal-Wallis rank sum test $P < 0.001$) in grazed plots than in the exclosed plots, with a relative abundance of 7.0% in grazed plots compared to below 1% in exclosed plots (Fig. S5, Supporting Information). OTUs assigned to *Crenothrix* and *Methylobacter* had higher relative abundances than other genera within Methylococcales, representing 22 out of 25 OTUs of that order and from 56% to 100% of the sequences (Fig. S7, Supporting Information). Both genera were relatively more abundant in grazed plots (Kruskal–Wallis rank sum test: $P < 0.05$ for *Crenothrix* and for *Methylobacter* $P < 0.01$). From the 8 bioindicator OTUs for the grazed plots, one *Methylobacter* OTU (X49) was identified as bioindicator (Fig. 4, Fig. S6, Supporting Information). Among 13 OTUs identified as bioindicators for the exclosed plots, none of them belonged to the MOB.

To obtain further insights into the active MOB community, we sequenced *pmoA* transcript cDNA libraries from the summer 2015 microcosms and the spring and summer 2016 *in situ* soil samples using the two different *pmoA* primer pairs (Table S1, Supporting Information). The RDA analyses gave similar overall trends for both datasets. Therefore, the results from the mb661R *pmoA* dataset are used as the primary data basis for analyses, while the A682R *pmoA* dataset is used as a reference point to discuss uncertainties arising due to primer pair selection. Sequencing of *pmoA* gene libraries using the mb661R primer provided us with 29 149 sequences per library on average after quality filtering, the smallest library containing 9007 and the largest 58 612 sequences, whereas for the A682R primer an average of 22 340 sequences per library was provided, the smallest library containing 2213 and the largest library containing 53 950 sequences.

MOB community *pmoA* transcription in the grazed plots differed significantly from the exclosed plots ($P < 0.001$) (Fig. 5, Fig. S8, Table S4, Supporting Information), following the differences in CH_4 oxidation rates. Sampling date also had a clear impact on the MOB *pmoA* expression in the grazed plots ($P < 0.001$), but not in the exclosed plots ($P = 0.467$).

The majority of *pmoA* transcripts belonged to the genus *Methylobacter* (Figs S9 and S10, Supporting Information). Furthermore, nearly all bioindicator OTUs (for grazed or exclosed plots) belonged to *Methylobacter* (Fig. 6). This indicates that a consortium of closely related species and strains within the same genus are primarily responsible for most of the CH_4 oxidation but are also very responsive to ecosystem change.

OTUs from only two other genera, *Methylosarcina* and *Methylomicrobium*, were identified as bioindicators (OTU M54, Fig. 6 and OTUs A65 and A66, Fig. S11, Supporting Information). The relative abundance of *Methylosarcina* was low (< 1% in both *pmoA* datasets).

Methylomicrobium was the second most active genus based on the mb661R *pmoA* dataset (10.7% of the sequences in grazed plots, 27.6% in exclosed plots, Fig. S9, Supporting Information). OTU *Methylomicrobium*-M1 was the OTU with the highest overall abundance. However, the transcriptional activity of this and other *Methylomicrobium* OTUs were similar in all plots (Fig. 6)

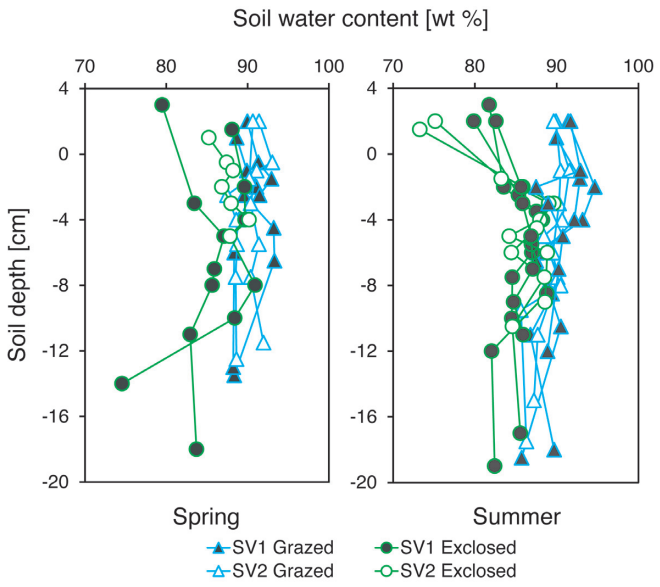

Figure 2. Soil water content in spring (left) and summer 2015 and 2016 (right), comparing grazed treatment (blue) and exclosed treatment (green). The water content was measured for the vegetation (>0 cm soil depth), at the soil/vegetation interface (0 cm) and until a soil depth of 20 cm (y-axis). Each point represents one measurement. Soil water content (x-axis) varied from 73 to 95 wt%. Soil depths were chosen in order to include visually distinguishable layers as well as many depths within the layers suspected to account for the majority of CH_4 oxidation (0–10 cm soil depth).

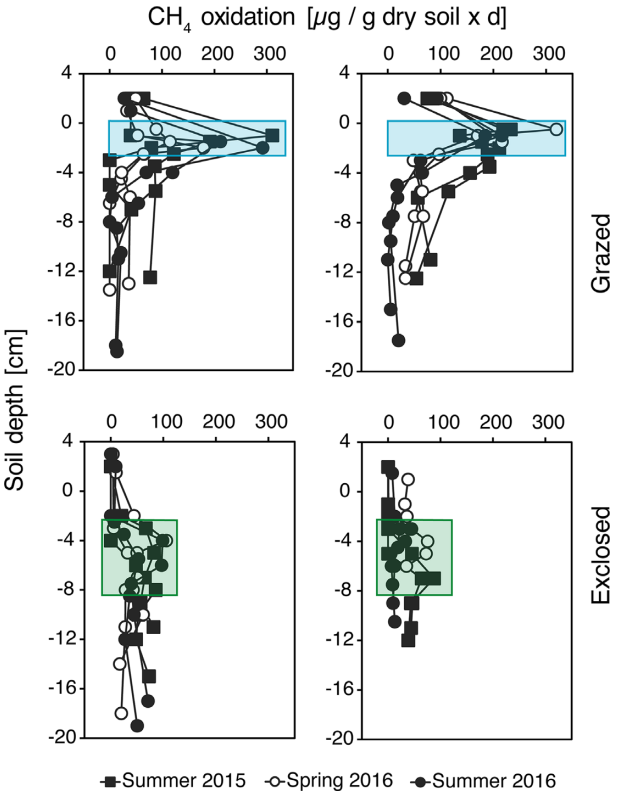

Figure 3. Potential CH_4 oxidation (μg CH_4 oxidized per g dry soil and per day) along vertical soils gradients for the grazed (two top figures) and exclosed treatments (two bottom figures). Filled symbols represent summer and open symbols represent spring. Each point represents one measurement. Oxidation rates from site SV1 and SV2 are shown on the left; and right- hand side respectively. The shaded area highlights the zone of maximum CH_4 oxidation activity. CH_4 oxidation measured above ground (i.e. vegetation) are > 0 on the y-axis, whereas below ground activity are < 0 on the y-axis.

excluding those OTUs as bioindicator for grazed or exclosed plots.

MOB transcriptional profile based on the A682R *pmoA* dataset was slightly different from the mb661R *pmoA* dataset. The major discrepancy was the large amount of unidentified MOB annotated as MOB-like (Fig. S10, Supporting Information). OTU A6 had the highest relative abundance within the MOB-like group with no significant differences between the grazed and the exclosed plots, ranking fourth in relative abundance behind *Methylobacter* OTUs A1, A3 and A4.

Phylogenetic analysis of the *pmoA* sequences of the bioindicator OTUs showed that most of them cluster within *Methylobacter*, in most cases closer to uncultivated environmental sequences than cultivated strains (Fig. 7). Interestingly, the bioindicators were all members of distinct clusters showing that these are phylogenetically different MOB strains.

DISCUSSION

Different ecosystem states change the potential for CH_4 oxidation

In our study, we investigated how the presence or absence of herbivory affected the potential for CH_4 oxidation and the methanotroph community in a high-Arctic peatland. Herbivore exclusion had promoted a higher proportion of vascular plants (Fig. 1) and less dense soil structure, reflected in higher O_2 concentrations, lower water content and higher soil temperatures (Fig. 2, Table S3, Figs S1 and S2, Supporting Information). The higher temperatures may be explained by better insulation being provided by the thicker vascular plant cover (Sjögersten, Van Der Wal and Woodin 2008; Sjögersten *et al.* 2011; Falk *et al.* 2015). In addition, visual observations of living roots in the exclosed plots but not in the grazed plots confirmed previous observations of higher root and vascular plant biomass in the exclosed plots (Sjögersten *et al.* 2011). Lower *in situ* CH_4 concentrations in the exclosed plots (Fig. S3, Supporting Information) contrast the

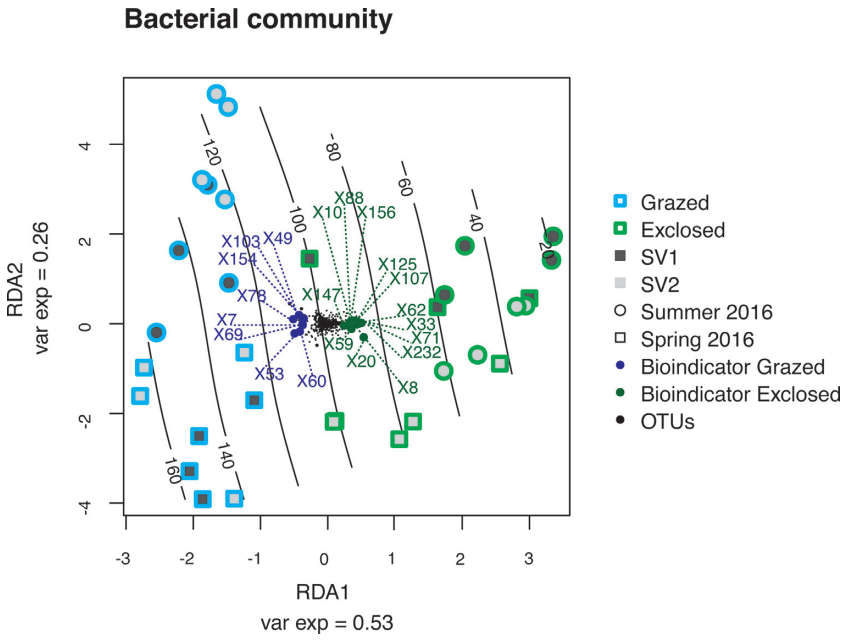

Figure 4. Treatment and season-dependent differences of bacterial communities at Solvatn peatland sites. The figure is based on redundancy analysis of the bacterial community (V3-V4 region of the 16S rRNA gene). Samples are labeled according to treatment: grazed (blue) and exclosed (green); sites: SV1 (dark grey) and SV2 (light grey); and sampling season: spring 2016 (square), summer 2016 (circle). Black lines indicate CH_4 oxidation potentials (μg CH_4 oxidized per g soil and day). Black dots show the distribution of non-bioindicator OTUs while green dots represent bioindicator OTUs for exclosed treatment and blue dots represent bioindicator OTUs for grazed treatment. Bioindicator identities are represented by the letter X followed by a number. Taxonomic information about the bioindicator OTUs is found in the V3-V4 heatmap (Fig. S6, Supporting Information).

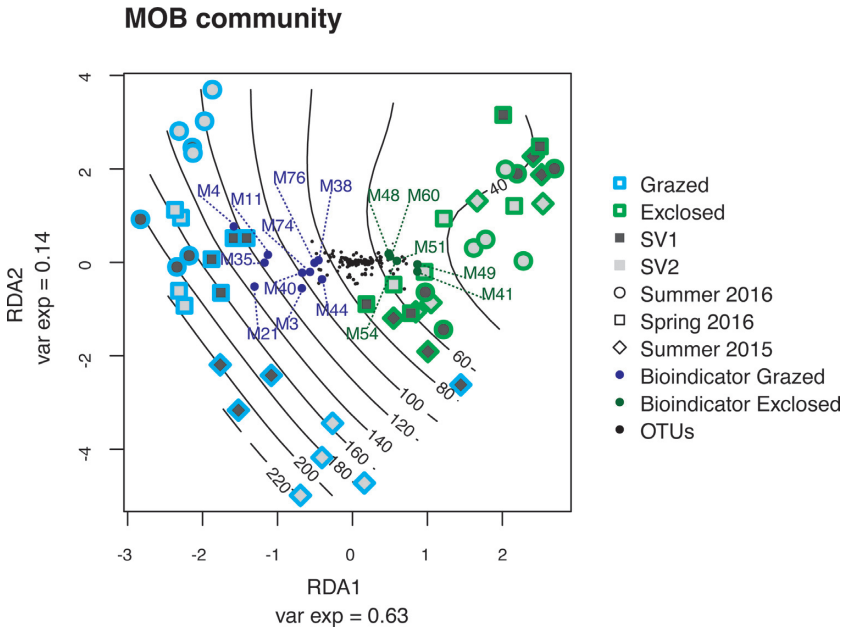

Figure 5. Treatment, site and season-dependent differences of MOB communities at Solvatn peatland sites. The figure is based on redundancy analysis of the MOB community (*pmoA* transcripts, primer pair A189F/mb661R). Samples are labeled according to treatment: grazed (blue) and exclosed (green); sites: SV1 (dark grey) and SV2 (light grey); and sampling season: summer 2015 (tilted square), spring 2016 (square), summer 2016 (circle). Black lines indicate CH_4 oxidation potential (μg CH_4 oxidized per g soil and day). Black dots show the distribution of non-bioindicator OTUs while green dots represent bioindicator OTUs for exclosed treatment and blue dots represent bioindicator OTUs for grazed treatment. Bioindicator identities are represented by the letter M followed by a number, marking them as OTUs from the mb661R *pmoA* dataset. Taxonomic information about the bioindicator OTUs is found in the heatmap in Fig. 6.

higher temperatures measured, as one would expect increased microbial activity at higher temperatures. However, the higher O_2 concentrations at 0–5 cm depth in the exclosed plots would promote CH_4 oxidation and inhibit CH_4 production, in line with our observations.

We did not observe any seasonally dependent differences in water content in grazed plots. Exclosed plots had overall lower water contents than the grazed plots and also slightly higher water contents in spring compared to summer, possibly due to recent snowmelt (Fig. 2).

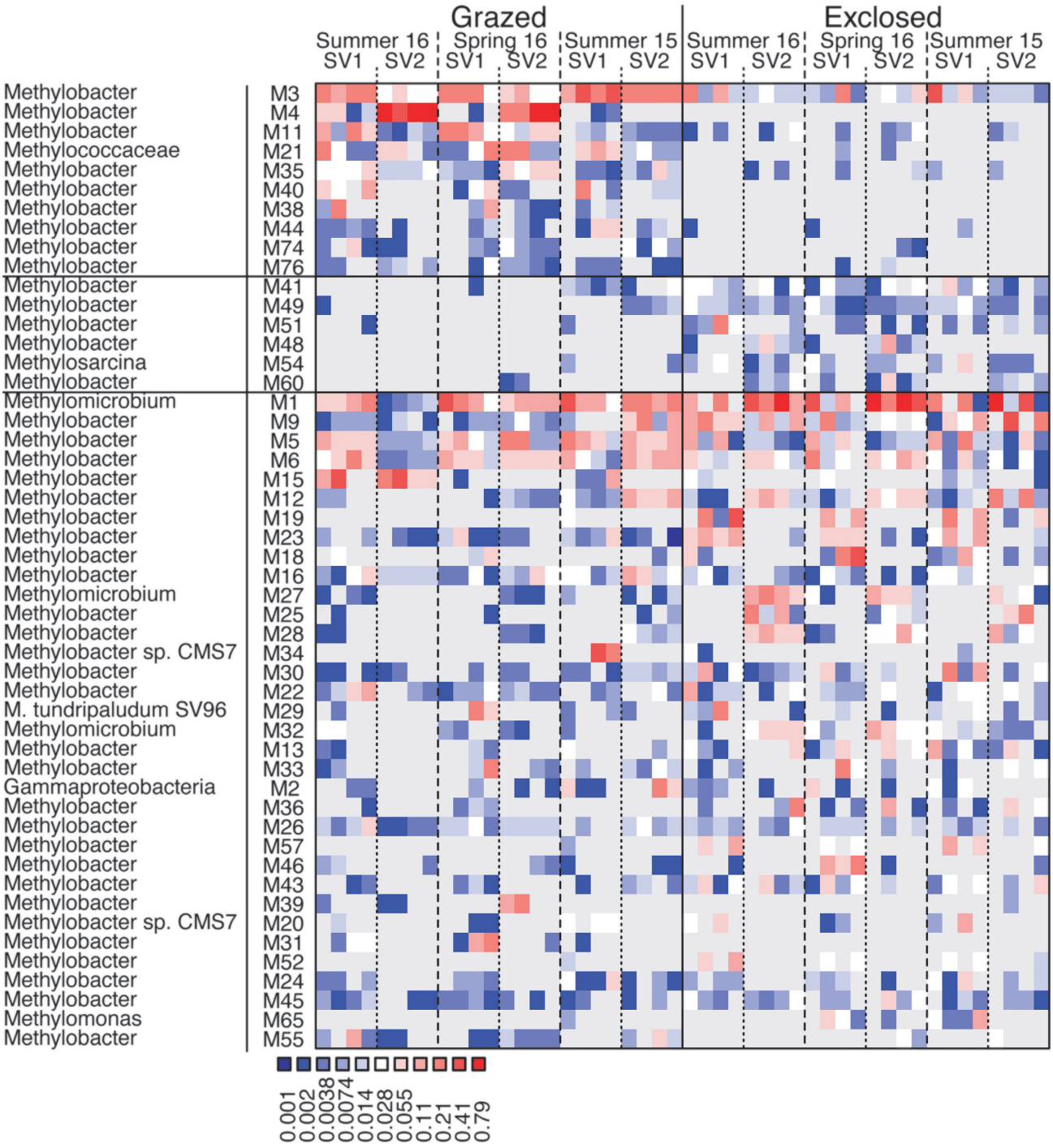

Figure 6. Relative abundances of MOB OTUs retrieved from *pmoA* transcripts *in situ* and *ex situ* (microcosm experiment). Bioindicator OTUs for the grazed treatment are shown in the uppermost section while the bioindicator OTUs for the exclosed treatment are shown in the middle section. In the lowest section we show the MOB OTUs with the highest relative abundance until representing 90% of the community. OTU names consist of the letter M plus a number, marking them as OTUs from the mb661R *pmoA* dataset. The color represents the relative abundance of a given OTU in a given sample.

The higher water content, higher *in situ* CH_4 concentrations and lower O_2 concentrations measured in the grazed plots were indicative of higher rates of CH_4 production in these soils (Table S3, Fig. 2, Figs S2 and S3, Supporting Information). However, due to the higher SOM content available for microbial degradation in exclosed plots it cannot be excluded that the amount of CH_4 produced in exclosed plots occasionally can surpass the CH_4 produced in grazed plots.

The potential CH_4 oxidation rates were highest in the grazed plots (Fig. 3) Furthermore, in these plots the zones of CH_4 oxidation were closer to the peat surface in grazed plots. In contrast to this, the lower *in situ* CH_4 concentrations and higher O_2 concentrations in the exclosed plots corresponded to a vertical shift of the maximum CH_4 oxidation zone from directly below the surface to between three and eight centimeters depth (Fig. 3). This matches the higher potential CH_4 oxidation rates measured in

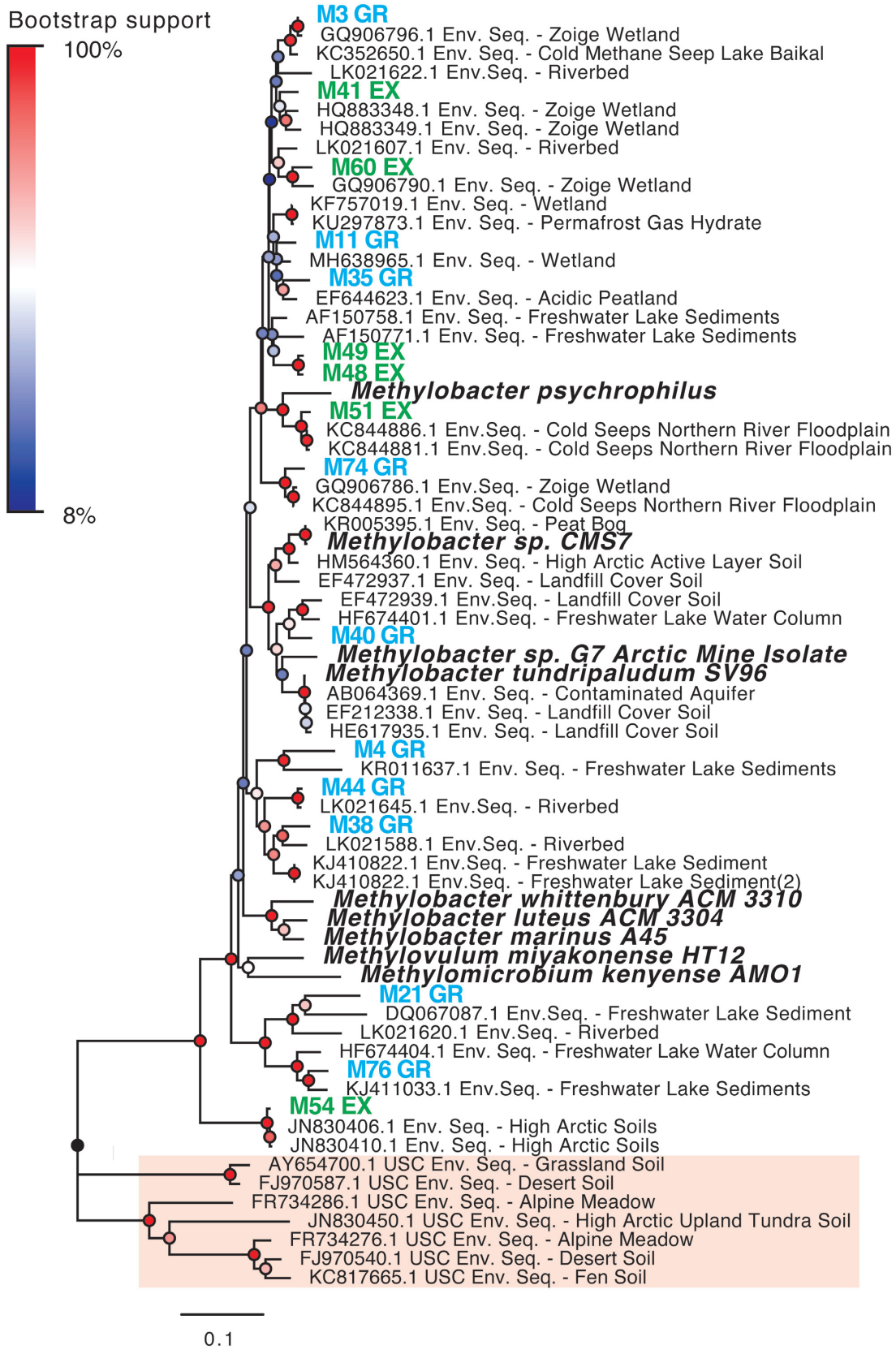

Figure 7. Neighbour-joining tree showing the phylogeny of the mb661R *pmoA* bioindicator OTUs (exclosed treatment in green, grazed treatment in blue), cultivated MOB strains (bold and italic) and related environmental sequences retrieved from Genbank (NCBI). Sequences belonging to the upland soil cluster gamma are used as outgroup to root the tree (shaded in red). Calculation was based on a 440-nucleotide alignment, using Jukes Cantor correction and 500 bootstraps. Bootstrap support is shown as node color ranging from blue (8%, lowest) to red (100%, highest). The length of the branches is based on the scale of 0.1 changes per nucleotide.

grazed areas of alpine meadows (Abell *et al.* 2009) and smaller CH_4 net-emissions measured in ungrazed areas of the Zackenberg valley (Greenland) and Yukon-Kuskokwim Delta (Western Alaska) (Falk *et al.* 2015; Kelsey *et al.* 2016). A possible explanation for the higher potential CH_4 oxidation in the grazed sites is differences in nitrogen (N) availability. Ammonia (NH_4) concentrations has been shown to correlate with higher CH_4 oxidation rates and type I MOB abundances in rice paddy soils (Bodelier and Laanbroek 2004). Sjögersten *et al.* (2011) also showed higher N in grazed plots than in exclosed plots which can explain the higher CH_4 oxidation observed in grazed plots in our study. Interestingly, it has been proposed that N fertilization favors a lower diversity (genus level) in rice paddy soils (Noll, Frenzel and Conrad 2008). As such, we would expect to observe higher methanotroph diversities in exclosed plots than grazed plots, but we did not.

Different bacterial and methanotroph communities in grazed and exclosed soils

Related to the higher potential CH_4 oxidation rates, we observed a considerably more transcriptionally active methanotroph community in grazed than exclosed plots (Fig. S6, Supporting Information). This difference was emphasized by the overall higher DNA and RNA content per gram dry soil in the zone of maximal CH_4 oxidation in grazed peat soils compared to exclosed peat soils (Fig. S4, Supporting Information). Furthermore, the higher relative abundances of methanotrophs in the grazed plots corresponded with higher CH_4 oxidation rates measured in the microcosm experiment *ex situ* (Fig. 3). Similarly, a link between CH_4 oxidation rates and transcript abundances was previously demonstrated (Reim *et al.* 2012; Siljanen *et al.* 2012) but we did not apply RT-qPCR and cannot directly compare this.

Methylobacter made up the majority of the methanotroph communities at Solvatn. From the genomes of several *Methylobacter* species, we know that these microorganisms oxidize CH_4 using the particulate methane monooxygenase. Our sequencing efforts targeting *pmoA* transcripts confirmed this, as the majority of *pmoA* transcripts were assigned to *Methylobacter* (Fig. 6 and Fig. S11, Supporting Information). Furthermore, we observed that a set of *Methylobacter* bioindicator OTUs were consistently more active in the maximal CH_4 oxidation zone of the exclosed plots while other OTUs were more active in the grazed plots, indicating that the different CH_4 and O_2 concentrations favor different *Methylobacter* OTUs. Similiarly, in stratified lakes the MOB communities were structured according to CH_4 and O_2 concentrations, providing for a niche-adapted community responsible for CH_4 oxidation dynamics (Mayr *et al.* 2020). An earlier microcosm study also supported the idea that closely related *Methylobacter* populations are adapted to different niches as they responded differently to O_2 tension (Oshkin *et al.* 2015).

CH_4 concentrations in Solvatn peat soil are high (Fig. S3, Supporting Information) while net net CH_4 emissions are low (Høj, Olsen and Torsvik 2005; Sjögersten *et al.* 2011). It has previously been suggested that such niche partitioning increases the exploitation of resources (Finke and Snyder 2008; Mayr *et al.* 2020). Thus, niche partitioning of closely related *Methylobacter* OTUs may explain the efficiency of CH_4 consumption in both grazed and exclosed peat soils at Solvatn.

Our study shows that phylogenetically distinct *Methylobacter* OTUs might find their ecological niches within micro niches of the same ecosystem as the most active fraction of the MOB community consisted of several closely related transcriptionally active *Methylobacter* populations (Figs. 6 and 7). Similar observations were reported from Lake Washington, Lake Pavin and the Canadian high Arctic (Costello and Lidstrom 1999; Martineau, Whyte and Greer 2010; Biderre-Petit *et al.* 2011), suggesting that our findings reflect a common occurrence. The bioindicator approach allows us to identify OTUs that respond to specific environmental changes in different ecosystems. By correlating past and future datasets this approach can help determining whether certain strains or species have the same roles and responses in other ecosystems or under other conditions.

It remains difficult to a draw a line between species and strains based on sequencing the *pmoA* genes or transcripts even though similarity cut-offs have been suggested for *pmoA* OTUs (Wen, Yang and Liebner 2016). A genome-based study revealed that a large variety of *Methylobacter* genomes which were earlier assigned as strains of *M. tundripaludum* SV96 are actually different species (Orata *et al.* 2018). Thus, some of the *pmoA* OTUs we have identified as bioindicators may be representative of different *Methylobacter* species, and so the OTU dynamics described here are in part reflecting the ecology of *Methylobacter* species.

CONCLUSION

Herbivory in Svalbard leads to reduced vascular plant and root biomass in peatlands, resulting in increased soil water content, higher *in situ* pore water CH_4 concentrations and reduced O_2 concentrations. These changes correspond with a shallower and more potent zone of maximal CH_4 oxidation in grazed peat compared to peat protected from grazing. Furthermore, the shallower CH_4 oxidation zone in grazed peat has a relatively more abundant and different MOB community than the exclosed peat, the major difference being the dominance of different *Methylobacter* OTUs. Nevertheless, *Methylobacter* comprise the major CH_4 filter in both peat soils, actively reducing the amount of CH_4 emitted to the atmosphere. This study emphasizes how herbivory leads to altered soil conditions that selects for different active MOB communities able to respond to increased CH_4 concentrations.

SUPPLEMENTARY DATA

Supplementary data are available at FEMSEC online.

ACKNOWLEDGMENTS

The funding for this study was provided by NORRUSS (Grant: 233645/H30) and Svalbard Science Forum (AFG Grant: 246113/E10 and AFG Grant: 256933/E10) from the Research Council of Norway. AT Tveit was supported by the Research Council of Norway FRIPRO Mobility Grant Project Time and Energy 251027/RU, co-founded by ERC under Marie Curie Grant 606895, and Tromsø Research Foundation starting grant project Cells in the Cold 16_SG_ATT. CVW Seppey was supported by the Research Council of Norway, projects BiodivERsA (270252/E50) and ERAnet-LAC (256132/H30). A significant part of the calculation was performed on the Norwegian National Infrastructures for High-Performance Computing and Data Storage UNINETT Sigma2, Projects NN9549K, NN9265K and NK9593K.

Conflicts of interest. None declared.

REFERENCES

Abell GCJ, Stralis-Pavese N, Sessitsch A *et al.* Grazing affects methanotroph activity and diversity in an alpine meadow soil. *Environ Microbiol Rep* 2009;**1**:457–65.

Amaral JA, Knowles R. Growth of methanotrophs in methane and oxygen counter gradients. *FEMS Microbiol Lett* 1995;**126**:215–20.

Anderson MJ, Ellingsen KE, McArdle BH. Multivariate dispersion as a measure of beta diversity. *Ecol Lett* 2006;**9**:683–93.

Bardgett RD, Manning P, Morriën E *et al.* Hierarchical responses of plant-soil interactions to climate change: Consequences for the global carbon cycle. *J Ecol* 2013;**101**:334–43.

Beck DAC, Kalyuzhnaya MG, Malfatti S *et al.* A metagenomic insight into freshwater methane-utilizing communities and evidence for cooperation between the Methylococcaceae and the Methylophilaceae. *Peer J* 2013;**2013**:1–23.

Biderre-Petit C, Jézéquel D, Dugat-Bony E *et al.* Identification of microbial communities involved in the methane cycle of a freshwater meromictic lake. *FEMS Microbiol Ecol* 2011;**77**:533–45.

Blees J, Niemann H, Wenk CB *et al.* Micro-aerobic bacterial methane oxidation in the chemocline and anoxic water column of deep south-alpine Lake Lugano (Switzerland). *Limnol Oceanogr* 2014;**59**:311–24.

Bodelier PLE, Laanbroek HJ. Nitrogen as a regulatory factor of methane oxidation in soils and sediments. *FEMS Microbiol Ecol* 2004;**47**:265–77.

Bornemann M, Bussmann I, Tichy L *et al.* Methane release from sediment seeps to the atmosphere is counteracted by highly active Methylococcaceae in the water column of deep oligotrophic Lake Constance. *FEMS Microbiol Ecol* 2016;**92**:1–11.

Börjesson G, Sundh I, Svensson B. Microbial oxidation of CH4 at different temperatures in landfill cover soils. *FEMS Microbiol Ecol* 2004;**48**:305–12.

Costello AM, Lidstrom ME. Molecular characterization of functional and phylogenetic genes from natural populations of methanotrophs in lake sediments. *Appl Environ Microbiol* 1999;**65**:5066–74.

Edgar RC. MUSCLE: Multiple sequence alignment with high accuracy and high throughput. *Nucleic Acids Res* 2004;**32**:1792–7.

Falk JM, Schmidt NM, Christensen TR *et al.* Large herbivore grazing affects the vegetation structure and greenhouse gas balance in a high Arctic mire. *Environ Res Lett* 2015;**10**:045001.

Finke DL, Snyder WE. Niche partitioning increases resource exploitation by diverse communities. *Science (80-)* 2008;**321**:1488–90.

Graef C, Hestnes AG, Svenning MM *et al.* The active methanotrophic community in a wetland from the High Arctic. *Environ Microbiol Rep* 2011;**3**:466–72.

Hanson RS, Hanson TE. Methanotrophic bacteria. *Microbiol Rev* 1996;**60**:439–71.

He R, Wooller MJ, Pohlman JW *et al.* Identification of functionally active aerobic methanotrophs in sediments from an Arctic lake using stable isotope probing. *Environ Microbiol* 2012;**14**:1403–19.

Hessen DO, Tombre IM, van Geest G *et al.* Global change and ecosystem connectivity: how geese link fields of central Europe to eutrophication of Arctic freshwaters. *Ambio* 2017;**46**:40–7.

Ho A, Kerckhof F-M, Lüke C *et al.* Conceptualizing functional traits and ecological characteristics of methane-oxidizing bacteria as life strategies. *Environ Microbiol Rep* 2013;**5**:335–45.

Holmes AJ, Costello A, Lidstrom ME *et al.* Evidence that particulate methane monooxygenase and ammonia monooxygenase may be evolutionarily related. *FEMS Microbiol Lett* 1995;**132**:203–8.

Høj L, Olsen RA, Torsvik VL. Archaeal communities in high-Arctic wetlands at Spitsbergen, Norway (78°N) as characterized by 16S rRNA gene fingerprinting. *FEMS Microbiol Ecol* 2005;**53**:89–101.

Kelsey KC, Leffler AJ, Beard KH *et al.* Interactions among vegetation, climate, and herbivory control greenhouse gas fluxes in a subarctic coastal wetland. *J Geophys Res Biogeosciences* 2016;**121**:2960–75.

Klindworth A, Pruesse E, Schweer T *et al.* Evaluation of general 16S ribosomal RNA gene PCR primers for classical and next-generation sequencing-based diversity studies. *Nucleic Acids Res* 2013;**41**:1–11.

Knief C. Diversity and habitat preferences of cultivated and uncultivated aerobic methanotrophic bacteria evaluated based on pmoA as molecular marker. *Front Microbiol* 2015;**6**:1–38.

Kruse J, Lennartz B, Leinweber P. A modified method for measuring saturated hydraulic conductivity and anisotropy of fen peat samples. *Wetlands* 2008;**28**:527–31.

Kumar S, Stecher G, Tamura K. MEGA7: Molecular evolutionary genetics analysis version 7.0 for bigger datasets. *Mol Biol Evol* 2016;**33**:1870–4.

Lane DJ. 16S/23S rRNA sequencing. *Nucleic Acid Techniques in Bacterial Systematics*, New York: John Wiley & Sons, 1991, 115–75.

Liebner S, Schwarzenbach SP, Zeyer J. Methane emissions from an alpine fen in central Switzerland. *Biogeochemistry* 2012;**109**:287–99.

Magoč T, Salzberg SL. FLASH: Fast length adjustment of short reads to improve genome assemblies. *Bioinformatics* 2011;**27**:2957–63.

Mahé F, Rognes T, Quince C *et al.* Swarm: robust and fast clustering method for amplicon-based studies. *Peer J* 2014;**2**, DOI:10.7717/peerj.593.

Martineau C, Whyte LG, Greer CW. Stable isotope probing analysis of the diversity and activity of Methanotrophic bacteria in soils from the Canadian high Arctic. *Appl Environ Microbiol* 2010;**76**:5773–84.

Mayr MJ, Zimmermann M, Guggenheim C *et al.* Niche partitioning of methane-oxidizing bacteria in the oxygen-methane counter gradient of stratified lakes. *ISME J* 2020;**14**:274–87.

McDonald IR, Bodrossy L, Chen Y *et al.* Molecular ecology techniques for the study of aerobic methanotrophs. *Appl Environ Microbiol* 2008;**74**:1305–15.

Niemann H, Steinle L, Blees J *et al.* Toxic effects of lab-grade butyl rubber stoppers on aerobic methane oxidation. *Limnol Oceanogr Methods* 2015;**13**:40–52.

Noll M, Frenzel P, Conrad R. Selective stimulation of type I methanotrophs in a rice paddy soil by urea fertilization revealed by RNA-based stable isotope probing. *FEMS Microbiol Ecol* 2008;**65**:125–32.

Oksanen J, Blanchet FG, Friendly M *et al.* vegan: Community Ecology Package. R. 2018, DOI: ISBN 0-387-95457-0.

Orata FD, Meier-Kolthoff JP, Sauvageau D *et al.* Phylogenomic analysis of the gammaproteobacterial Methanotrophs (order Methylococcales) calls for the reclassification of members at the genus and species evels. *Front Microbiol* 2018;**9**:1–17.

Oshkin IY, Beck DAC, Lamb AE *et al.* Methane-fed microbial microcosms show differential community dynamics and pinpoint taxa involved in communal response. *ISME J* 2015;**9**:1119–29.

Oshkin IY, Wegner C-E, Lüke C *et al*. Gammaproteobacterial methanotrophs dominate cold methane seeps in floodplains of west siberian rivers. *Appl Environ Microbiol* 2014;**80**:5944–54.

Oswald K, Milucka J, Brand A *et al*. Light-dependent aerobic methane oxidation reduces methane emissions from seasonally stratified lakes. *PLoS One* 2015;**10**:e0132574.

Parish F, Sirin A, Charman D *et al*. *Assessment on Peatlands, Biodiversity and Climate Change: Main Report. Global Environment Centre, Kuala Lumpur and Wetlands International, Wageningen*, 2008, 179.

Pearson WR. Flexible sequence similarity searching with the FASTA3 program package. In: Misener S, Krawetz SA , (eds.). *Methods in Molecular Biology*, Totowa, NJ: Humana Press, 2000, 185–219.

Quast C, Pruesse E, Yilmaz P *et al*. The SILVA ribosomal RNA gene database project: Improved data processing and web-based tools. *Nucleic Acids Res* 2013;**41**:590–6.

Rambaut A. FigTree, v. 1.4.4. 2018.

R Core Team. R Core Team (2018). R: A language and environment for statistical computing. R Foundation for statistical computing, Vienna, Austria. Available online at https://www.R-project.org/. 2018.

Reay DS, Smith KA, Hewitt CN. Methane: importance, sources and sinks. In: Reay DS, Hewitt CN, Smith KA, Grace J , (eds.). *Greenhouse Gas Sinks*, Wallingford, Oxfordshire, UK: CABI, 2007, 143–51.

Reim A, Lüke C, Krause S *et al*. One millimetre makes the difference: high-resolution analysis of methane-oxidizing bacteria and their specific activity at the oxic-anoxic interface in a flooded paddy soil. *ISME J* 2012;**6**:2128–39.

Roberts D. Package ' labdsv.' 2016.

Rognes T, Flouri T, Nichols B *et al*. VSEARCH: a versatile open source tool for metagenomics. *Peer J* 2016;**4**:e2584.

Semrau JD, Chistoserdov A, Lebron J *et al*. Particulate methane monooxygenase genes in methanotrophs. *J Bacteriol* 1995;**177**:3071–9.

Semrau JD, DiSpirito AA, Yoon S. Methanotrophs and copper. *FEMS Microbiol Rev* 2010;**34**:496–531.

Siljanen HMP, Saari A, Bodrossy L *et al*. Seasonal variation in the function and diversity of methanotrophs in the littoral wetland of a boreal eutrophic lake. *FEMS Microbiol Ecol* 2012;**80**:548–55.

Singleton CM, McCalley CK, Woodcroft BJ *et al*. Methanotrophy across a natural permafrost thaw environment. *ISME J* 2018;**12**:2544–58.

Sjögersten S, van der Wal R, Loonen MJJE *et al*. Recovery of ecosystem carbon fluxes and storage from herbivory. *Biogeochemistry* 2011;**106**:357–70.

Sjögersten S, Van Der Wal R, Woodin SJ. Habitat type determines herbivory controls over CO2 fluxes in a warmer Arctic. *Ecology* 2008;**89**:2103–16.

Smith GJ, Angle JC, Solden LM *et al*. Members of the genus Methylobacter are inferred to account for the majority of aerobic methane oxidation in oxic soils from a freshwater eetland. *MBio* 2018;**9**:e00815–18.

Solheim B, Endal A, Vigstad H. Nitrogen fixation in Arctic vegetation and soils from Svalbard, Norway. *Polar Biol* 1996;**16**:35–40.

Stępniewska Z, Goraj W, Kuźniar A *et al*. Methane oxidation by endophytic bacteria inhabiting Sphagnum sp. and some vascular plants. *Wetlands* 2018;**38**:411–22.

Tsutsumi M, Iwata T, Kojima H *et al*. Spatiotemporal variations in an assemblage of closely related planktonic aerobic methanotrophs. *Freshw Biol* 2011;**56**:342–51.

Tveit A, Schwacke R, Svenning MM *et al*. Organic carbon transformations in high-Arctic peat soils: key functions and microorganisms. *ISME J* 2013;**7**:299–311.

Tveit AT, Urich T, Frenzel P *et al*. Metabolic and trophic interactions modulate methane production by Arctic peat microbiota in response to warming. *Proc Natl Acad Sci* 2015;**112**:E2507–16.

Urich T, Lanzén A, Qi J *et al*. Simultaneous assessment of soil microbial community structure and function through analysis of the meta-transcriptome. *PLoS One* 2008;**3**:e2529.

Wartiainen I, Hestnes AG, McDonald IR *et al*. Methylobacter tundripaludum sp. nov., a methane-oxidizing bacterium from Arctic wetland soil on the Svalbard islands, Norway (78° N). *Int J Syst Evol Microbiol* 2006;**56**:109–13.

Wartiainen I, Hestnes AG, Svenning MM. Methanotrophic diversity in high arctic wetlands on the islands of Svalbard (Norway)–denaturing gradient gel electrophoresis analysis of soil DNA and enrichment cultures. *Can J Microbiol* 2003;**49**:602–12.

Wen X, Yang S, Liebner S. Evaluation and update of cutoff values for methanotrophic pmoA gene sequences. *Arch Microbiol* 2016;**198**:629–36.

Yun J, Ma A, Li Y *et al*. Diversity of methanotrophs in Zoige wetland soils under both anaerobic and aerobic conditions. *J Environ Sci* 2010;**22**:1232–8.

Zhang L, Adams JM, Dumont MG *et al*. Distinct methanotrophic communities exist in habitats with different soil water contents. *Soil Biol Biochem* 2019;**132**:143–52.

Supplementary Data

Supplementary Table 1: Sampling overview

	Summer 2015	Spring 2016	Summer 2016
In situ soil parameters (temperature, O_2 and CH_4 concentration)	X	X	X
Ex situ soil parameters (soil water content, soil organic matter content)	X	X	X
CH_4 oxidation measurements *ex situ* (microcosms)	X	X	X
16S rRNA gene analysis of *in situ* bacterial community		X	X
pmoA transcript analysis of *in situ* MOB community		X	X
pmoA transcript analysis of *ex situ* MOB community (microcosms)	X		

Supplementary Table 2: Pipeline overview for V3-V4 and *pmoA* (with both primer sets) amplicon sequence analysis. Steps 1-5 describe the processing of raw sequences until Swarm clustering and are therefore not applicable (n/a) for OTU counts, which is described in step 7 and 8. Sequences from the V3-V4 dataset were not checked for frameshift mutations and step 5 is therefore not applicable (n/a).

		V3V4		mb661		A682	
		Sequences	OTUs	Sequences	OTUs	Sequences	OTUs
1	raw sequences	1707324	(n/a)	2635949	(n/a)	2869266	(n/a)
2	good quality	706371	(n/a)	1606840	(n/a)	1189725	(n/a)
3	with good primers	647378	(n/a)	1567342	(n/a)	1162401	(n/a)
4	not chimera	352308	(n/a)	1496771	(n/a)	1151186	(n/a)
5	respecting frameshift	(n/a)	(n/a)	1399165	(n/a)	1073560	(n/a)
6	clustering	352197	53468	1399164	15909	1073533	13942
7	good sequence length and taxonomy	346132	52629	1399144	15897	1072313	13727
8	high occurrence	155893	1310	1366774	220	1044851	223

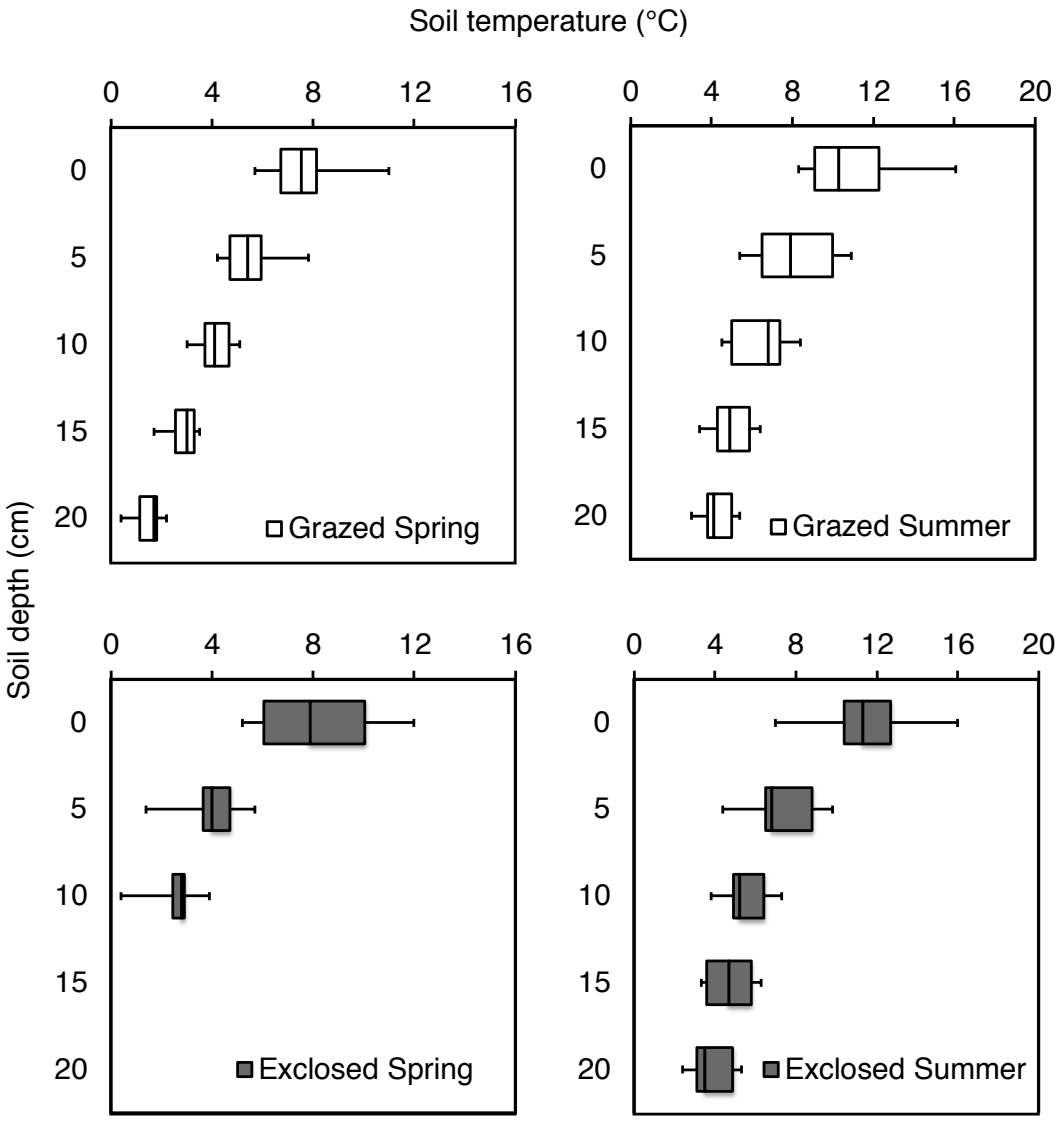

Supplementary Fig. 1A and 1B: Soil temperatures measured along vertical soil gradients comparing grazed treatment (two top figures) and exclosed treatment (two bottom figures) in spring (left hand side) and summer (right hand side). Whiskers indicate min and max temperature measured; boxes consist of 25% quartile, median and 75% quartile.

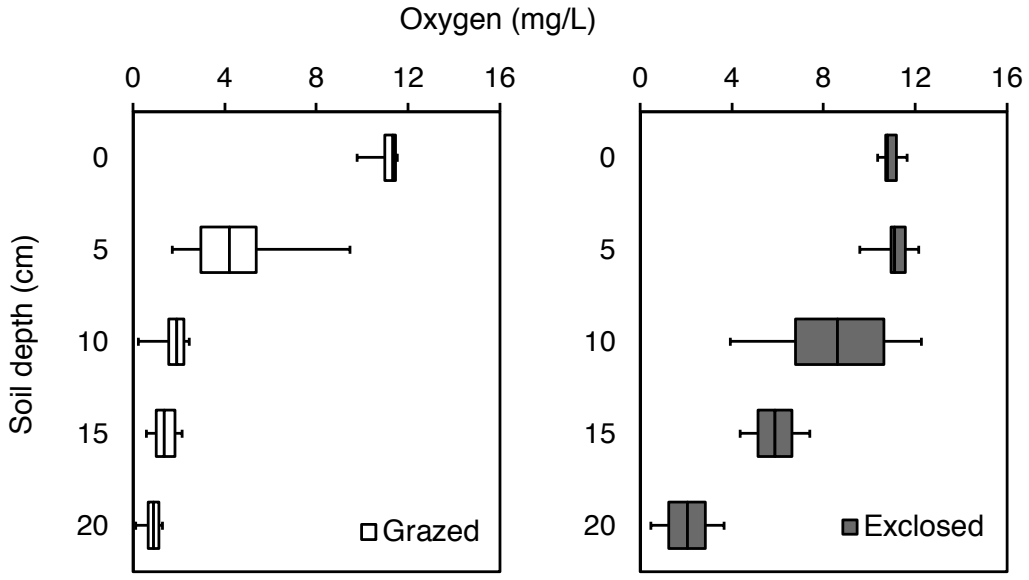

Supplementary Fig. 2: O_2 profiles along vertical soil gradients (y-axis) comparing grazed treatment (left) and exclosed treatment (right). Measurements were taken in 5 cm intervals in summer 2015, spring 2016 and summer 2016 at both sites, SV1 and SV2. Whiskers indicate min and max O_2 concentration measured; boxes consist of 25% quartile, median and 75% quartile.

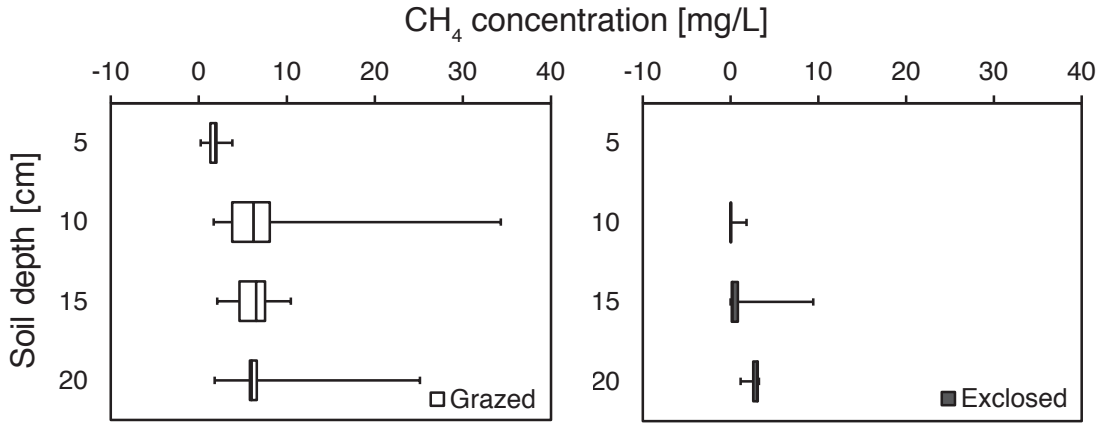

Supplementary Fig. 3: CH_4 pore water concentration measurements [mg/L] along vertical soil gradients (y-axis) comparing grazed treatment (left) and exclosed treatment (right). The data used in this figure are from summer 2015, spring 2016 and summer 2016 and were taken at both sites, SV1 and SV2. Whiskers indicate max and min CH_4 concentrations; Boxes consist of 25% quartile, median and 75% quartile.

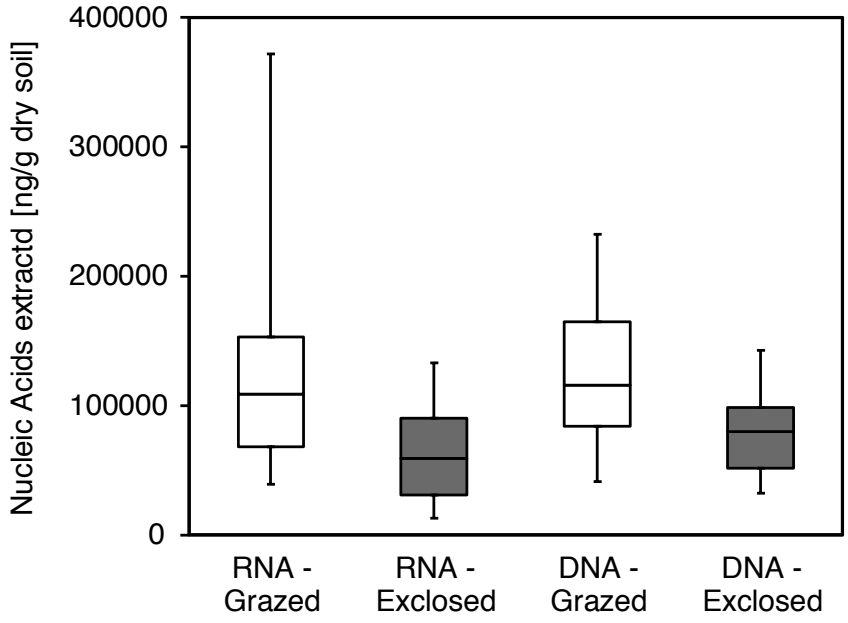

Supplementary Fig. 4: RNA and DNA extracted per gram dry soil for grazed (white) and exclosed (grey) treatments as indicator for community size. Whiskers indicate min. and max. values; boxes consist of 25% quartile, median and 75% quartile.

Supplementary Table 3: Soil parameter ranges for grazed treatment (left) and exclosed treatment (right). Measurements at a depth of 0 cm are taken at the soil/vegetation interface.

	Grazed						Exclosed					
	Spring			**Summer**			**Spring**			**Summer**		
Depth [cm]	Temp. [°C]	O_2 [mg/L]	CH_4 [mg/L]	Temp. [°C]	O_2 [mg/L]	CH_4 [mg/L]	Temp. [°C]	O_2 [mg/L]	CH_4 [mg/L]	Temp. [°C]	O_2 [mg/L]	CH_4 [mg/L]
0	5.7-11.0	10.9-11.5	-	8.3-16.1	9.8-11.3	-	5.2-12.0	10.4-11.5	-	7.0-16.0	10.7-11.6	-
5	4.2-7.8	1.7-4.5	1.0-2.0	5.4-10.9	7.1-9.5	0.2-3.8	1.4-5.7	9.6-12.1	-	4.4-9.8	11.0-11.4	<0.1
10	3.0-5.1	1.5-2.3	3.3-8.1	4.5-8.4	0.2-2.4	1.7-34.3	0.4-3.9	4.0-12.3	< 0.1-1.8	3.8-7.3	8.1-9.9	< 0.1-0.1
15	1.7-3.5	0.6-2.2	4.6-7.5	3.4-6.4	1.0-1.9	2.1-10.4	1.0-2.5	7.4	< 0.1-1.4	3.3-6.3	4.4	<0.1-9.4
20	0.4-2.2	0.1-1.2	5.5-6.6	3.0-5.4	0.7-1.3	1.8-25.1	0.4-2.1	3.6	-	2.4-5.3	0.5	1.1-3.2

Supplementary Table 4: p-value overview from RDA for each dataset (*pmoA*: mb661, A682; V3-V4). Community column is split in total (all samples), grazed (samples from grazed treatment only) and exclosed (samples from exclosed treatment only). Sampling date shows the effect significance of the sampling period, Grazing shows the effect significance of the treatment and CH_4 Oxidation Rate shows the relation significance between the potential CH_4 oxidation measured in the microcosms and the communities. The last column shows the interaction between Sampling Date and Grazing, Site and Grazing. Interactions between the effect of Sampling Date and Grazing are not applicable (n/a) for the grazed and exclosed sub-datasets. Numbers lower then 0.05 show high interaction whereas numbers higher than 0.05 indicate low interaction.

Sequence Dataset	Community	Sampling Date	Grazing	CH_4 Ox. Rate	Interaction - Sampling Date:Grazing
V3V4	Total	0.007	<0.001	0.613	0.130
	Grazed	0.004	(n/a)	0.300	(n/a)
	Exclosed	0.124	(n/a)	0.673	(n/a)
mb661	Total	0.033	<0.001	0.651	0.099
	Grazed	<0.001	(n/a)	0.277	(n/a)
	Exclosed	0.467	(n/a)	0.149	(n/a)
A682	Total	0.019	<0.001	0.614	0.051
	Grazed	<0.001	(n/a)	0.230	(n/a)
	Exclosed	0.453	(n/a)	0.270	(n/a)

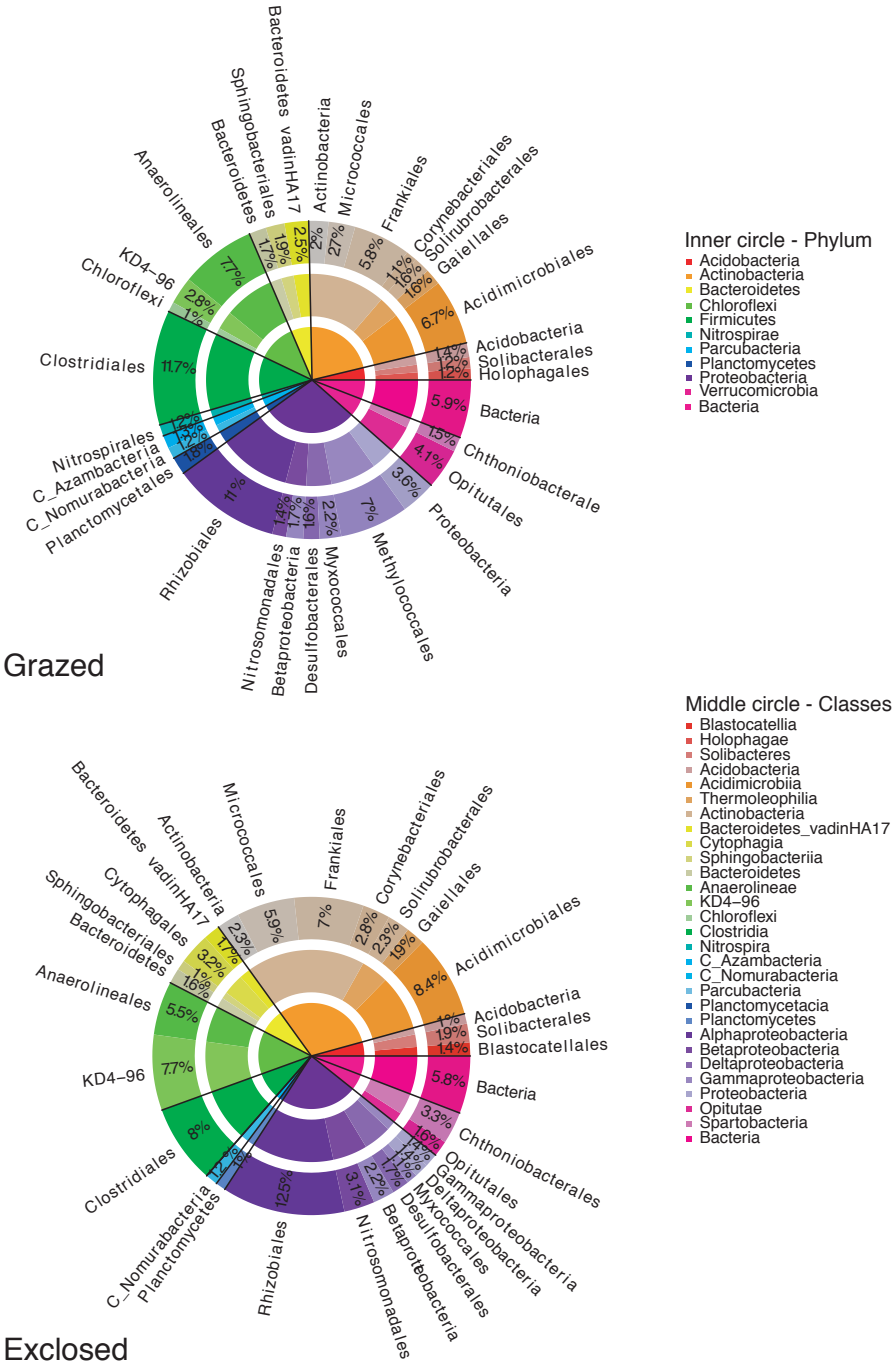

Supplementary Fig. 5: Distribution of bacterial taxa in grazed and exclosed treatments. Only taxa with a relative abundance > 1% are represented. Relative abundances are listed in the outermost ring of the chart and are given in %. The different rings represent different taxonomic levels, starting with phyla in the innermost ring followed by class and order moving outward.

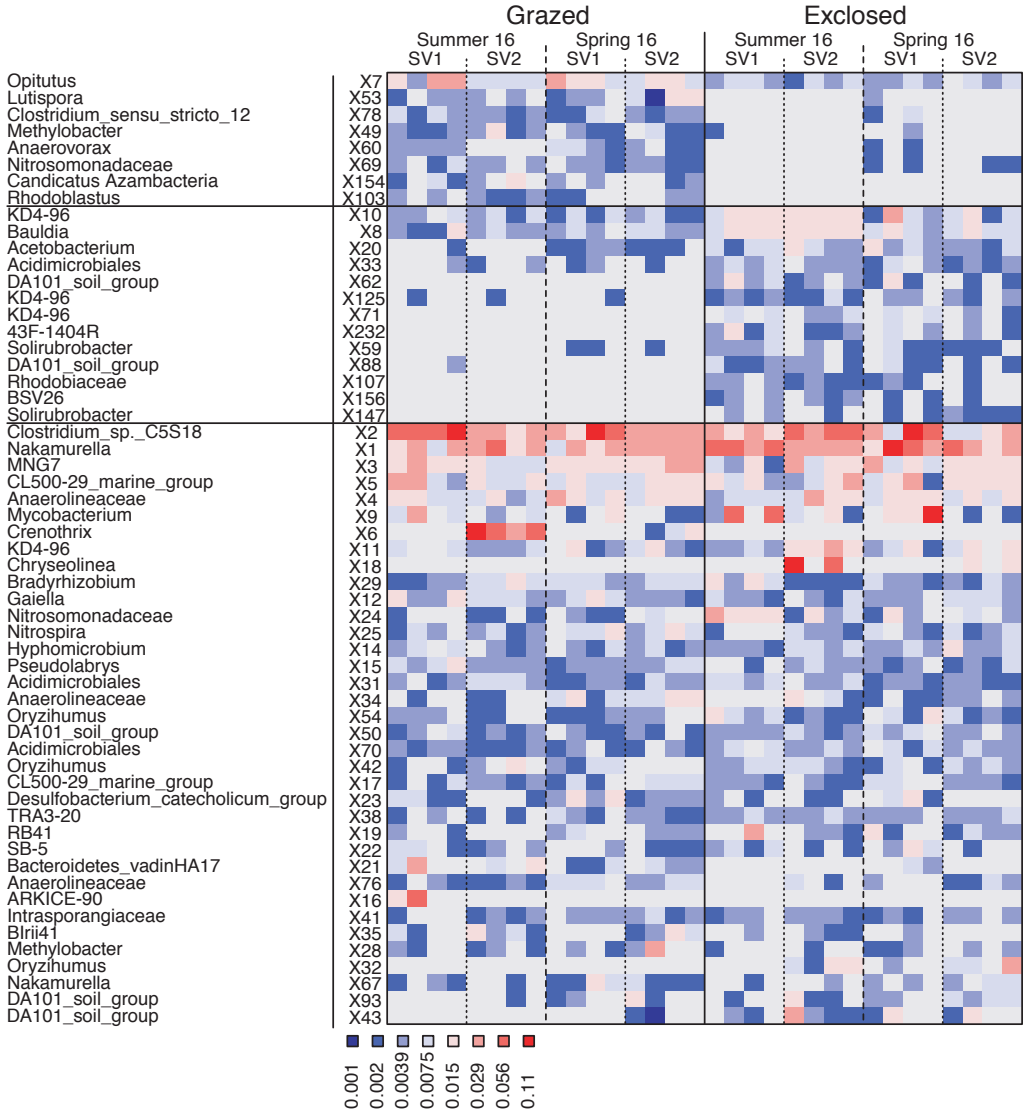

Supplementary Fig. 6: Relative abundances of bacterial OTUs retrieved from 16S rRNA genes *in situ*. Bioindicator OTUs for the grazed treatment are shown in the uppermost section while the bioindicator OTUs for the exclosed treatment are shown in the middle section. In the lowest section we show the OTUs with the highest relative abundances until representing 50% of the community. OTU names consist of the letter X plus a number, marking them as OTUs from the V3-V4 dataset. The color represents the relative abundance of a given OTU in a given sample.

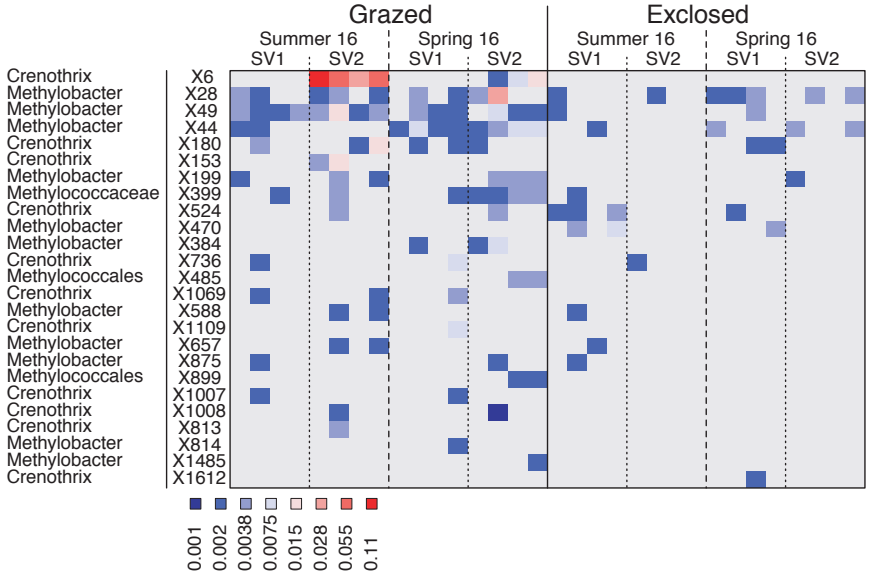

Supplementary Fig. 7: Heatmap showing the increase in OTU abundance *in situ* assigned to the order Methylococcales in grazed treatment, which is visible in Supplementary Figs 5 and 6. OTU names consist of the letter X plus a number, marking them as OTUs from the V3V4 dataset. The color represents the relative abundance of a given OTU in a given sample.

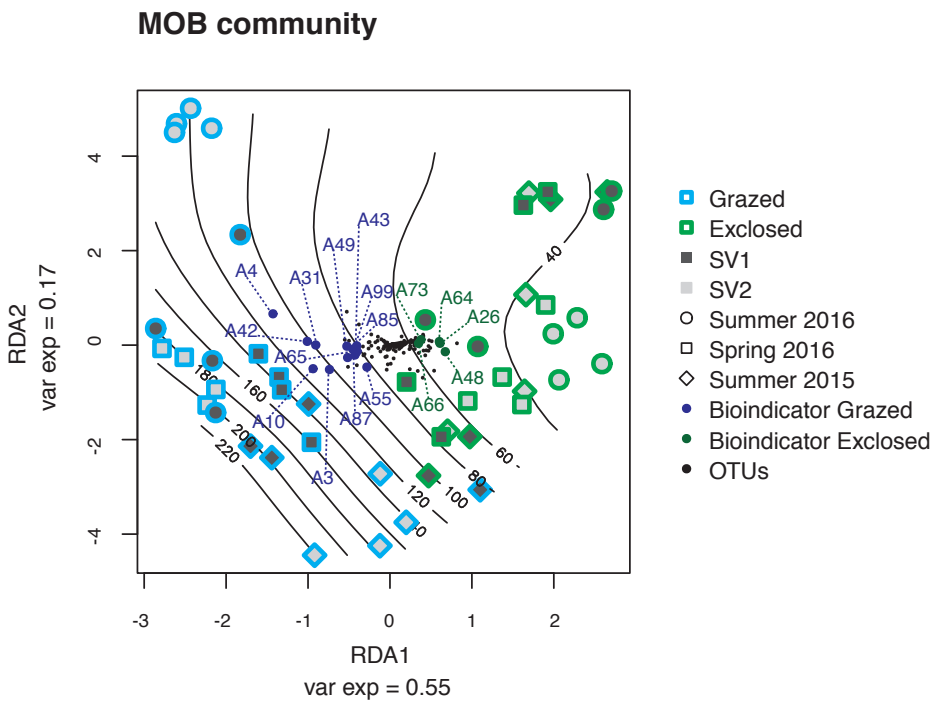

Supplementary Fig.8: Treatment and season-dependent differences in the MOB communities at Solvatn peatland sites. The figure is based on redundancy analysis of the MOB community (*pmoA* transcripts, primer pair A189F/A682R). Samples are labeled according to treatment: grazed (blue) and exclosed (green); sites: SV1 (dark grey) and SV2 (light grey); and sampling season: summer 2015 (tilted square), spring 2016 (square), summer 2016 (circle). Black lines indicate CH_4 oxidation potential (μg CH_4 oxidized per g soil and day). Black dots show the distribution of non-bioindicator OTUs, while green dots represent bioindicator OTUs for exclosed treatment and blue dots represent bioindicator OTUs for grazed treatment. Bioindicator identities are represented by the letter A followed by a number, marking them as OTUs from the A682R *pmoA* dataset. Taxonomic information can be obtained from the heatmap in Supplementary Fig. 11.

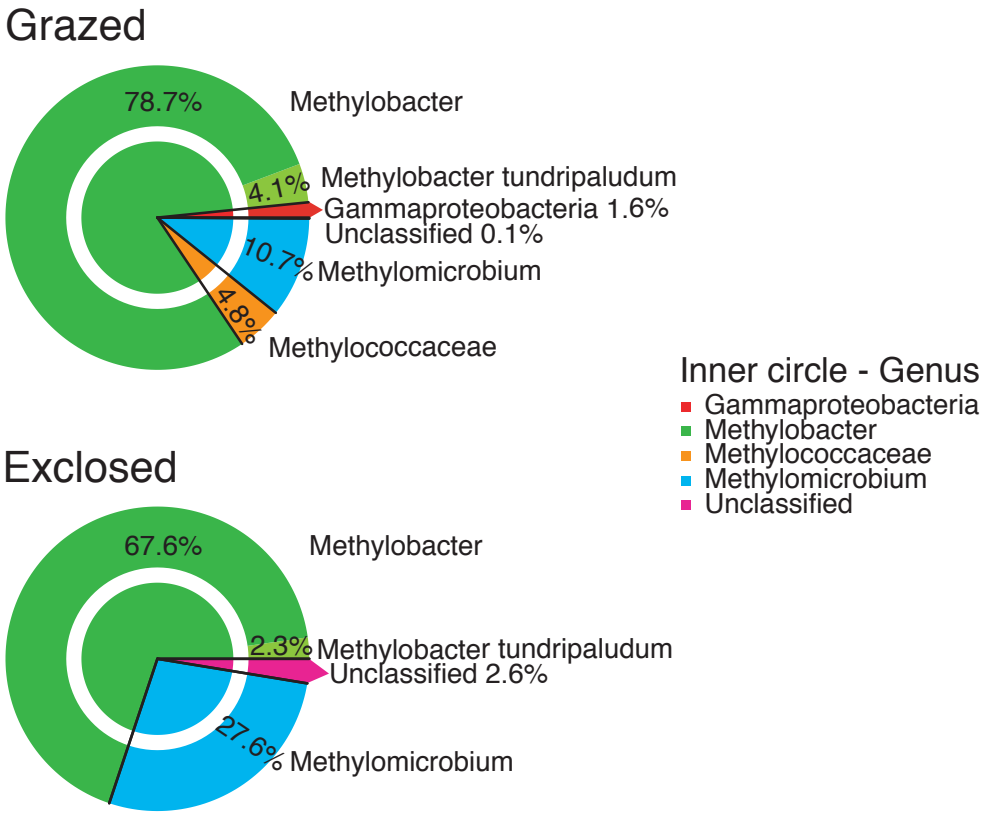

Supplementary Fig. 9: Distribution of MOB taxa (A189F/mb661R primer) in grazed and exclosed treatments. Only taxa with a relative abundance >1% are represented. Relative abundances are listed in the outermost ring of the chart and are given in %. The different rings represent different taxonomic levels, with genus in the innermost ring followed by species in the outermost ring.

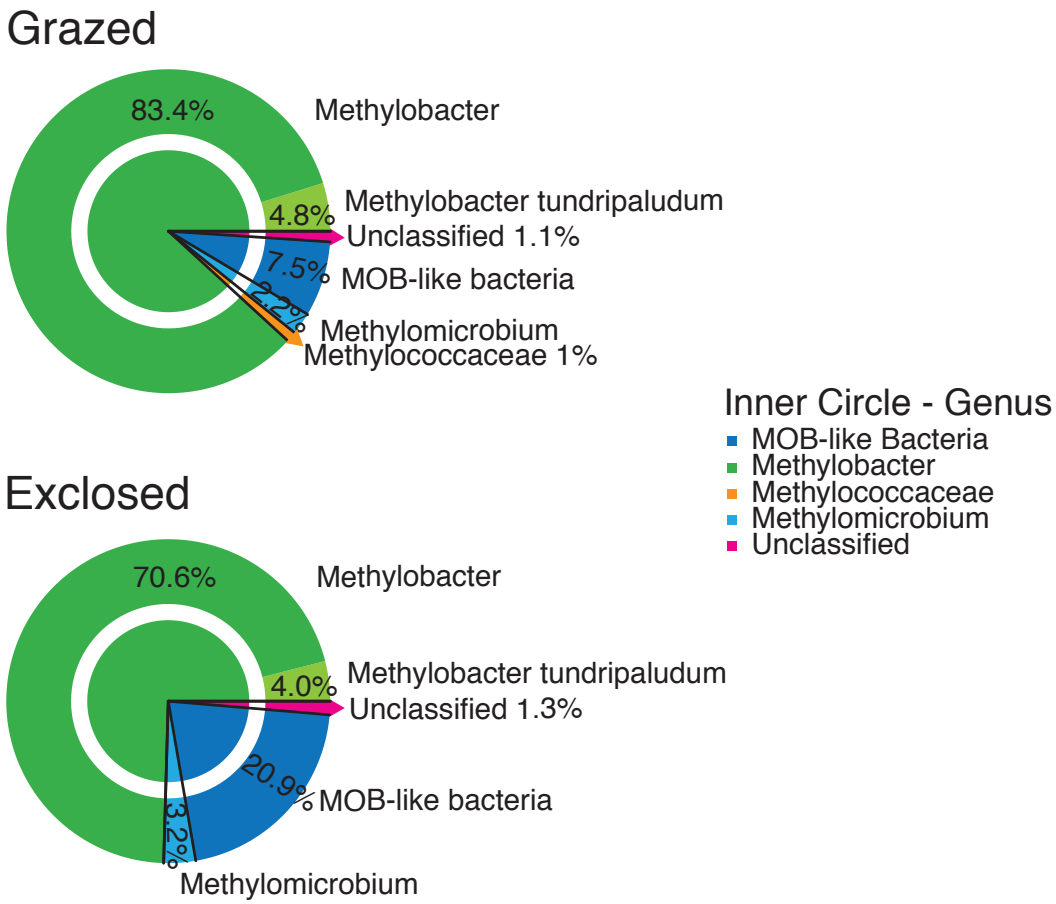

Supplementary Fig. 10: Distribution of MOB taxa (A189F/A682R primer) in grazed and exclosed treatments. Only taxa with a relative abundance >1% were included. Relative abundances are listed in the outermost ring of the chart and are given in %. The different rings represent different taxonomic levels, with genus in the innermost ring followed by species in the outermost ring.

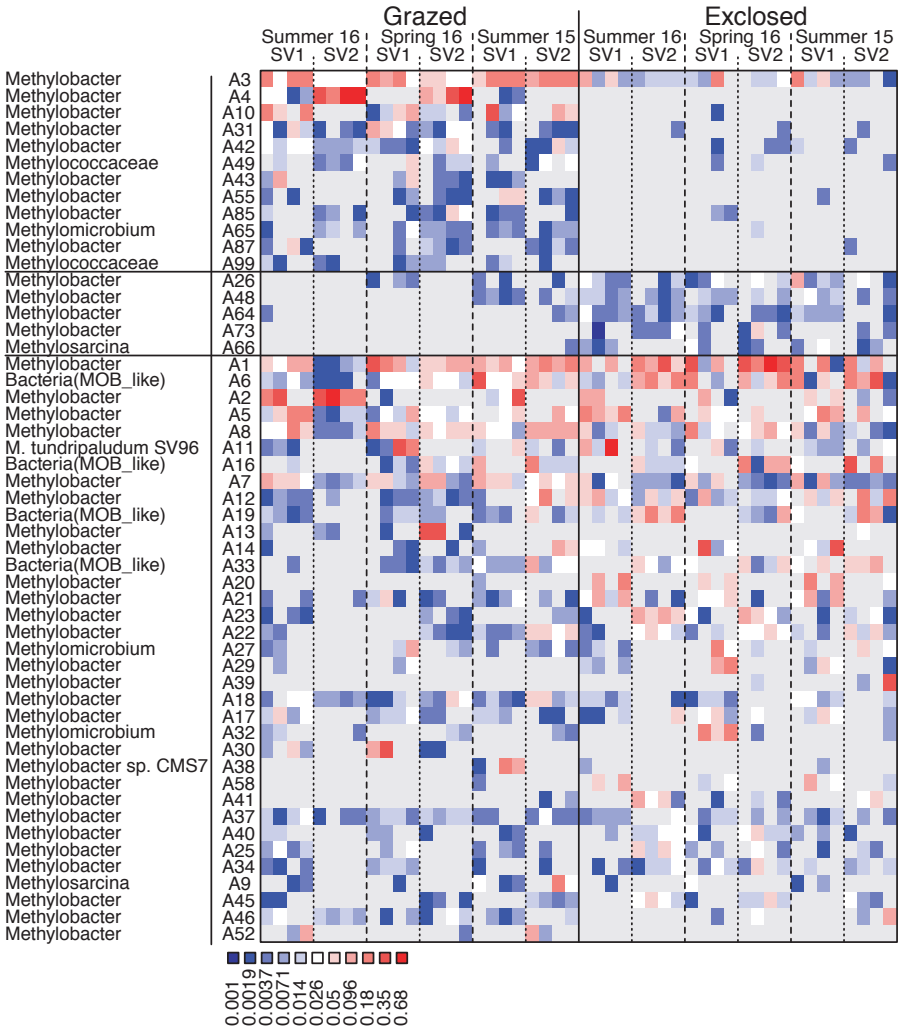

Supplementary Fig. 11: Relative abundances of MOB OTUs retrieved from *pmoA* transcripts *in situ* and *ex situ* (microcosm experiment). Bioindicator OTUs for the grazed treatment are shown in the uppermost section while the bioindicator OTUs for the exclosed treatment are shown in the middle section. In the lowest section we show the MOB OTUs with the highest relative abundance until representing 90% of the community. OTU names consist of the letter A plus a number, indicating them as OTUs from the A682R *pmoA* dataset. The color represents the relative abundance of a given OTU in a given sample

Paper II

microorganisms

MDPI

Article

The Influence of Above-Ground Herbivory on the Response of Arctic Soil Methanotrophs to Increasing CH_4 Concentrations and Temperatures

Edda M. Rainer [1,*], Christophe V. W. Seppey [1,2], Caroline Hammer [1], Mette M. Svenning [1] and Alexander T. Tveit [1]

[1] Department of Arctic and Marine Biology, UiT, The Arctic University of Norway, 9037 Tromsø, Norway; seppey@uni-potsdam.de (C.V.W.S.); c.hammer@boku.ac.at (C.H.); mette.svenning@uit.no (M.M.S.); alexander.t.tveit@uit.no (A.T.T.)

[2] Institute of Environmental Sciences and Geography, University of Potsdam, Karl-Liebknecht-Str. 24-25, 14476 Potsdam, Germany

* Correspondence: edda.m.rainer@uit.no

Abstract: Rising temperatures in the Arctic affect soil microorganisms, herbivores, and peatland vegetation, thus directly and indirectly influencing microbial CH_4 production. It is not currently known how methanotrophs in Arctic peat respond to combined changes in temperature, CH_4 concentration, and vegetation. We studied methanotroph responses to temperature and CH_4 concentration in peat exposed to herbivory and protected by exclosures. The methanotroph activity was assessed by CH_4 oxidation rate measurements using peat soil microcosms and a pure culture of *Methylobacter tundripaludum* SV96, qPCR, and sequencing of pmoA transcripts. Elevated CH_4 concentrations led to higher CH_4 oxidation rates both in grazed and exclosed peat soils, but the strongest response was observed in grazed peat soils. Furthermore, the relative transcriptional activities of different methanotroph community members were affected by the CH_4 concentrations. While transcriptional responses to low CH_4 concentrations were more prevalent in grazed peat soils, responses to high CH_4 concentrations were more prevalent in exclosed peat soils. We observed no significant methanotroph responses to increasing temperatures. We conclude that methanotroph communities in these peat soils respond to changes in the CH_4 concentration depending on their previous exposure to grazing. This "conditioning" influences which strains will thrive and, therefore, determines the function of the methanotroph community.

Keywords: methanotroph; methane oxidation; pmoA amplicon sequencing; *Methylobacter*; grazing pressure; peat soil microcosms; temperature; Arctic

Citation: Rainer, E.M.; Seppey, C.V.W.; Hammer, C.; Svenning, M.M.; Tveit, A.T. The Influence of Above-Ground Herbivory on the Response of Arctic Soil Methanotrophs to Increasing CH_4 Concentrations and Temperatures. *Microorganisms* **2021**, *9*, 2080. https://doi.org/10.3390/microorganisms9102080

Academic Editor: Vitaly V. Kadnikov

Received: 27 August 2021
Accepted: 23 September 2021
Published: 2 October 2021

1. Introduction

Vegetation in parts of the Arctic has changed severely due to increased grazing by geese [1–3]. The higher geese numbers are closely linked to climate and land-use changes, as food sources are increasing in their overwintering grounds [4,5]. Herbivory-induced changes in vegetation lead to changes in below-ground biota and their productivity [6–8] and affect the balance of greenhouse gases in wetlands, with higher methane (CH_4) emissions from areas subjected to grazing [8–11]. The exclusion of herbivores from patches of Arctic peatlands led to the restoration of vascular plant growth [12], and it was shown that higher abundances of vascular plants alter the polysaccharide composition in these soils, further changing the soil microbial community [13].

At the same time, the Arctic is warming two to three times faster than the global average, an effect known as Arctic amplification [14–16]. A result of this is the acceleration of permafrost thaw and a thickening of the active layer, with longer periods of non-frozen topsoil [17]. Thawing permafrost contains organic carbon, which can be metabolized

by microbes that emit carbon dioxide (CO_2) and CH_4. It has been shown that even small increases in temperatures can lead to substantial increases in CH_4 production by peat soil microorganisms under anoxic conditions [18–21]. Increased CH_4 production can potentially lead to increased CH_4 emissions, further increasing global temperatures through radiative forcing.

CH_4 production is counterbalanced by methane-oxidizing bacteria (MOB; methanotrophs). MOB act as a biological filter for CH_4 and play a key role in mitigating CH_4 emissions from peat and other soils. Many MOB live at the oxic/anoxic interface in peatland soils [22,23], oxidizing CH_4 for energy harvest and biomass synthesis. MOB are a diverse group of bacteria belonging to the phyla *Gamma-* and *Alphaproteobacteria* and *Verrucomicrobia* [24]. The diversity of MOB communities is affected by environmental variables such as pH and oxygen (O_2). Many cold and neutral pH soils are inhabited by low-diversity communities of MOB, dominated by the genus *Methylobacter,* e.g., [25–27]. In contrast, cold acidic soils are more likely to be dominated by members of the *Alphaproteobacteria*, such as the genera *Methylocystis* and *Methylocapsa* [24,28–30].

MOB found in Arctic soils have temperature growth patterns ranging from psychrotrophic to mesophilic; these MOB communities can, therefore, respond to large temperature changes [26,31–33]. However, physiological and ecological temperature responses and how these affect community CH_4 oxidation rates are not well understood. In line with our limited understanding of this, studies have shown that temperature effects on CH_4 oxidation rates are inconsistent, ranging from, for example, strong temperature responses in landfill soils [34] to variable responses in permafrost soils [35] and a lack of responses in forest soils [36]. On the contrary, the physiological responses of different MOB species to temperature based only on growth are highly predictable [37]. The relationship between temperature, growth rates, and soil CH_4 oxidation rates depends on numerous variables, such as soil CH_4 and nutrient concentrations, enzyme kinetics, physiological acclimation, and growth responses of individual strains and overall MOB population sizes. Additionally, the types and numbers of different strains responsible for oxidation are also likely to affect CH_4 oxidation rates.

Due to the numerous controls on MOB communities and their activities, it may be anticipated that the type of soil habitat strongly influences potential CH_4 oxidation rates. In adjacent but chemically and structurally different permafrost soil habitats, different CH_4 oxidation rates were observed, with higher rates in soils exposed to the highest CH_4 concentrations [35]. Substrate availability, that is, CH_4 concentrations, have been shown to control CH_4 oxidation rates in both lakes and forest soils [38,39]. Similarly, peat exposed to herbivory displayed differently structured microbiota, including altered MOB habitats and higher CH_4 oxidation potentials than peat protected from herbivory by barnacle geese [13,27].

However, it is still unclear how peat MOB communities respond to changes in temperature and CH_4 production. It is also unknown how herbivory influences this response. The objective of this study was to investigate the effect of increasing CH_4 concentrations and temperatures on MOB community activities in samples representing two different Arctic peat soil ecosystem states—(1) peat exposed to geese grazing for more than 20 years, and (2) peat protected from grazing for the last 20 years.

2. Materials and Methods

2.1. Field Site and Sampling

Samples were collected in August 2016 at Solvatn. The Solvatn peatland (N78°55.550, E11°56.611) is located close to the Ny Ålesund research station and settlement in Svalbard. It is heavily grazed by Barnacle geese (*Branta leucopsis*) and dominated by brown mosses, primarily *Calliergon richardsonii* [40]. Exclosures established in 1998 protect parts of the peatland vegetation from grazing geese [12], allowing for the growth of vascular plants that are otherwise suppressed by grazing. From one site, named SV1 in a recent study [27], two blocks (approximately 30 × 15 × 30 cm) were cut from the peat soil protected from

grazing (SV1 EX1 and SV1 EX2) as well as from the adjacent grazed peat soils (SV1 GR1 and SV1 GR2) and directly transferred to zip-lock plastic bags. All four blocks were kept cool during transportation from the field sites to the on-site laboratory (approximately 5 min) and then frozen at −20 °C upon arrival. The blocks were further shipped, frozen, to the laboratory in Tromsø, Norway, and stored at −20 °C until being used for the microcosm experiments. The experiments were not carried out in the field laboratory due to lacking infrastructure. Consequently, the samples were stored frozen to avoid extended storage in a non-frozen condition that could lead to system changes. These soils are exposed to freezing conditions for most of the year, including freeze and thaw occurrences during spring and autumn. Nevertheless, to evaluate the effects of freezing, CH_4 oxidation rates were quantified both immediately after thawing and again after a three-week incubation. We also added an additional pre-incubation period to one of our two experiments to test whether prolonged incubation would lead to even higher oxidation rates. Details of this step are presented in Section 2.2.

2.2. Soil Microcosms

This study was based on two peat soil microcosm experiments, referred to as Exp I and Exp II. The microcosms were organized in a fully crossed factor design to study the combined effect of two CH_4 concentrations and two temperatures on the two grazing treatments (grazed and exclosed peat).

The zone of maximal CH_4 oxidation in the Arctic peat soil, as previously identified in situ [27], was used for the experiments. In grazed soils, this zone was located at a depth of 0.5–2.0 cm, while in exclosed soils, it was located at a depth of 4–8 cm [27].

The experimental temperatures were 8 °C and 15 °C. The lower temperature of 8 °C is a frequently encountered surface soil temperature at this high latitude during summer (5.4–10.0 °C for grazed soils and 4.4–9.8 °C for exclosed soils at a depth of 5 cm, [27]), while 15 °C is at the high end of temperatures recorded in the vegetation layer of Arctic peat soil in summer [27,41,42]. The experimental headspace CH_4 concentrations were 0.1% (about 2 µM of dissolved CH_4 at 8 °C and 1.7 µM of dissolved of CH_4 at 15 °C) and 1% (about 20 µM of dissolved CH_4 at 8 °C and about 17 µM of dissolved CH_4 at 15 °C), imitating commonly occurring CH_4 concentrations in the upper layers of these soils. Soil CH_4 concentrations previously observed ranged from 100.7–237.4 µM (avg 153.5 µM) in grazed sites at a depth of 5 cm and from 0.4–3.7 µM (avg 1.5 µM) in exclosed sites at a depth of 10 cm [27].

For Exp I, peat blocks were thawed at 8 °C overnight. Layers 0–2 cm deep of the grazed peat soil and layers 5–7 cm deep of the exclosed peat soil were cut from the peat blocks. Then, 4 g of peat soil were weighed into 50 mL serum bottles (16 bottles with grazed and 16 bottles with exclosed peat soil). Each vial was closed with butyl rubber stoppers (Wheaton) and aluminum crimp caps [43].

We injected 0.07 mL CH_4 (95% *v/v*) into 16 bottles (8 bottles per grazing treatment) to obtain a headspace concentration of 0.1% CH_4, while 16 bottles (8 bottles per grazing treatment) were injected with 0.7 mL CH_4 (95% *v/v*) for a headspace concentration of 1% CH_4. For each grazing treatment, four bottles with 0.1% CH_4 and four bottles with 1% CH_4 were incubated at 8 °C and at 15 °C, respectively. In total, the experiment consisted of 32 bottles.

At the start of the experiment, the initial CH_4 oxidation rates were calculated from four CH_4 concentration measurements made within the first 20–40 h for each bottle. At each time point, 0.5 mL gas samples were retrieved from the headspace with a pressure-lock syringe (Vici Precision Sampling, LA, USA) and injected directly onto a Haysep-D packed column of a GC-FID (SRI Instruments, CA, USA). The elution time was 1.8 min for CH_4, and the instrument was set to maximum sensitivity. The CH_4 concentrations were calculated by comparing them to the injected standard gases (Messer, Switzerland). After the first four sampling time-points, an incubation period of three weeks started, during which the CH_4 headspace concentrations were maintained at 0.1% or 1%. The CH_4

was consumed rapidly in some of the microcosms and was, therefore, supplied at regular intervals to ensure that the concentrations never dropped below 0.05% or 0.8% CH_4 for the 0.1% or 1% conditions, respectively.

At the end of the incubation period, the CH_4 oxidation rates were estimated with the four measurements described above for the start of the experiment. After the CH_4 oxidation rate measurements, the peat soil from each microcosm was transferred into sterile 15 mL tubes and flash frozen in liquid N_2 to be used for RNA extraction.

After evaluating the results of the first experiment, we decided to perform a second experiment (Exp II) with a slightly altered setup, designed to provide even more certainty on three potentially crucial factors—soil depth, pre-incubation length, and pre-incubation temperature.

Twice the number of microcosm replicates for all conditions (64 bottles in total) were used in Exp II to better represent the variability in potential CH_4 oxidation rates between the two grazing treatments. We also included a pre-incubation week at 4 °C for all microcosms. For the 15 °C microcosms, this was followed by another pre-incubation week at 8 °C to avoid abrupt large temperature increases unlikely to occur in nature. Because of this additional week, the microcosms incubated at 15 °C were incubated for one week longer than the 8 °C microcosms, while the incubation at the final temperature (i.e., 8 or 15 °C) was the same for both sets of microcosms. In Exp II, we targeted a soil layer 4 cm thick to ensure that the entire zone of the highest CH_4 oxidation potential [27] was included. The considerable variation in the CH_4 oxidation rates between some replicates in Exp I suggest that the selection of a narrow 2 cm layer could have excluded the most active zone, in some cases, due to local variations. Therefore, we sampled a layer at a depth of 0–4 cm for the grazed treatment and at a depth of 4–8 cm for the exclosed treatment for Exp II. The bottles were then prepared in the same way as for Exp I.

The soil water content was determined gravimetrically by drying 5 g of soil from each layer at 150 °C in triplicate. The determined water content was used to calculate the soil dry weight and the CH_4 oxidation rate per gram of dry soil for each microcosm.

To consider the different solubility of CH_4 in pore water at 8 °C and 15 °C, the CH_4 oxidation rates for the same dissolved concentrations of CH_4 were estimated. Assuming first-order rate kinetics, as previously shown in [44], we log-transformed the decline in CH_4 over time and fitted linear regression models to the transformed plots. The slopes of the linear models correspond to the rate constants. By multiplying the respective rate constants by a CH_4 concentration that would result in the same dissolved CH_4 concentrations at 8 and 15 °C, we obtained adjusted rates at these temperatures. The fit of the linear model was evaluated and considered to have a satisfactory coefficient of determination, giving the following values: R^2—8 °C = 0.71 to 0.99, R^2—15 °C = 0.71 to 0.99; 147 of the 192 linear models had an R^2 of > 0.9.

2.3. CH_4 Oxidation of Methylobacter Tundripaludum SV96

M. tundripaludum SV96 was cultivated in NMS medium [45] for 10–14 days at 8 and 15 °C under a headspace CH_4 concentration of approximately 13% (20 mL of a mixture of 95% CH_4 and 5% CO_2). To reach exponential growth, the culture was transferred to fresh medium three times during this period. Serum bottles were incubated on rotary shakers at 150 rpm. Exponentially growing cells were harvested and diluted in sterile 0.5 mM phosphate buffer (pH = 6.8) to a density of about 5×10^7 cells per ml. Then, 21.6 mL of this diluted cell suspension was distributed into 125 mL serum bottles (3 bottles per concentration and temperature; 24 in total), which were then closed with butyl rubber stoppers (Wheaton) and aluminum crimp caps. Headspace atmospheres were prepared by injecting different amounts of CH_4 (0.2, 0.6, 1.5, and 3 mL of 95% CH_4 and 5% CO_2) to create a series of CH_4 headspace concentrations (about 1900, 5400, 13,000, and 25,000 ppm, respectively) with three bottles per CH_4 concentration. In addition, a negative control that contained only phosphate buffer and no bacterial cells was measured.

The CH_4 concentrations were measured at four time points (including time point zero, right after the headspace preparation) over the course of eight hours. To measure the headspace CH_4 concentration, 0.5 mL of gas was collected with a pressure-lock syringe (VICI) and directly injected into a GC-FID, as was described for the soil microcosms. Starting at time point one, 340 µL of cell suspension was collected from each of the bottles after the CH_4 measurements to estimate the cell density. The cell density was measured by optical density (OD) at 410 nm. The densities were converted into cell numbers with a standard of cell numbers and OD measurements specifically made for *M. tundripaludum* SV96. The standard was established by cultivating *M. tundripaludum* SV96 to 14 different optical densities ranging from 0.0085 OD410 to 0.7295 OD410 and counting, for each OD, the number of cells at that optical density using a counting chamber under a light microscope. The cell counts ranged from 6.1 to 726.6 $\times$ 10^5, corresponding to a linear model R^2 of 0.92. The estimation of cell numbers allowed us to adjust the CH_4 oxidation rates to the number of cells as this number increased throughout the experiment. Between measurements, the flasks were incubated at the respective temperatures on a rotary shaker at 150 rpm [46].

The headspace and dissolved CH_4 concentrations were calculated from the measured peak areas using a range of defined standards. Concentrations were converted into masses of CH_4 using the ideal gas law, while Henry's law was used to estimate the corresponding mass of dissolved CH_4. All numbers were adjusted for the removal of gases and medium during the sampling. The CH_4 oxidation rates calculated between each time point were then normalized to the time between measurements and the number of cells in the medium to obtain a rate (µmol of CH_4 oxidized per 10^8 cells per hour).

Assuming first-order rate kinetics, as previously shown in [44], we log-transformed the cell-normalized decline in CH_4 over time and fitted linear regression models to the transformed plots. The slopes of the linear models correspond to the rate constants. By multiplying the respective rate constant by the desired concentration of CH_4, we obtained the rates of oxidation at these concentrations [44]. The fit of the linear models was evaluated and considered to have satisfactory coefficients of determination, giving the following values: R^2—8 °C = 0.83–0.99, R^2—15 °C = 0.72–0.99; 24 of the 28 linear models had an R^2 of > 0.9.

2.4. RNA Extraction

Nucleic acids were extracted from the peat soil samples from Exp I. The samples were homogenized using a mortar and pestle while suspended in liquid nitrogen. The nucleic acids were extracted from 0.2 g of peat soil (two technical replicates per sample) using a modified version of Griffiths' protocol [42,47]. For RNA extraction, the two replicates were pooled, and DNA was removed (RQ1 DNase, Promega, Madison, WI, USA), which was followed by RNA clean-Up (MegaClear™ Transcription Clean-Up Kit, Ambion™, Thermo Fisher Scientific, Waltham, MA, USA) and ethanol precipitation. The RNA quality was controlled by gel electrophoresis and a Nanodrop (Thermo Fisher Scientific, Waltham, MA, USA). The RNA was reverse transcribed using Superscript IV (Thermo Fisher Scientific, Waltham, MA, USA) and the cDNA was used as a template for PCR with the primer pair A189F/mb661R [48] to confirm the presence of the *pmoA* gene transcript. The cDNA samples were sent for amplicon generation and sequencing with Illumina MiSeq at the IMGM laboratories in Planegg, Germany. For the amplicon generation, both the A189F/mb661 and A189F/A682R primers sets were applied, further referred to as the mb661R and A682R datasets [48,49]. The *pmoA* transcript amplicons were generated in a 2-step target-specific (TS) PCR (using 10 ng of cDNA as a template) for 25 cycles, followed by a 12-cycle index PCR using 1 µL from the TS PCR products. The polymerase used for amplification was the Q5® High-Fidelity polymerase from NEB (Ipswich, MA, USA).

2.5. PmoA Transcript Numbers

The cDNA samples were diluted to 2.5 ng/µL for quantification with qPCR. For the standard curve, genomic DNA of *M. tundripaludum* SV96 was checked for integrity using gel electrophoresis and quantified using Qubit Fluorometric Quantification (Thermo Fischer Scientific, Waltham, MA, USA). Copy numbers of *pmoA* were calculated based on genomic information and the measured concentration. The standard curve was generated using dilutions of the DNA from *M. tundripaludum* SV96, yielding 7.15×10^6 to 7.15 *pmoA* copies. The diluted cDNA samples and the diluted standards were analyzed in triplicate. The negative controls (no template) were analyzed simultaneously in at least six replicates. The master mix and primer for the qPCR were the SsoFast Evergreen Supermix (Biorad, Hercules, CA, USA) and the A189/mb661R primer pair [48], respectively. The thermal profile for qPCR amplification [50] was used with the following modifications: Fluorescence data acquisition was performed at 78 °C for 30 s, and a total of 35 cycles were performed after the initial 10 cycles of touchdown qPCR. Melting curve analysis was performed from 65 °C to 95 °C. The calculations for each replicate were performed within the qPCR software (CFX Manager, Biorad, Hercules, CA, USA) based on the standard curve. The number of *pmoA* transcripts per gram of dry soil was calculated based on the average of the three replicates.

2.6. Bioinformatics

2.6.1. Databases

For the taxonomical assignation, a de-replicated database was built with sequences trimmed according to the corresponding *pmoA* primer sets. Sequences used for the two *pmoA* databases [51] were complemented with three *Methylobacter* sequences (GenBank id=AJ414658.1, KC878619.1, and the sequence from an Arctic coalmine isolate from Svalbard (not published)).

2.6.2. Pipeline

Reads were merged using the program Flash (v. 1.2.8; [52]) and low-quality sequences were discarded if they had a 50 nucleotide fragment with an average Phred score below 20 prior to trimming the primers. Chimeras were removed using the program Vsearch (v. 2.4.4; [53]), both against a database (for *pmoA* primers [51]) and de novo. To avoid frameshift errors, only sequences without stop codon errors or framing errors (the nucleotide number is not divisible by three) were kept. OTU clustering was performed using Swarm (v. 2.1.13; [54]), and taxonomically assigned using the best alignment between the dominant sequence of each OTU and the database, using Ggsearch36 (v. 36.3.8f; [55]). Finally, the OTUs were selected according to their dominant sequence length (mb661: (465,474)), A682: (492,495)) to remove obvious sequencing errors. An overview of all the steps in the pipeline is given in Supplementary Table S1.

2.6.3. Community Analyses

To normalize for sequencing depth, we used the relative abundance of the two MOB communities. To avoid noise caused by low-abundance OTUs in a given sample, every OTU representing less than a thousandth of the community in this sample was considered as absent from that sample. This denoising step removed less than 5% of the reads.

2.6.4. Redundancy Analysis (RDA)

Prior to analyses, the community matrices were log-normalized according to the methods of [56] (function decostand, package vegan v. 2.4-2; [57]). For each primer pair, the effects of elevated CH_4 and elevated temperature were estimated for the microbial communities using a redundancy analysis (RDA, function capscale, package vegan v. 2.4-2; [57]). To only consider the effect of the CH_4 and temperature treatments, the effects of the peat block replicates were considered random variables. The effect of the factors, as well as the significance of the ordination axes were tested with a permutation test

(10,000 permutations, function anova.cca, package vegan v. 2.4-2; [57]). To disentangle the effects of interactions between the grazing treatments, an RDA was calculated for each grazing treatment and tested in the same fashion as the analysis performed on all samples.

2.6.5. Bioindicators

For each primer pair and grazing treatment, the "responding bioindicator OTUs" for both CH_4 concentrations were identified using an indicator species analysis (indval; function indval, package labdsv v. 1.8-0; [58]). An OTU was selected as a "responding bioindicator OTU" if the probability of reaching a higher indicator value than that of the bioindicator after 10,000 permutations was lower than 0.01. "Responding bioindicator OTUs" were only reported in heatmaps.

We further selected the "unconditional bioindicator OTUs" by one of two criteria—(1) OTUs that respond to either 0.1% or 1% CH_4 in both the grazed and exclosed peat soil microcosms; (2) OTUs that respond to either 0.1% or 1% CH_4 in the grazed peat soil and are absent from exclosed peat soil microcosms, or the other way around.

2.6.6. Phylogenetic Analysis

For the phylogenetic analysis, only "unconditional bioindicator OTUs" were included. Phylogenetic trees were then built from the "unconditional bioindicator OTU" sequences and closely related sequences were retrieved from the NCBI GenBank to better assess their taxonomy. These closely related sequences were obtained by aligning the bioindicator sequences (using BLASTn) against the NCBI nucleotide database and selecting the two-highest scoring matches. A set of cultivated gammaproteobacterial MOB sequences were retrieved in addition to a set of *pmoA* sequences belonging to upland-soil cluster (USC)-gamma, the latter serving as an outgroup to root the tree. Sequences were aligned in MEGA10 [59] using MUSCLE with UPGMB clustering [60]. The length of the alignment was inspected visually for an overlap in all sequences and a section of 452 bp (the mb661R dataset) was chosen for phylogenetic analysis. A phylogenetic tree was constructed in MEGA10 using the neighbor-joining method with the Jukes–Cantor correction and 500 bootstraps [59]. In addition, phylogenetic trees using the maximum likelihood and the minimum evolution method (with the Jukes–Cantor correction and 500 bootstraps each) were generated and compared to the first tree.

3. Results

3.1. CH_4 Oxidation Rates Changing in Response to CH_4 Concentrations

Incubation under microcosm headspace atmospheres with 1% CH_4 resulted in higher CH_4 oxidation rates than with 0.1% CH_4 for both grazed and exclosed peat soils. This effect was observed both before and after the three-week incubation period (Figure 1 and Supplementary Figure S1). Additionally, the CH_4 oxidation rates were always higher after the three-week incubation (Supplementary Figures S2 and S3), showing that the MOB community responded positively to prolonged incubation at stable conditions after thawing. However, the oxidation rates after the three-week incubation period were similar in Exp I (Supplementary Figure S2) and Exp II (Supplementary Figure S3), confirming that the additional pre-incubation at 4 °C and 8 °C in Exp II had negligible effects on the CH_4 oxidation rate. This suggests that within the first three weeks, this MOB community had reached its full potential under the present conditions. Overall, higher CH_4 oxidation rates were observed in the grazed peat soils.

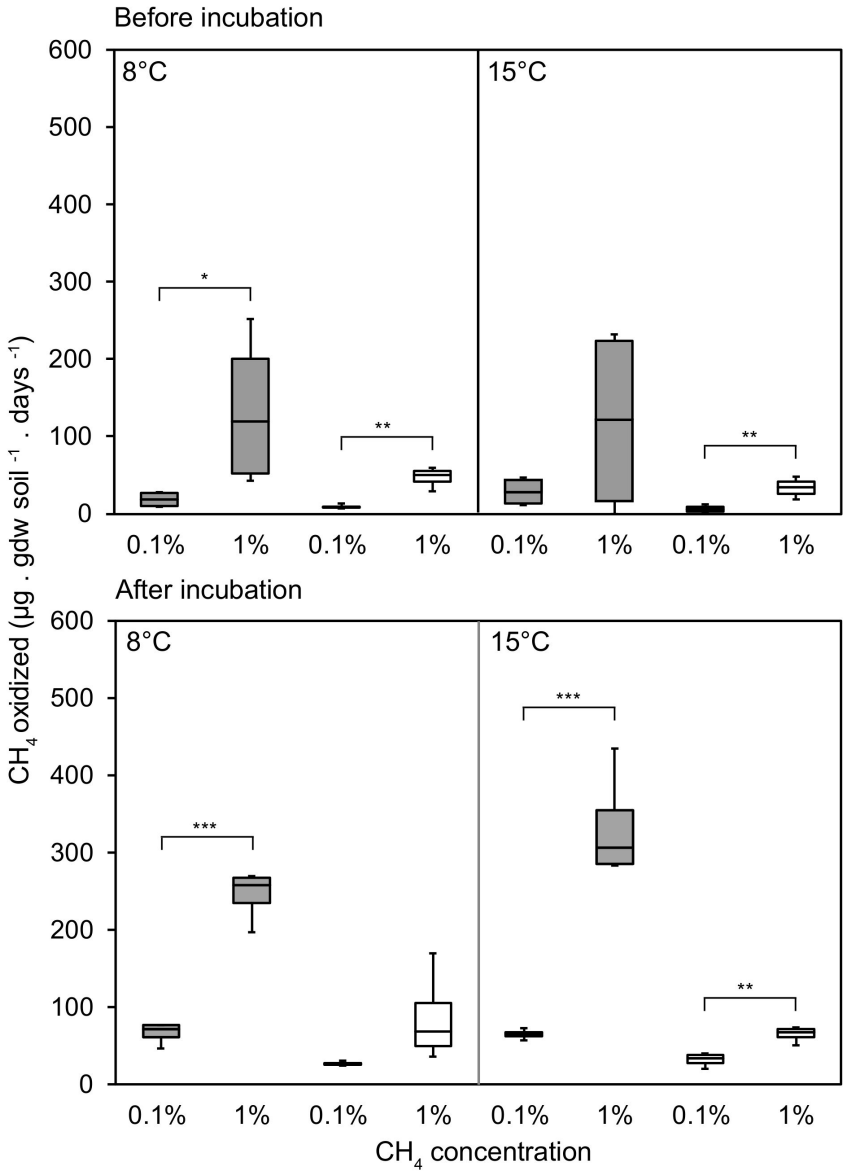

Figure 1. CH_4 oxidation rates from Exp I, emphasizing the comparison between 0.1% and 1% headspace CH_4 concentrations. Results are shown for measurements collected before (top) and after (bottom) the three-week incubation period, and at 8 (left) and 15 °C (right). Grazed microcosms are shown in gray; exclosed microcosms in white. Comparison using linear mixed models with peat blocks as random variables shows significant differences in the CH_4 oxidation rates between CH_4 concentrations (* $p < 0.05$; ** $p < 0.01$; *** $p < 0.001$).

3.2. CH_4 Oxidation in Response to Temperature

We observed mostly minor and insignificant temperature effects on CH_4 oxidation rates in grazed and exclosed peat soils, both before and after the three-week incubation (Figure 2 and Supplementary Figure S4). Exceptions to this were the significantly higher CH_4 oxidation rates at 15 °C compared to 8 °C in grazed peat soils at 0.1% CH_4 before the three-week incubation in both experiments. In exclosed peat soils from Exp II, significantly higher CH_4 oxidation rates at 15 °C were also measured at 1% CH_4 before the incubation, while significantly lower rates were measured in exclosed peat soil microcosms at 0.1% CH_4 after the incubation.

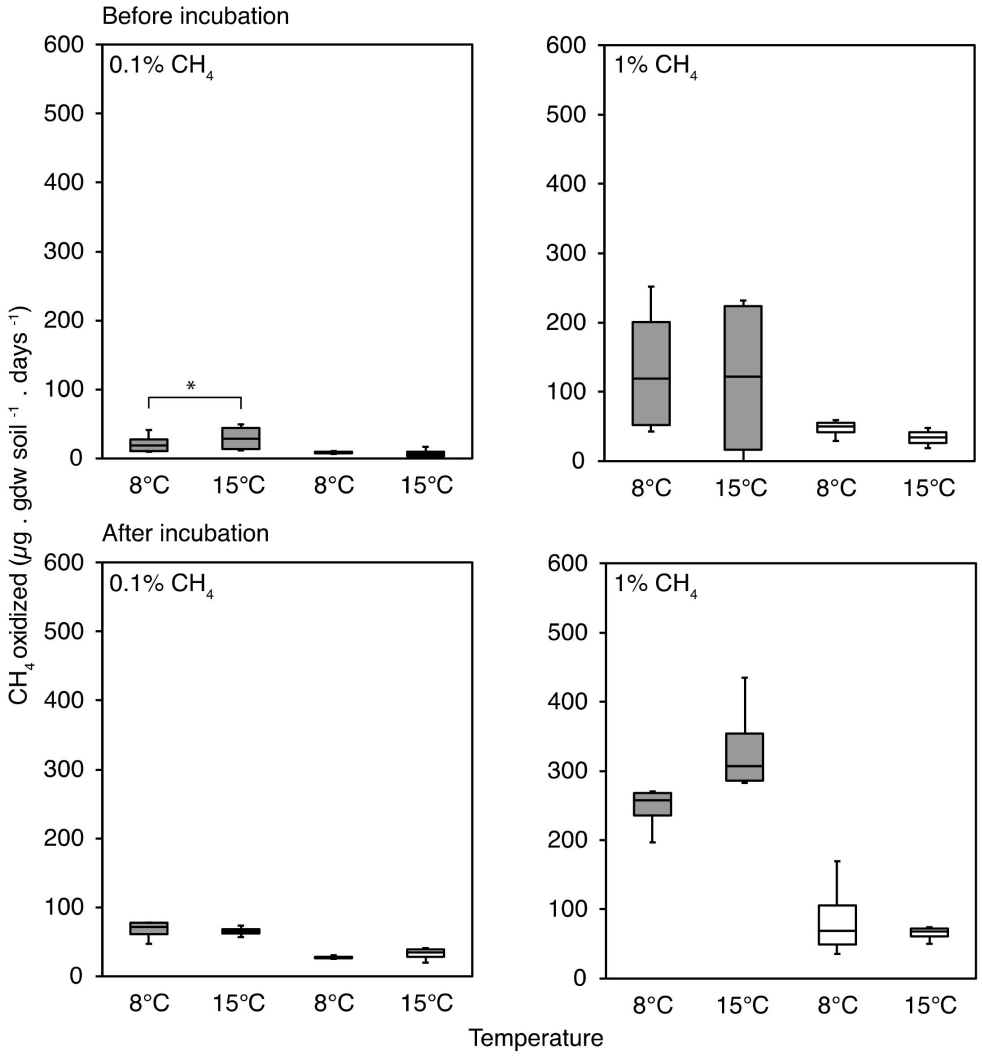

Figure 2. CH_4 oxidation rates from Exp I, emphasizing the comparison between 8 °C and 15 °C. Results are shown for measurements collected before (top) and after (bottom) the three-week incubation period, and at 0.1% (left) and 1% CH_4 (right). Grazed microcosms are shown in gray; exclosed microcosms in white. Comparison using linear mixed models with peat blocks as random variables shows significant differences in the CH_4 oxidation rates between temperatures (* p = 0.05–0.01).

3.3. CH_4 Oxidation in a Pure Culture of M. Tundripaludum SV96 in Response to Temperature

M. tundripaludum SV96 was isolated from the peat soil habitat sampled for the experiments above [32]. To better understand the soil oxidation rates and temperature responses described above, we designed a CH_4 oxidation experiment with *M. tundripaludum* SV96 using the same two temperatures (8 °C and 15 °C) and CH_4 concentrations (0.1% and 1%) for comparison. We observed the highest CH_4 oxidation rates per cell number at 1% CH_4 concentration and we also observed a clear effect of temperature at this concentration, with approximately twice as high CH_4 oxidation rates at 15 °C compared to 8 °C (Figure 3).

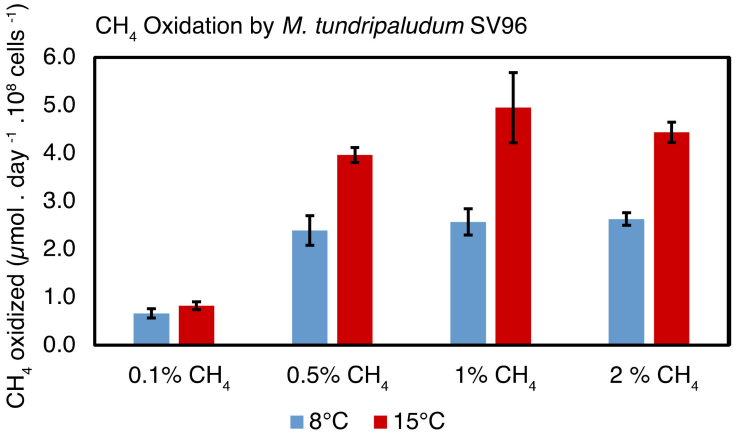

Figure 3. CH_4 oxidation per cell for *Methylobacter tundripaludum* SV96 at 8 °C (blue) and 15 °C (red) with CH_4 headspace concentrations ranging from 0.1% to 2%.

However, the temperature effect on the CH_4 oxidation rate at 0.1% headspace concentration was much smaller and not significant ($p = 0.3$). Adjusting the rate according to the CH_4 solubility, we observed a similarly small but significant difference ($p = 0.006$, Supplementary Figure S7).

3.4. MOB Community

3.4.1. *PmoA* Transcript Numbers

A higher number of *pmoA* transcripts at 1% CH_4 than at 0.1% CH_4 was detected in the grazed peat soils. This difference was significant at 15 °C (linear mixed model (lmm) $p = 0.04$), but not at 8 °C (lmm $p = 0.28$) (Figure 4). In the exclosed peat soils, no significant differences in *pmoA* transcript numbers related to the CH_4 concentration were detected. Overall, the *pmoA* transcript numbers were lower for the exclosed peat soils than for the grazed peat soils (0.1% CH_4 lmm $p = 0.04$ at 15 °C; 1% CH_4 lmm $p = 0.01$ at 8 °C, and $p = 0.02$ at 15 °C). An exception was found at 0.1% CH_4 at 8 °C (lmm $p = 0.07$), suggesting a transcriptionally less active MOB community was responsible for the lower CH_4 oxidation rates in the exclosed peat soils.

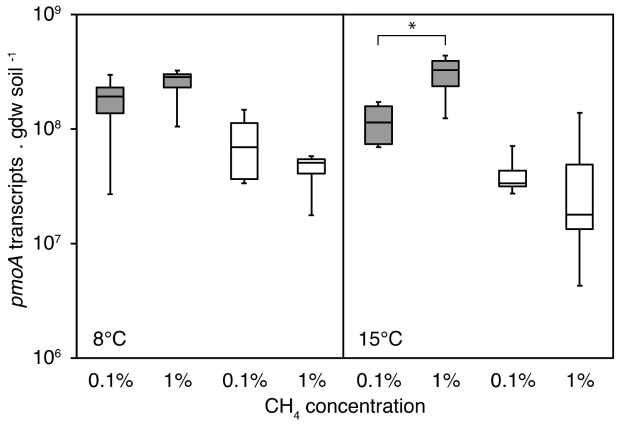

Figure 4. MOB *pmoA* transcript number after the three-week incubation at 0.1% and 1% CH_4 in grazed (gray) and exclosed sites (white). The left panel shows microcosms incubated at 8 °C and the right panel shows microcosms incubated at 15 °C. The y-axis shows *pmoA* transcript numbers per gram dry soil, log-transformed. Pairwise comparison using linear mixed models with peat blocks as random variables shows significant differences in the *pmoA* transcripts (* $p = 0.05$–0.01).

3.4.2. Transcriptionally Active MOB

The active MOB communities were identified by sequencing *pmoA* transcripts from Exp I. The CH_4 concentration had a significant effect on the composition of MOB community transcripts ($p < 0.001$ for both the mb661R and the A682R dataset) (Figure 5 and Supplementary Figure S8). Temperature, on the other hand, had no significant effect on the MOB community transcript composition ($p = 0.264$ for mb661R and $p = 0.449$ for A682R datasets).

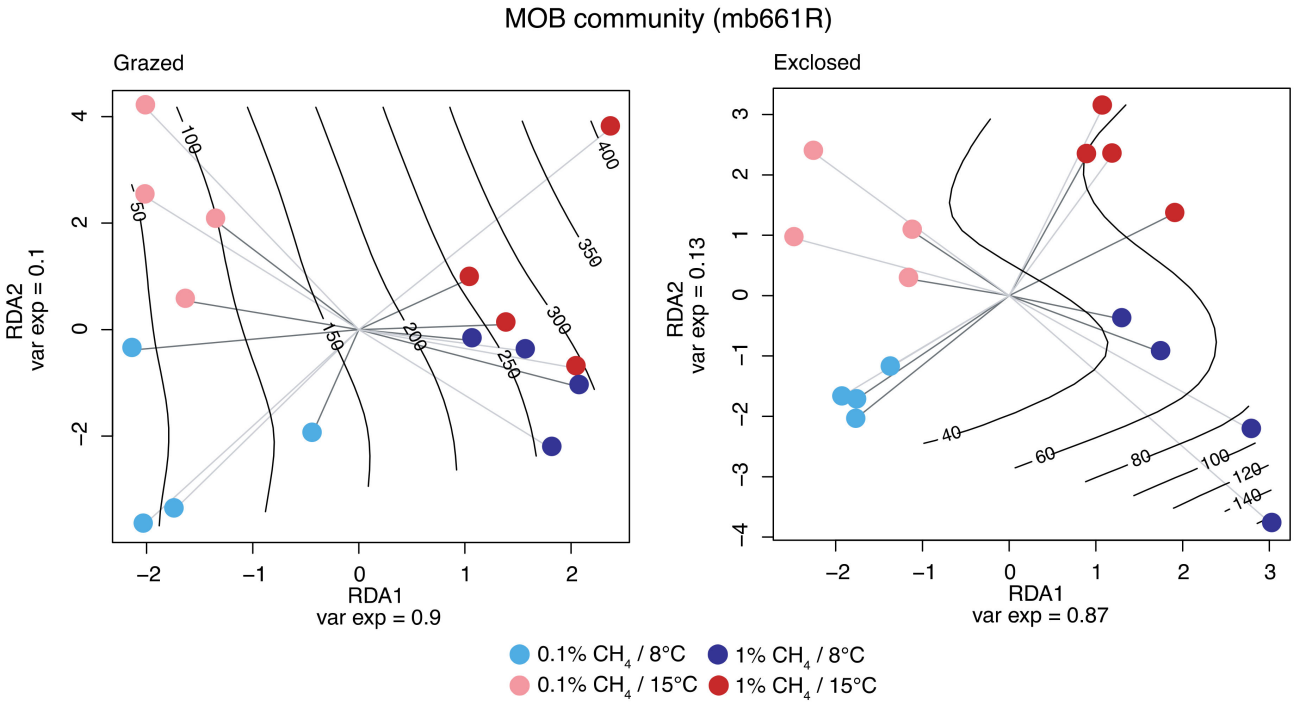

Figure 5. Redundancy analysis of the effect of CH_4 concentration and temperature on the MOB communities after incubation (*pmoA* transcripts using the A189F/mb661R primer pair). The effect of CH_4 concentration and temperature was corrected according to the peat block replicates (represented by gray shaded lines). Samples are labeled according to CH_4 concentration (light colors—0.1% CH_4, dark colors—1% CH_4) and temperature (blue—8 °C and red—15 °C). The black lines indicate a projection of the measured CH_4 oxidation rates (µg of CH_4 oxidized per gram dry soil and day).

The majority of the detected MOB *pmoA* transcripts in both the mb661R and the A682R dataset belonged to the family *Methylococcacaea* (Figure 6 and Supplementary Figure S9). However, the samples incubated at 0.1% CH_4 contained smaller fractions of *Methylococcacaea* than the samples incubated at 1% CH_4 (Figure 6 and Supplementary Figure S9).

Methylobacter OTUs dominated the 0.1% CH_4 incubations with average relative abundances of 48.9% (grazed soils) and 44.7% (exclosed soils) (Figure 6, mb661R). In the 1% CH_4 incubations, *Methylobacter* OTUs made up even larger fractions, with abundances of 71.8% (grazed soils) and 68.4% (exclosed soils) (Figure 6). Contrary to *Methylobacter*, OTUs within *Methylomicrobium* and unclassified Type 1a MOB OTUs had higher relative abundances in the 0.1% CH_4 incubations than in the 1% CH_4 incubations.

Similar observations were made in the A682R dataset (Supplementary Figure S9). The lowest relative abundances of *Methylobacter pmoA* transcripts were observed at 0.1% CH_4, making up 60.9% (grazed soils) and 72.9% (exclosed soils). In the 1% CH_4 incubations, *Methylobacter* OTUs made up larger fractions of 75.9% (grazed soils) and 79.9% (exclosed soils). *Methylosarcina pmoA* transcripts, which were not detected in the mb661R dataset, had the highest relative abundances in the 0.1% CH_4 incubations, with 37.6% (grazed soils) and 12.3% (exclosed soils). At 1% CH_4, these OTUs made up only 21.8% (grazed soils) and 7.7% (exclosed soils).

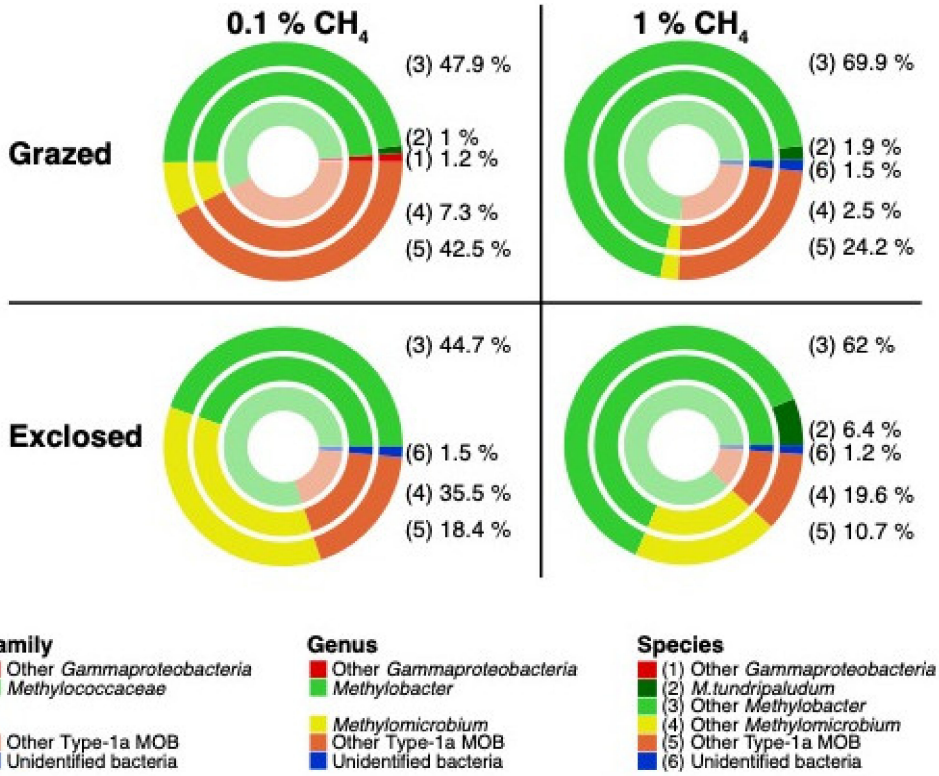

Figure 6. Distribution of MOB taxa (A189F/mb661R primer set) in grazed and exclosed peat soils after incubation at 0.1% CH_4 and at 1% CH_4 (16 soil samples per concentration and 16 soil samples per grazing condition). As temperature had no significant effect on the MOB community, these 16 samples include both the 8 and 15 °C incubations. OTU clustering was performed using Swarm [54] and taxonomically assigned by using the best alignment between the dominant sequence of each OTU and the database using Ggsearch36 [55]. Taxa with a relative abundance of > 1% are represented at the full taxonomic resolution, whereas those taxa not reaching the 1% threshold were added to their broader taxonomic group, one level lower in taxonomic resolution. The different rings represent different taxonomic levels from family to genus to species, moving from the innermost ring outward. Relative abundances for the species level are given in %.

In the 0.1% CH_4 incubations, the relative abundances of OTUs matching *M. tundripaludum* SV96 were 1.0% (grazed soils) and <1.0% (exclosed soils) (Figure 6, mb661R dataset). In the 1% CH_4 incubations, the relative abundances were higher, at 1.9% (grazed soils) and 6.4% (exclosed soils). The same patterns were observed in the A682R dataset (Supplementary Figure S9), with <1.0% (grazed and exclosed soils) and >4.2% (grazed and exclosed soils) at 1% CH_4. This shows that *M. tundripaludum* SV96 is a small but active part of the MOB community in these soils at high CH_4 concentrations.

To identify the MOB OTUs that were preferentially activated by either 0.1% or 1% CH_4, we screened our datasets for OTUs that were consistently more abundant at one or the other CH_4 concentration and called them "responsive bioindicator OTUs". From those OTUs, we selected the OTUs that behaved the same in the grazing treatments (grazed and exclosed peat soil) or that were only present in one of the treatments and called those "unconditional bioindicator OTUs" (see Section 2.6.5. for details about the bioindicator selection).

In the grazed soils, we identified 12 "responsive bioindicator OTUs". Seven (mb661R) and three (A682R) OTUs had higher relative abundances at 0.1% CH_4, and one OTU in each of the datasets (mb661R and A682R) had a higher relative abundance at 1% CH_4 (Figures 7 and 8 and Supplementary Figures S10 and S11). In the exclosed peat soil microcosms, we identified 15 "responsive bioindicator OTUs". Three (mb661R) and two (A682R) OTUs had higher relative abundances at 0.1% CH_4, whereas six (mb661R) and four (A682R) OTUs had a higher relative abundance of transcripts at 1% CH_4 (Figures 7 and 8 and Supplementary Figures S10 and S11).

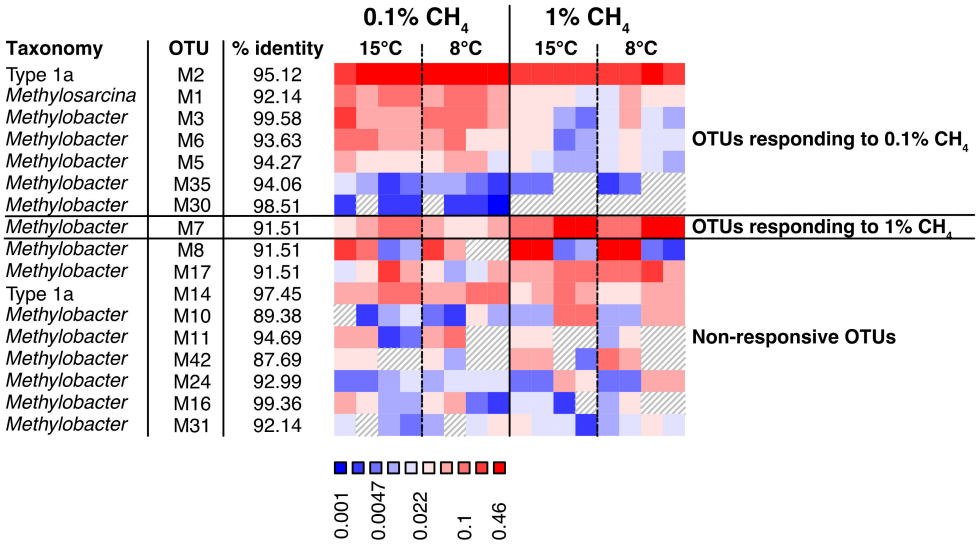

Figure 7. Relative abundances of *pmoA* transcripts representing MOB OTUs (A189F/mb661R primer pair) from grazed peat soil microcosms after incubation at 0.1% and 1% CH_4 concentrations. OTUs with higher relative abundance at 0.1% CH_4 are shown in the first block (left), and those with higher relative abundance at 1% CH_4 in the second block (right). The non-responsive OTUs with the highest relative abundance are shown in the third block. The number of OTUs included in the figure make up 90% of the total MOB community transcription. OTUs are identified by the letter M (indicating that these are part of the mb661R dataset) and a number. The percentage of identity between the OTU and the best hit in the database is given next to the OTU identification. The highest possible taxonomic rank identified was chosen for each OTU. Relative abundances reach from low abundances (blue) to high (red).

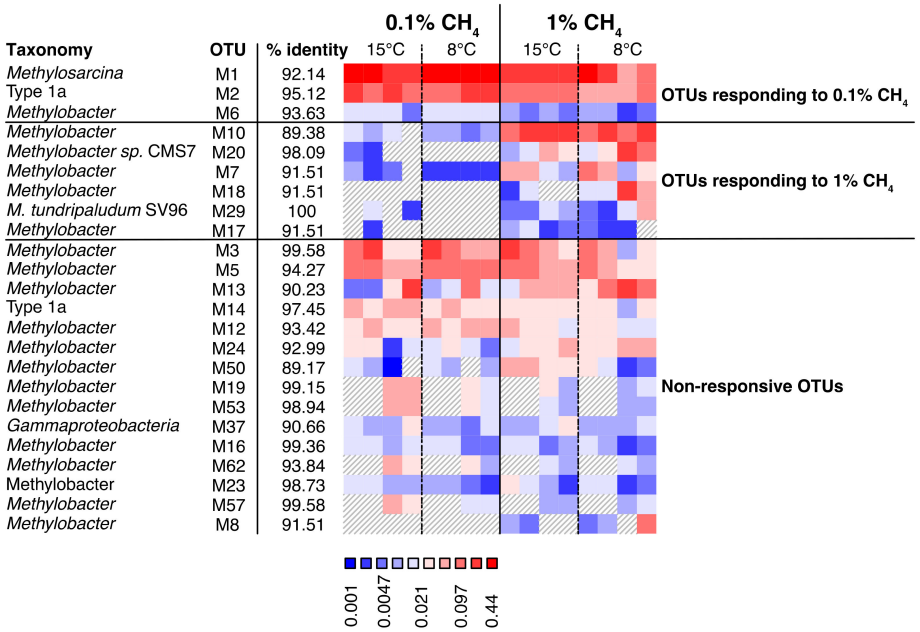

Figure 8. Relative abundances of *pmoA* transcripts representing MOB OTUs (A189F/mb661R primer pair) from exclosed peat soil microcosms after incubation at 0.1% and 1% CH_4 concentrations. OTUs with higher relative abundance at 0.1% CH_4 are shown in the first block (left) and those with higher relative abundance at 1% CH_4 in the second block (right). The non-responsive OTUs with the highest relative abundance are shown in the third block. The number of OTUs included in the figure make up 90% of the total MOB community transcription. OTUs are identified by the letter M (indicating that these are part of the mb661R dataset) and a number. The percentage of identity between the OTU and the best hit in the database is given next to the OTU identification. The highest possible taxonomic rank identified was chosen for each OTU. Relative abundances reach from low abundances (blue) to high (red).

The *pmoA* sequences categorized as "unconditional bioindicator OTUs" were subsequently aligned with a set of reference sequences, including blast search hits and cultivated strains, and used to infer the phylogenetic relationships of the "unconditional bioindicator OTUs" from the mb661R and A682R datasets, respectively (Figure 9 and Supplementary Figure S12). The *Methylobacter* OTUs identified as "unconditional bioindicator OTUs" for 0.1% CH_4 clustered separately from those that were "unconditional bioindicator OTUs" for 1% CH_4 (Figure 9 and Supplementary Figure S12). The two Arctic strains, *M. tundripaludum* SV96 [32] and *Methylobacter* sp. CMS7 [31], clustered with two of the 1% CH_4 bioindicator OTUs, respectively (Figure 9), whereas the remaining bioindicator OTUs clustered with environmental sequences (including lake sediments and landfill cover soils rather than cultivated strains).

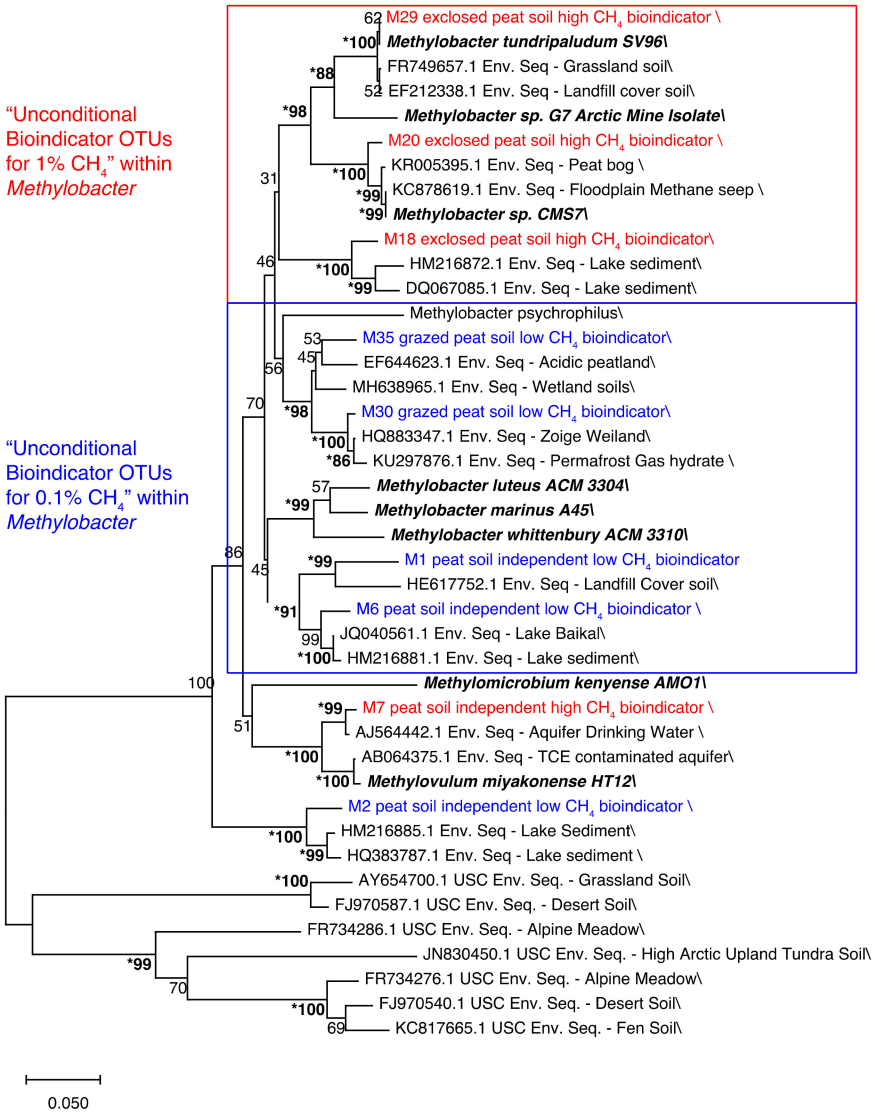

Figure 9. Phylogenetic representation of the "unconditional bioindicator OTUs" for 0.1% CH_4 (blue) and 1% CH_4 (red) incubations (mb661R dataset), cultivated MOB (bold, italic), and closely related environmental sequences retrieved from the NCBI GenBank. All OTUs included were identified as bioindicators both in the grazed and the exclosed peat soil microcosms, or in only one of the soil types, being absent from the other soil type. The first type is called "peat soil independent". The other type of OTUs, which were specifically assigned as bioindicators for one of the peat soil types, are labeled

as either grazed or exclosed. The tree is based on a 456-nucleotide alignment, using the neighbor-joining method with the Jukes–cantor correction and 500 bootstraps. The length of the branches is based on a scale of 0.05 changes per nucleotide. Bootstrap values of >80 in 3 models that were used to construct the tree (neighbor-joining, maximum likelihood, and minimum evolution) are marked with * and written in bold.

4. Discussion

4.1. CH_4 Response

4.1.1. Activity

Higher CH_4 concentrations led to higher CH_4 oxidation rates immediately after addition, but the effect was stronger after a three-week incubation period at maintained CH_4 concentrations. Thus, while the initial rates reflected the oxidation potential of the MOB community shortly after thawing, the latter rates were influenced by MOB growth, physiological acclimation, or community response. Responses of the MOB communities to increasing CH_4 concentrations were shown in a study of lake overturn, where population shifts over several months corresponded with the ability of the MOB community to mitigate the majority of the CH_4 [61]. In the same study, a growth response was also indicated in the MOB community, which was responsible for the oxidation of the CH_4. Such an effect of CH_4 concentrations on the MOB response and capacity was also shown in a study of atmospheric CH_4 oxidation by conventional MOB, where conditioning with high CH_4 concentrations allowed for atmospheric CH_4 uptake [62]. The highest CH_4 oxidation rates and strongest response after the three-week incubation in our experiment were observed in grazed peat soil microcosms. These soils contained in situ CH_4 concentrations of up to 237.4 µM (100.7–237.4 µM of dissolved CH_4 at SV1) in the pore water at 5 cm and 2139.0 µM (469.4–2139.0 µM dissolved CH_4) at a depth of 10 cm [27]. In comparison, exclosed peat soils contained only up to 3.7 µM of CH_4 (0.4–3.7 µM CH_4 at SV1) at a depth of 10 cm and 578.0 µM (0.53–578 µM of CH_4) at a depth of 15 cm. Thus, the 0.1% incubations (with a concentration of about 1.7–2 µM of dissolved CH_4) were lower than in situ CH_4 concentrations in grazed peat at depths of 5 and 10 cm and about in situ CH_4 concentrations in exclosed soils at a depth of 10 cm. The 1% incubations (with a concentration of about 17–20 µM of dissolved CH_4) were lower than the in situ CH_4 concentrations in grazed soils below 5 cm, whereas they were higher than in situ CH_4 concentrations of exclosed soils at a depth of 10 cm. It should be noted that the samples for our experiments were collected from the surface (Exp I: 0–2 cm, Exp II: 0–4 cm) in grazed soils and above 10 cm (Exp I: 5–7 cm, Exp II: 4–8 cm). Thus, the microorganisms in these hotspots for CH_4 oxidation would have been exposed to lower CH_4 concentrations than indicated by the available in situ pore water CH_4 measurements. Measurements at 0–5 and 0–10 cm in the grazed and exclosed sites, respectively, were not possible due to the lack of pore water at these depths.

Nevertheless, these results show that the MOB responses were related to the dissolved CH_4 concentrations in the respective soil pore waters, with stronger MOB responses to added CH_4 in the soils with higher in situ CH_4 concentrations.

4.1.2. MOB Transcript Numbers

We observed that a transcriptionally more active MOB community was responsible for the higher CH_4 oxidation rates in the grazed peat soils compared to the exclosed peat soils. Positive correlations between *pmoA* transcript numbers and CH_4 oxidation rates have been shown before [23,63]. However, within each grazing treatment, we did not observe a correlation between *pmoA* transcript numbers and CH_4 oxidation rates. Reasons for this may be changes in population sizes or changes in particulate methane monooxygenase kinetics due to a shift in the MOB community.

4.1.3. MOB Transcript Composition

CH_4 concentration had a significant impact on the relative abundance of *pmoA* transcripts for different members of the MOB community in both grazed and exclosed peat

soils (Figure 5). These results corroborate previous results, suggesting that in situ CH_4 concentrations shape the MOB community in the Solvatn peatland [27]. The relative abundances of *Methylobacter* OTUs were higher at a 1% CH_4 concentration in both the grazed and exclosed plots (Figure 6 and Supplementary Figure S9). In contrast to this, there was a lower relative abundance of *Methylomicrobium* and *Methylosarcina* OTU transcripts at a 1% CH_4 concentration in both the grazed and exclosed plots. *Methylobacter* has been shown to thrive in colder, CH_4-rich, environments with a neutral pH, and our study confirms that this genus thrives when CH_4 concentrations are high.

Furthermore, we identified a strong treatment-dependent community transcriptional response, with some OTUs responding positively to 1% CH_4 (the majority of reacting OTUs were *Methylobacter*), while others responded to 0.1% CH_4 (Figures 7 and 8 and Supplementary Figures S10 and S11). Interestingly, a larger number of OTUs responded to 0.1% CH_4 in the grazed peat soil microcosms, where in situ CH_4 concentrations were the highest, while more OTUs responded to 1% CH_4 in the exclosed peat soil microcosms, which had the lowest in situ CH_4 concentrations [27]. This suggests that high and low in situ CH_4 concentrations select for different MOB strains, respectively, and that the largest group of strains respond to the condition that is most different from the in situ condition. We suspect that this is because the responding strains had low transcriptional activity in the original soil and became more active during steady exposure to a 0.1% CH_4 headspace concentration. Furthermore, our findings show that such effects are observable within three weeks and correlate with changes in the CH_4 oxidation rates. This indicates the co-existence of closely related strains that prefer either high or low CH_4 concentrations, respectively, and that these populations can replace each other within an Arctic summer. Similar observations were made in lakes, where changes in apparent half-saturation constants and CH_4 uptake rates at the CH_4 saturation correlated with changes in *pmoA* expression and for which MOB strains (99% identity) were responsible [61]. It is tempting to draw a line between which strains are active and use this as a basis for inferring whether the strains have high or low apparent affinities for CH_4. However, cell numbers and cellular enzyme contents also influence uptake rates, and the relative contribution of enzyme kinetics, cell numbers, and cellular protein content to the observed rates remains unknown in most studies, including our own. Nevertheless, the different CH_4 uptake rates seem to correspond with different compositions of active MOB strains.

4.1.4. Phylogeny

Most of the bioindicators belonged to the genus *Methylobacter*. Some of the "unconditional bioindicator OTUs" for 1% CH_4 clustered with high-Arctic *Methylobacter* isolates retrieved from CH_4-rich ecosystems [31,32], while the phylogenetic clusters containing the "unconditional bioindicator OTUs" for 0.1% CH_4 did not contain closely related isolates. Atmospheric MOB are phylogenetically distinct but closely related to conventional MOB [24,64] and are characterized by a more efficient energy metabolism [44]. Similarly, phylogenetically different populations of ammonia-oxidizing Archaea are associated with different ammonia oxidation uptake rates [65,66], and different ammonia oxidation kinetics reflect different life strategies [65]. Thus, the phylogenetic separation of OTUs with a higher abundance in the microcosms with high CH_4 concentrations from those preferring low CH_4 concentrations might indicate the existence of closely related but phylogenetically and functionally distinct *Methylobacter* strains that co-exist in the same environment. In addition to indicating the phylogenetic separation of function, these results also suggest a bias in enrichment and culturing approaches, as most isolates cluster with OTUs that are active at high CH_4 concentrations.

4.2. Temperature Response

Rising temperatures are often affiliated with increases in metabolic activity [67], as shown by the temperature response in growth rates of pure cultures of methanotrophs [37]. In line with this, we did see significant effects of temperature on cellular CH_4 oxidation

rates in *M. tundripaludum* SV96, although the differences were minor at 0.1% CH_4. In comparison, temperature had small and inconsistent effects on soil CH_4 oxidation rates and *pmoA* transcript abundances at both 0.1% and 1% CH_4. Inconsistent temperature effects on CH_4 oxidation might be caused by several factors, such as changes in cell growth, growth efficiency, cell numbers, cellular protein contents, and types of active MOB strains, all of which may be affected by substrate and nutrient concentrations. In a study of Arctic lakes, CH_4 oxidation rates were not increasing with increasing temperature when the substrate was limiting [38]. Thus, there might be a physiological response to temperature that, due to CH_4 limitation, looks like a lack of temperature response. This could be the case in some of our microcosms, particularly at the lowest (0.1%) CH_4 concentration, possibly explaining the small temperature effect seen at 0.1% CH_4 in the experiment with *M. tundripaludum* SV96. CH_4 oxidation has frequently been observed as being less temperature-sensitive than CH_4 production, but this phenomenon has not yet been explained [35]. Future studies should, therefore, address intracellular physiological responses in MOB at different temperatures and not only quantify CH_4 oxidation rates and growth. Temperatures from 8 °C to 15 °C do occur in the topsoil on warm summer days in Svalbard [27], and although the community must be physiologically capable of responding to such temperature changes, we are still not aware of how.

Shifts in the active members of the MOB community may also influence the temperature response of a microbial community, but we did not observe any consistent transcriptional shifts among the active members with a change in temperature. Thus, within the temperature range covered in this study, shifts in the transcriptionally active community did not seem to be a significant response.

5. Conclusions

We found that MOB in Arctic peat soils from Svalbard respond to changes in CH_4 concentrations, but the nature of the response depends on whether the peat has been exposed to herbivory. Herbivory "conditioning" simultaneously influenced the presence and activity of different MOB strains, community CH_4 oxidation, and the effect of increased CH_4 concentration on CH_4 oxidation rates. Temperature, on the other hand, had only minor effects on the MOB community and its CH_4 uptake. However, as CH_4 production is expected to increase with higher temperatures, we hypothesize that the resulting higher peat soil CH_4 concentrations will influence MOB activity and CH_4 oxidation potential, but this shift will be influenced by the extent of the herbivory.

Supplementary Materials: The following are available online at https://www.mdpi.com/article/10.3390/microorganisms9102080/s1, Figure S1: CH_4 oxidation rates from Exp II emphasizing the comparison between 0.1 % and 1 % headspace CH_4 concentrations. Figure S2: CH_4 oxidation rates from Exp I before and and after the three-week incubation. Figure S3: CH_4 oxidation rates from Exp II before and and after the three-week incubation. Figure S4: CH_4 oxidation rates from Exp II emphasizing the comparison between 8 and 15 °C. Figure S5: CH_4 oxidation rates from Exp I emphasizing the comparison between 8 °C and 15 °C (corrected for dissolved CH_4). Figure S6: CH_4 oxidation rates from Exp II emphasizing the comparison between 8 °C and 15 °C (corrected for dissolved CH_4). Figure S7: CH_4 oxidation per cell for *Methylobacter tundripaludum* SV96. Table S1: Number of sequences and OTUs at the different stages of the bioinformatic pipeline. Figure S8: Redundancy analysis of the effect of CH_4 concentration and temperature on the MOB communities after incubation (*pmoA* transcripts using the A189F/A682R primer pair). Figure S9: Distribution of MOB taxa (A189F/A682R primer set) in grazed and exclosed peat soils after incubation at 0.1% CH_4 and at 1% CH_4. Figure S10: Relative abundances of *pmoA* transcripts representing MOB OTUs (A189F/A682R primer pair) from grazed peat soil microcosms after incubation at 0.1 % and 1% CH_4 concentration. Figure S11: Relative abundances of *pmoA* transcripts representing MOB OTUs (A189F/A682R primer pair) from exclosed peat soil microcosms after incubation at 0.1 % and 1% CH_4 concentration. Figure S12: Phylogenetic representation of the "unconditional bioindicator OTUs" for 0.1% CH_4 (blue) and 1% CH_4 (red) incubations, cultivated MOB (bold, italic) and closely related environmental sequences retrieved from the NCBI GenBank

Author Contributions: E.M.R. conceived the study with input from A.T.T and M.M.S.; E.M.R., C.H. and M.M.S. established the microcosm experiments. C.H. conducted the microcosm experiments and E.M.R. the growth and rate measurements in pure culture; C.H. extracted the RNA, prepared them for sequencing, and ran the qPCR experiments with assistance from E.M.R.; E.M.R and A.T.T. analyzed the gas uptake rates.; C.V.W.S. analyzed the sequences and performed the statistics; E.M.R. wrote the manuscript with input from all authors. All authors have read the manuscript and agreed to publish the manuscript in its present state.

Funding: The funding for this study was provided by NORRUSS (233645/H30) and Svalbard Science Forum (AFG grant: 256933/E10) from the Research Council of Norway. ATT was supported by the Research Council of Norway FRIPRO Mobility Grant Project Time and Energy 251027/RU, co-founded by ERC under Marie Curie Grant 606895, and Tromsø Research Foundation starting grant project Cells in the Cold 16_SG_ATT. CVWS was supported by the Research Council of Norway, projects BiodivERsA (270252/E50) and ERAnet-LAC(256132/H30).

Data Availability Statement: Reads will be available upon acceptance of the manuscript.

Conflicts of Interest: The authors declare no conflict of interest.

References

1. Kuijper, D.P.J.; Bakker, J.P.; Cooper, E.J.; Ubels, R.; Jónsdóttir, I.S.; Loonen, M.J.J.E. Intensive grazing by Barnacle geese depletes High Arctic seed bank. *Can. J. Bot.* **2006**, *84*, 995–1004. [CrossRef]
2. Jefferies, R.L.; Rockwell, R.F. Foraging geese, vegetation loss and soil degradation in an Arctic salt marsh. *Appl. Veg. Sci.* **2002**, *5*, 7–16. [CrossRef]
3. Handa, I.T.; Harmsen, R.; Jefferies, R.L. Patterns of vegetation change and the recovery potential of degraded areas in a coastal marsh system of the Hudson Bay lowlands. *J. Ecol.* **2002**, *90*, 86–99. [CrossRef]
4. Hessen, D.O.; Tombre, I.M.; van Geest, G.; Alfsnes, K. Global change and ecosystem connectivity: How geese link fields of central Europe to eutrophication of Arctic freshwaters. *Ambio* **2017**, *46*, 40–47. [CrossRef]
5. Tombre, I.M.; Oudman, T.; Shimmings, P.; Griffin, L.; Prop, J. Northward range expansion in spring-staging barnacle geese is a response to climate change and population growth, mediated by individual experience. *Glob. Chang. Biol.* **2019**, *25*, 3680–3693. [CrossRef]
6. Bardgett, R.D.; Wardle, D.A. Herbivore-mediated linkages between aboveground and belowground communities. *Ecology* **2003**, *84*, 2258–2268. [CrossRef]
7. Wardle, D.A.; Bardgett, R.D.; Klironomos, J.N.; Setälä, H.; Van Der Putten, W.H.; Wall, D.H. Ecological linkages between aboveground and belowground biota. *Science* **2004**, *304*, 1629–1633. [CrossRef]
8. Foley, K.M.; Beard, K.H.; Atwood, T.B.; Waring, B.G. Herbivory changes soil microbial communities and greenhouse gas fluxes in a high-latitude wetland. *Microb. Ecol.* **2021**, 1–10. [CrossRef]
9. Falk, J.M.; Schmidt, N.M.; Christensen, T.R.; Ström, L. Large herbivore grazing affects the vegetation structure and greenhouse gas balance in a high Arctic mire. *Environ. Res. Lett.* **2015**, *10*, 45001. [CrossRef]
10. Winton, R.S.; Richardson, C.J. Top-down control of methane emission and nitrogen cycling by waterfowl. *Ecology* **2017**, *98*, 265–277. [CrossRef] [PubMed]
11. Kelsey, K.C.; Leffler, A.J.; Beard, K.H.; Schmutz, J.A.; Choi, R.T.; Welker, J.M. Interactions among vegetation, climate, and herbivory control greenhouse gas fluxes in a subarctic coastal wetland. *J. Geophys. Res. Biogeosciences* **2016**, *121*, 2960–2975. [CrossRef]
12. Sjögersten, S.; van der Wal, R.; Loonen, M.J.J.E.; Woodin, S.J. Recovery of ecosystem carbon fluxes and storage from herbivory. *Biogeochemistry* **2011**, *106*, 357–370. [CrossRef]
13. Bender, K.M.; Svenning, M.M.; Hu, Y.; Richter, A.; Schückel, J.; Jørgensen, B.; Liebner, S.; Tveit, A.T. Microbial responses to herbivory-induced vegetation changes in a high-Arctic peatland. *Polar Biol.* **2021**, *44*, 899–911. [CrossRef]
14. Cohen, J.; Screen, J.A.; Furtado, J.C.; Barlow, M.; Whittleston, D.; Coumou, D.; Francis, J.; Dethloff, K.; Entekhabi, D.; Overland, J.; et al. Recent Arctic amplification and extreme mid-latitude weather. *Nat. Geosci.* **2014**, *7*, 627–637. [CrossRef]
15. Francis, J.A.; Vavrus, S.J.; Cohen, J. Amplified Arctic warming and mid-latitude weather: New perspectives on emerging connections. *Wiley Interdiscip. Rev. Clim. Chang.* **2017**, *8*, 1–11. [CrossRef]
16. Serreze, M.C.; Barry, R.G. Processes and impacts of Arctic amplification: A research synthesis. *Glob. Planet. Change* **2011**, *77*, 85–96. [CrossRef]
17. Tarnocai, C.; Canadell, J.G.; Schuur, E.A.G.; Kuhry, P.; Mazhitova, G.; Zimov, S. Soil organic carbon pools in the northern circumpolar permafrost region. *Glob. Biogeochem. Cycles* **2009**, *23*, 1–11. [CrossRef]
18. Tveit, A.T.; Urich, T.; Frenzel, P.; Svenning, M.M. Metabolic and trophic interactions modulate methane production by Arctic peat microbiota in response to warming. *Proc. Natl. Acad. Sci. USA* **2015**, *112*, E2507–E2516. [CrossRef]
19. Metje, M.; Frenzel, P. Methanogenesis and methanogenic pathways in a peat from subarctic permafrost. *Environ. Microbiol.* **2007**, *9*, 954–964. [CrossRef]

20. Metje, M.; Frenzel, P. Effect of temperature on anaerobic ethanol oxidation and methanogenesis in acidic peat from a Northern Wetland. *Appl. Environ. Microbiol.* **2005**, *71*, 8191–8200. [CrossRef] [PubMed]
21. Høj, L.; Olsen, R.A.; Torsvik, V.L. Archaeal communities in High Arctic wetlands at Spitsbergen, Norway (78° N) as characterized by 16S rRNA gene fingerprinting. *FEMS Microbiol. Ecol.* **2005**, *53*, 89–101. [CrossRef]
22. Brune, A.; Frenzel, P.; Cypionka, H. Life at the oxic-anoxic interface: Microbial activities and adaptations. *FEMS Microbiol. Rev.* **2000**, *24*, 691–710. [CrossRef]
23. Reim, A.; Lüke, C.; Krause, S.; Pratscher, J.; Frenzel, P. One millimetre makes the difference: High-resolution analysis of methane-oxidizing bacteria and their specific activity at the oxic-anoxic interface in a flooded paddy soil. *ISME J.* **2012**, *6*, 2128–2139. [CrossRef] [PubMed]
24. Knief, C. Diversity and habitat preferences of cultivated and uncultivated aerobic methanotrophic bacteria evaluated based on pmoA as molecular marker. *Front. Microbiol.* **2015**, *6*, 1346. [CrossRef]
25. Wartiainen, I.; Hestnes, A.G.; Svenning, M.M. Methanotrophic diversity in high arctic wetlands on the islands of Svalbard (Norway)-denaturing gradient gel electrophoresis analysis of soil DNA and enrichment cultures. *Can. J. Microbiol.* **2003**, *49*, 602–612. [CrossRef] [PubMed]
26. Martineau, C.; Whyte, L.G.; Greer, C.W. Stable isotope probing analysis of the diversity and activity of Methanotrophic bacteria in soils from the Canadian high Arctic. *Appl. Environ. Microbiol.* **2010**, *76*, 5773–5784. [CrossRef] [PubMed]
27. Rainer, E.M.; Seppey, C.V.W.; Tveit, A.T.; Svenning, M.M. Methanotroph populations and CH4 oxidation potentials in High Arctic peat are altered by herbivory induced vegetation change. *FEMS Microbiol. Ecol.* **2020**, *96*, 1–12. [CrossRef] [PubMed]
28. Tveit, A.T.; Kiss, A.; Winkel, M.; Horn, F.; Hájek, T.; Svenning, M.M.; Wagner, D.; Liebner, S. Environmental patterns of brown moss- and Sphagnum-associated microbial communities. *Sci. Rep.* **2020**, *10*, 1–16. [CrossRef] [PubMed]
29. Dedysh, S.N.; Didriksen, A.; Danilova, O.V.; Belova, S.E.; Liebner, S.; Svenning, M.M. *Methylocapsa palsarum* sp. nov., a methanotroph isolated from a subarctic discontinuous permafrost ecosystem. *Int. J. Syst. Evol. Microbiol.* **2015**, *65*, 3618–3624. [CrossRef]
30. Dedysh, S.N.; Berestovskaya, Y.Y.; Vasylieva, L.V.; Belova, S.E.; Khmelenina, V.N.; Suzina, N.E.; Trotsenko, Y.A.; Liesack, W.; Zavarzin, G.A. *Methylocella tundrae* sp. nov., a novel methanotrophic bacterium from acidic tundra peatlands. *Int. J. Syst. Evol. Microbiol.* **2004**, *54*, 151–156. [CrossRef] [PubMed]
31. Belova, S.E.; Oshkin, I.Y.; Glagolev, M.V.; Lapshina, E.D.; Maksyutov, S.S.; Dedysh, S.N. Methanotrophic bacteria in cold seeps of the floodplains of northern rivers. *Microbiology* **2013**, *82*, 743–750. [CrossRef]
32. Wartiainen, I.; Hestnes, A.G.; McDonald, I.R.; Svenning, M.M. *Methylobacter tundripaludum* sp. nov., a methane-oxidizing bacterium from Arctic wetland soil on the Svalbard islands, Norway (78° N). *Int. J. Syst. Evol. Microbiol.* **2006**, *56*, 109–113. [CrossRef]
33. Berestovskaya, Y.Y.; Vasil'eva, L.V.; Chestnykh, O.V.; Zavarzin, G.A. Methanotrophs of the psychrophilic microbial community of the Russian arctic tundra. *Microbiology* **2002**, *71*, 460–466. [CrossRef]
34. Einola, J.K.M.; Kettunen, R.H.; Rintala, J.A. Responses of methane oxidation to temperature and water content in cover soil of a boreal landfill. *Soil Biol. Biochem.* **2007**, *39*, 1156–1164. [CrossRef]
35. Zheng, J.; RoyChowdhury, T.; Yang, Z.; Gu, B.; Wullschleger, S.D.; Graham, D.E. Impacts of temperature and soil characteristics on methane production and oxidation in Arctic tundra. *Biogeosciences* **2018**, *15*, 6621–6635. [CrossRef]
36. King, G.M.; Adamsen, A.P.S. Effects of temperature on methane consumption in a forest soil and in pure cultures of the methanotroph Methylomonas rubra. *Appl. Environ. Microbiol.* **1992**, *58*, 2758–2763. [CrossRef]
37. Kevbrina, M.V.; Okhapkina, A.A.; Akhlynin, D.S.; Kravchenko, I.K.; Nozhevnikova, A.N.; Gal'chenko, V.F. Growth of mesophilic methanotrophs at low temperatures. *Microbiology* **2001**, *70*, 384–391. [CrossRef]
38. Lofton, D.D.; Whalen, S.C.; Hershey, A.E. Effect of temperature on methane dynamics and evaluation of methane oxidation kinetics in shallow Arctic Alaskan lakes. *Hydrobiologia* **2014**, *721*, 209–222. [CrossRef]
39. Zeng, L.; Tian, J.; Chen, H.; Wu, N.; Yan, Z.; Du, L.; Shen, Y.; Wang, X. Changes in methane oxidation ability and methanotrophic community composition across different climatic zones. *J. Soils Sediments* **2019**, *19*, 533–543. [CrossRef]
40. Solheim, B.; Endal, A.; Vigstad, H. Nitrogen fixation in Arctic vegetation and soils from Svalbard, Norway. *Polar Biol.* **1996**, *16*, 35–40. [CrossRef]
41. Graef, C.; Hestnes, A.G.; Svenning, M.M.; Frenzel, P. The active methanotrophic community in a wetland from the High Arctic. *Environ. Microbiol. Rep.* **2011**, *3*, 466–472. [CrossRef]
42. Tveit, A.; Schwacke, R.; Svenning, M.M.; Urich, T. Organic carbon transformations in high-Arctic peat soils: Key functions and microorganisms. *ISME J.* **2013**, *7*, 299–311. [CrossRef]
43. Niemann, H.; Steinle, L.; Blees, J.; Bussmann, I.; Treude, T.; Krause, S.; Elvert, M.; Lehmann, M.F. Toxic effects of lab-grade butyl rubber stoppers on aerobic methane oxidation. *Limnol. Oceanogr. Methods* **2015**, *13*, 40–52. [CrossRef]
44. Tveit, A.T.; Schmider, T.; Hestnes, A.G.; Lindgren, M.; Didriksen, A.; Svenning, M.M. Simultaneous oxidation of atmospheric methane, carbon monoxide and hydrogen for bacterial growth. *Microorganisms* **2021**, *9*, 153. [CrossRef] [PubMed]
45. Whittenbury, R.; Phillips, K.C.; Wilkinson, J.F. Enrichment, Isolation and Some Properties of Methane-utilizing Bacteria. *J. Gen. Microbiol.* **1970**, *61*, 205–218. [CrossRef] [PubMed]
46. Tays, C.; Guarnieri, M.T.; Sauvageau, D.; Stein, L.Y. Combined effects of carbon and nitrogen source to optimize growth of proteobacterial methanotrophs. *Front. Microbiol.* **2018**, *9*, 1–14. [CrossRef]

47. Urich, T.; Lanzén, A.; Qi, J.; Huson, D.H.; Schleper, C.; Schuster, S.C. Simultaneous assessment of soil microbial community structure and function through analysis of the meta-transcriptome. *PLoS ONE* **2008**, *3*, e2527. [CrossRef]
48. Costello, A.M.; Lidstrom, M.E. Molecular characterization of functional and phylogenetic genes from natural populations of methanotrophs in lake sediments. *Appl. Environ. Microbiol.* **1999**, *65*, 5066–5074. [CrossRef]
49. Holmes, A.J.; Costello, A.; Lidstrom, M.E.; Murrell, J.C. Evidence that particulate methane monooxygenasre and ammonia monooxygenase may be related. *FEMS Microbiol. Lett.* **1995**, *132*, 203–208. [CrossRef]
50. Henneberger, R.; Lüke, C.; Mosberger, L.; Schroth, M.H. Structure and function of methanotrophic communities in a landfill-cover soil. *FEMS Microbiol. Ecol.* **2012**, *81*, 52–65. [CrossRef]
51. Wen, X.; Yang, S.; Liebner, S. Evaluation and update of cutoff values for methanotrophic pmoA gene sequences. *Arch. Microbiol.* **2016**, *198*, 629–636. [CrossRef]
52. Magoč, T.; Salzberg, S.L. FLASH: Fast length adjustment of short reads to improve genome assemblies. *Bioinformatics* **2011**, *27*, 2957–2963. [CrossRef]
53. Rognes, T.; Flouri, T.; Nichols, B.; Quince, C.; Mahé, F. VSEARCH: A versatile open source tool for metagenomics. *PeerJ* **2016**, *4*, e2584. [CrossRef]
54. Mahé, F.; Rognes, T.; Quince, C.; de Vargas, C.; Dunthorn, M. Swarm: Robust and fast clustering method for amplicon-based studies. *PeerJ* **2014**, *2*, e593. [CrossRef]
55. Pearson, W.R. Flexible Sequence Similarity Searching with the FASTA3 Program Package. In *Methods in Molecular Biology*; Misener, S., Krawetz, S.A., Eds.; Humana Press: Totowa, NJ, USA, 2000; pp. 185–219.
56. Anderson, M.J.; Ellingsen, K.E.; McArdle, B.H. Multivariate dispersion as a measure of beta diversity. *Ecol. Lett.* **2006**, *9*, 683–693. [CrossRef] [PubMed]
57. Oksanen, J.; Blanchet, F.G.; Friendly, M.; Kindt, R.; Legendre, P.; McGlinn, D.; Minchin, P.R.; O'Hara, R.B.; Simpson, G.L.; Solymos, P.; et al. Vegan: Community Ecology Package. 2018. Available online: https://cran.r-project.org/web/packages/vegan/index.html (accessed on 24 January 2018).
58. Roberts, D. Package'labdsv'. 2016. Available online: https://cran.r-project.org/web/packages/labdsv/labdsv.pdf (accessed on 24 January 2016).
59. Kumar, S.; Stecher, G.; Li, M.; Knyaz, C.; Tamura, K. MEGA X: Molecular Evolutionary Genetics Analysis across computing platforms. *Mol. Biol. Evol.* **2018**, *35*, 1547–1549. [CrossRef]
60. Edgar, R.C. MUSCLE: Multiple sequence alignment with high accuracy and high throughput. *Nucleic Acids Res.* **2004**, *32*, 1792–1797. [CrossRef] [PubMed]
61. Mayr, M.J.; Zimmermann, M.; Dey, J.; Brand, A.; Wehrli, B.; Bürgmann, H. Growth and rapid succession of methanotrophs effectively limit methane release during lake overturn. *Commun. Biol.* **2020**, *3*, 1–9. [CrossRef]
62. Cai, Y.; Zheng, Y.; Bodelier, P.L.E.; Conrad, R.; Jia, Z. Conventional methanotrophs are responsible for atmospheric methane oxidation in paddy soils. *Nat. Commun.* **2016**, *7*, 1–10. [CrossRef] [PubMed]
63. Siljanen, H.M.P.; Saari, A.; Bodrossy, L.; Martikainen, P.J. Seasonal variation in the function and diversity of methanotrophs in the littoral wetland of a boreal eutrophic lake. *FEMS Microbiol. Ecol.* **2012**, *80*, 548–555. [CrossRef]
64. Tveit, A.T.; Hestnes, A.G.; Robinson, S.L.; Schintlmeister, A.; Dedysh, S.N.; Jehmlich, N.; Von Bergen, M.; Herbold, C.; Wagner, M.; Richter, A.; et al. Widespread soil bacterium that oxidizes atmospheric methane. *Proc. Natl. Acad. Sci. USA* **2019**, *116*, 8515–8524. [CrossRef] [PubMed]
65. Kits, K.D.; Sedlacek, C.J.; Lebedeva, E.V.; Han, P.; Bulaev, A.; Pjevac, P.; Daebeler, A.; Romano, S.; Albertsen, M.; Stein, L.Y.; et al. Kinetic analysis of a complete nitrifier reveals an oligotrophic lifestyle. *Nature* **2017**, *549*, 269–272. [CrossRef] [PubMed]
66. Alves, R.J.E.; Wanek, W.; Zappe, A.; Richter, A.; Svenning, M.M.; Schleper, C.; Urich, T. Nitrification rates in Arctic soils are associated with functionally distinct populations of ammonia-oxidizing archaea. *ISME J.* **2013**, *7*, 1620–1631. [CrossRef] [PubMed]
67. Dijkstra, P.; Thomas, S.C.; Heinrich, P.L.; Koch, G.W.; Schwartz, E.; Hungate, B.A. Effect of temperature on metabolic activity of intact microbial communities: Evidence for altered metabolic pathway activity but not for increased maintenance respiration and reduced carbon use efficiency. *Soil Biol. Biochem.* **2011**, *43*, 2023–2031. [CrossRef]

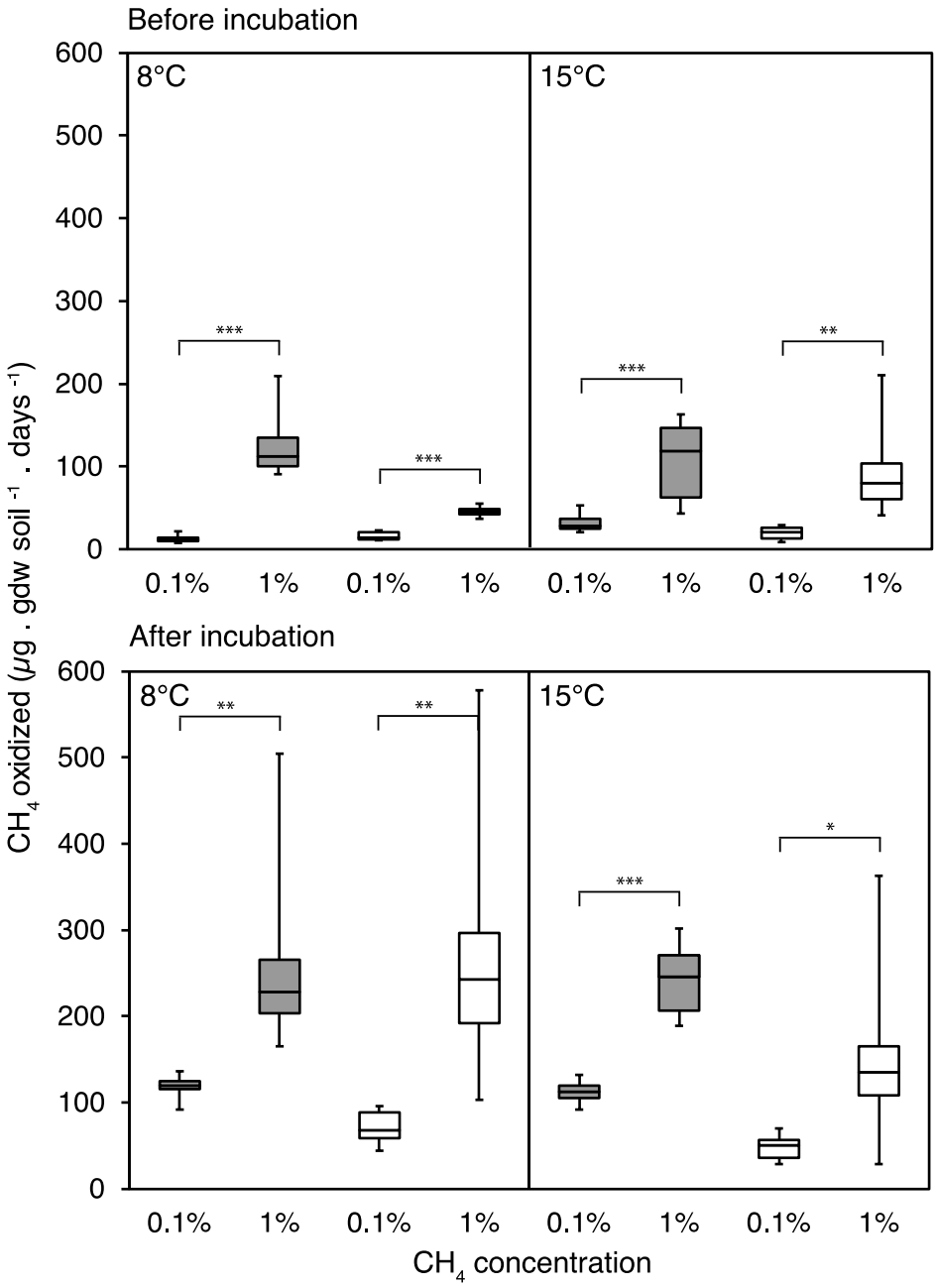

Supplementary Figure S1. CH_4 oxidation rates from Exp II emphasizing the comparison between 0.1% and 1% headspace CH_4 concentrations. Results are shown for measurements collected before (top) and after (bottom) the three-week incubation, and at 8 (left) and 15 °C (right). Grazed microcosms are shown in gray; exclosed microcosms in white. Comparison using linear mixed models with peat blocks as random variables shows significant differences in the CH_4 oxidation rates between CH_4 concentrations (*$p < 0.05$; ** $p < 0.01$; *** $p < 0.001$).

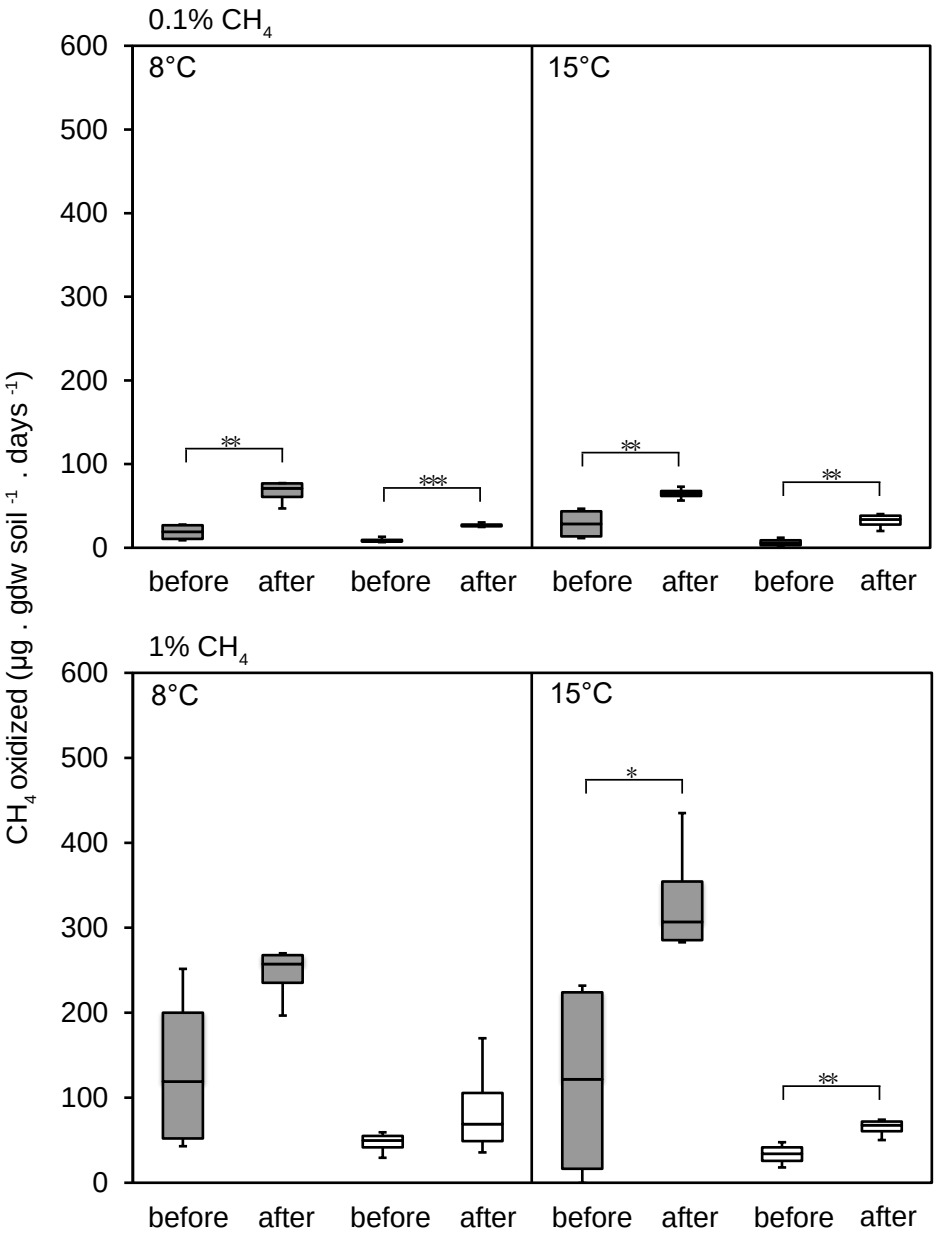

Supplementary Figure S2. CH_4 oxidation rates from Exp I before and and after the three-week incubation, at 8 °C (left) and 15 °C (right) and 0.1% (top) and 1% CH_4 headspace concentrations (bottom). Grazed peat soil microcosms are shown in gray; exclosed peat soil microcosms in white. Comparison using linear mixed models with peat blocks as random variables shows significant differences in the CH_4 oxidation rates before and after the incubation (*$p < 0.05$; ** $p < 0.01$; *** $p < 0.001$).

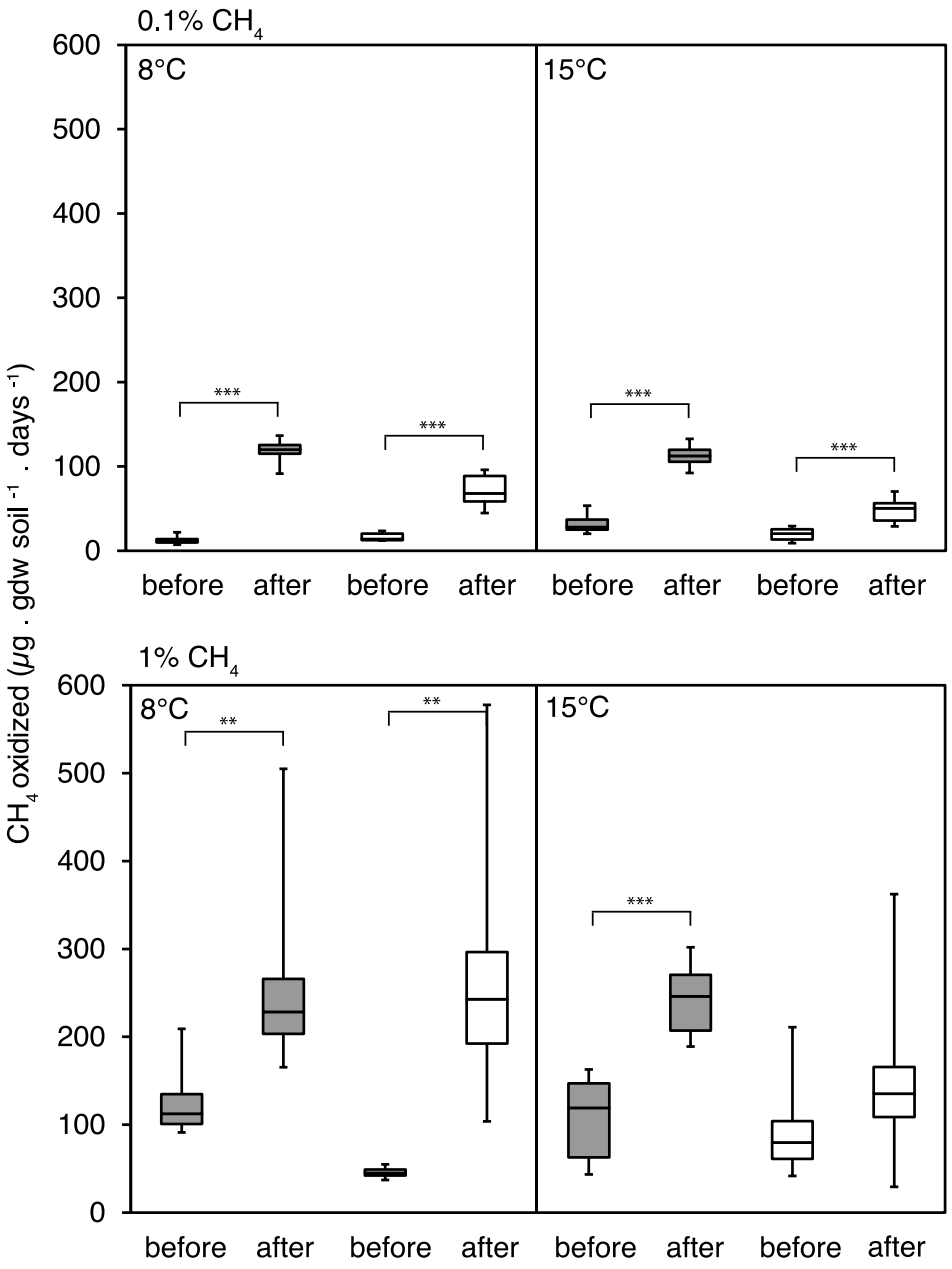

Supplementary Figure S3. CH_4 oxidation rates from Exp II before and and after the three-week incubation at 8°C (left) and 15 °C (right) and 0.1% (top) and 1% CH_4 headspace concentrations (bottom). Grazed peat soil microcosms are shown in gray; exclosed peat soil microcosms in white. Comparison using linear mixed models with peat blocks as random variables shows significant differences in the CH_4 oxidation before and after the incubation (* $p < 0.05$; ** $p < 0.01$; *** $p < 0.001$).

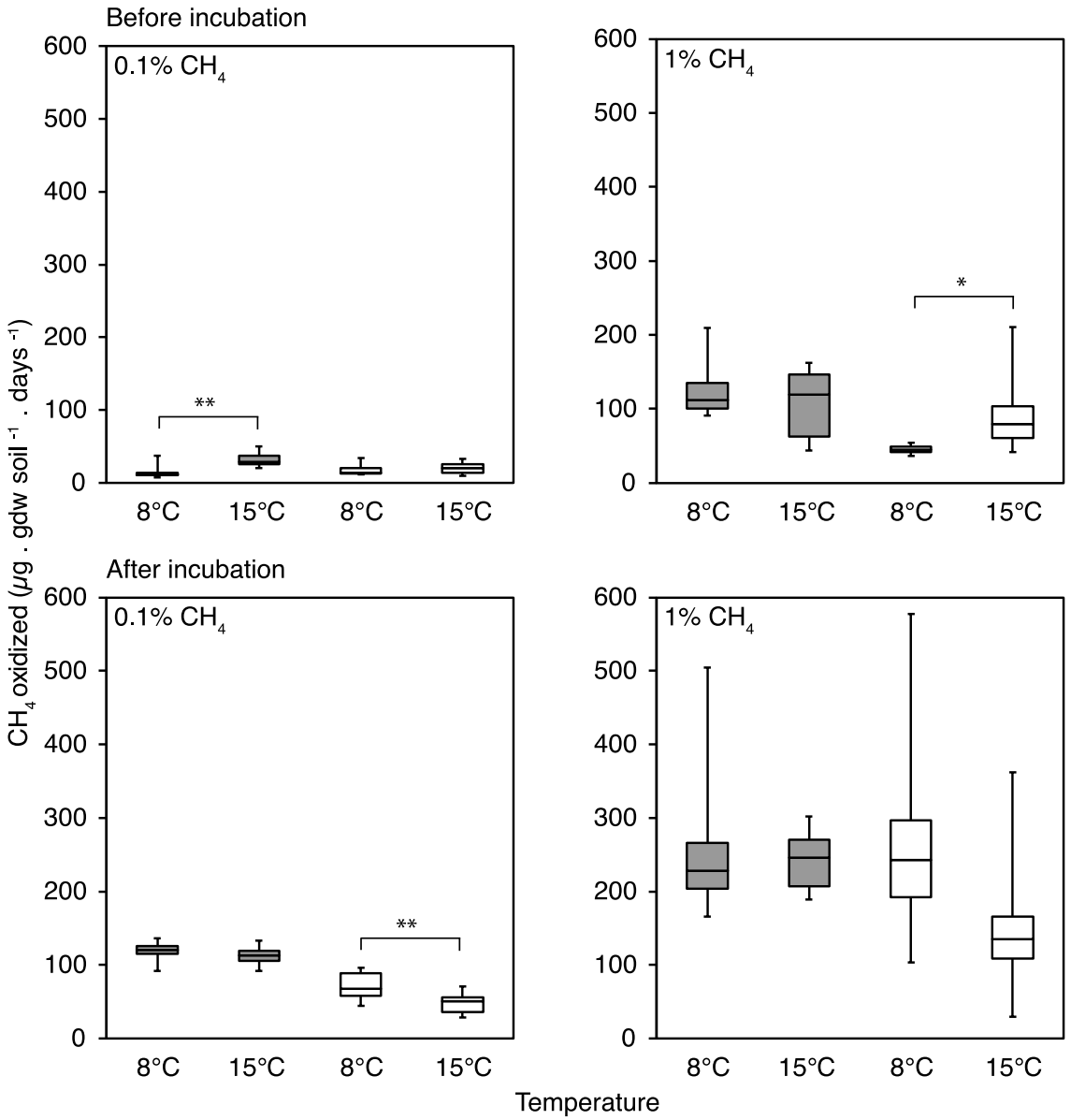

Supplementary Figure S4. CH_4 oxidation rates from Exp II emphasizing the comparison between 8 °C and 15 °C. Results are shown for measurements collected before (top) and after (bottom) the three-week incubation, and at 0.1% (left) and 1% CH_4 (right). Grazed microcosms are shown in gray; exclosed microcosms in white.Comparison using linear mixed models with peat blocks as random variables shows significant differences in the CH_4 oxidation rates between temperatures (* $p < 0.05$; ** $p < 0.01$).

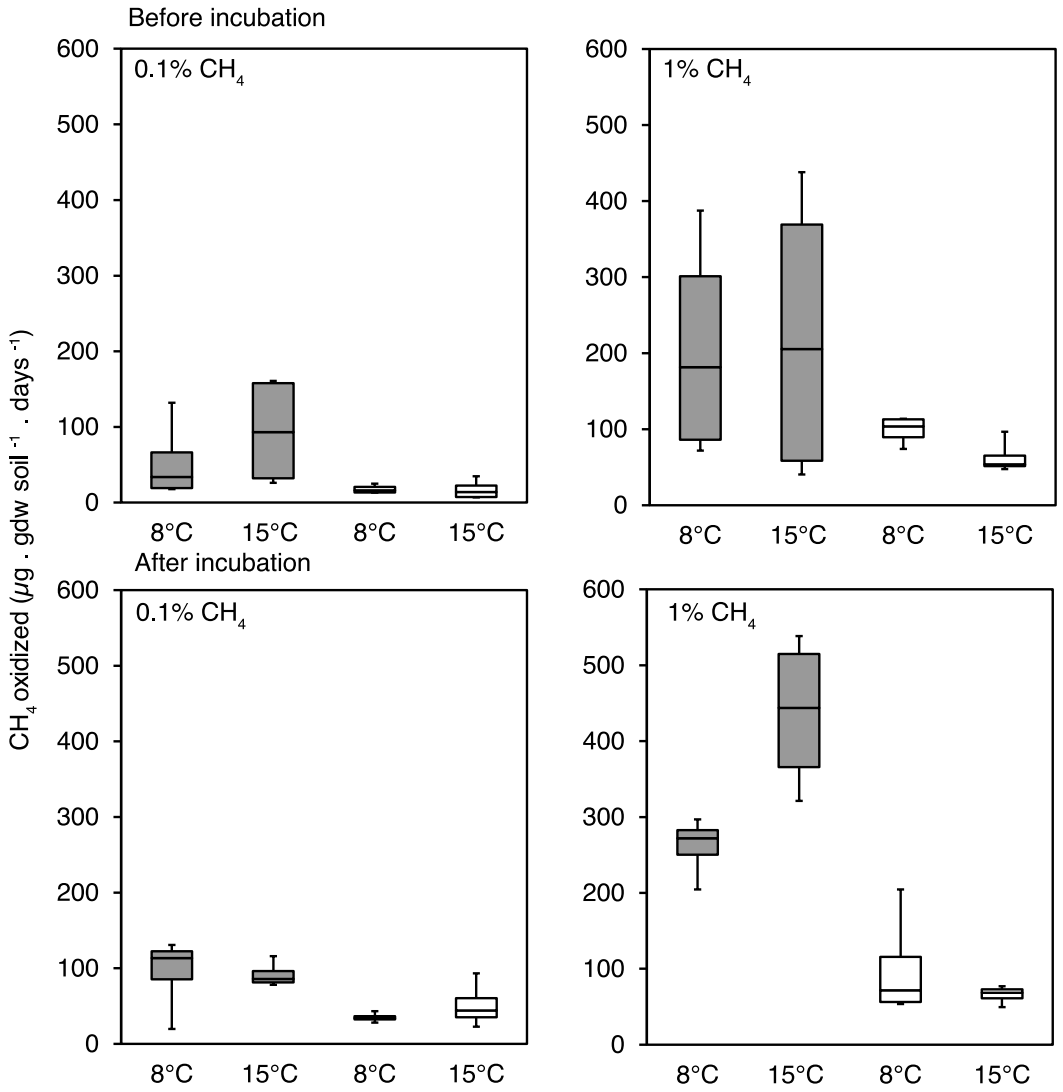

Supplementary Figure S5. CH_4 oxidation rates from Exp I emphasizing the comparison between 8 °C and 15 °C. Results are shown for measurements collected before (top) and after (bottom) the three-week incubation, and at 0.1% (left) and 1% CH_4 (right). The CH_4 oxidation rates presented here are corrected for the different amounts of CH_4 dissolved at 8 °C and 15 °C. Grazed microcosms are shown in gray; exclosed microcosms in white. Comparison using linear mixed models with peat blocks as random variables shows significant differences in the CH_4 oxidation rates between temperatures (* $p < 0.05$).

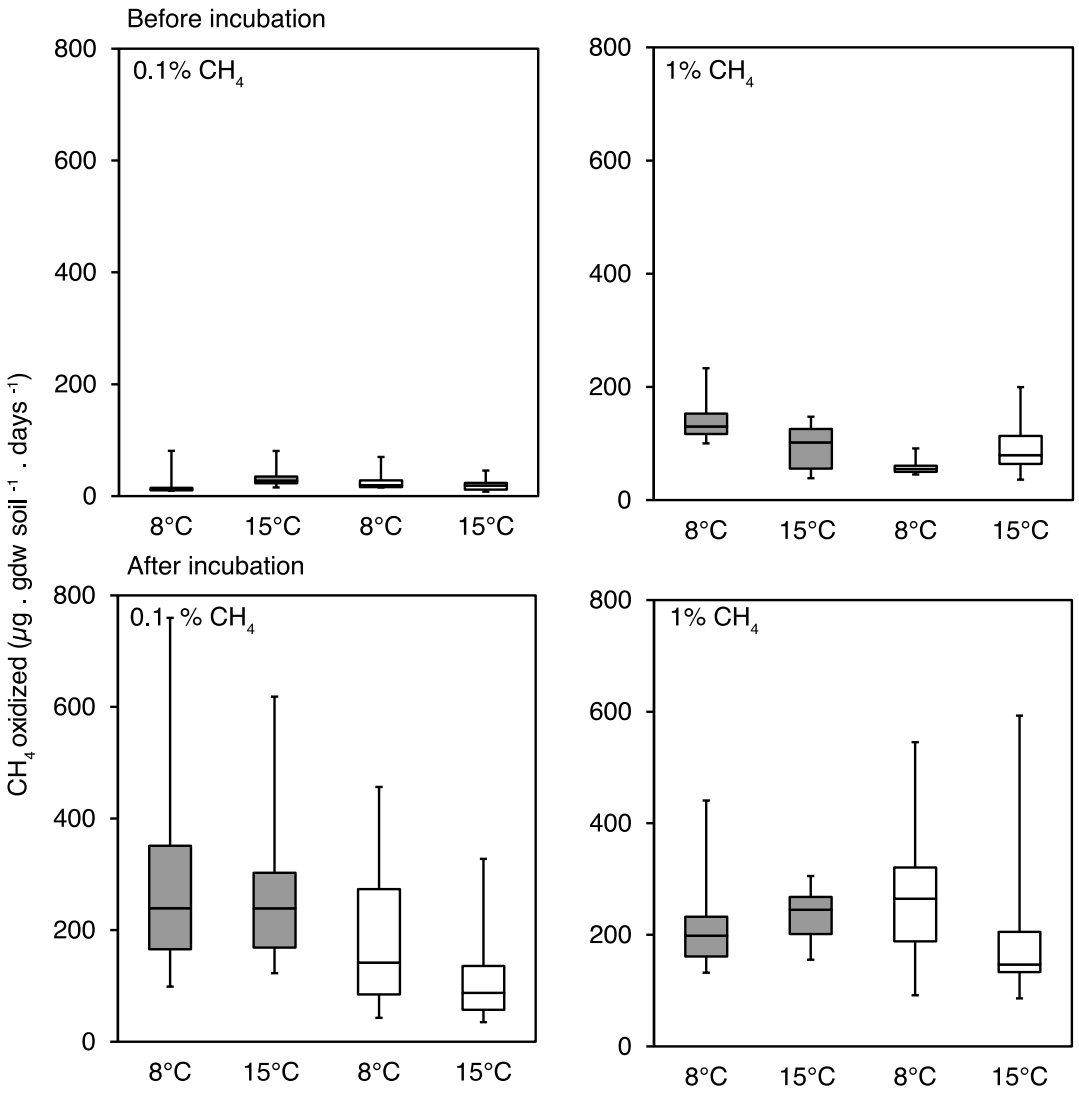

Supplementary Figure S6. CH_4 oxidation rates from Exp II emphasizing the comparison between 8 °C and 15 °C. Results are shown for measurements collected before (top) and after (bottom) the three-week incubation, and at 0.1% (left) and 1% CH_4 (right). The CH_4 oxidation rates presented here are corrected for the different amounts of CH_4 dissolved at 8 °C and 15 °C. Grazed microcosms are shown in gray; exclosed microcosms in white. Comparison using linear mixed models with peat blocks as random variables shows significant differences in the CH_4 oxidation between temperatures (* $p < 0.05$; ** $p < 0.01$).

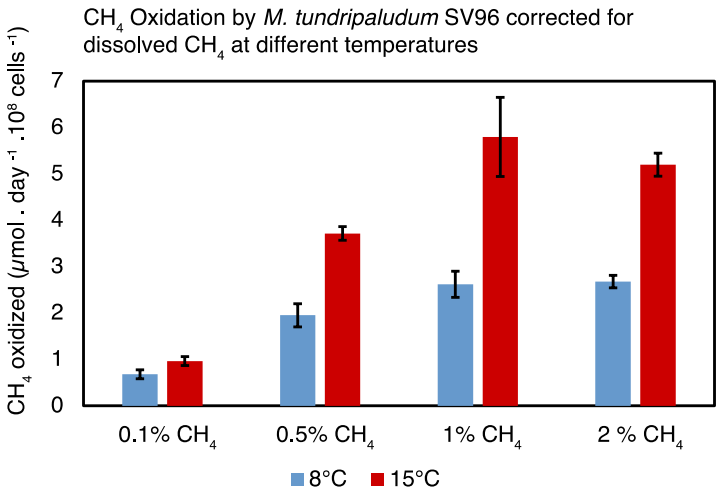

Supplementary Figure S7. CH_4 oxidation per cell for *Methylobacter tundripaludum* SV96 at 8 °C (blue) and 15 °C (red), with CH_4 headspace concentrations ranging from 0.1to 2%. The CH_4 oxidation rates have been corrected for the amount of CH_4 dissolved at 8 °C and 15 °C.

Supplementary Table S1. Number of sequences and OTUs at the different stages of the bioinformatic pipeline.

Pipeline step	Sequences		OTUs	
primer set	mb661	A682	mb661	A682
merging	2068297	1033135	---	---
quality check	1270623	438874	---	---
trimming	1240464	426302	---	---
chimera removal	1162251	422389	---	---
frameshift removal	1096123	394153	---	---
clustering	1096121	394153	11641	5075
length selection	1096106	393547	11631	4952

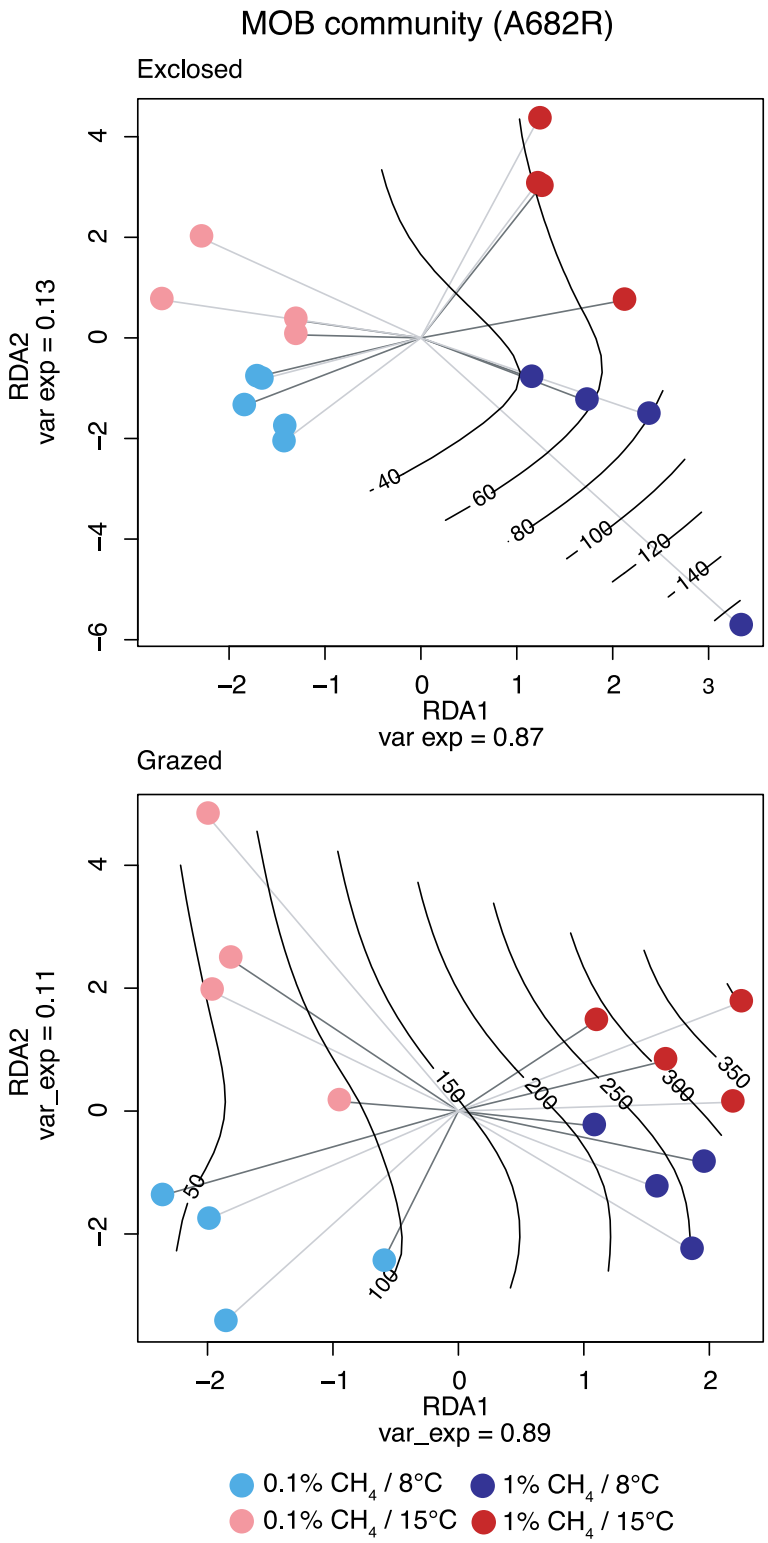

Supplementary Figure S8. Redundancy analysis of the effect of CH_4 concentration and temperature on the MOB communities after incubation (*pmoA* transcripts using the A189F/A682R primer pair). The effect of CH_4 concentration and temperature was corrected according to the peat block replicates (represented by gray shaded lines). Samples are labeled according to CH_4 concentration (light colors — 0.1% CH_4, dark colors — 1%CH_4) and temperature (blue — 8 °C and red — 15 °C). The black lines indicate a projection of the measured CH_4 oxidation rates (µg of CH_4 oxidized per gram dry soil and day).

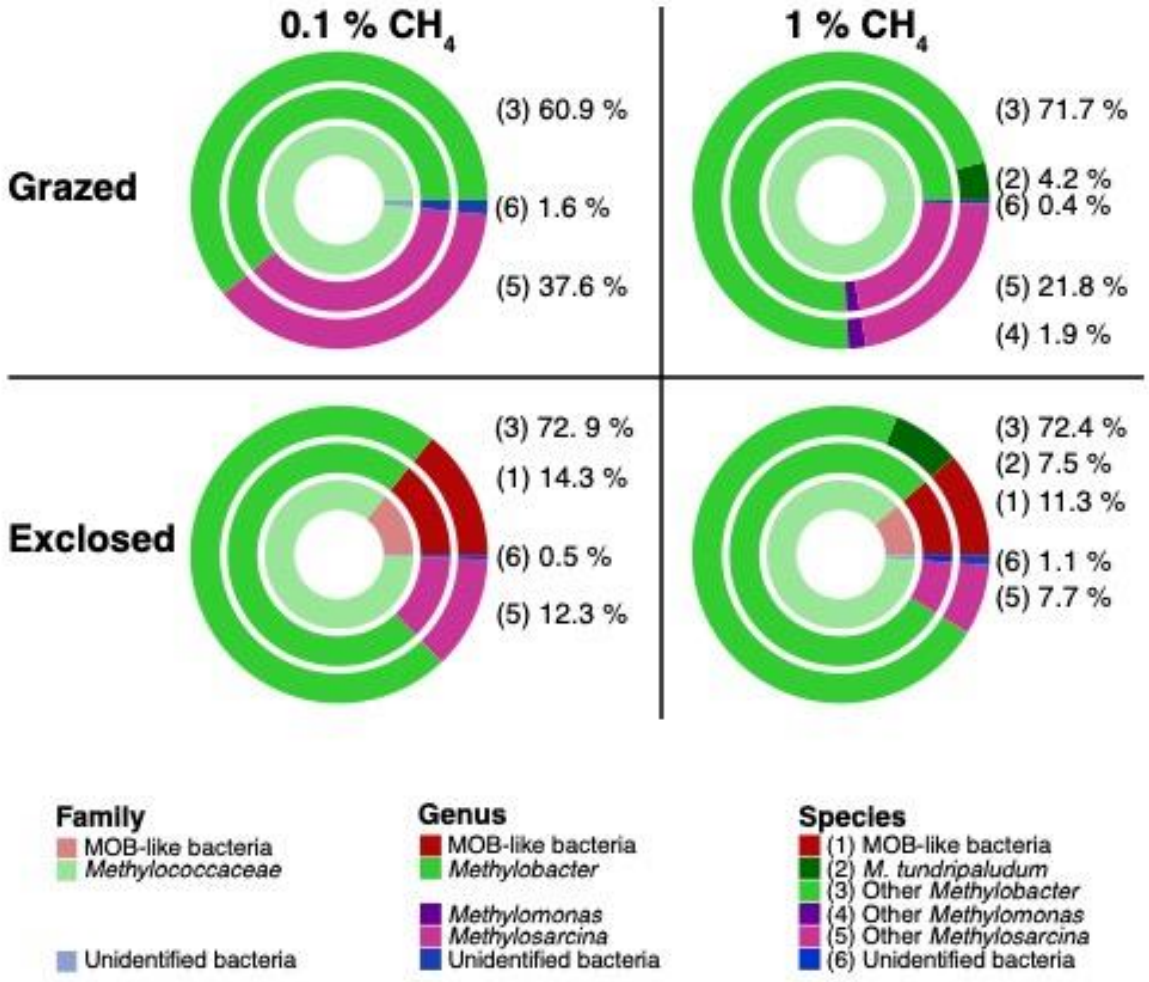

Supplementary Figure S9. Distribution of MOB taxa (A189F/A682R primer set) in grazed and exclosed peat soils after incubation at 0.1% CH_4 and at 1% CH_4 (16 soil samples per concentration and 16 soil samples per grazing condition). As temperature had no significant effect on the MOB community, these 16 samples include both the 8 °C and 15 °C incubations. Taxa with a relative abundance of > 1% are represented at the full taxonomic resolution, whereas those taxa not reaching the 1% threshold were added to their broader taxonomic group, one lvel lower in taxonomic resolution. The different rings represent different taxonomic levels from family to genus to species moving from the innermost ring outward. Relative abundances for the species level are given in %.

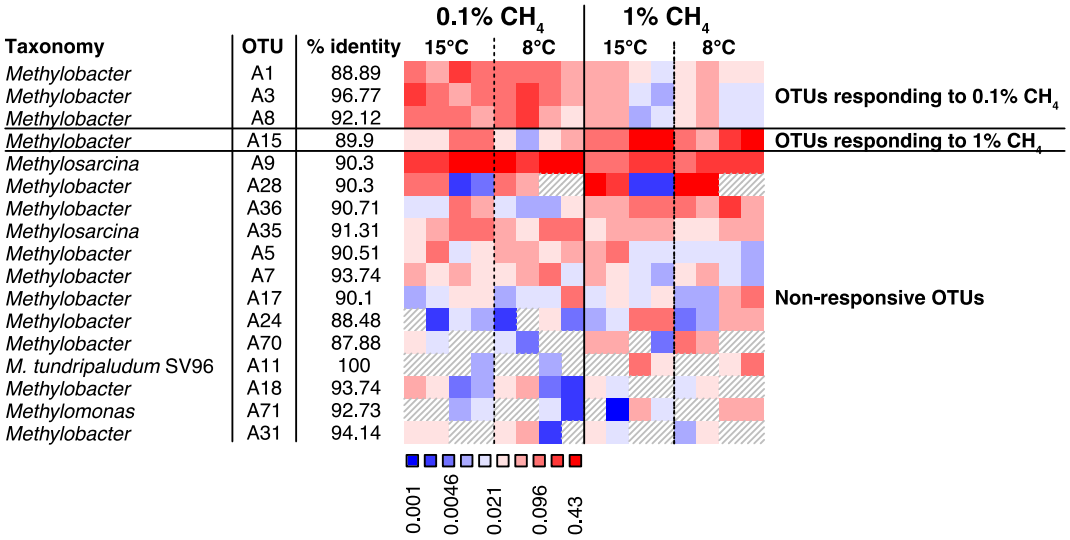

Supplementary Figure S10. Relative abundances of *pmoA* transcripts representing MOB OTUs (A189F/A682R primer pair) from grazed peat soil microcosms after incubation at 0.1% and 1% CH_4 concentrations. OTUs with higher relative abundance at 0.1% CH_4 are shown in the first block (left) and those with higher relative abundance at 1% CH_4 in the second block (right). The non-responsive OTUs with the highest relative abundance are shown in the third block. The number of OTUs included in the figure make up 90% of the total MOB community transcription. OTUs are identified as the letter A (indicating that these are part of the A682R dataset) and a number. The percentage of identity between the OTUs and the best hit in the database is given next to the OTU identification. Relative abundances reach from low abundances (blue) to high (red).

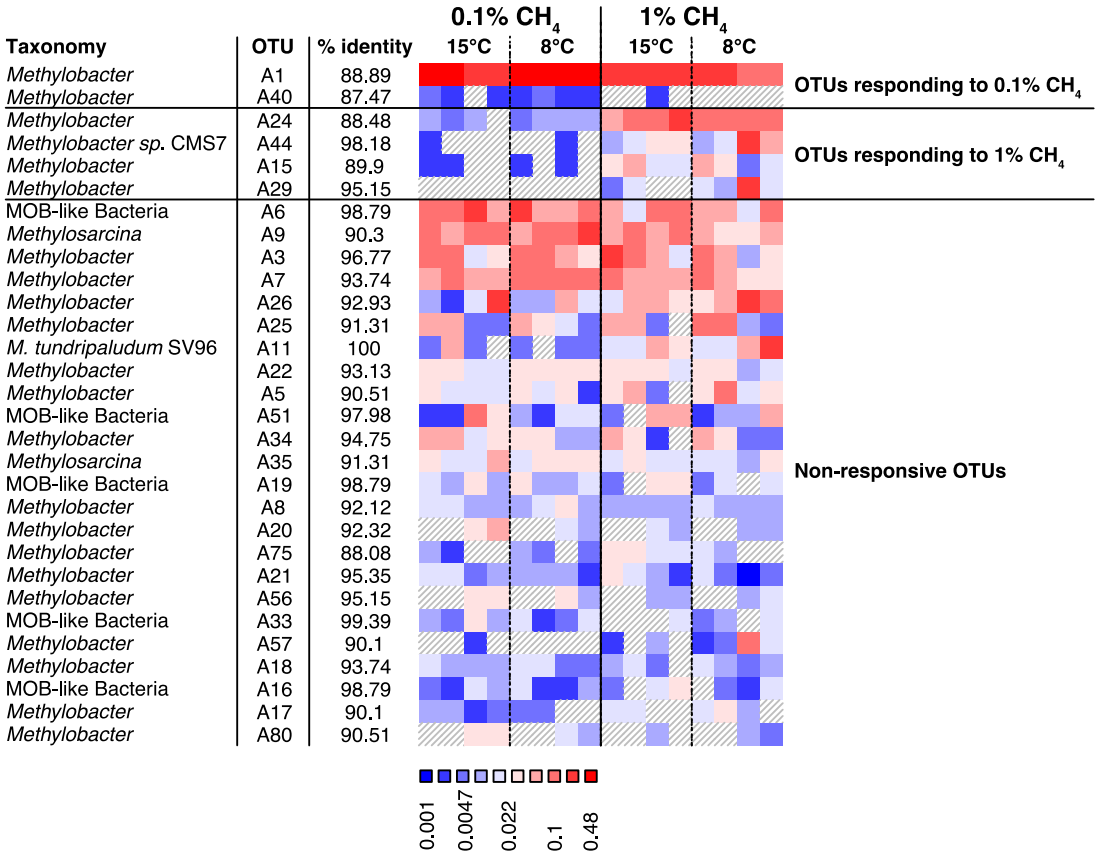

Supplementary Figure S11. Relative abundances of *pmoA* transcripts representing MOB OTUs (A189F/A682R primer pair) from exclosed peat soil microcosms after incubation at 0.1% and 1% CH_4 concentration. OTUs with higher relative abundance at 0.1% CH_4 are shown in the first block (left) and those with higher relative abundance at 1% CH_4 in the second block (right). The non-responsive OTUs with the highest relative abundance are shown in the third block. The number of OTUs included in the figure make up 90% of the total MOB community transcription. OTUs are identified as the letter A (indicating that these are part of the A682R dataset) and a number. The percentage of identity between the OTU and the best hit in the database is given next to the OTU identification. Relative abundances reach from low abundances (blue) to high (red).

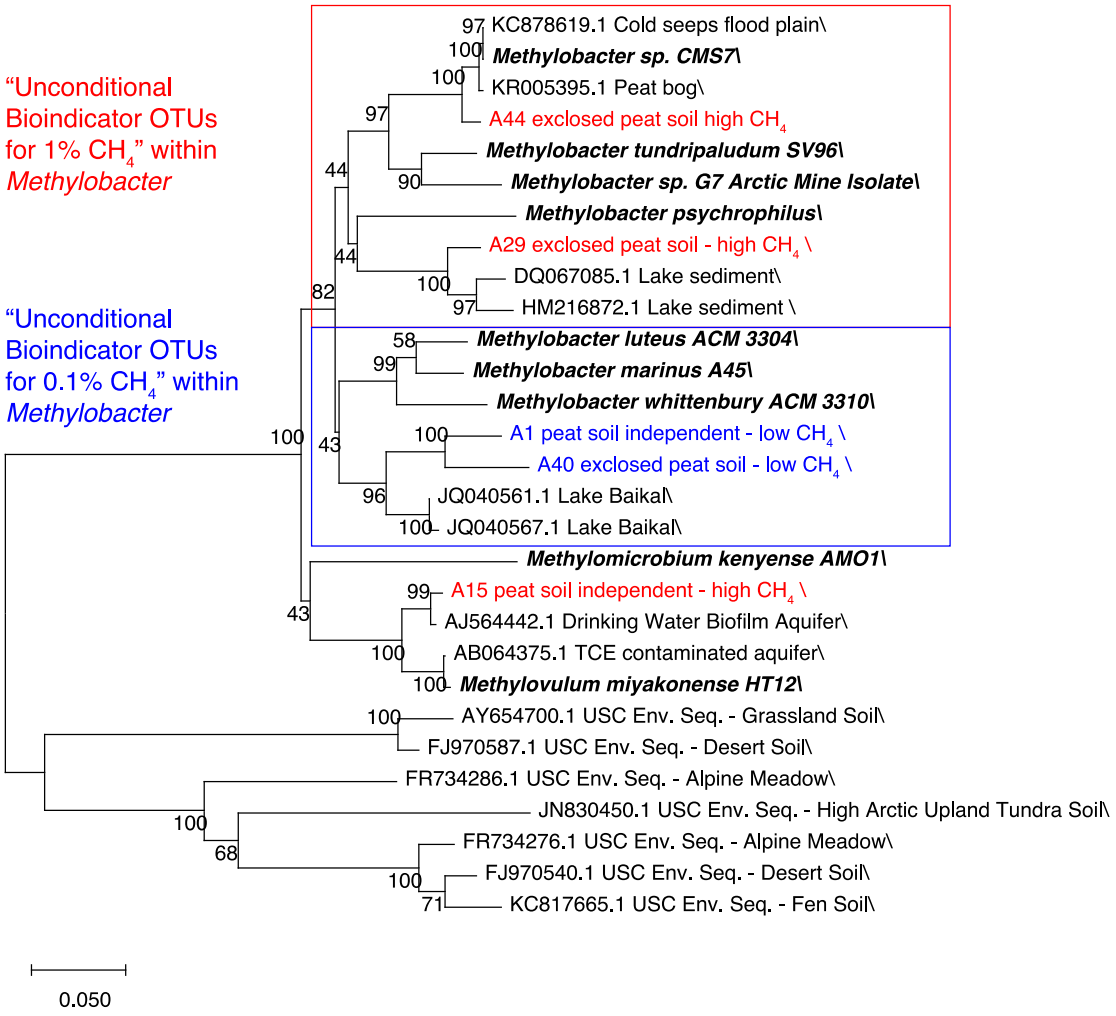

Supplementary Figure S12. Phylogenetic representation of the "unconditional bioindicator OTUs" for 0.1% CH_4 (blue) and 1% CH_4 (red) incubations, cultivated MOB (bold, italic) and closely related environmental sequences retrieved from the NCBI GenBank. All OTUs included were identified as bioindicators both in the grazed and the exclosed peat soil microcosms, or in only one of the soil types, being absent from the other soil type. The first type is called "peat soil independent". The other type of OTUs, which were specifically assigned as bioindicators for one of the peat soil types, are labeled as either grazed or exclosed. The tree is based on a 452 nucleotide alignment, using the neighbor-joining method with the Jukes-cantor correction and 500 bootstraps. The length of the branches is based on a scale of 0.05 changes per nucleotide.

microorganisms

MDPI

Correction

Correction: Rainer et al. The Influence of Above-Ground Herbivory on the Response of Arctic Soil Methanotrophs to Increasing CH_4 Concentrations and Temperatures. *Microorganisms* 2021, *9*, 2080

Edda M. Rainer [1,*], Christophe V. W. Seppey [1,2], Caroline Hammer [1], Mette M. Svenning [1] and Alexander T. Tveit [1]

[1] Department of Arctic and Marine Biology, UiT, The Arctic University of Norway, 9037 Tromsø, Norway; seppey@uni-potsdam.de (C.V.W.S.); c.hammer@boku.ac.at (C.H.); mette.svenning@uit.no (M.M.S.); alexander.t.tveit@uit.no (A.T.T.)

[2] Institute of Environmental Sciences and Geography, University of Potsdam, Karl-Liebknecht-Str. 24-25, 14476 Potsdam, Germany

* Correspondence: edda.m.rainer@uit.no

The authors wish to make the following corrections to this paper [1]:

Data Availability Statement: Reads will be available upon acceptance of the manuscript.

To the correct version, as follows:

Data Availability Statement: The data presented in this study are openly available in the European Nucleotide Archive (ENA), project PRJEB48225.

The authors would like to apologize for any inconvenience caused to the readers by these changes.

Reference

1. Rainer, E.M.; Seppey, C.V.W.; Hammer, C.; Svenning, M.M.; Tveit, A.T. The Influence of Above-Ground Herbivory on the Response of Arctic Soil Methanotrophs to Increasing CH_4 Concentrations and Temperatures. *Microorganisms* **2021**, *9*, 2080. [CrossRef] [PubMed]

Citation: Rainer, E.M.; Seppey, C.V.W.; Hammer, C.; Svenning, M.M.; Tveit, A.T. Correction: Rainer et al. The Influence of Above-Ground Herbivory on the Response of Arctic Soil Methanotrophs to Increasing CH_4 Concentrations and Temperatures. *Microorganisms* 2021, *9*, 2080. *Microorganisms* **2021**, *9*, 2535. https://doi.org/10.3390/microorganisms9122535

Received: 29 November 2021
Accepted: 1 December 2021
Published: 8 December 2021

Paper III

Glycogen storage and ribosome regulation controls methanotroph temperature acclimation

Alexander T. Tveit[a*], Andrea Söllinger[a], Edda Marie Rainer[a], Alena Didriksen[a], Anne Grethe Hestnes[a], Liabo Motleleng[a], Hans-Jörg Hellinger[b], Thomas Rattei[b], Mette M. Svenning[a]

[a]*Department of Arctic and Marine Biology, UiT The Arctic University of Norway, Post Box 6050 Langnes, 9037 Tromsø, Norway.*

[b]*Division of Computational Systems Biology, Department of Microbiology and Ecosystem Science, University of Vienna, Althanstrasse 14, Vienna, Austria.*

*Corresponding author: Alexander Tøsdal Tveit (*alexander.t.tveit@uit.no)*

Abstract

Methanotrophs oxidize up to 90 % of the CH_4 produced in natural and anthropogenic ecosystems. Often living close to the surface, these organisms must frequently acclimate to temperature change. We have studied temperature acclimation in *Methylobacter tundripaludum* SV96, a member of the widespread genus *Methylobacter*, by comparing its physiological states at 8, 15, 21 and 27 °C. At CH_4 saturation, we observed that more CH_4 was oxidized per cell division at 8 and 15 °C than at 21 and 27 °C. This higher substrate use at low temperature corresponded with an upregulation of carbon assimilation directed towards glycogen storage and large shifts in cellular glycogen concentrations depending on temperature. The entire protein biosynthesis machinery, including transcription for nucleotide and amino acid metabolism and rRNA proteins, was upregulated at 15°C; a catalytic compensation to increase rates of protein biosynthesis. We conclude that storage of excess carbon as glycogen and regulation of the protein biosynthesis machinery are vital temperature acclimation tools that control carbon and energy flows in *M. tundripaludum* SV96. Comparative experiments showed that while temperature responses differed between *Methylobacter* species, large temperature driven shifts in CH_4 uptake and growth efficiency were common. Our findings suggest substantial influence of physiological temperature acclimation on global CH_4 cycling.

Key words: Methane, methanotrophs, temperature, cell physiology, cell metabolism, gene expression

1. Introduction

Species within the genus *Methylobacter* have been identified as the most abundant and active methanotrophs in many ecosystems including peat soils, ponds, lakes, sediments, rice paddies and landfills [1-9]. These environments are among the biggest contributors to global methane (CH_4) emissions [10]. High-emitting ecosystems often contain high CH_4 concentrations (>100 µM) [11-14], meaning that *Methylobacter* species are frequently exposed to, and presumably adapted to, CH_4 uptake saturation.

Soils experience a mix of stable temperatures and large temperature fluctuations driven by day/night cycles and weather changes, and these fluctuations depend on soil type, depth, latitude, altitude and season [15-18]. Highly variable temperature effects on soil CH_4 oxidation rates have been observed, ranging from, e.g., strong temperature responses in landfills [19] to variable responses in permafrost soils [20] and minor effects under atmospheric CH_4 concentrations in forest soils [21] or high CH_4 concentrations (0.1 – 1 %) in peat [22]. According to one study, temperature responses seem to depend on the soil type and CH_4 concentration [23]. Also, CH_4 oxidation has frequently been observed as being less temperature sensitive than CH_4 production but this phenomenon has not yet been explained [20]. Despite the apparent importance of microbial temperature acclimation, we do not yet have a clear understanding of how methanotrophs and other microorganisms in the environment acclimate physiologically to temperature changes and how this relates to substrate turnover and growth.

Temperature adaptations in bacteria occur at many levels, e.g. genetic changes that influence the amino acid composition of enzymes [24], horizontal gene transfer that influences cell structure or temperature kinetics [25], modifications of membrane fatty acid composition [26] and changes in gene expression patterns or regulatory networks [27]. For example, in response to short-term cold shock, some bacteria adapt the DNA curvature and initiate translation blocks to favour translation of cold-response transcripts [28]. Bacterial cells have also been shown to grow to larger sizes and sustain larger intracellular pools of ATP to compensate for kinetic limitations at low temperatures [29, 30]. Similarly, in plants, ribulose bisphosphate cycle intermediates accumulate and offset reductions in catalytic efficiency at lowered temperatures [31]. Some studies suggest that accumulation of carbon and energy storage polymers can have a role in temperature acclimation of microorganisms, including transcriptional upregulation of polyhydroxyalkanoate storage in anoxic peat at low

temperature (< 10 °C) [32], and glycogen storage as a survival mechanism at low temperature in *E. coli* [33].

Central to the cellular response of bacteria to altered conditions, including temperatures, is the genetic information processing machinery [34]. Ribosomal tuning was shown through, e.g., studies on *E. coli* to be a major cellular tool to optimize growth rates and physiological states in response to changes in their external conditions, including temperature, e.g., [35, 36]. Recently, studies of soil microbial responses to long term warming have revealed that the higher growth rates at higher temperatures are accompanied by a reduction in the number of ribosomes [37, 38], confirming that adjustments of the protein biosynthesis machinery is a major temperature acclimation mechanism in nature. So far, physiological evaluations of temperature acclimation mechanisms in pure cultures are mostly restricted to *E. coli*.

Due to their central role as a CH_4 sink and frequent exposure to temperature change, methanotroph temperature acclimation may have a considerable influence on global CH_4 cycling. The objective with this study was to understand how the methanotroph *Methylobacter tundripaldum* SV96, originally isolated from arctic peat soil [39] but frequently detected in sub-Arctic and temperate zones, acclimate to four different temperatures representative for summer conditions in areas where this species is active, e.g., [13, 40].

To understand the physiological response of *M. tundripaludum* SV96 we combined growth and CH_4 oxidation kinetics with transcriptomics and quantification of cellular RNA, protein and glycogen. The acclimation time prior to experiments allow focus on acclimation responses over stress responses. Furthermore, we performed comparative growth and CH_4 oxidation kinetics experiments with two other *Methylobacter* species to address variation in temperature acclimation.

We show that regulation of glycogen storage and the protein biosynthesis machinery are central temperature acclimation mechanisms in *M. tundripaludum* SV96. While temperature responses differed between *Methylobacter* species, large shifts in CH_4 uptake and growth efficiency were common to their respective temperature acclimation strategies.

2. Results and Discussion

Growth kinetics of *M. tundripaludum* SV96 at 8, 15, 21 and 27 °C (assuming Michaelis-Menten kinetics) demonstrated large differences in specific growth rates between temperatures and CH_4 concentrations (Fig. 1A; p.adjust < 0.05). At CH_4-uptake saturation, cells divided fastest at 15 °C, followed by 21 °C, 8 °C and 27 °C ($V_{max(app)}$, p.adjust < 0.05). With decreasing CH_4 concentrations below ~0.01 µM, the specific growth rate at 8°C increased substantially relative to the other temperatures (Fig. 1A, upper panel). Three growth control experiments with higher CH_4 headspace concentrations (20 % in headspace and > 0.3 µM dissolved) showed similar patterns of growth at the different temperatures, but with slightly higher growth rates at 21°C relative to 15 °C, and at 27 °C relative to 8 °C (Fig. S2A, B, C).

At CH_4-uptake saturation, higher CH_4 consumption rates ($V_{max(app)}$, p.adjust < 0.05) were detected at 15°C than at 21 °C (Fig. 1B). Likewise, much more CH_4 was oxidized at 8 °C than at 27 °C (Fig. S3). At lower CH_4 concentrations, there were rather small differences in CH_4 consumption (Fig 1B). Consequently, the growth efficiency (number of cell divisions per CH_4 molecules oxidized) is much lower at 8 and 15 °C than at 21 and 27 °C (Fig. 1C). With a decrease in CH_4 concentration, growth efficiency increased at all temperatures, with largest increase at 8°C, followed by 15 °C, 27 °C and 21 °C. The observation that high temperature (21 and 27 °C) leads to more efficient growth at high CH_4 concentrations and low temperature (8 and 15 °C) leads to more efficient growth at low CH_4 concentrations, demonstrated radical shifts in cellular resource use at different temperatures and CH_4 concentrations. It also indicated an unclear relation between growth rate and efficiency as both fast and slow growing cells grew efficiently and inefficiently, depending on temperature and CH_4 concentration. These findings disagree with a proposed model in which fast and slow growth are suggested to be inefficient, while the highest efficiency is obtained during intermediate growth rates [41]. However, growth in that study refers to cellular biomass growth, while we consider microbial growth to equal cell division and cell biomass to vary independently of cell division due to changes in cell size and contents [42, 43].

This inefficient growth at low temperatures and CH_4 uptake saturation (Fig. S3) interested us as it means more CH_4 is harvested prior to cell division at low temperature than at high temperature. Saturating CH_4 concentrations are common in high-emitting ecosystems and many of these ecosystems are cold; as an example, 25 % of the Arctic landmass is covered

by wetlands [44]. Thus, our observation means that a considerable amount of global CH_4 has an unknown physiological fate. Consequently, we focused on identifying potential explanations for the additional CH_4 consumed at low temperature. From literature we learn that excess substrates may be consumed during cell division to cover costs for ROS (reactive oxygen species) protection, protein repair, compensations to prevent low metabolic turnover rates [45, 46], leakage from cells [47], larger or denser cells [30, 42] or storage polymers [48]. Recent studies also demonstrate how adjustments of the protein biosynthesis machinery can consume or liberate cellular resources during temperature acclimation [38, 46]. To identify which mechanisms are involved in acclimation of *M. tundripaludum* SV96, we extracted nucleic acids for transcriptomics from cells incubated at 8, 15, 21 and 27 °C and saturating CH_4 concentrations (> 0.1 mM dissolved CH_4) during logarithmic growth.

Cellular RNA and DNA content in *M. tundriplaudum* SV96.

A fast growing *E. coli* cell, contains as a percentage of dry weight, approximately 55 % protein, 20 % RNA (primarily rRNA), 9 % lipids and 3 % DNA [49]. The RNA to DNA ratio in *M. tundripaludum* SV96 was lower than reported for fast growing *E. coli*, and varied between temperatures with averages of 2.3, 3.7, 3.6 and 2.8, at 8, 15, 21 and 27 °C, respectively (Fig. 2). All differences, except between 15 and 21 °C, and 8 and 27 °C were significant (p.adjust < 0.05), demonstrating temperature related differences in cellular RNA content. The DNA quantities extracted per 10^8 *M. tundripaludum* SV96 cells were not significantly different between temperatures (p.adjust > 0.077) (Fig. 2). The RNA quantities were significantly different between all temperatures (p.adjust < 0.05) except 21 and 15 °C (p.adjust = 0.0612) (Fig. 2), in line with the RNA/DNA ratios. The majority of cellular RNA is ribosomal RNA (82 – 90 %) and total RNA is therefore proportional to the cellular amount of ribosomal RNA (rRNA) [50]. Ribosomes make up a large fraction of bacterial cell biomass [51], with rRNA constituting up to 20 % of cell DW (dry weight) [52] and ribosomal proteins making up 2 – 40 % of total proteins [35], and therefore potentially more than 20 % of cell DW. Thus, tuning of the cellular ribosome concentration is a major mechanism involved in optimizing growth rates in *E. coli* [35]. Furthermore, ribosomes are estimated to account for ~50 % of the energy consumption of rapidly growing *E. coli* [53]. Correspondingly, one of the most powerful bacterial growth laws states that the relationship between bacterial growth and cellular ribosome content is linear [35, 46]. However, the poor correlation between cellular RNA

concentration and growth rate (R^2 = 0.57) for *M. tundripaludum* SV96 is not consistent with this assumption. A recent study suggested that due to the effect of temperature itself on enzymatic rates, growth and ribosome concentrations do not correlate well [46], matching our observations.

Transcriptomics.

The inefficient growth at 15 °C and CH_4 saturation (Fig. S3) may be partly explained by the high cellular RNA (Fig. 2), as more CH_4 is needed to build more ribosomes. However, the RNA content was similar at 21 and 15 °C, despite much more efficient growth at 21 °C. This raised the question whether other mechanisms could explain the large differences in growth efficiency between temperatures.

Three mRNA enriched transcriptome libraries from each of the temperatures (Fig. S1 A) were sequenced, resulting in a total of 12 mRNA libraries. The mRNA fraction ranged from 30 % to 99 % mRNA after rRNA depletion, leaving between 2.2 million and 15.3 million mRNA reads aligned to the *M. tundripaludum* SV96 genome (Supplementary dataset 1, S6).

Central carbon and energy metabolisms.

We observed significantly higher expression of particulate methane monooxygenase (pMMO) and methanol dehydrogenase (MDH) at 15, 21 and 27 °C than at 8 °C (Fig. 3). Thus, the high oxidation rates at 8 and 15 °C relative to 21 and 27 °C (Fig. S3), despite lower or similar expression of pMMO at low temperatures, suggest that *M. tundripaludum* SV96 carries a low temperature-adapted pMMO. Furthermore, the small changes in $K_{m(app)}$ with temperature (Fig. 1B) indicates that this adaptation is not related to substrate affinity, but rather the ability of the enzyme to convert substrate to product more quickly at low temperature (higher K_{cat}).

We also observed increased transcription for NADH generating tetrahydromethanopterin (TH_4MPT) pathway C_1 transfer to CO_2 at 15 °C (Fig. 3), suggesting an overall upregulation of energy conservation. However, there were no distinctive upregulation of oxidative phosphorylation at 15 °C (Fig. 3). Rather, we observed increased transcription of genes for different enzyme systems with the same functional role (e.g., complexes I, IV and V) at 15 and 21 °C, respectively. Isozymes; enzymes with different amino acid sequences that catalyse the same reaction; have previously been suggested as an important part of microbial

temperature acclimation [54, 55]. However, the discrete functional roles of different functionally analogous but non-homologous enzyme systems with roles in oxidative phosphorylation are generally not well understood [56].

We observed significant upregulation at 15 °C for a large proportion of the genes leading from CH_4 oxidation through the Ribulose monophosphate pathway (RuMP) fructose bisphosphate branch 1 (FBP 1) towards nucleotide biosynthesis (Fig. 3). This was in line with the high cellular RNA content at 15 °C (Fig. 2) and also in accordance with transcriptional upregulation of translation, amino acid biosynthesis, nucleotide metabolism and protein metabolism in *E. coli* exposed to higher temperatures [57, 58].

Nucleotide biosynthesis, transcription, and translation.

Nucleotide biosynthesis pathways receive the precursors 2-Oxo-glutarate and D-ribulose-5P from the TCA cycle and RuMP, respectively; molecules which are needed to serve the purine and pyrimidine pathways (Fig. 4). We observed significant upregulation at 15 °C for 30 out of 46 pathway steps needed for nucleotide biosynthesis from these two precursors, matching the upregulation of RuMP towards nucleotide biosynthesis.

Among the genes encoding the DNA-directed RNA polymerase, only the β subunit, *rpoB* (α; *rpoA*, β′; *rpoC*, β; *rpoB*) was significantly upregulated at 15 °C (Fig. S4). The genes for three out of four enzymes that compose the RNA degradosome; RNase E, Enolase, and polynucleotide phosphorylase; were also upregulated at 15 °C, while the gene encoding ATP dependent RNA helicase (*rhlE*) was not (Fig. S4). Genes encoding enzymes for protein folding; *groE*, *groL* and *gnaK were upregulated at 15 °C* (Fig. S4). This increased investment into transcription, RNA degradation and protein folding at 15 °C was matched by the overall upregulation of the small subunit (SSU) and large subunit (LSU) ribosomal proteins, with 15 out of 29 LSU and 14 out of 19 SSU proteins being significantly higher expressed at 15 °C (Fig. 5). These observations were further supported by the overall upregulation of amino acid biosynthesis at 15 °C, with many individual pathway steps (43 out of 79) being significantly upregulated at 15 °C relative to the other temperatures (Fig. S5). It is important to note that this overall upregulation of the protein biosynthesis machinery does not imply that we also find higher protein synthesis rates at 15 °C than at 21 °C. The reason is that all synthesis rates, including the synthesis of ribosomes and proteins, are directly influenced by temperature [46]. However, the upregulation does increase protein biosynthesis rates relative to the rates that

would have been obtained without upregulation and can therefore be considered as upregulation of protein biosynthesis itself. Such catalytic compensation comes at a cost, in line with the higher CH_4 consumption per cell division at 15 °C than at 21 °C (Fig. S3 C). Similar catalytic compensation at low temperature was previously seen in the upregulation of ATP and RuBisCO in bacteria and plants, respectively [29, 31], and also suggested as part of the bacterial response to soil warming [38].

We wanted to test the hypothesis that the regulatory adjustments of the protein biosynthesis machinery acted as a catalytic compensation mechanism, resulting in stable cellular RNA and protein concentrations, except at 8 °C where we expected fewer ribosomes (see Fig. 2) and proteins. Therefore, we extracted total RNA and protein from cells cultivated at 8, 15, 21 and 27 °C in a new growth experiment (Fig. S1C, Fig. S2C). The RNA:DNA ratio followed a similar pattern as observed previously, with lower but not significantly different (p.adjust ≥ 0.089) RNA:DNA ratios at 8 °C relative to the higher temperatures (Fig. 6A). Correspondingly, Protein:DNA ratios were also lower at 8 °C, and not significantly different (p.adjust ≥ 0.22) from the other temperatures (Fig. 6B). Summarized, our observations demonstrate consistently lower cellular RNA at 8 °C, although not always significant, and indicates lower cellular protein content at this temperature. However, the lack of differences between 15, 21 and 27 °C means that the observed transcriptional adjustments often resulted in similar cellular concentrations of ribosomes and proteins at different temperatures. Stable ribosome concentrations across a broad temperature range and declines at extremes, were also seen in E. coli between ~25 and 37 °C [46].

Can glycogen storage explain high CH_4 consumption per cell division at 8°C?

The lack of upregulated protein biosynthesis at 8 °C implies that the high CH_4 consumption per cell division at this temperature remained unexplained. Higher rates of energy conservation and CO_2 production through the H_4MPT pathway (Fig. 3) at 8 °C could have accounted for the low growth efficiency. However, the CO_2 production per CH_4 molecule consumed was highest at 21 °C, followed by 8 and 15 °C (Fig. S6), offering no explanation.

Some bacteria are known to store superfluous carbon and energy as, e.g., Glycogen or poly-β-hydroxybutyrate [59]. In searching the genome of *M. tundripaludum* SV96 for carbon storage pathway genes we identified all steps from CH_4 oxidation, via the initial steps of RuMP-FBP (Fig. 3), to glycogen synthesis. Starting from formaldehyde, the genes for 6 out of the 8

steps needed to produce glycogen were upregulated at 8 °C and 15 °C (Fig. 7A). However, for the final step from amylose to glycogen, catalyzed by a 1,4-alpha-glucan branching enzyme (EC: 2.4.1.18), there were two gene copies. These copies were transcriptionally tuned opposite to each other in relation to temperature, suggesting this as an important regulatory step for glycogen synthesis. As glycogen accumulation could potentially account for the high CH_4 consumption at low temperature, we tested whether cells of *M. tundripaludum* SV96 had accumulated different quantities of glycogen at different temperatures. When cells were harvested in early stationary phase, more glycogen had accumulated at 8 °C, than 15 and 21, in line with the overall transcriptional patterns, but accumulation was much higher at 27 °C (Fig. 7B). This suggests that fast CH_4 uptake rates relative to the specific growth rates at 8 and 15 °C creates an incentive for the cells to store the surplus as glycogen, in comparison to the situation at 21 °C, and that cells at 27 °C are not at all able to spend all the resources consumed and rather directs them to storage. However, when the cells were harvested in the logarithmic phase, we observed that cells accumulated highest concentrations of glycogen at 21 °C, indicating that during fast growth glycogen acts as an intermediate carbon and energy storage. Thus, glycogen accumulation failed to directly account for the high substrate consumption at low temperature. However, we propose that glycogen acts as a key buffer compound for balancing the distribution of carbon and energy resources between growth and storage during temperature acclimation. Furthermore, this cellular tool also seems to have a key role in cell adjustments between growth states for *M. tundripaludum* SV96 as previously described for yeast and *E. coli* [60].

Growth, membranes, cell walls and exopolysaccharides. FtsZ is a key enzyme in bacterial cell division, being involved in Z-ring formation, a constricting structure at the division site [61, 62]. The gene expression pattern for FtsZ and related proteins reflected the growth rates of the culture at different temperatures with similar expression levels at 15 and 21 °C and lower expression at 8 and 27 °C (Fig. S7). This further corresponds to the upregulation of genes for cell wall synthesis at both 15 and 21 °C. At 27 °C we observed a strong upregulation of genes for exopolysaccharides (Fig. S8A). As *M. tundripaludum* SV96 does not grow above 30 °C [39], these responses might reflect the adjustments needed for survival at high temperatures. Correspondingly, increased expression of polysaccharides is often associated with sub-optimal conditions, including temperatures outside the growth optimum range [63, 64].

Exopolysaccharides are thought to protect cells from high temperatures by strengthening their structural integrity. On the other hand, desaturation of fatty acids is a common response in bacteria exposed to low temperature in an attempt to increase membrane fluidity, e.g., [26, 65]. We observed significant upregulation of fatty acid desaturase at 8 °C and 15 °C, relative to 21 and 27 °C (Fig. S7B).

Temperature effects on growth and CH_4 oxidation kinetics in different methanotrophic species. To further improve our understanding of the ecological relevance of temperature acclimation for CH_4 oxidation in different environments we performed the same CH_4 oxidation and growth experiments reported in Fig. 1 for two additional species from the genus *Methylobacter.* This genus is widespread and abundant in soils and aquatic environments (Fig. 8A) and can therefore be considered an important contributor to global CH_4 cycling.

Methylobacter sp. G7 is closely related to *M. tundripaludum* SV96, while *Methylobacter luteus* IMV-B-3098 is more distantly related (Fig. S9). *Methylobacter* sp. G7 originates from a biofilm inside the coalmine G7 close to Longyearbyen, Svalbard (78°13'00"N 15°38'00"E). The coalmine has a stable temperature of 10 °C. *Methylobacter* sp. G7 has not been published as a novel species to date, but its gene identities to *M. tundripaludum* SV96 (94.35 % for *pmoA* and 98.88 % for the 16S rRNA gene), different fatty acid profile (Supplementary dataset 1, S26) and adaptation to temperature suggests that it might represent a novel *Methylobacter* species. *Methylobacter* sp. G7 did not grow at 27 °C, and therefore the experiments with this strain were carried out at 4, 8, 15 and 21 °C. The highest growth rate for *Methylobacter* sp. G7 under CH_4 saturation was at 8°C, followed by 4, 15 and 21 °C. The highest CH_4 oxidation rates were at 21 and 8 °C, followed by 15 and 4 °C (Fig. S10). This gives the highest growth efficiency, under CH_4 saturation, at 4 °C, followed by 8, 15 and 21 °C. This temperature response pattern is very different from *M. tundripaludum* SV96 (Fig. 1), but the two strains share a large increase in growth efficiency at lower CH_4 concentrations and low temperature. *M. luteus* is a mesophilic species and typically found in freshwater or marine sediments or sewage [66]. *M. luteus* IMV-B-3098, the strain used in this study, had the highest cell division and CH_4 oxidation rates at 27 °C, followed by 21 °C (Fig. S11). Its highest growth efficiency was at 15 °C, but its changes in growth efficiency with CH_4 concentration and temperature were considerably smaller than for the two other strains. Common to all three *Methylobacter* strains were large influences of temperature and CH_4 concentrations on their physiology, affecting CH_4 consumption and growth efficiency.

Important cellular mechanisms controlling temperature acclimation and carbon cycling. Adjustments of ribosomes and storage compounds allow cells to manage their resources effectively [48, 53], while the utilization of storage compounds have been suggested as a major buffer mechanism to balance cell stoichiometry, with potentially large implications for soil microbial ecology [67].

We conclude that regulation of the protein biosynthesis machinery and glycogen storage are key temperature acclimation mechanisms in *M. tundripaludum* SV96, a type strain and widespread member of the genus *Methylobacter* (Fig. 8B). Furthermore, the large changes in CH_4 consumption and growth efficiency with temperature for the three *Methylobacter* strains demonstrate a substantial influence of temperature acclimation on methanotroph function. Considering the importance of temperature changes in surface environments, and the widespread distribution of *Methylobacter* in CH_4-emitting ecosystems, temperature acclimation is therefore likely to exert considerable influence on global CH_4 cycling. However, the extent of this influence depends on methanotroph ecology as different species and strains dominate different environments and respond distinctively to changes in temperature and CH_4 concentrations.

3. Materials and Methods

Cultures (all experiments, see Fig. S1 and Supplementary dataset 1). During stock culture maintenance, pre-incubations and experiments, *M. tundripaludum* SV96 [39], (DSMZ 17260), *Methylobacter* sp. G7 (unpublished) and *Methylobacter* luteus IMV-B-3098 (ATCC 49878T) [68] were cultivated on nitrate mineral salt (NMS) medium [69], see [70] for trace element solution, with a headspace of ambient air with CH_4 added to a concentration of 20 %. Liquid cultures were initially prepared from a frozen stock (Fig. S1). Prior to distribution of inoculum to the respective acclimation temperatures, the cultures were maintained at room temperature (~20°C) or 15 °C (*Methylobacter* sp. G7) for a period of at least six weeks. Then, the cultures were divided in four parts, one part for each experimental temperature for acclimation.

Acclimation (all experiments, see Fig. S1 and Supplementary dataset 1). During acclimation, cells were incubated in 80 mL NMS medium under ~80 % air and ~20 % CH_4 (12 mL of 100 %

CH_4 was injected into a 40 mL headspace containing air) at 8, 15, 21 and 27 °C (*M. tundripaludum* SV96 and *M. luteus* IMV-B-3098), or 4, 8, 15 and 21°C (*Methylobacter* sp. G7) (Fig. S1). The volumes required to obtain these concentrations, resulted in ~1.3 atm headspace pressure at room temperature inside the incubation bottles. The bottles were sealed with butyl rubber plugs (3 mm thick, Chromacol, Munich, Germany) and aluminium crimp caps (Chromacol, Munich, Germany). During acclimation, the cultures were transferred to new NMS medium three times to maintain the cells in logarithmic growth and finally obtain cultures in early logarithmic phase at a density of 1-5 x 10^8 cells mL^{-1}. These cultures were diluted to approximately 5 x 10^7 cells mL^{-1} in new NMS medium for growth, growth kinetics, CH_4 oxidation kinetics, CO_2 production, transcriptomics, glycogen measurements, nucleic acids extractions and protein extractions (Fig S1). During acclimation and subsequent experiments, cultures were shaken horizontally at 50 rpm. The cultures were always allowed acclimation for the time needed to surpass 10 generations (7 – 12 days).

Shaking speed and mass transfer limitations. Strains that consume gases can experience mass transfer limitations due to low substrate solubility if, e.g., high cell densities result in CH_4 uptake rates that are higher than the CH_4 dissolution rates. Gas solubility decreases with increasing temperature. Therefore, estimates of activity must be related to the estimated dissolved concentration and mass transfer limitation must be prevented. Faster shaking or higher headspace gas concentrations increase the rate of gas dissolution, but the former is more often used to prevent mass transfer limitation. We applied 50 rpm shaking (KS501, Ika Labortechnik, Staufen, Germany) in the main experiment and all support experiments except those carried out at 150 rpm for comparison of shaking speed effects (Fig. S1 and Supplementary dataset 1). At 50 rpm, the CH_4 uptake per 10^8 *M. tundripaludum* SV96 cells was linear at all temperatures and CH_4 concentrations. For the different temperatures, 8, 15, 21 and 27 °C, averages of R^2 (21 linear regressions per temperature in triplicates for each of seven concentrations) were 0.91, 0.91, 0.88 and 0.79, respectively (Supplementary dataset 1, S3). At the two lowest concentrations, where mass transfer limitations are most probable, R^2 values were above 0.9 for all temperatures. This confirms zero order kinetics at all temperatures and CH_4 concentrations, despite increasing cell density with time (Supplementary dataset 1, S2), meaning that cells growing at 50 rpm are not exposed to mass transfer limitations of gaseous substrates. However, because higher shaking speeds are often used to prevent mass transfer

limitations, we tested the effect of higher shaking speed on *M. tundripaludum* SV96 at 15 and 21 °C. When shaking at 150 rpm growth rates were ~0.035 – 0.073 cell divisions per cell per hour at 15 and 21 °C and CH_4 saturation (Fig. S1F, G, H and Supplementary dataset 1, S10 – S12). In comparison, when shaking at 50 rpm at the same temperatures, growth rates were 0.061 – 0.11 cell divisions per cell per hour at CH_4 saturation (Fig. S1A, B, C and Supplementary dataset 1, S1, S2, S7, S8). This demonstrates slower average growth at 150 rpm than at 50 rpm.

Cell growth experiments (Fig. S1A, B, C, D, E, F). Subsamples of acclimated logarithmic-phase cultures (75ml) at the different temperatures were diluted to approximately 5×10^7 cells mL^{-1} with NMS. Then, 22-mL aliquots (in triplicate) of each diluted culture were transferred to 125-mL glass bottles with 80 % air and 20 % CH_4 in a headspace atmosphere with 1.3 atm pressure. This resulted in 0.36 – 0.51 mM dissolved CH_4 and 20 % headspace CH_4 concentration, depending on the temperature, well within the threshold of CH_4 saturation for *M. tundripaludum* SV96. Approximately 0.1 mM CH_4 is needed for saturation, see Fig. 1B. Bottles were sealed with butyl rubber plugs (3 mm thick, Chromacol, Munich, Germany) and aluminium crimp caps (Chromacol, Munich, Germany). The bottles were incubated at 8, 15, 21 and 27 °C and 50 rpm (Fig. S1A – E) or 150 rpm (Fig. S1F) for up to 36 hours. See supplementary dataset 1 (S1, S7, S8, S9, S10) for incubation time and sampling time points for each experiment. At time zero and at the regular intervals, 300 µL of cell suspension (in duplicate) was transferred to a Nunclon Delta Surface plate (Thermo Scientific, Waltham, MA, USA) and the cell density was measured (Spectra Max 250 microplate reader, Molecular Devices, San José, CA, USA) at 600 nm (NMS medium as blank). For OD measurements, blanks were subtracted from measurements.

Glycogen experiment (Fig. S1E). The cells were acclimated and cultivated under 20 % CH_4 in air as described above in the acclimation and growth experiment sections. Five replicate bottles with 20 mL culture and 20 % CH_4 in air were incubated per temperature in darkness with 50 rpm shaking for 48 hours to reach high cell density in logarithmic growth phase, or transition zone between logarithmic and early stationary phase at 15 and 21 °C. At 27 °C and 8 °C it took 60 and 90 hours, respectively, to reach those same cell densities Supplementary dataset 1, S24). In addition to a standardization of the cell densities of the different growth phases, the initial inoculum volume was larger in those incubations that were harvested in the transition phase to reach this phase within the same amount of time. At two time-points

during incubation, 2 – 10 mL of culture was sampled for glycogen measurements, depending on the culture density. The culture was centrifuged in 2ml Safe Lock tubes at 25 000 x g and 4 °C for 10 minutes to collect cell pellets. The pellets were washed in 1ml 1x PBS and stored at -80 °C. After thawing on ice, the pellets were resuspended in 400µl ice cold milliQ water, transferred to lysis matrix E tubes (MP biomedicals, Irvine, CA, USA) for bead beating at 4.0 m s^{-1} for 15 seconds before heat treatment at 99 °C for 10 minutes and centrifugation at 10 000 x g at 4 °C for 10 minutes. The recovered lysate was kept on ice while preparing the kit reagents and standard dilutions according to the manufacturer's recommendations (Glycogen assay kit, ab65620, Abcam, Cambridge, UK) for fluorometric analysis. In brief, each sample was pipetted in four wells mixing 25 µl lysate with 25 µl hydrolysis buffer to get duplicate readings of sample + sample background control. The samples and standards were added 1 µl hydrolysis enzyme each, followed by incubation at room temperature for 30 min. All wells were then added 50 µl reaction mix, incubated another 30 min at room temperature, followed by glycogen quantification using a plate reader (GloMax® Explorer, Promega, Madison, WI, USA), by measurement of oxidized glucose from hydrolyzed glycogen that is labeled with an OxiRed probe emitting fluorescence at 587 nm.

CH_4 oxidation kinetics, growth kinetics and CO_2 production rate (Fig. S1A, D, F, G, H, I, J). Subsamples of acclimated exponential-phase cultures (75 mL) were diluted to approximately 5×10^7 cells mL^{-1} with NMS medium, giving a total volume of 150 – 200 mL. Then, 21.6 mL aliquots of these diluted cultures were transferred to 125 mL glass bottles. We used triplicate aliquots for each of seven CH_4 concentrations, for a total of 21 bottles per temperature and 84 bottles per strain (Fig. S1A, G, H, I and J). For each temperature, two negative controls of 21.6 mL phosphate buffer in 125 mL glass flasks were prepared per CH_4 concentration to reveal technical issues (56 negative controls in total per strain). Seven volumes (200 µl; 600 µl; 1,5 mL; 3 mL; 6 mL; 12 mL; 15 mL) of a gas mix containing 95 % CH_4 and 5 % N_2 were injected into three flasks per volume with a plastic syringe (BD Plastipak, Franklin Lakes, NJ, USA) with a sterile 0.5 × 16 mm needle (BD Microlance, Franklin Lakes, NJ, USA) from a multi-layer polypropylene gas bag (RESTEK, Bad Homburd vor der Höhe, Germany) to create the seven different CH_4 concentrations. Final headspace concentrations of CH_4 ranged between 1000 and 130 000 p.p.m.v. while dissolved concentrations of CH_4, ranged between 1.5 and 260 µM, depending also on temperature. The gas pressures in the bottles were then adjusted to a total

headspace pressure of ~1.3 atm at 20 °C by injecting additional volumes of air and N_2. When adding CH_4 and N_2 gas, the bottle pressure increases, resulting in lower than atmospheric concentrations of other atmospheric gases. However, partial pressures stay approximately the same, and so does the availability for the cells. The experiments lasted up to 9 hours, during which time gas samples were collected at 4 – 5 time points, including the experiment start (t0). See supplementary dataset 1 for the length of respective experiments, exact time points and number of samples collected for each individual experiment. For CH_4 and CO_2 measurements, 1 mL of headspace gas was sampled with a pressure-lock 1 mL gas syringe (VICI Precision Sampling, Baton Rouge, LA, USA) with a side-port needle (0.020" × 0.012" × 2"; VICI Precision Sampling, Baton Rouge, LA, USA). The pressure in the syringe was adjusted to ambient pressure, before injection on a gas chromatograph (SRI 8610C, fitted with an 8600-PKDC 3 cm 9'Haysep D Column and a flame ionization detector, SRI Instruments, Torrence, CA, USA). The pressure in the bottles and the ambient pressures were monitored using a manometer (LEO 1, Keller AG, Winterthur, Switzerland). Calibration gases were injected at the same temperature and pressure (ambient) as the samples, allowing calculation of gas species concentrations and, using the bottles pressures, the mass of the gas of interest in the injected sample. Calibration was performed using certified standards (Messer AG, Bad Soden am Taunus, Germany). From the second measurement and onward, 340 µL of the liquid culture was sampled in parallel to the headspace gas. The optical densities of these liquid samples were determined as described in the growth section above. These estimates of cell growth together with the above mentioned OD600 to cell count standard (Supplementary dataset 1, S15) were used for the final calculations of CH_4 oxidation and CO_2 production per cell division in Fig. 1, Fig. S3, Fig. S10 and Fig. S11. For the CO_2 production rates, we only used headspace concentration of 130 000 p.p.m.v. CH_4 (15 mL 100 % CH_4 injected). Five bottles and two negative controls per temperature were injected with CH_4 to reach this concentration, which corresponds to the highest concentration used in the CH_4 oxidation kinetics experiments (between 130 and 260 µM dissolved CH_4 depending on the temperature). All concentrations are well within the saturating range of CH_4 concentrations at all temperatures used in this study. Gas samples were injected on a gas chromatograph (SRI 8610C, fitted with an 8600-PKDC 3 cm 9'Haysep D Column and a flame ionization detector fitted with a methanizer to allow conversion of CO_2 to CH_4 , SRI Instruments, Torrence, CA, USA). Otherwise, the methodological approach was the same as for the CH_4 uptake experiments. The CO_2

experiment was only performed at 8, 15 and 21 °C as this was sufficient to answer our questions. We did not observe changes in headspace gas concentrations of the negative controls in any of the above-mentioned experiments.

OD600 to cell number conversion. In order to normalize CH_4 oxidation rates and other rates to cell numbers, standard curves correlating optical density (OD_{600}) to cell numbers were created for the three cultures, *M. tundripaludum* SV96, *M. luteus* IMV-B-3098 and *Methylobacter* sp. G7. This was done using a Helber cell counting chamber, with defined volumes of cell culture from a dilution series counted using light microscopy. For each cell density, 24 x 1/25 mm^2 in two 1 mm grids of known volume were screened. The average of these counts was used to calculate the number of cells per volume liquid with known optical density (Supplementary dataset 1, S15).

Calculations. Specific growth rates were calculated as the slope of the natural logarithm of optical densities against time, during logarithmic growth. Mixing ratios of CH_4 and CO_2 were calculated by comparison to certified standards. Masses of headspace and dissolved CH_4 and total CO_2 (sum of all CO_2 species) at different temperatures were calculated from the mixing ratios of CH_4 and CO_2 using Henry's Law, assuming an ideal state, knowing the ambient pressure, temperature, headspace volume of the bottle, headspace pressure, liquid volume, respective temperature-dependent solubility constants of the gases. Some deviations from a real-life situation can be expected to arise from calculations assuming an ideal state. However, errors from gas solubility effects of non-ideal pH and salinity are identical across the experimental temperature gradient and is therefore considered not to affect the data-basis for the conclusions. All calculations accounted for removal of gas and liquid for measurements. We calculated the CH_4 oxidation and CO_2 production rates from slopes of linear models fitted to the concentrations measured during experiments and adjusted to the number of cells in the culture. Briefly, the oxidation between any two time points was normalized to the number of cells in the culture at that time (per 10^8 cells), and as such the CH_4 or CO_2 estimated for any given time point represented what would have been measured had a population of 10^8 cells been active throughout the experiment. Growth efficiencies (Fig. 1, Fig. S10, Fig. S11) were calculated as the specific growth rate (cell divisions $cell^{-1}$ $hour^{-1}$) divided by CH_4 oxidation rates (µmol CH_4 oxidized 10^8 $cells^{-1}$ $hour^{-1}$) and multiplied by 10^8 to give cell divisions per µmol CH_4 oxidized. The data used to estimate growth efficiency were

the values predicted for each measurement time-point by the non-linear Michaelis-Menten regression models. For estimates of specific growth rates, CH_4 oxidation and growth efficiency at CH_4 saturation (Fig. S3), $V_{max(app)}$ values predicted from the Michaelis-Menten kinetics models were used (see below for $V_{max(app)}$ estimation). For µmol of CO_2 produced per µmol CH_4 oxidized (Fig. S6), the CO_2 production per 10^8 cells was divided by the CH_4 oxidation per 10^8 cells at the same condition from Fig. 1.

Statistics for physiological data. Tests of significant differences in RNA, DNA and protein content, CO_2 production rates, growth rates and glycogen content between cells at different temperatures were done using the built-in function for the t-test in R ("pairwise.t.test"). P values were corrected for multiple testing using the method of Benjamini and Hochberg [71] within the R function "p.adjust" [72]. The Michaelis-Menten CH_4 oxidation and growth kinetics of *M. tundripaludum* SV96, *M. luteus* IMV-B-3098 and *Methylobacter* sp. G7 were modelled using the "nls" function of the nlstools R package, specifying the "michaelis" model and providing start values for $K_{m(app)}$ and $V_{max(app)}$ (Km=0.002, Vmax=0.02). Kinetics coefficients and corresponding p values were extracted from these models using the "summary" function. Modelled growth and CH_4 oxidation rates were predicted using the "predict" function and used to estimate cell divisions per µmol CH_4 oxidized at different dissolved CH_4 concentrations. Four-parameter logistics curves to model the growth efficiency (cell divisions per µmol CH_4 oxidized) at different dissolved CH_4 concentrations were fitted using the "drm" function of the "drc" package. Functions of the "R.utils" and "plyr" packages were used in addition to built-in functions to handle the data in R, while "ggplot2", in addition to built-in functions, was used to plot the data.

RNA and DNA extraction and sequencing (Fig. 2 and Fig. 6). Six cultures of *M. tundripaludum* SV96 were acclimated at each of the temperatures, 8, 15, 21 or 27 °C. After acclimation, the cultures were cultivated to a sufficient cell density for extraction in logarithmic phase growth as described above. Cultures at 8 and 27 °C were incubated for 36 hours and cultures at 15 and 21 °C for 16 hours prior to harvest. This allowed the cells to reach sufficient density for the downstream approaches. The cultures were pelleted by centrifugation and re-suspended in 740 µL TE buffer (pH 8). Further, 40 µL lysozyme (50 mg/mL) was added, and the suspensions were incubated for 5 min at room temperature. Then, 40 µL of 10% SDS and 8 µL of proteinase K (10 mg/mL) were added, and the samples were incubated at 37 °C for 1 h.

Next, 100 µL of 5 M NaCl and 100 µL Cetyl trimethylammonium bromide (50g/L) /NaCl (20g/L) were added, and the samples were incubated at 65 °C for 10 min. Nucleic acids were then extracted with one volume phenol/chloroform/isoamyl alcohol and then with chloroform/isoamyl alcohol and precipitated with 0.6 volumes of isopropanol. DNA was removed using the TURBO DNA-free kit (Ambion, Thermo Fisher Scientific, Waltham, MA, USA). For the second RNA and DNA extraction (Fig. 6), the cell pellets (in 2 ml Eppendorf) were kept on dry ice to prevent thawing and 375 µl of phosphate buffer (PBS, pH 8.0), 125 µl of TRIZMA-NaCl-CTAB (TNC) and 400 µl of phenol/chloroform/isoamylalcohol 25:24:1 were added to each tube (lysis matrix E, MP biomedicals, Irvine, CA, USA) and exposed to bead beating (MP biomedicals, Irvine, CA, USA) for 30 s at 4.0 m s^{-1}. After bead beating, extractions were performed as previously described for soil [38, 73].

DNA and RNA were quantified using Qubit (Thermo Fisher scientific, Waltham, MA, USA). RNA quality was assessed using automated gel electrophoresis with Experion^{TM} (Bio-Rad, Hercules, CA, USA), demonstrating high quality RNA with 23S to 16S rRNA ratios of 1.6 – 2.4. The quantity of RNA and DNA per 10^8 cells was calculated by dividing the mass of extracted RNA by the number of cells used for the extraction. Three extracts per temperature were processed further. Ribosomal RNA was removed from the total RNA of these 12 samples using the Ribo-Zero rRNA Removal Kit (Bacteria, Epicentre, Illumina, San Diego, CA, USA), and the remaining RNA was sequenced. Transcriptomic libraries were prepared from the rRNA depleted samples using the Illumina Truseq RNA-seq library preparation kit v1 and sequenced using 2 × 100 bp paired-end technology on the Illumina High-Seq 2000 platform. This procedure allowed the generation of high-coverage transcriptomes for the quantitative analysis of gene transcription.

Protein extractions. Proteins were extracted as previously described with some modifications [74]. Briefly, A volume of 1 ml TRIzol was added to each cell pellet in a lysis matrix E tube (MP biomedicals, Irvine, CA, USA) and the tubes were immediately placed in a bead beater (MP biomedicals, Irvine, CA, USA) and processed for 30 s at 4.0 m s^{-1}, followed by phenol:chloroform extraction, and addition of 100 % ethanol. The phenol-ethanol supernatant was transferred into a new tube for protein isolation with isopropanol. The resultant protein pellets were washed with 0.3 M guanidine hydrochloride in 95% ethanol and

re-suspended in 200 µl of 1% SDS prior to quantification with Qubit (Thermofisher scientific, Waltham, MA, USA).

Computational analyses. Sequences were trimmed with Trimmomatic, using default settings (Bolger et al., 2014), to remove Illumina adapters (ILLUMINACLIP:ADAPTERS:2:30:10), removing bases from the start and end of the sequence if below a quality threshold of three (LEADING:3, TRAILING:3), and remove four-base-pair sequence sections that fell below a quality threshold of 15 (SLIDINGWINDOW:4:15), as well as any sequences shorter than 36 bp (MINLEN:36). The rRNA sequences were sorted out with SortMeRNA [75], using default settings and the 5S, 16S and 23S rRNA gene copies from the *M. tundripaludum* SV96 genome as reference sequences. Non-ribosomal RNA was mapped to the *M. tundripaludum* SV96 genome using BWA *sampe* (to generate alignments in the SAM format given paired-end reads aligner) [76] with default settings. The number of different genome features present in the transcriptomes were counted using FeatureCounts [77]. Features were counted if both read pairs were assigned to the same feature, and these were then counted as one fragment. Gene expression data was analysed using R [72]. To compare expression between samples, matrices holding the counts of genome features in each of the 12 transcriptomes were normalized using the median of ratios method available in the R package DEseq2 [78]. This method uses the median of ratios of transcript counts for different genes in a sample to their respective geometric means (the mean of transcript counts for a particular gene across all samples). To test whether differential expression between different temperatures were significant, we applied the Wald test with multiple testing correction using the false discovery rate (FDR) controlling method of Benjamini and Hochberg [71], the default statistical test for differential expression in DEseq2. This method is highly robust with three or more replicates, with very few false positives (< 5%) regardless of fold change thresholds [79], but it is prone to false negatives at low replication numbers (≤ 6). This means that the risk that significant biological patterns across multiple genes are false positives, is negligible, even with three replicates. However, there is significant risk of failing to identify many of the changes that really occur.

Gene expression data were visualized using the R package *Heatmap3*. Based on the genome of *M. tundripaludum* SV96 [80], we reconstructed central carbon and energy metabolisms, pathways of protein biosynthesis and functions relevant to cell division and other cell structures by manually curating the annotations for the genome of

M. tundripaludum SV96 available in Genoscope (https://mage.genoscope.cns.fr/microscope/mage/viewer.php?O_id=818). The *M. tundripaludum* SV96 genome is also available from NCBI with accession number NZ_AEGW00000000.2.

16S rRNA gene maps. The maps showing global distribution of *Methylobacter* was generated as recently described [81]. This section is under progress and will be finished prior to journal submission.

Data deposition and scripts for computational analyses. The RNA-seq data from this study have been deposited under the accession project number PRJNA390985 in the NCBI short read archive (SRA). The individual experiment identification numbers for each of the 12 datasets are found in supplementary dataset 1, S7. Scripts for RNA-seq pre-processing, gene expression analysis, statistical tests, modelling and visualization in R, are provided online (*online archive will be determined prior to journal submission*). Physiological data are provided in supplementary dataset 1 and online (*online archive will be determined prior to journal submission*). The processed and normalized transcript counts and statistics for the differential gene expression analyses are provided in supplementary dataset 2.

ACKNOWLEDGMENTS

This work was supported by the Research council of Norway FRIPRO Mobility grant project Time & Energy 251027/RU, co-funded by the European Research Council (ERC) under Marie Curie grant agreement no 608695, and Tromsø Research Foundation starting grant project Cells in the Cold 17_SG_ATT. The computations were performed on resources provided by UNINETT Sigma2 - the National Infrastructure for High Performance Computing and Data Storage in Norway, account no. NN9639K and NS9593K.

1 **Figures**

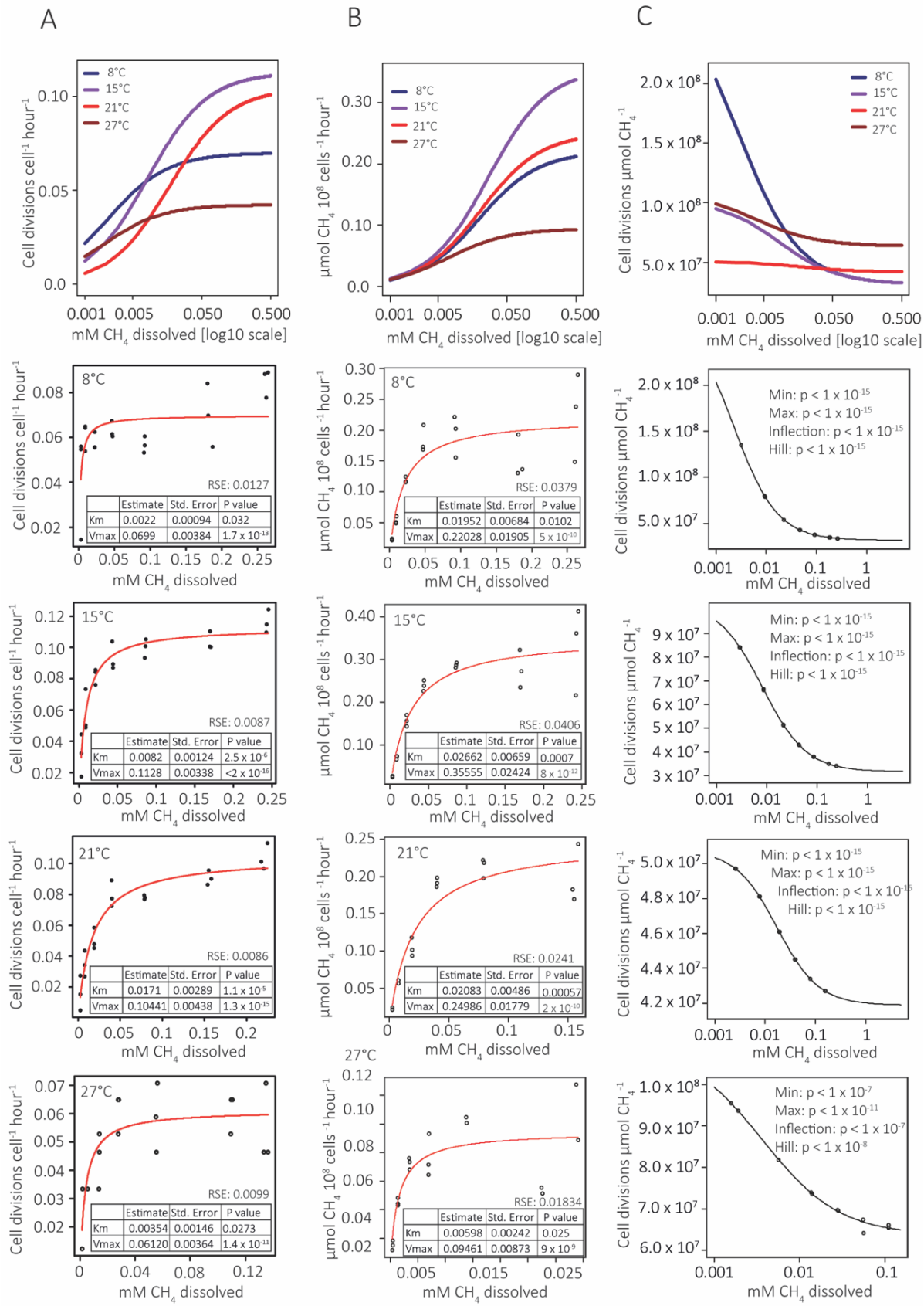
A
B
C
8°C
15°C
21°C
27°C
Cell divisions cell⁻¹ hour⁻¹
µmol CH4 10⁸ cells⁻¹ hour⁻¹
Cell divisions µmol CH4⁻¹
mM CH4 dissolved [log10 scale]
mM CH4 dissolved
RSE: 0.0127
RSE: 0.0379
RSE: 0.0087
RSE: 0.0406
RSE: 0.0086
RSE: 0.0241
RSE: 0.0099
RSE: 0.01834
Estimate | Std. Error | P value
Km | 0.0022 | 0.00094 | 0.032
Vmax | 0.0699 | 0.00384 | 1.7 x 10⁻¹³
Km | 0.01952 | 0.00684 | 0.0102
Vmax | 0.22028 | 0.01905 | 5 x 10⁻¹⁰
Km | 0.0082 | 0.00124 | 2.5 x 10⁻⁶
Vmax | 0.1128 | 0.00338 | <2 x 10⁻¹⁶
Km | 0.02662 | 0.00659 | 0.0007
Vmax | 0.35555 | 0.02424 | 8 x 10⁻¹²
Km | 0.0171 | 0.00289 | 1.1 x 10⁻⁵
Vmax | 0.10441 | 0.00438 | 1.3 x 10⁻¹⁵
Km | 0.02083 | 0.00486 | 0.00057
Vmax | 0.24986 | 0.01779 | 2 x 10⁻¹⁰
Km | 0.00354 | 0.00146 | 0.0273
Vmax | 0.06120 | 0.00364 | 1.4 x 10⁻¹¹
Km | 0.00598 | 0.00242 | 0.025
Vmax | 0.09461 | 0.00873 | 9 x 10⁻⁹
Min: p < 1 x 10⁻¹⁵
Max: p < 1 x 10⁻¹⁵
Inflection: p < 1 x 10⁻¹⁵
Hill: p < 1 x 10⁻¹⁵
Min: p < 1 x 10⁻⁷
Max: p < 1 x 10⁻¹¹
Inflection: p < 1 x 10⁻⁷
Hill: p < 1 x 10⁻⁸

2

Figure 1. Growth kinetics, CH_4 oxidation kinetics and cell divisions per CH_4 oxidation at different temperatures for *M. tundripaludum* SV96. Specific growth rates (cell divisions per cell per hour) are shown for different dissolved CH_4 concentrations at different temperatures in **(A)**. The first panel of (A) shows a combination of growth kinetics for the four different temperatures, 8, 15, 21 and 27 °C. The X-axis is on a log10 scale to better resolve the differences between temperatures in the low and high end of concentrations. Panel two to five are the individual growth kinetics at the temperatures 8, 15, 21 and 27 °C, respectively. CH_4 oxidation rates per cell for different dissolved CH_4 concentrations at different temperatures are shown in **(B)**. The first panel of (B) is a combination of the CH_4 oxidation kinetics at the four different temperatures, 8, 15, 21 and 27 °C. X-axis is on log10 scale to better resolve the differences between temperatures in the lower end or higher end of concentrations. Second to fifth panel are the individual CH_4 oxidation kinetics at the temperatures 8, 15, 21 and 27 °C, respectively. $K_{m(app)}$, $V_{max(app)}$, standard errors and p values for the coefficient's estimates, and residual standard errors of the models were estimated using non-linear regression, applying a Michaelis-Menten function (see the materials and methods section "statistics for physiological measurements"). Cell divisions per µmol CH_4 oxidized at different dissolved CH_4 concentrations and temperatures are shown in **(C)**. The first panel of (C) shows these growth efficiency curves for all temperatures combined. Panel two to five show the models for each temperature. These growth efficiency estimates were calculated from the predicted rates in (A) and (B) by dividing specific growth rate predictions by CH_4 oxidation rate predictions to obtain cell divisions per µmol CH_4 oxidized. Four-parameter logistics curves (dose-response model) were fitted to the resulting quotients. P values for the four parameters (min, max, infle of the dose-response models for different temperatures are shown in panel two to five in (C), respectively. In all panels, the x-axis is displayed on a log10 scale. The corresponding data can be found in supplementary dataset 1, S2, S3 and S4.

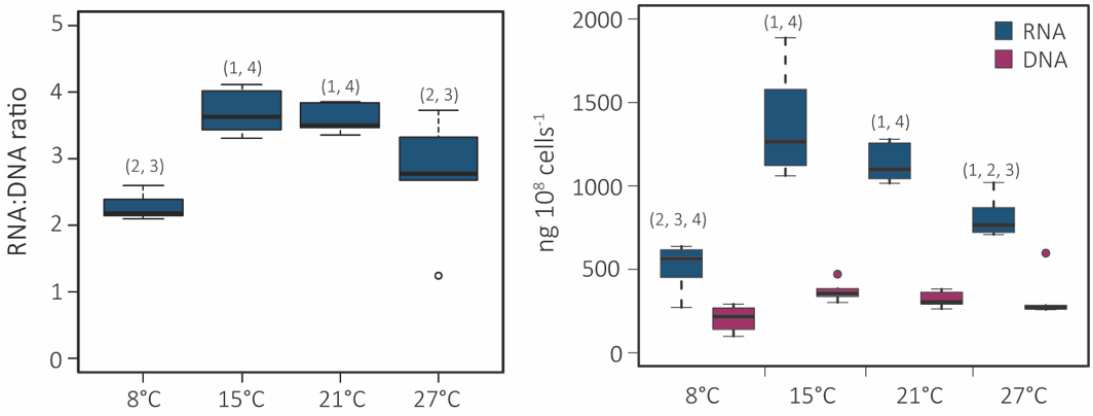

Figure 2. Cellular RNA (blue) and DNA (purple) in *M. tundripaludum* SV96 at 8, 15, 21 and 27 °C. In **(A)** boxplots show the concentrations of RNA and DNA in *M. tundripaludum* SV96 cells. In **(B)**, boxplots show the RNA:DNA ratios. Differences between means were evaluated using unpaired one-tailed t-tests. Significant differences (p.adjust < 0.05, multiple testing correction using Benjamini-Hochberg correction) to 8 °C (1), 15 °C (2), 21 °C (3) and 27 °C (4) are indicated with numbers above the individual boxes. The corresponding data can be found in supplementary dataset 1, S5.

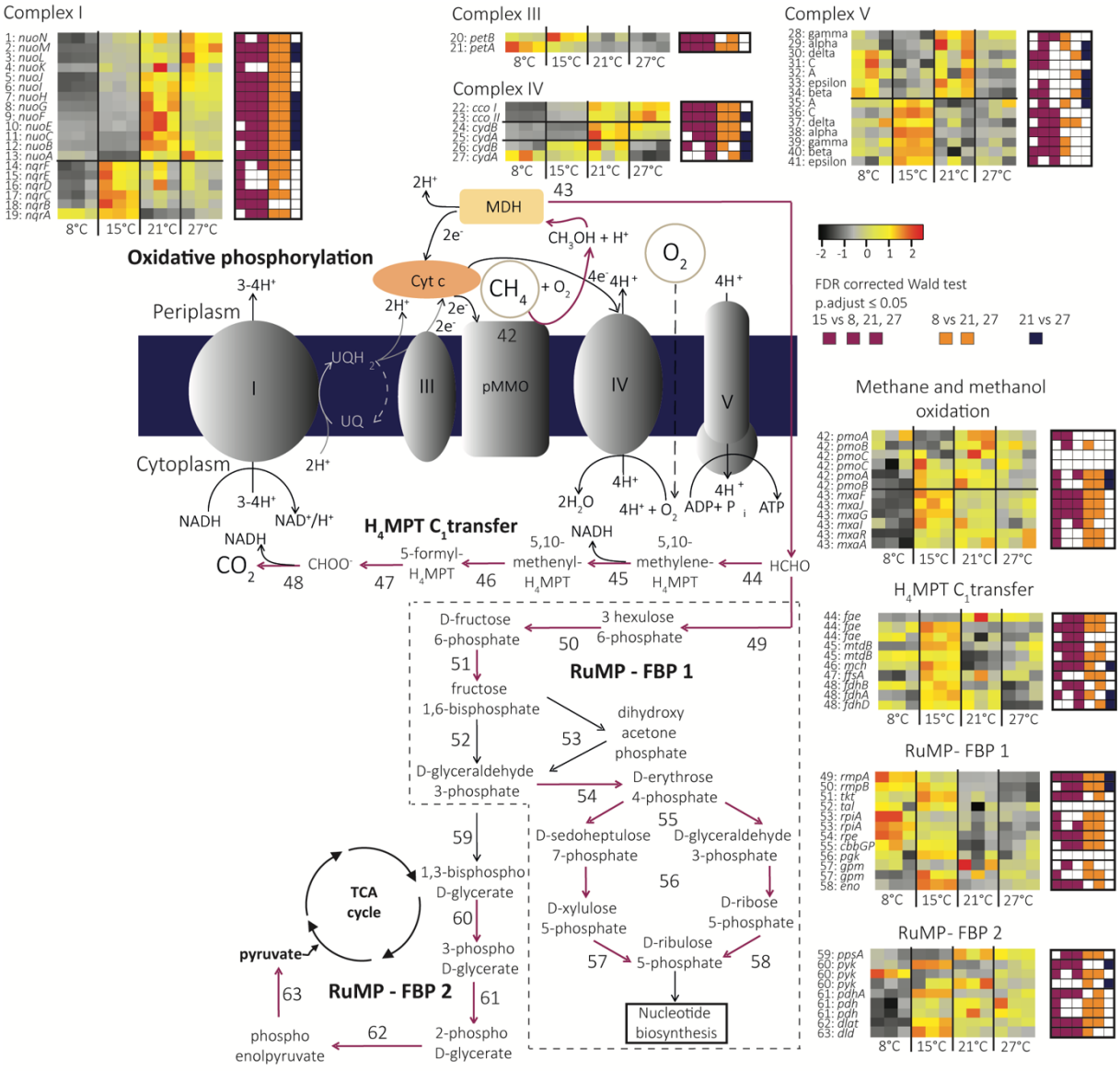

Figure 3. Gene transcription for central carbon and energy metabolisms in *M. tundripaludum* SV96. Heatmaps indicate changes in the relative abundance of transcripts in the transcriptomes at 8, 15, 21 and 27 °C. The colour scale reflects z-score normalized relative abundances, with black being lowest relative abundance, followed by grey, yellow, orange and red, corresponding to increasing relative abundances. Significant differences (p.adjust < 0.05) in transcript relative abundances are displayed in square plots to the right of each heatmap, purple indicating significant difference between 15 °C and 8, 21 and 27 °C, respectively, when moving from left to right. Orange indicates significant differences between 8 °C and 21 and 27 °C. Dark blue indicates significant differences between 21 and 27 °C. P values are estimated with a Wald test, implemented in DESeq2 and corrected for multiple testing using Benjamini-Hochberg correction which adjusts for the false discovery rate. Purple arrows indicate

upregulation, meaning that at least one of the genes encoding the enzyme responsible for catalysing the reaction represented by this pathway step is significantly higher expressed at 15 °C than at two or three of the other temperatures. All adjusted p. values, normalized counts, genome IDs, full protein names and E.C. numbers for the genes are provided in Supplementary dataset 2, S1.

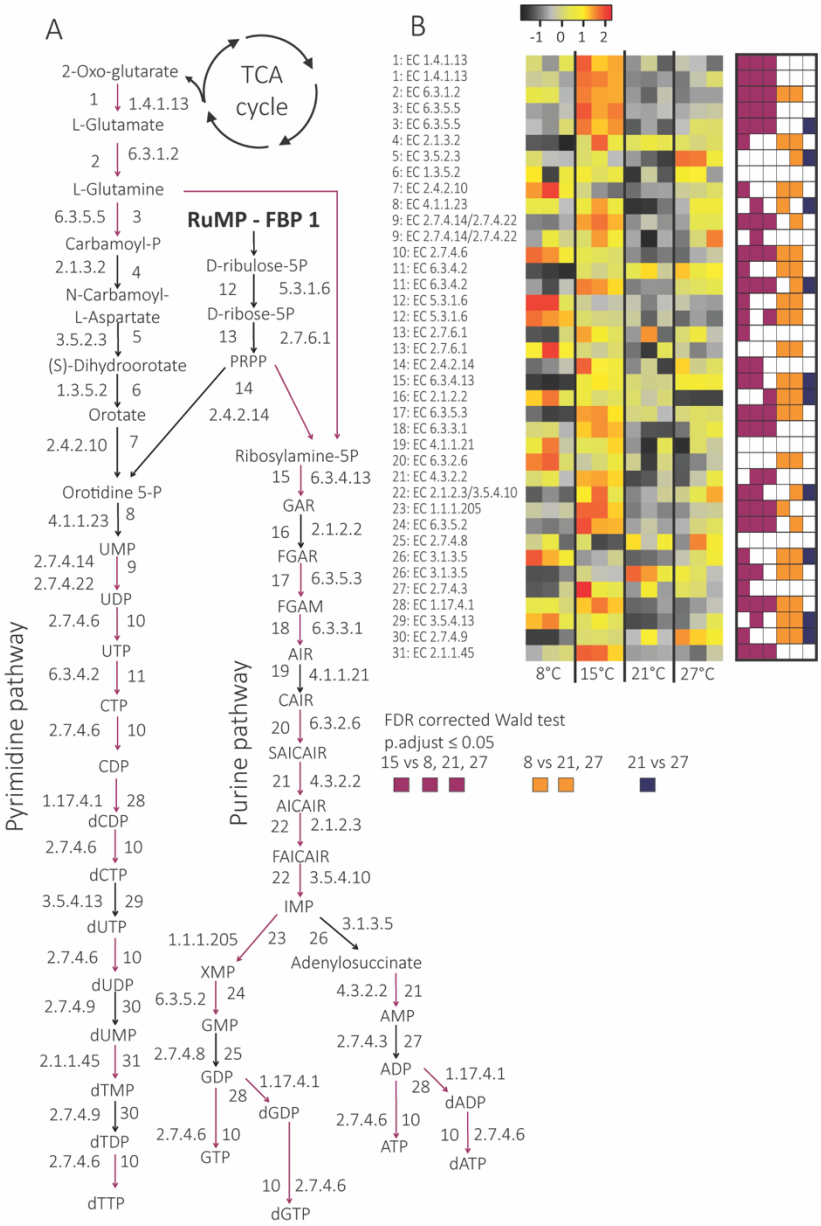

Figure 4. Gene transcription for nucleotide metabolism in *M. tundripaludum* SV96. Heatmaps indicate changes in the relative abundance of transcripts in the transcriptomes at 8, 15, 21 and 27 °C. The colour scale reflects z-score normalized relative abundances, with black being lowest relative abundance, followed by grey, yellow, orange and red, corresponding to increasing relative abundances. Significant differences (p.adjust < 0.05) in transcript relative abundances are displayed in square plots to the right of each heatmap, purple indicating significant difference between 15 °C and 8, 21 and 27 °C, respectively, when moving from left to right. Orange indicates significant differences between 8 °C and 21 and 27 °C. Dark blue indicates significant differences between 21 and 27 °C. P values are estimated with a Wald test, implemented in DESeq2 and corrected for multiple testing using Benjamini-

Hochberg correction which adjusts for the false discovery rate. Purple arrows indicate that at least one of the genes encoding the enzyme responsible for catalysing the reaction represented by this pathway step is significantly higher expressed at 15 °C than at two or three of the other temperatures. All adjusted p. values, normalized counts, genome IDs, full protein names and gene names are given in Supplementary dataset 2, S2.

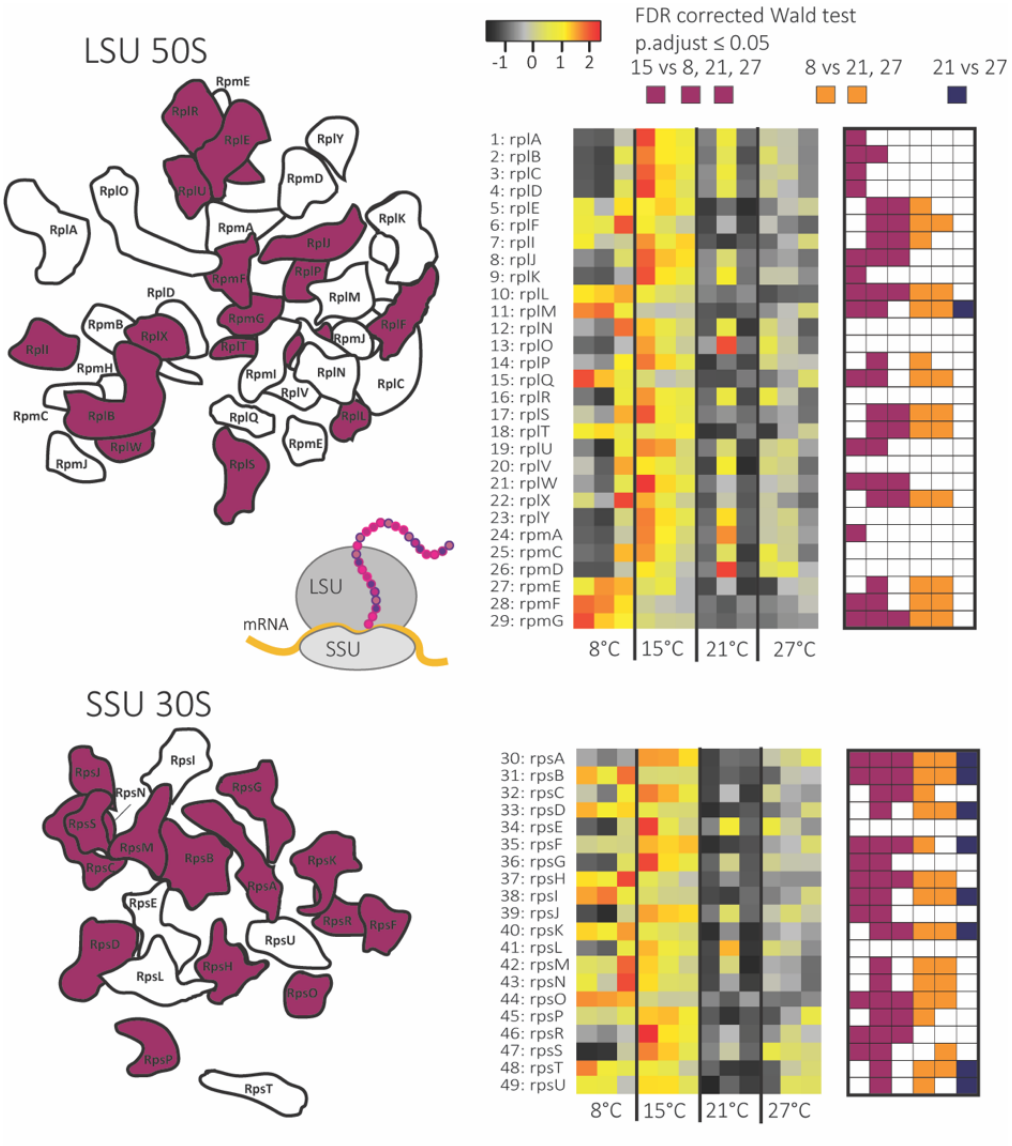

Figure 5. Gene transcription for ribosomal proteins in *M. tundripaludum* SV96. Heatmaps indicate changes in the relative abundance of transcripts in the transcriptomes at 8, 15, 21 and 27 °C. The colour scale reflects z-score normalized relative abundances, with black being lowest relative abundance, followed by grey, yellow, orange and red, corresponding to increasing relative abundances. Significant differences (p.adjust < 0.05) in transcript relative abundances are displayed in square plots to the right of each heatmap, purple indicating significant difference between 15 °C and 8, 21 and 27 °C, respectively, when moving from left to right. Orange indicates significant differences between 8 °C and 21 and 27 °C. Dark blue indicates significant differences between 21 and 27 °C. P values are estimated with a Wald test, implemented in DESeq2 and corrected for multiple testing using Benjamini-Hochberg

correction which adjusts for the false discovery rate. Purple ribosomal proteins in the visualization of the ribosomal protein structure on the left of the heatmaps indicate that at least one of the genes encoding the enzyme responsible for catalysing the reaction represented by this pathway step is significantly higher expressed at 15 °C than at two or three of the other temperatures. All adjusted p. values, normalized counts, genome id's and full protein names are given in Supplementary dataset 2, S3. Rpl and rpm: large ribosomal subunit proteins; rps: small ribosomal subunit proteins.

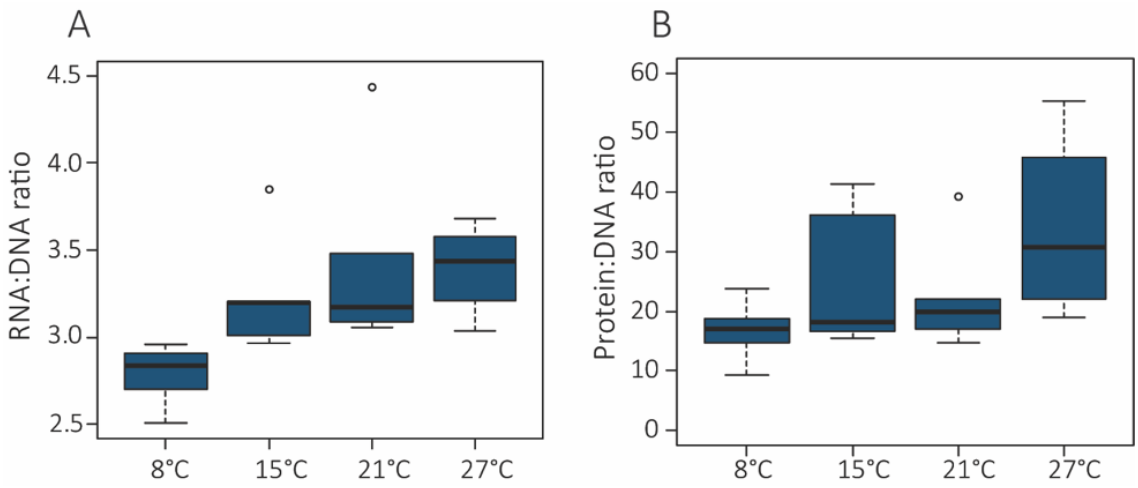

Figure 6. RNA (A) and protein (B) per cell at 8, 15, 21 and 27 °C. In **(A)** boxplots show the RNA:DNA ratio in *M. tundripaludum* SV96 cells. In **(B)**, boxplots show the protein:DNA ratios. Differences between means were evaluated using unpaired one-tailed t-tests. Significant differences were considered after multiple testing correction using Benjamini-Hochberg correction. No significant differences were detected (p.adjust > 0.05). The corresponding data can be found in supplementary dataset 1, S23.

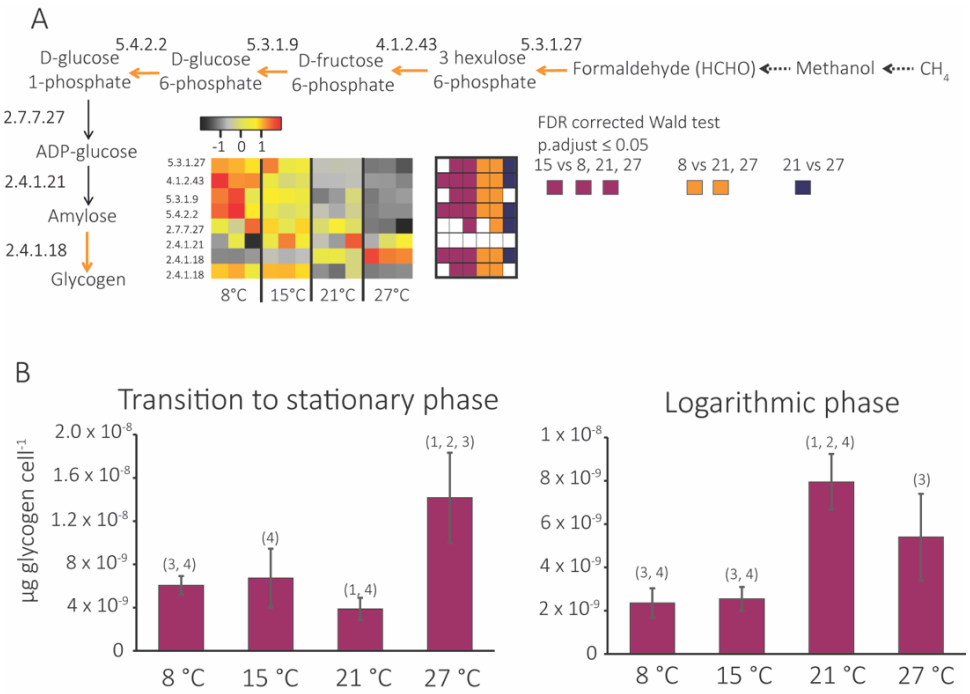

Figure 7. Gene expression for glycogen synthesis (A), and glycogen accumulation per cell (B) in *M. tundripaludum* SV96. Heatmaps (A) indicate changes in the relative abundance of transcripts in the transcriptomes at 8, 15, 21 and 27 °C. The colour scale reflects z-score normalized relative abundances, with black being lowest relative abundance, followed by grey, yellow, orange and red, corresponding to increasing relative abundances. Significant differences (p.adjust < 0.05) in transcript relative abundances are displayed in square plots to the right of each heatmap, purple indicating significant difference between 15 °C and 8, 21 and 27 °C, respectively, when moving from left to right. Orange indicates significant differences between 8 °C and 21 and 27 °C. Dark blue indicates significant differences between 21 and 27 °C. P values are estimated with a Wald test, implemented in DESeq2 and corrected for multiple testing using Benjamini-Hochberg correction which adjusts for the false discovery rate. Orange arrows indicate that at least one of the genes encoding the enzyme responsible for catalysing the reaction represented by this pathway step is significantly higher expressed at 8 °C than at two or three of the other temperatures. All adjusted p. values, normalized counts, genome IDs and full protein names are given in Supplementary dataset 2, S4. Bargraphs (B) show the µg glycogen per cell, estimated from a cell lysate with a known cell number. Considering the possibility of incomplete lysis, the numbers are likely conservative estimates. Error bars indicate standard deviation. Numbers above bars indicate to which of the other bars there are significant differences (p.adjust < 0.05).

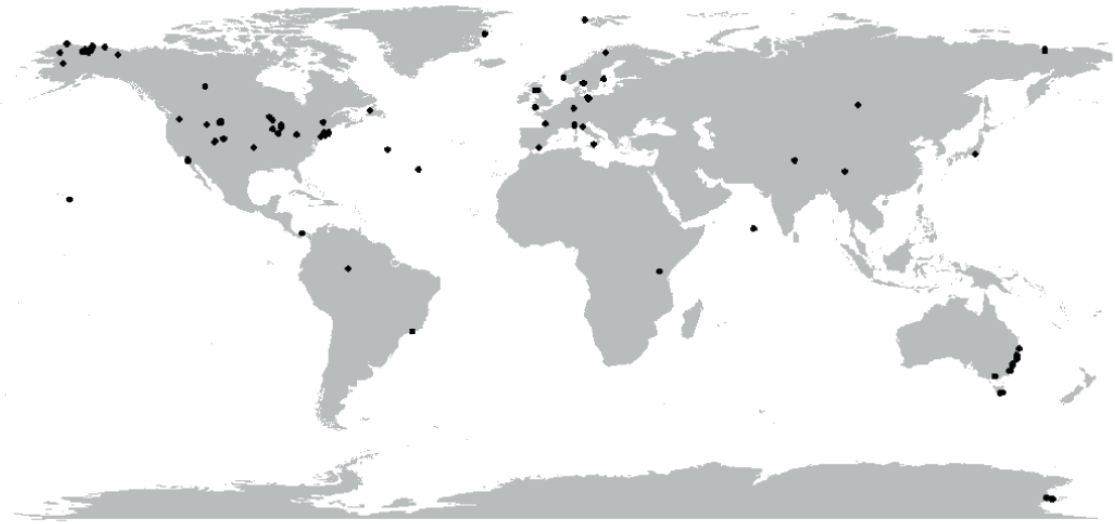

Figure 8. Geographical distribution of *Methylobacter* (A) and *M. tundripaludum* SV96 (B). Figure shows a preliminary version of (A) where each dot on the map indicates the occurrence of a member of *Methylobacter* in that location by detection of a sufficiently similar 16S rRNA gene sequence to confirmed members of the genus.

References

1. Tveit, A., et al., *Organic carbon transformations in high-Arctic peat soils: key functions and microorganisms.* Isme J, 2013. **7**(2): p. 299-311.
2. Graef, C., et al., *The active methanotrophic community in a wetland from the High Arctic.* Environmental Microbiology Reports, 2011. **3**(4): p. 466-472.
3. Liebner, S., et al., *Diversity of Aerobic Methanotrophic Bacteria in a Permafrost Active Layer Soil of the Lena Delta, Siberia.* Microbial Ecology, 2009. **57**(1): p. 25-35.
4. Martineau, C., L.G. Whyte, and C.W. Greer, *Stable Isotope Probing Analysis of the Diversity and Activity of Methanotrophic Bacteria in Soils from the Canadian High Arctic.* Applied and Environmental Microbiology, 2010. **76**(17): p. 5773-5784.
5. He, R., et al., *Identification of functionally active aerobic methanotrophs in sediments from an arctic lake using stable isotope probing.* Environ Microbiol, 2012. **14**(6): p. 1403-19.
6. Dieser, M., et al., *Molecular and biogeochemical evidence for methane cycling beneath the western margin of the Greenland Ice Sheet.* ISME J, 2014. **8**: p. 2305-2316.
7. Lüke, C., et al., *Macroecology of methane-oxidizing bacteria: the β-diversity of pmoA genotypes in tropical and subtropical rice paddies.* Environ Microbiol, 2014. **16**(1): p. 72-83.
8. Sundh, I., D. Bastviken, and L.J. Tranvik, *Abundance, activity, and community structure of pelagic methane-oxidizing bacteria in temperate lakes.* Appl Environ Microbiol, 2005. **71**(11): p. 6746-52.
9. Meyer-Dombard, D.R., J.E. Bogner, and J. Malas, *A Review of Landfill Microbiology and Ecology: A Call for Modernization With 'Next Generation' Technology.* Frontiers in Microbiology, 2020. **11**: p. 1127.
10. Rosentreter, J.A., et al., *Half of global methane emissions come from highly variable aquatic ecosystem sources.* Nature Geoscience, 2021. **14**(4): p. 225-230.
11. Matveev, A., et al., *High methane emissions from thermokarst lakes in subarctic peatlands.* Limnology and Oceanography, 2016. **61**: p. S150-S164.

12. Abdalla, M., et al., *Emissions of methane from northern peatlands: a review of management impacts and implications for future management options.* Ecology and evolution, 2016. **6**(19): p. 7080-7102.
13. Rainer, E.M., et al., *Methanotroph populations and CH_4 oxidation potentials in high-Arctic peat are altered by herbivory induced vegetation change.* FEMS Microbiology Ecology, 2020. **96**(10): p. fiaa140.
14. Angle, J.C., et al., *Methanogenesis in oxygenated soils is a substantial fraction of wetland methane emissions.* Nature Communications, 2017. **8**: p. 1567.
15. Raney, P.A., J.D. Fridley, and D.J. Leopold, *Characterizing Microclimate and Plant Community Variation in Wetlands.* Wetlands, 2014. **34**(1): p. 43-53.
16. Westermann, S., et al., *The annual surface energy budget of a high-arctic permafrost site on Svalbard, Norway.* The Cryosphere, 2009. **3**(2): p. 245-263.
17. Liu, X. and T. Luo, *Spatiotemporal Variability of Soil Temperature and Moisture across two Contrasting Timberline Ecotones in the Sergyemla Mountains, Southeast Tibet.* Arctic, Antarctic, and Alpine Research, 2011. **43**(2): p. 229-238.
18. Illston, B.G. and C.A. Fiebrich, *Horizontal and vertical variability of observed soil temperatures.* Geoscience Data Journal, 2017. **4**(1): p. 40-46.
19. Einola, J., R. Kettunen, and J. Rintala, *Responses of methane oxidation to temperature and water content in cover soil of a boreal landfill.* Soil Biology & Biochemistry, 2007. **39**: p. 1156-1164.
20. Zheng, J., et al., *Impacts of temperature and soil characteristics on methane production and oxidation in Arctic tundra.* Biogeosciences, 2018. **15**(21): p. 6621-6635.
21. King, G.M. and A.P. Adamsen, *Effects of Temperature on Methane Consumption in a Forest Soil and in Pure Cultures of the Methanotroph Methylomonas rubra.* Applied and Environmental Microbiology, 1992. **58**(9): p. 2758-2763.
22. Rainer, E.M., et al., *The Influence of Above-Ground Herbivory on the Response of Arctic Soil Methanotrophs to Increasing CH_4 Concentrations and Temperatures.* Microorganisms, 2021. **9**(10): p. 2080.
23. Whalen, S.C. and W.S. Reeburgh, *Moisture and temperature sensitivity of CH_4 oxidation in boreal soils.* Soil Biology and Biochemistry, 1996. **28**(10): p. 1271-1281.

24. Siddiqui, K.S., et al., *Role of lysine versus arginine in enzyme cold-adaptation: modifying lysine to homo-arginine stabilizes the cold-adapted α-amylase from Pseudoalteramonas haloplanktis.* Proteins, 2006. **64**(2): p. 486-501.
25. López-García, P., et al., *Bacterial gene import and mesophilic adaptation in archaea.* Nat Rev Micro, 2015. **13**(7): p. 447-456.
26. Marr, A.G. and J.L. Ingraham, *EFFECT OF TEMPERATURE ON THE COMPOSITION OF FATTY ACIDS IN ESCHERICHIA COLI.* Journal of Bacteriology, 1962. **84**(6): p. 1260-1267.
27. Yamaguchi-Shinozaki, K. and K. Shinozaki, *Transcriptional regulatory networks in cellular responses and tolerance to dehydration and cold stresses.* Annu Rev Plant Biol, 2006. **57**: p. 781-803.
28. Lopez-Maury, L., S. Marguerat, and J. Bähler, *Tuning gene expression to changing environments: from rapid responses to evolutionary adaptation.* Nat Rev Genet, 2008. **9**(8): p. 583-593.
29. Amato, P. and B.C. Christner, *Energy metabolism response to low-temperature and frozen conditions in Psychrobacter cryohalolentis.* Appl Environ Microbiol, 2009. **75**(3): p. 711-718.
30. Wiebe, W.J., W.M. Sheldon, and L.R. Pomeroy, *Bacterial growth in the cold: evidence for an enhanced substrate requirement.* Appl Environ Microbiol, 1992. **58**(1): p. 359-364.
31. Holaday, A.S., et al., *Changes in Activities of Enzymes of Carbon Metabolism in Leaves during Exposure of Plants to Low Temperature.* Plant Physiology, 1992. **98**(3): p. 1105-1114.
32. Tveit, A.T., et al., *Metabolic and trophic interactions modulate methane production by Arctic peat microbiota in response to warming.* Proc Natl Acad Sci U S A, 2015. **112**(19): p. E2507-16.
33. Wang, M., et al., *Glycogen Metabolism Impairment via Single Gene Mutation in the glgBXCAP Operon Alters the Survival Rate of Escherichia coli Under Various Environmental Stresses.* Frontiers in Microbiology, 2020. **11**: p. 588099.
34. Lan, G. and Y. Tu, *Information processing in bacteria: memory, computation, and statistical physics: a key issues review.* Reports on progress in physics. Physical Society (Great Britain), 2016. **79**(5): p. 052601.

35. Bosdriesz, E., et al., *How fast-growing bacteria robustly tune their ribosome concentration to approximate growth-rate maximization.* The FEBS journal, 2015. **282**(10): p. 2029-2044.
36. Ryals, J., R. Little, and H. Bremer, *Temperature dependence of RNA synthesis parameters in Escherichia coli.* Journal of Bacteriology, 1982. **151**(2): p. 879-886.
37. Walker, T.W.N., et al., *Microbial temperature sensitivity and biomass change explain soil carbon loss with warming.* Nature Climate Change, 2018. **8**(10): p. 885-889.
38. Söllinger, A., et al., *Down-regulation of the bacterial protein biosynthesis machinery in response to weeks, years, and decades of soil warming.* Science Advances, 2022. **8**(12): p. eabm3230.
39. Wartiainen, I., et al., *Methylobacter tundripaludum sp. nov., a methane-oxidizing bacterium from Arctic wetland soil on the Svalbard islands, Norway (78 ° N).* Int J Syst Evol Microbiol, 2006. **56**: p. 109-13.
40. Reddy, K.R., et al., *Effect of temperature on methane oxidation and community composition in landfill cover soil.* Journal of Industrial Microbiology and Biotechnology, 2019. **46**(9-10): p. 1283-1295.
41. Lipson, D.A., *The complex relationship between microbial growth rate and yield and its implications for ecosystem processes.* Frontiers in Microbiology, 2015. **6**(615).
42. Trueba, F.J., et al., *Effects of temperature on the size and shape of Escherichia coli cells.* Archives of Microbiology, 1982. **131**(3): p. 235-240.
43. Cotner, J.B., W. Makino, and B.A. Biddanda, *Temperature affects stoichiometry and biochemical composition of Escherichia coli.* Microb Ecol, 2006. **52**(1): p. 26-33.
44. Kåresdotter, E., et al., *Mapping the Vulnerability of Arctic Wetlands to Global Warming.* Earth's Future, 2021. **9**(5): p. e2020EF001858.
45. Dijkstra, P., et al., *Effect of temperature on metabolic activity of intact microbial communities: Evidence for altered metabolic pathway activity but not for increased maintenance respiration and reduced carbon use efficiency.* Soil Biology and Biochemistry, 2011. **43**(10): p. 2023-2031.
46. Mairet, F., J.-L. Gouzé, and H. de Jong, *Optimal proteome allocation and the temperature dependence of microbial growth laws.* npj Systems Biology and Applications, 2021. **7**(1): p. 14.

47. Nercessian, O., et al., *Bacterial populations active in metabolism of C1 compounds in the sediment of Lake Washington, a freshwater lake.* Appl Environ Microbiol, 2005. **71**(11): p. 6885-99.
48. Wilkinson, J.F., *CARBON AND ENERGY STORAGE IN BACTERIA.* J Gen Microbiol, 1963. **32**: p. 171-176.
49. Neidhardt, F.C., J.L. Ingraham, and M. Schaechter. *Physiology of the bacterial cell : a molecular approach*. 1990.
50. Blazewicz, S.J., et al., *Evaluating rRNA as an indicator of microbial activity in environmental communities: limitations and uses.* The ISME journal, 2013. **7**(11): p. 2061-2068.
51. Bremer, H. and P.P. Dennis, *Modulation of Chemical Composition and Other Parameters of the Cell at Different Exponential Growth Rates.* EcoSal Plus, 2008. **3**(1).
52. Failmezger, J., et al., *Quantifying ribosome dynamics in Escherichia coli using fluorescence.* FEMS Microbiology Letters, 2017. **364**(6): p. fnx055.
53. Li, G.-W., et al., *Quantifying absolute protein synthesis rates reveals principles underlying allocation of cellular resources.* Cell, 2014. **157**(3): p. 624-635.
54. Bradford, M.A., *Thermal adaptation of decomposer communities in warming soils*. Front Microbiol, 2013. **4**: p.333.
55. German, D.P., S.S. Chacon, and S.D. Allison, *Substrate concentration and enzyme allocation can affect rates of microbial decomposition.* Ecology, 2011. **92**(7): p. 1471-1480.
56. Hreha, T.N., et al., *The three NADH dehydrogenases of Pseudomonas aeruginosa: Their roles in energy metabolism and links to virulence.* PLOS ONE, 2021. **16**(2): p. e0244142.
57. Matsumoto, Y., et al., *Growth rate-coordinated transcriptome reorganization in bacteria.* BMC Genomics, 2013. **14**: p. 808.
58. Gadgil, M., V. Kapur, and W.-S. Hu, *Transcriptional Response of Escherichia coli to Temperature Shift.* Biotechnology Progress, 2005. **21**(3): p. 689-699.
59. Wilkinson, J.F., *The problem of energy-storage compounds in bacteria.* Experimental Cell Research, 1959. **7**: p. 111-130.
60. Wilson, W.A., et al., *Regulation of glycogen metabolism in yeast and bacteria.* FEMS microbiology reviews, 2010. **34**(6): p. 952-985.

61. Rothfield, L.I. and S.S. Justice, *Bacterial cell division: the cycle of the ring.* Cell, 1997. **88**(5): p. 581-584.
62. Männik, J., B.E. Walker, and J. Männik, *Cell cycle-dependent regulation of FtsZ in Escherichia coli in slow growth conditions.* Molecular microbiology, 2018. **110**(6): p. 1030-1044.
63. De Vuyst, L. and B. Degeest, *Heteropolysaccharides from lactic acid bacteria.* FEMS Microbiology Reviews, 1999. **23**(2): p. 153-177.
64. Poli, A., G. Anzelmo, and B. Nicolaus, *Bacterial exopolysaccharides from extreme marine habitats: production, characterization and biological activities.* Marine drugs, 2010. **8**(6): p. 1779-1802.
65. Gounot, A.M., *Bacterial life at low temperature: physiological aspects and biotechnological implications.* J Appl Bacteriol, 1991. **71**(5): p. 386-397.
66. Bowman, J.P., *The Family Methylococcaceae*, in *The Prokaryotes: Gammaproteobacteria*, E. Rosenberg, et al., Editors. 2014, Springer Berlin Heidelberg: Berlin, Heidelberg. p. 411-440.
67. Mason-Jones, K., et al., *Microbial storage and its implications for soil ecology.* The ISME Journal, 2022. **16**(3): p. 617-629.
68. BOWMAN, J.P., et al., *Revised Taxonomy of the Methanotrophs: Description of Methylobacter gen. nov., Emendation of Methylococcus, Validation of Methylosinus and Methylocystis Species, and a Proposal that the Family Methylococcaceae Includes Only the Group I Methanotrophs.* International Journal of Systematic and Evolutionary Microbiology, 1993. **43**(4): p. 735-753.
69. Whittenbury, R., K.C. Phillips, and J.F. Wilkinson, *Enrichment, isolation and some properties of methane-utilizing bacteria.* J Gen Microbiol, 1970. **61**(2): p. 205-18.
70. Pfennig, N., *Beobachtungen über das Schwärmen von Chromatium okenii.* Archiv für Mikrobiologie, 1962. **42**: p. 90-95.
71. Benjamini, Y. and Y. Hochberg, *Controlling the False Discovery Rate: A Practical and Powerful Approach to Multiple Testing.* Journal of the Royal Statistical Society. Series B (Methodological), 1995. **57**(1): p. 289-300.
72. R Core Team 2009, *R: A language and environment for statistical computing*. 2009, R Foundation for Statistical Computing: Vienna, Austria.

73. Angel, R., P. Claus, and R. Conrad, *Methanogenic archaea are globally ubiquitous in aerated soils and become active under wet anoxic conditions.* Isme j, 2012. **6**(4): p. 847-862.
74. Gierse, L.C., et al., *A Multi-Omics Protocol for Swine Feces to Elucidate Longitudinal Dynamics in Microbiome Structure and Function.* Microorganisms, 2020. **8**(12): p. 1887.
75. Kopylova, E., L. Noe, and H. Touzet, *SortMeRNA: fast and accurate filtering of ribosomal RNAs in metatranscriptomic data.* Bioinformatics, 2012. **28**(24): p. 3211-3217.
76. Li, H. and R. Durbin, *Fast and accurate short read alignment with Burrows-Wheeler transform.* Bioinformatics, 2009. **25**(14): p. 1754-60.
77. Liao, Y., G.K. Smyth, and W. Shi, *featureCounts: an efficient general purpose program for assigning sequence reads to genomic features.* Bioinformatics, 2014. **30**(7): p. 923-30.
78. Anders, S. and W. Huber, *Differential expression analysis for sequence count data.* Genome Biol, 2010. **11**(10): p. R106.
79. Schurch, N.J., et al., *How many biological replicates are needed in an RNA-seq experiment and which differential expression tool should you use?* RNA, 2016. **22**(6): p. 839-51.
80. Svenning, M.M., et al., *Genome Sequence of the Arctic Methanotroph Methylobacter tundripaludum SV96.* Journal of Bacteriology, 2011. **193**(22): p. 6418-6419.
81. Wang, J., et al., *Global Geographic Diversity and Distribution of the Myxobacteria.* Microbiol Spectr, 2021. **9**(1): p. e0001221.
82. Kimura, M., *A simple method for estimating evolutionary rates of base substitutions through comparative studies of nucleotide sequences.* J Mol Evol, 1980. **16**(2): p. 111-120.
83. Kumar, S., et al., *MEGA X: Molecular Evolutionary Genetics Analysis across Computing Platforms.* Mol Biol Evol, 2018. **35**(6): p. 1547-1549.

Supplementary Figures

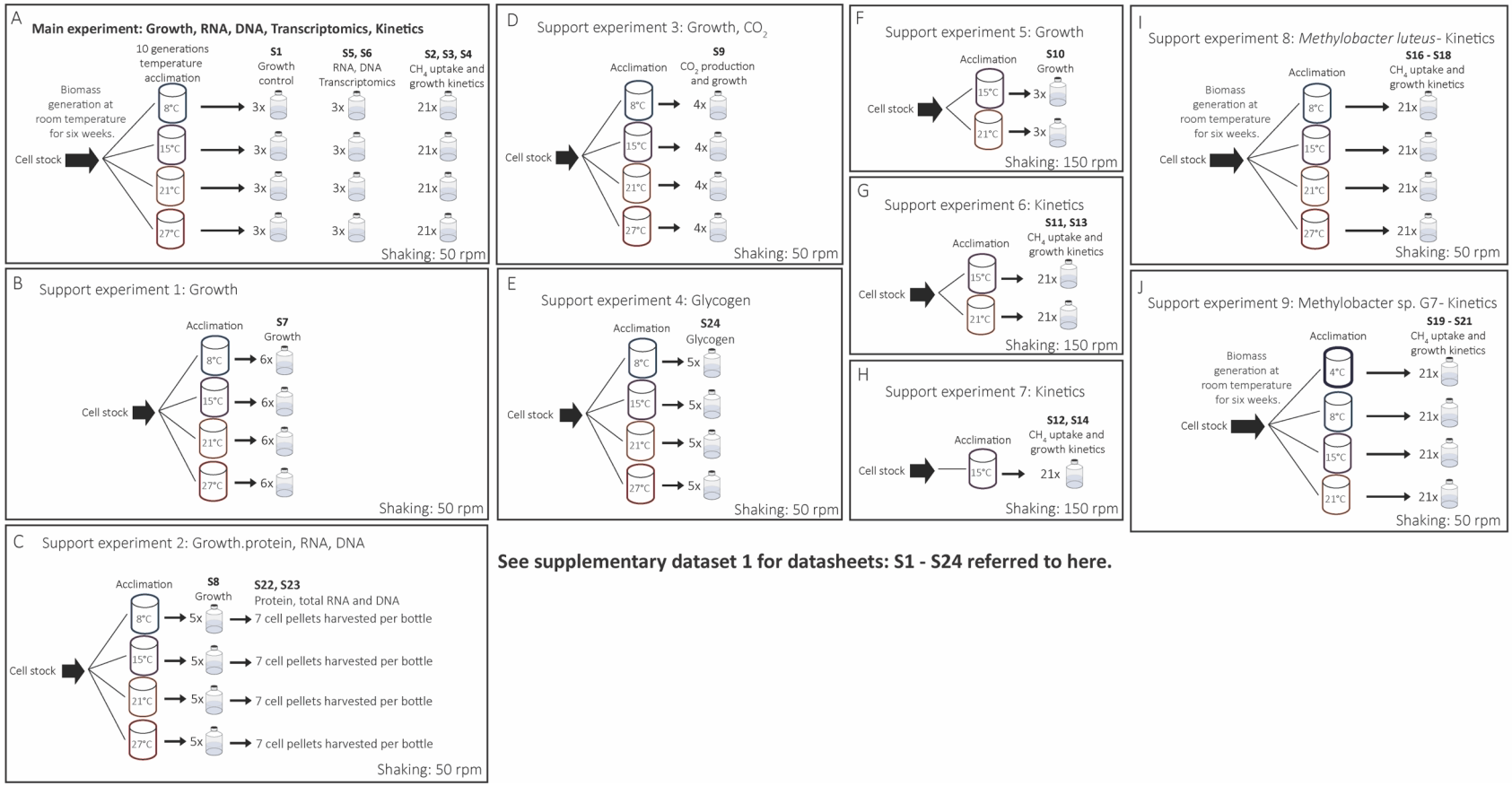

See supplementary dataset 1 for datasheets: S1 - S24 referred to here.

Figure S1. Experimental setup. Each box indicates an independent experiment. “Cell stock” represent a frozen cell culture as starting point for cultivation. Temperature acclimation times varied due to the different growth rates at different temperatures, thus being standardized to 10 generations of acclimation. Numbers in front of bottles indicate the number of replicates. The corresponding dataset to each experiment is indicated above the respective experiments, the numbers S1 – S24 referring to the individual tabs in supplementary dataset

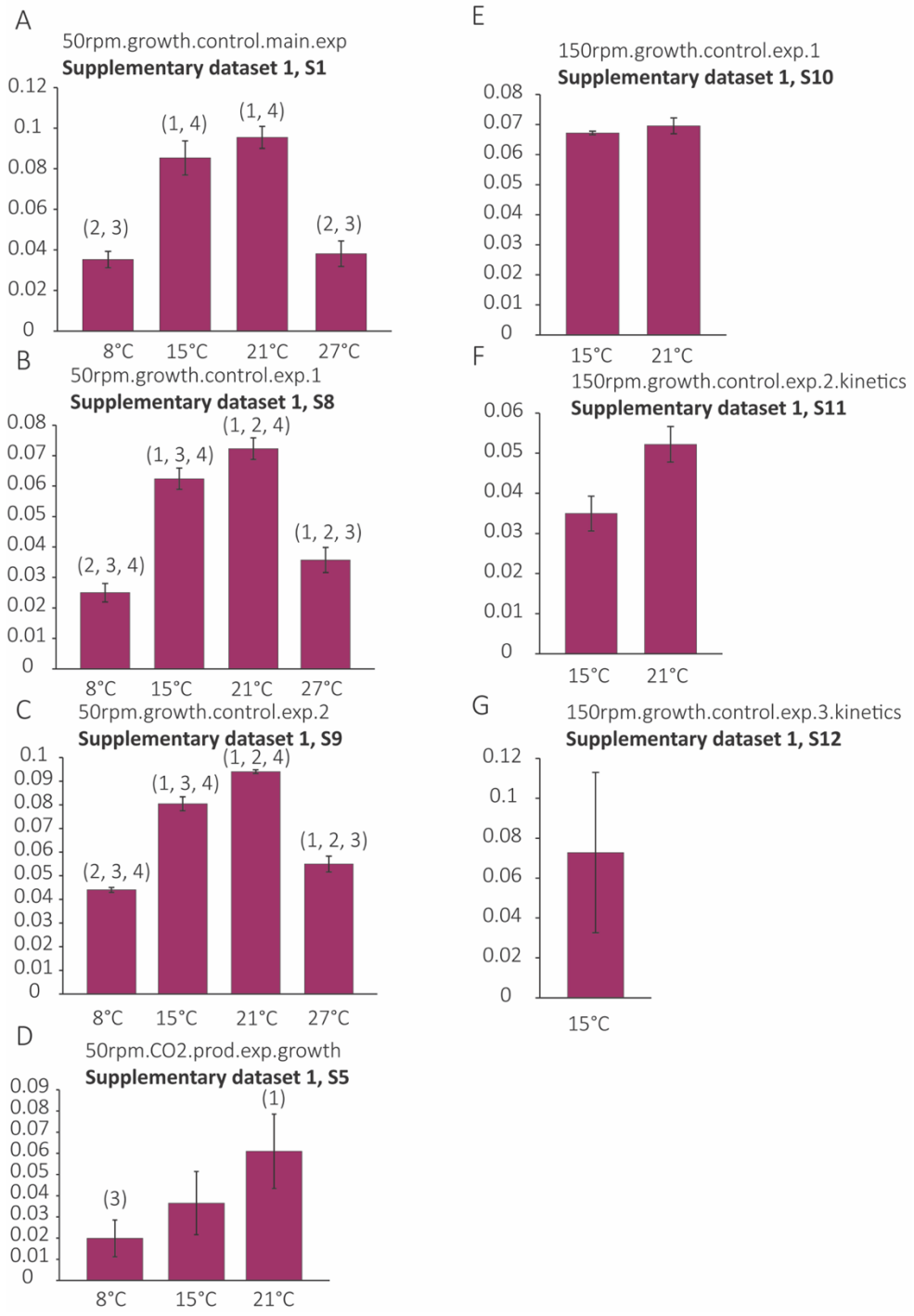

Figure S2. Specific growth rate control experiments. Bar graphs show the specific growth rates of *M. tundripaludum* SV96 at different temperatures, under a headspace of partial pressures of air components plus 20% CH_4. The corresponding dataset to each experiment is indicated next to the title of each bar graph, the numbers S1 – S12 referring to the individual tabs in supplementary dataset 1. Significant differences (p.adjust < 0.05, multiple testing correction using Benjamini-Hochberg correction) to 8 °C (1), 15 °C (2), 21 °C (3) and 27 °C (4) are indicated with numbers above the individual bars. Error bars represent standard deviation.

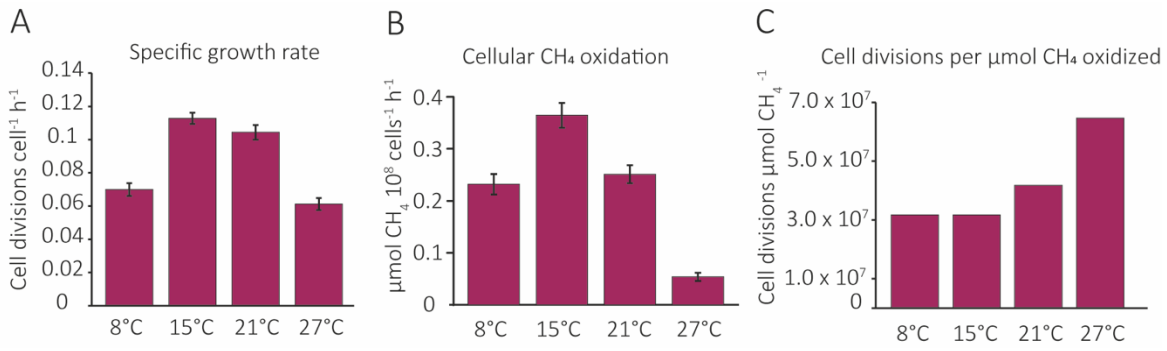

Figure S3. Specific growth rate (A), CH_4 oxidation (B) and cell division efficiency (C) based on Vmax estimates from kinetics in Fig. 1. Error bars represent the standard error of model estimates. Significances for individual estimates are shown in Fig. 1.

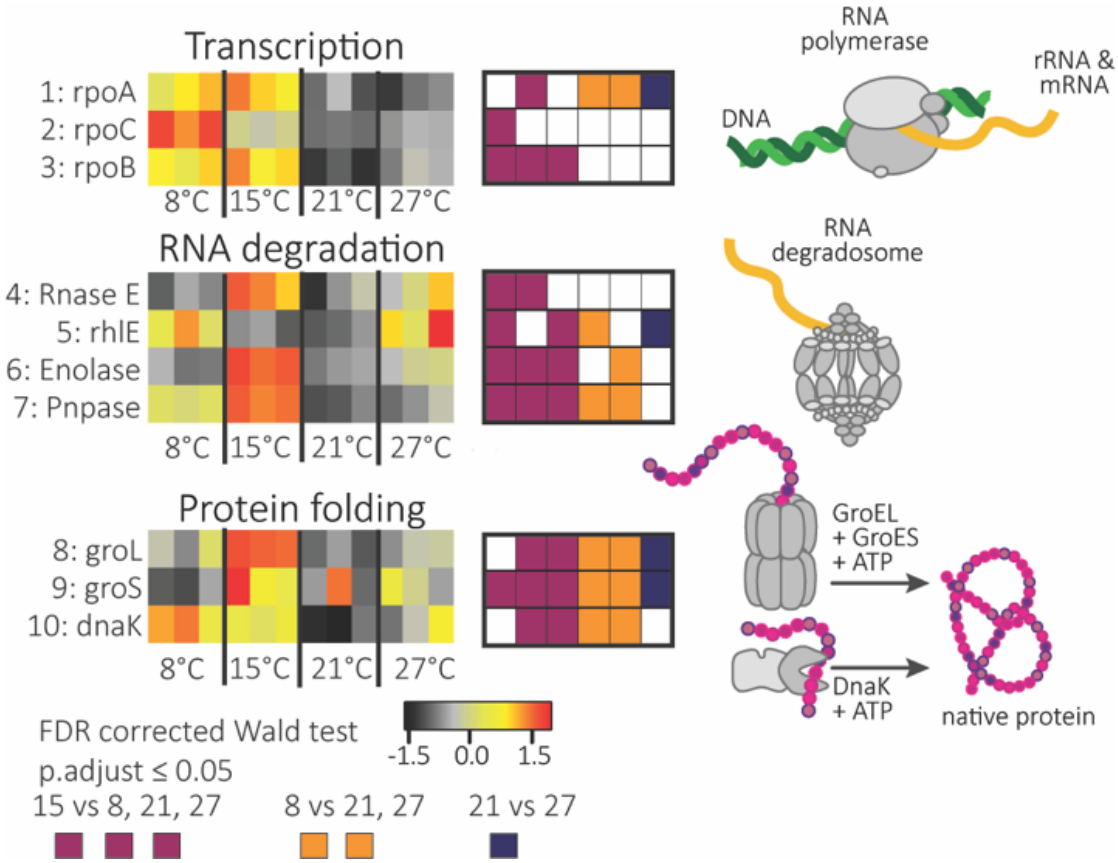

Figure S4. Gene transcription for RNA polymerase, RNA degradation and protein folding. Heatmaps indicate changes in the relative abundance of transcripts in the transcriptomes at 8, 15, 21 and 27 °C. The colour scale reflects z-score normalized relative abundances, with black being lowest relative abundance, followed by grey, yellow, orange and red, corresponding to increasing relative abundances. Significant differences (p.adjust < 0.05) in transcript relative abundances are displayed in square plots to the right of each heatmap, purple indicating significant difference between 15 °C and 8, 21 and 27 °C, respectively, when moving from left to right. Orange indicates significant differences between 8 °C and 21 and 27 °C. Dark blue indicates significant differences between 21 and 27 °C. P values are estimated with a Wald test, implemented in DESeq2 and corrected for multiple testing using Benjamini-Hochberg correction, which adjusts for the false discovery rate. All adjusted p. values, normalized counts, genome IDs and full protein names are given in Supplementary dataset 2,

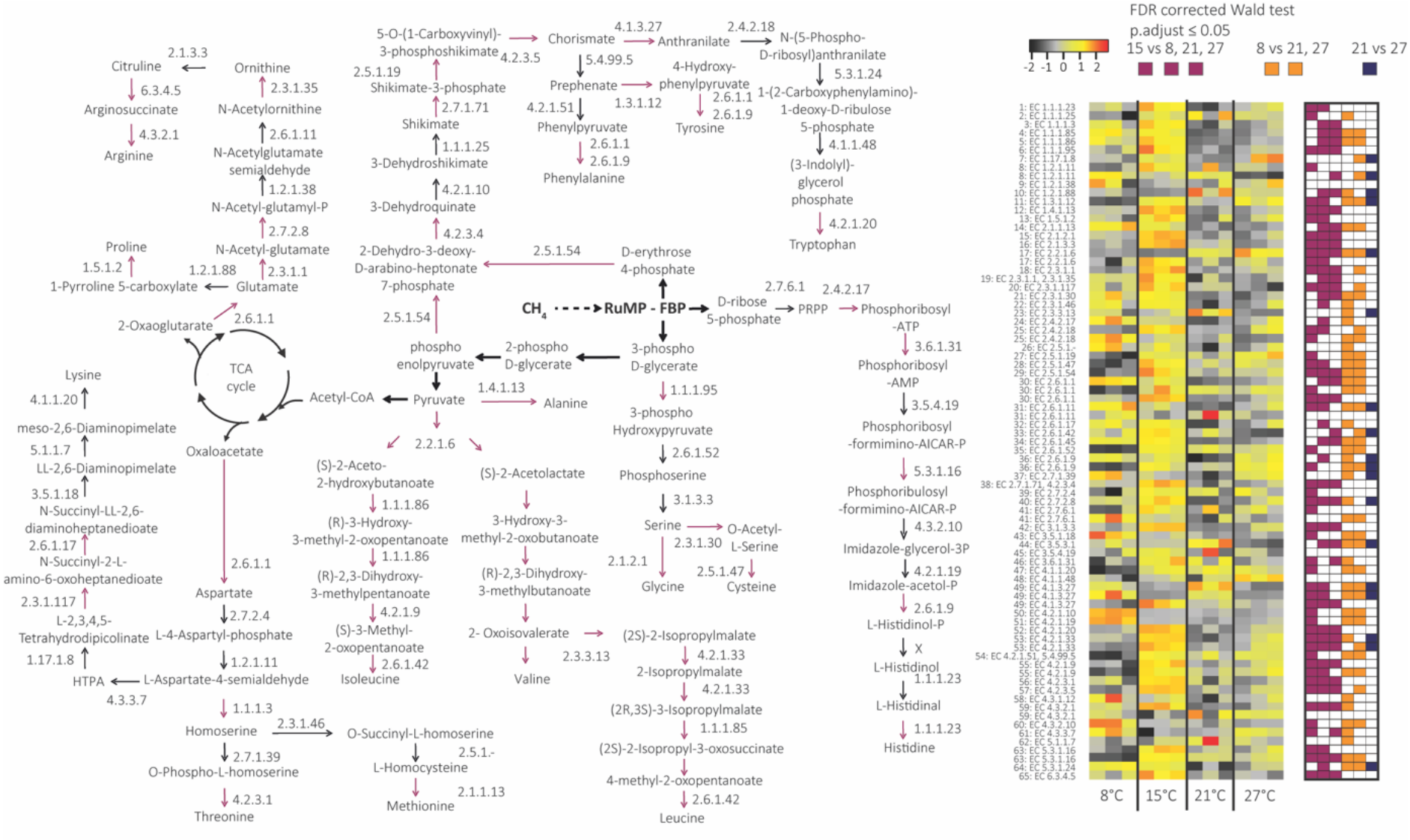
FDR corrected Wald test
p.adjust ≤ 0.05
15 vs 8, 21, 27
8 vs 21, 27
21 vs 27
-2 -1 0 1 2
8°C
15°C
21°C
27°C
CH4 ----> RuMP - FBP
TCA cycle
Citruline
Ornithine
Arginosuccinate
Arginine
N-Acetylornithine
N-Acetylglutamate semialdehyde
N-Acetyl-glutamyl-P
N-Acetyl-glutamate
Proline
1-Pyrroline 5-carboxylate
Glutamate
2-Oxaoglutarate
Lysine
meso-2,6-Diaminopimelate
LL-2,6-Diaminopimelate
N-Succinyl-LL-2,6-diaminoheptanedioate
N-Succinyl-2-L-amino-6-oxoheptanedioate
L-2,3,4,5-Tetrahydrodipicolinate
HTPA
Oxaloacetate
Aspartate
L-4-Aspartyl-phosphate
L-Aspartate-4-semialdehyde
Homoserine
O-Phospho-L-homoserine
Threonine
O-Succinyl-L-homoserine
L-Homocysteine
Methionine
5-O-(1-Carboxyvinyl)-3-phosphoshikimate
Shikimate-3-phosphate
Shikimate
3-Dehydroshikimate
3-Dehydroquinate
2-Dehydro-3-deoxy-D-arabino-heptonate 7-phosphate
Chorismate
Anthranilate
N-(5-Phospho-D-ribosyl)anthranilate
Prephenate
4-Hydroxy-phenylpyruvate
Phenylpyruvate
Tyrosine
Phenylalanine
1-(2-Carboxyphenylamino)-1-deoxy-D-ribulose 5-phosphate
(3-Indolyl)-glycerol phosphate
Tryptophan
D-erythrose 4-phosphate
D-ribose 5-phosphate
PRPP
Phosphoribosyl-ATP
Phosphoribosyl-AMP
Phosphoribosyl-formimino-AICAR-P
Phosphoribulosyl-formimino-AICAR-P
Imidazole-glycerol-3P
Imidazole-acetol-P
L-Histidinol-P
L-Histidinol
L-Histidinal
Histidine
phospho enolpyruvate
2-phospho D-glycerate
3-phospho D-glycerate
3-phospho Hydroxypyruvate
Phosphoserine
Serine
O-Acetyl-L-Serine
Glycine
Cysteine
Pyruvate
Acetyl-CoA
Alanine
(S)-2-Aceto-2-hydroxybutanoate
(R)-3-Hydroxy-3-methyl-2-oxopentanoate
(R)-2,3-Dihydroxy-3-methylpentanoate
(S)-3-Methyl-2-oxopentanoate
Isoleucine
(S)-2-Acetolactate
3-Hydroxy-3-methyl-2-oxobutanoate
(R)-2,3-Dihydroxy-3-methylbutanoate
2- Oxoisovalerate
Valine
(2S)-2-Isopropylmalate
2-Isopropylmalate
(2R,3S)-3-Isopropylmalate
(2S)-2-Isopropyl-3-oxosuccinate
4-methyl-2-oxopentanoate
Leucine

1

Figure S5. Gene transcription for amino acid metabolism in *M. tundripaludum* SV96. Heatmaps indicate changes in the relative abundance of transcripts in the transcriptomes at 8, 15, 21 and 27 °C. The colour scale reflects z-score normalized relative abundances, with black being lowest relative abundance, followed by grey, yellow, orange and red, corresponding to increasing relative abundances. Significant differences (p.adjust < 0.05) in transcript relative abundances are displayed in square plots to the right of each heatmap, purple indicating significant difference between 15 °C and 8, 21 and 27 °C, respectively, when moving from left to right. Orange indicates significant differences between 8 °C and 21 and 27 °C. Dark blue indicates significant differences between 21 and 27 °C. P values are estimated with a Wald test, implemented in DESeq2 and corrected for multiple testing using Benjamini-Hochberg correction which adjusts for the false discovery rate. Purple arrows indicate that at least one of the genes encoding the enzyme responsible for catalysing the reaction represented by this pathway step is significantly higher expressed at 15 °C than at two or three of the other temperatures. All adjusted p. values, normalized counts, genome IDs, gene names and full protein names are given in Supplementary dataset 2, S6.

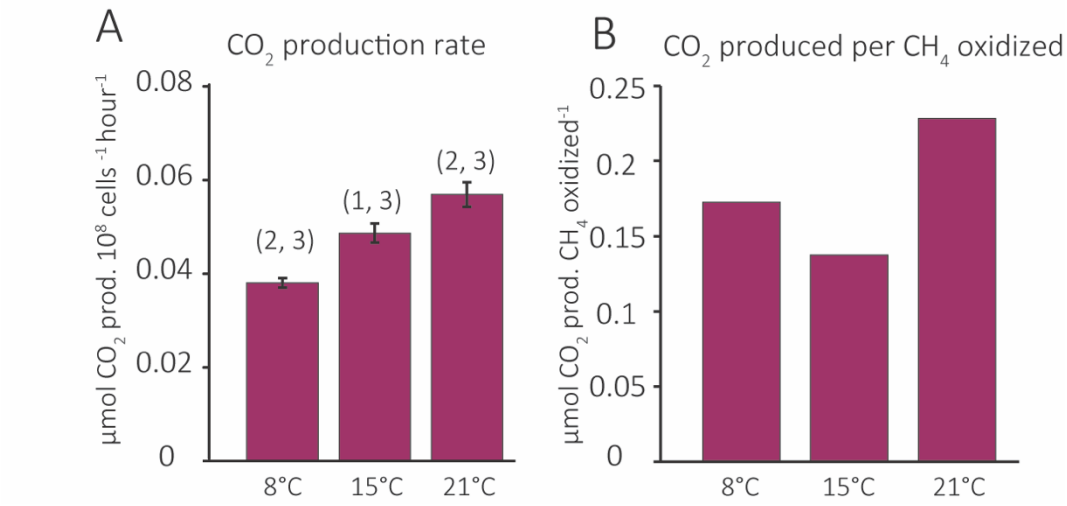

Figure S6. CO_2 production at CH_4 uptake saturation by *M. tundripaludum* SV96. Bar graphs show the CO_2 production rate per 10^8 cells (A) per specific growth rates and (B) per CH_4 oxidation of *M. tundripaludum* SV96 at different temperatures, under a headspace of air and 20% CH_4. The corresponding dataset to each experiment is indicated next to the title of each experiment, the number S5 referring to the individual tab in supplementary dataset 1 that holds the data. Significant differences (p.adjust < 0.05, multiple testing correction using Benjamini-Hochberg correction) to 8 °C (1), 15 °C (2) and 21 °C (3) are indicated with numbers above the individual bars. Error bars represent standard deviation. The lack of error bars in (B) is due to the data used in the calculation being from different experiments and thus only based on averages. The corresponding data can be found in supplementary dataset 1, S9.

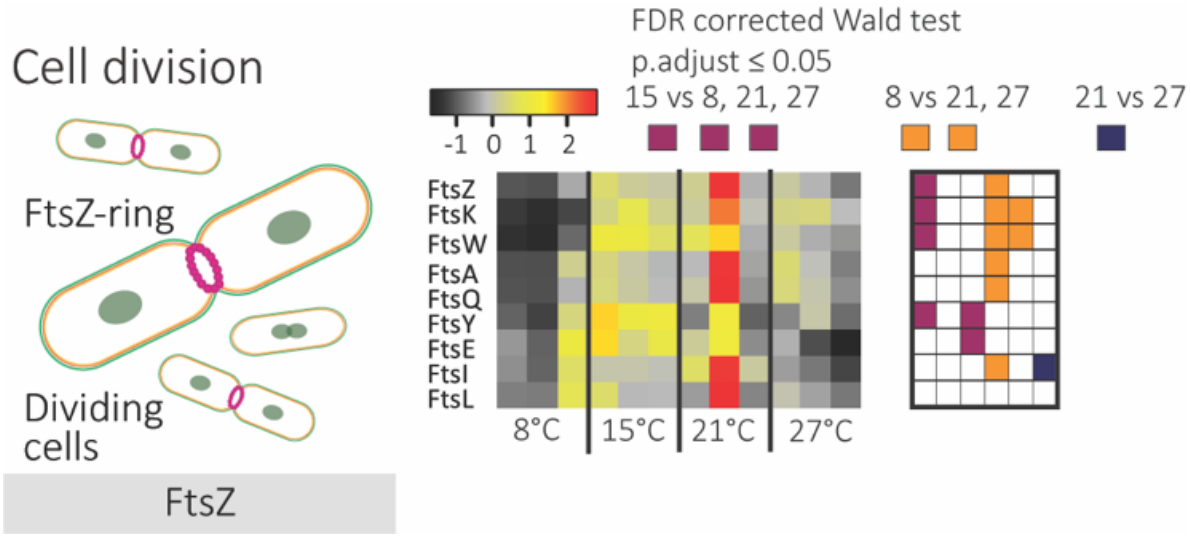

Figure S7. Gene transcription for cell division in *M. tundripaludum* SV96. Heatmaps indicate changes in the relative abundance of transcripts in the transcriptomes at 8, 15, 21 and 27 °C. The colour scale reflects z-score normalized relative abundances, with black being lowest relative abundance, followed by grey, yellow, orange and red, corresponding to increasing relative abundances. Significant differences (p.adjust < 0.05) in transcript relative abundances are displayed in square plots to the right of each heatmap, purple indicating significant difference between 15 °C and 8, 21 and 27 °C, respectively, when moving from left to right. Orange indicates significant differences between 8 °C and 21 and 27 °C. Dark blue indicates significant differences between 21 and 27 °C. P values are estimated with a Wald test, implemented in DESeq2 and corrected for multiple testing using Benjamini-Hochberg correction which adjusts for the false discovery rate. All adjusted p. values, normalized counts, genome IDs, gene names and full protein names are given in Supplementary dataset 2, S7.

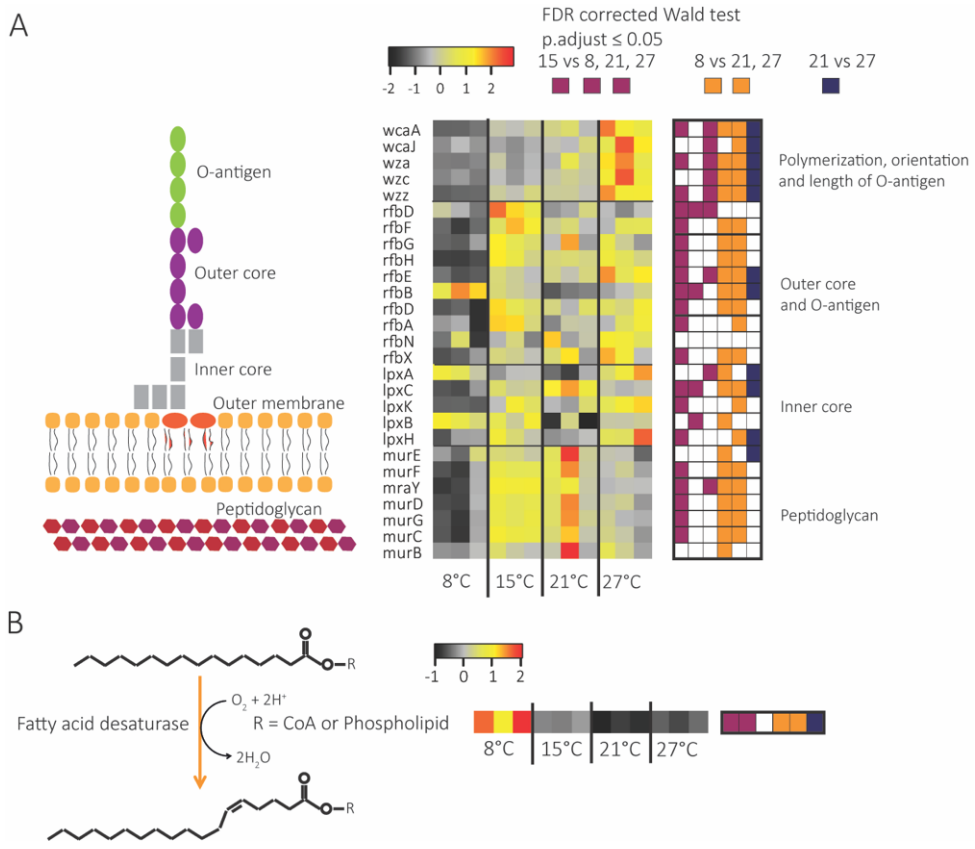

Figure S8. Gene transcription for cell wall synthesis, exopolysaccharides and fatty acid desaturation in *M. tundripaludum* SV96. (A) shows transcriptional patterns and significance tests for cell wall and exopolysaccharide synthesis. (B) shows fatty acid desaturase transcription and corresponding significance tests. Heatmaps indicate changes in the relative abundance of transcripts in the transcriptomes at 8, 15, 21 and 27 °C. The colour scale reflects z-score normalized relative abundances, with black being lowest relative abundance, followed by grey, yellow, orange and red, corresponding to increasing relative abundances. Significant differences (p.adjust < 0.05) in transcript relative abundances are displayed in square plots to the right of each heatmap, purple indicating significant difference between 15 °C and 8, 21 and 27 °C, respectively, when moving from left to right. Orange indicates significant differences between 8 °C and 21 and 27 °C. Dark blue indicates significant differences between 21 and 27 °C. P values are estimated with a Wald test, implemented in DESeq2 and corrected for multiple testing using Benjamini-Hochberg correction which adjusts for the false discovery rate. The orange arrow in (B) indicates significantly higher relative abundance of transcripts at 8 °C than at two or three of the other temperatures. All adjusted p. values, normalized counts, genome IDs, E.C. numbers, gene names and full protein names are given in Supplementary dataset 2, S8.

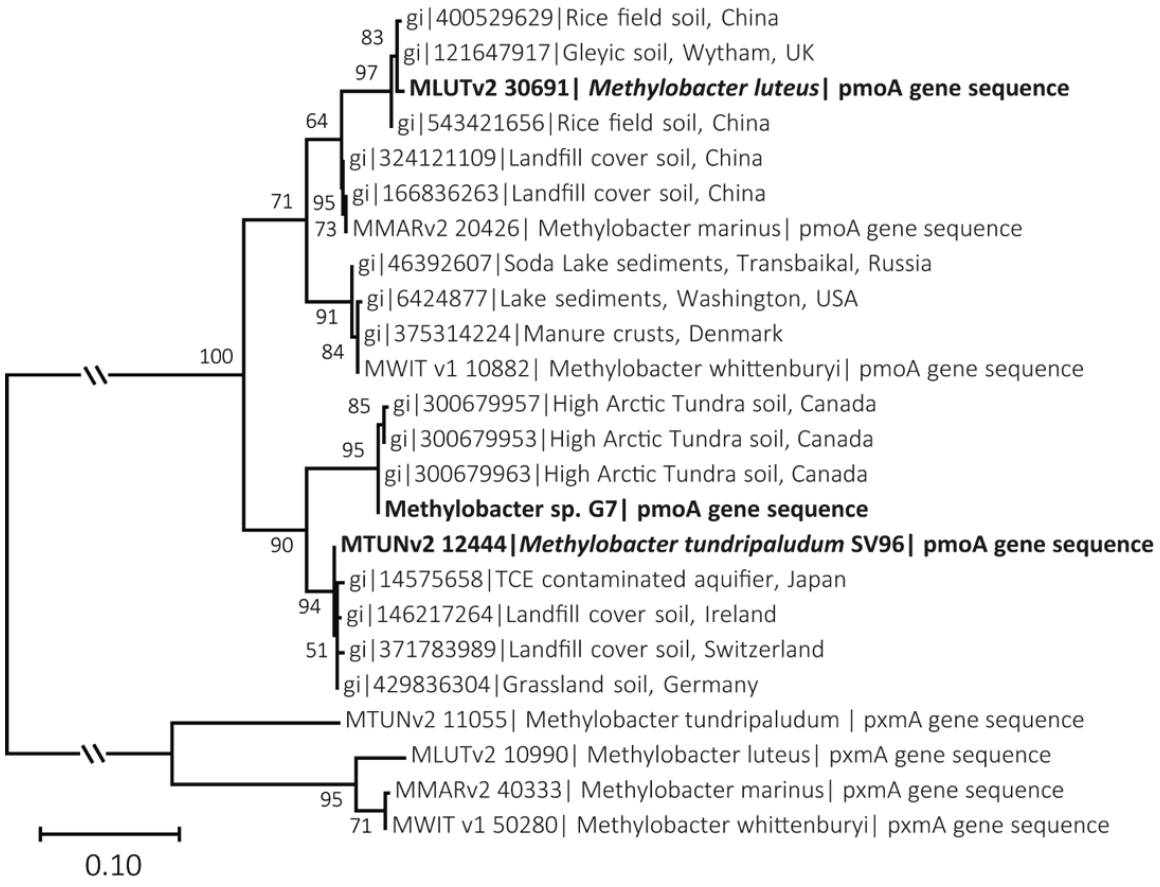

Figure S9. Phylogenetic tree of *pmoA* sequences belonging within the genus *Methylobacter*. Sequence names include gene identifier, ecosystem type of origin, and country of origin. The evolutionary history was inferred by using the Maximum Likelihood method and Kimura 2-parameter model [82]. The tree with the highest log likelihood (-2368.76) is shown. The percentage of trees in which the associated taxa clustered together is shown next to the branches. Initial tree(s) for the heuristic search were obtained automatically by applying Neighbor-Join and BioNJ algorithms to a matrix of pairwise distances estimated using the Maximum Composite Likelihood (MCL) approach, and then selecting the topology with superior log likelihood value. The tree is drawn to scale, with branch lengths measured in the number of substitutions per site. This analysis involved 24 nucleotide sequences. Codon positions included were 1st+2nd+3rd+Noncoding. There was a total of 471 positions in the final dataset. Evolutionary analyses were conducted in MEGA X [83].

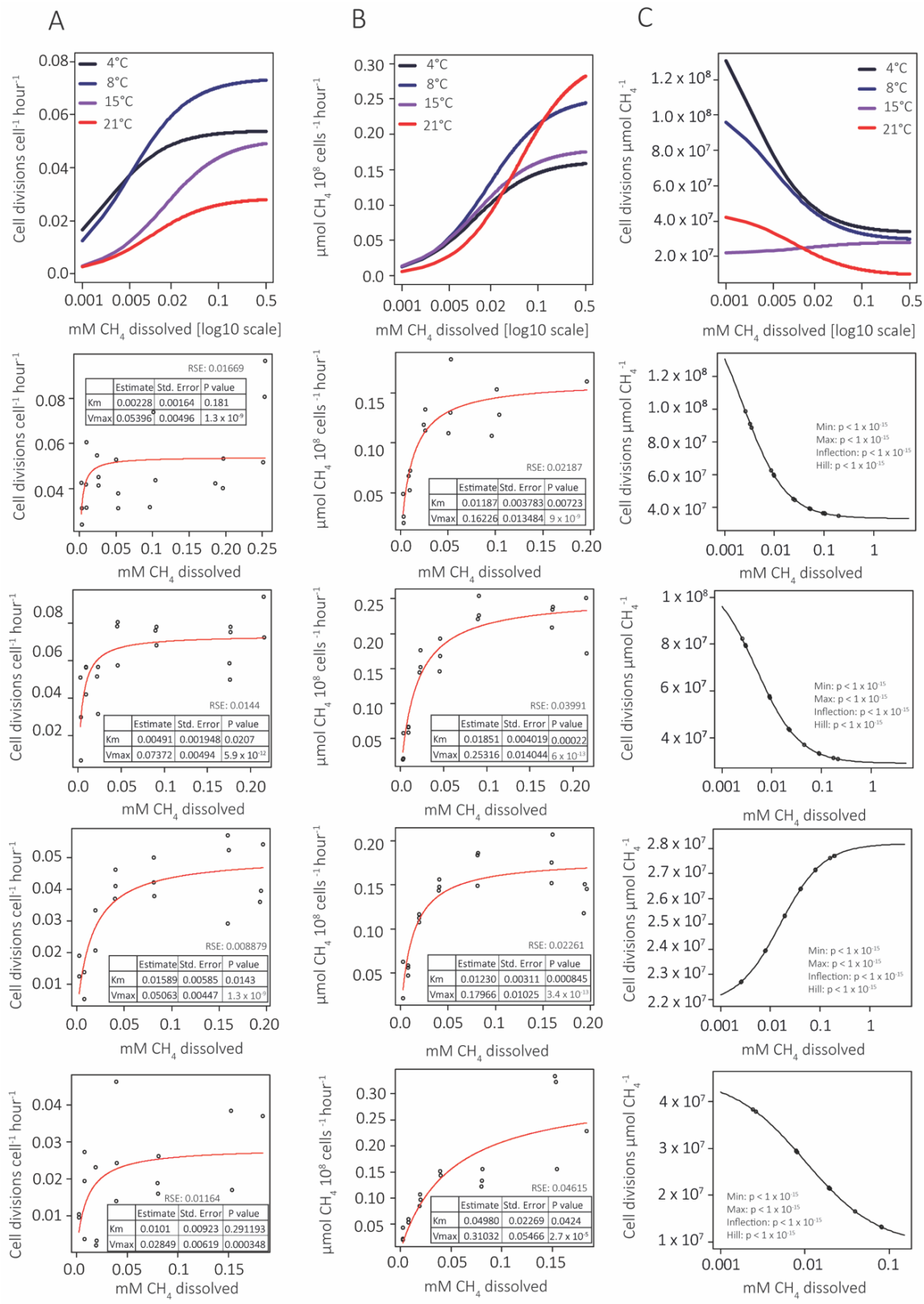
A
B
C
4°C
8°C
15°C
21°C
Cell divisions cell^{-1} hour^{-1}
µmol CH_4 10^8 cells $^{-1}$hour^{-1}
Cell divisions µmol CH_4^{-1}
mM CH_4 dissolved [log10 scale]
mM CH_4 dissolved
RSE: 0.01669
Estimate Std. Error P value
Km 0.00228 0.00164 0.181
Vmax 0.05396 0.00496 1.3 x 10^{-9}
RSE: 0.02187
Km 0.01187 0.003783 0.00723
Vmax 0.16226 0.013484 9 x 10^{-9}
RSE: 0.0144
Km 0.00491 0.001948 0.0207
Vmax 0.07372 0.00494 5.9 x 10^{-12}
RSE: 0.03991
Km 0.01851 0.004019 0.00022
Vmax 0.25316 0.014044 6 x 10^{-13}
RSE: 0.008879
Km 0.01589 0.00585 0.0143
Vmax 0.05063 0.00447 1.3 x 10^{-9}
RSE: 0.02261
Km 0.01230 0.00311 0.000845
Vmax 0.17966 0.01025 3.4 x 10^{-13}
RSE: 0.01164
Km 0.0101 0.00923 0.291193
Vmax 0.02849 0.00619 0.000348
RSE: 0.04615
Km 0.04980 0.02269 0.0424
Vmax 0.31032 0.05466 2.7 x 10^{-5}
Min: p < 1 x 10^{-15}
Max: p < 1 x 10^{-15}
Inflection: p < 1 x 10^{-15}
Hill: p < 1 x 10^{-15}

1

Figure S10. Growth kinetics, CH_4 oxidation kinetics and cell divisions per CH_4 oxidation at different temperatures for Methylobacter sp. G7. Specific growth rates (cell divisions per cell per hour) are shown for different dissolved CH_4 concentrations in **(A)**. The first panel is a combination of the growth kinetics at the four different temperatures, 4, 8, 15 and 21°C. X-axis is on log10 scale to better resolve the differences between temperatures in the lower end or higher end of concentrations. Second to fifth panel are the individual growth kinetics at the temperatures 4, 8, 15 and 21°C, respectively. CH_4 oxidation rates per cell for different dissolved CH_4 concentrations are shown in **(B)**. The first panel is a combination of the CH_4 oxidation kinetics at the four different temperatures, 4, 8, 15 and 21°C. X-axis is on log10 scale to better resolve the differences between temperatures in the lower end or higher end of concentrations. Second to fifth panel are the individual CH_4 oxidation kinetics at the temperatures 4, 8, 15 and 21°C, respectively. $K_{m(app)}$, $V_{max(app)}$, standard errors and p values for these estimates, respectively, and residual standard errors of the models were estimated using non-linear regression, applying a Michaelis-Menten function (see materials and methods section "statistics for physiological measurements"). Cell divisions per µmol CH_4 oxidized for different dissolved CH_4 concentrations are shown in **(C)**. The first panel of (C) shows these growth efficiency curves for all temperatures combined. Panel two to five show the models for each temperature. Estimates of specific growth rates and CH_4 oxidation rates at different dissolved CH_4 concentrations were predicted from models in **(A)** and **(B)**. Dividing specific growth rate estimates by CH_4 oxidation rates, we obtained Cell divisions per µmol CH_4 oxidized. Four-parameter logistics curves (dose-response model) were fitted to the quotients. P values for the four parameters are shown for the individual models in panel two to five. In all panels, x-axis is displayed on a log10 scale.

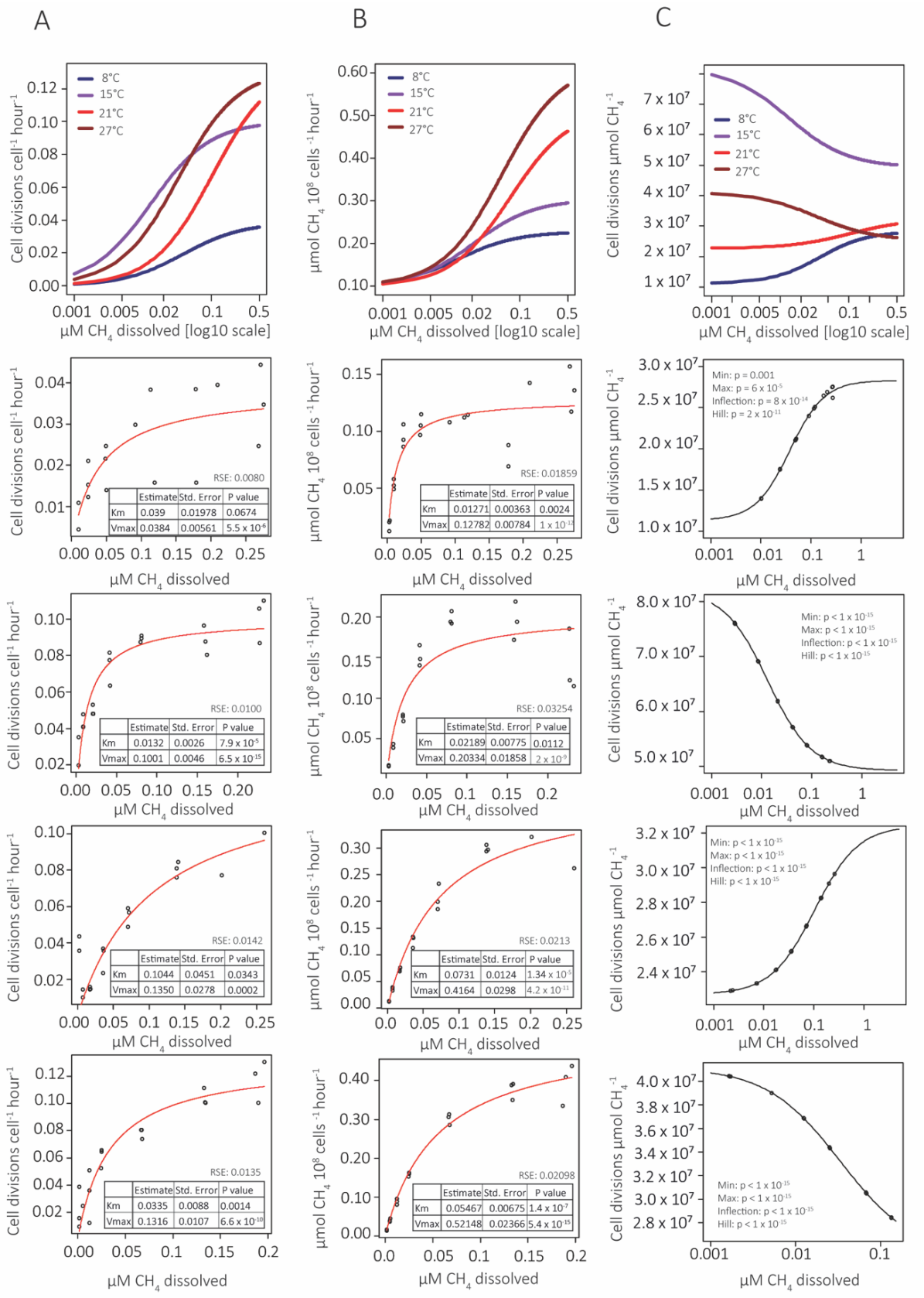
A
B
C
8°C
15°C
21°C
27°C
Cell divisions cell-1 hour-1
µmol CH4 10^8 cells -1 hour-1
Cell divisions µmol CH4-1
µM CH4 dissolved [log10 scale]
µM CH4 dissolved
RSE: 0.0080
Estimate Std. Error P value
Km 0.039 0.01978 0.0674
Vmax 0.0384 0.00561 5.5 x 10-6
RSE: 0.01859
Km 0.01271 0.00363 0.0024
Vmax 0.12782 0.00784 1 x 10-15
Min: p = 0.001
Max: p = 6 x 10-5
Inflection: p = 8 x 10-14
Hill: p = 2 x 10-11
RSE: 0.0100
Km 0.0132 0.0026 7.9 x 10-5
Vmax 0.1001 0.0046 6.5 x 10-15
RSE: 0.03254
Km 0.02189 0.00775 0.0112
Vmax 0.20334 0.01858 2 x 10-9
Min: p < 1 x 10-15
Max: p < 1 x 10-15
Inflection: p < 1 x 10-15
Hill: p < 1 x 10-15
RSE: 0.0142
Km 0.1044 0.0451 0.0343
Vmax 0.1350 0.0278 0.0002
RSE: 0.0213
Km 0.0731 0.0124 1.34 x 10-3
Vmax 0.4164 0.0298 4.2 x 10-11
Min: p < 1 x 10-15
Max: p < 1 x 10-15
Inflection: p < 1 x 10-15
Hill: p < 1 x 10-15
RSE: 0.0135
Km 0.0335 0.0088 0.0014
Vmax 0.1316 0.0107 6.6 x 10-10
RSE: 0.02098
Km 0.05467 0.00675 1.4 x 10-7
Vmax 0.52148 0.02366 5.4 x 10-15
Min: p < 1 x 10-15
Max: p < 1 x 10-15
Inflection: p < 1 x 10-15
Hill: p < 1 x 10-15

1

Figure S11. Growth kinetics, CH_4 oxidation kinetics and cell divisions per CH_4 oxidation at different temperatures for *M. luteus* IMV-B-3098. Specific growth rates (cell divisions per cell per hour) are shown for different dissolved CH_4 concentrations in **(A)**. The first panel is a combination of the growth kinetics at the four different temperatures, 8, 15, 21 and 27 °C. X-axis is on log10 scale to better resolve the differences between temperatures in the lower end or higher end of concentrations. Second to fifth panel are the individual growth kinetics at the temperatures 8, 15, 21 and 27 °C, respectively. CH_4 oxidation rates per cell for different dissolved CH_4 concentrations are shown in **(B)**. The first panel is a combination of the CH_4 oxidation kinetics at the four different temperatures, 8, 15, 21 and 27 °C. X-axis is on log10 scale to better resolve the differences between temperatures in the lower end or higher end of concentrations. Second to fifth panel are the individual CH_4 oxidation kinetics at the temperatures 8, 15, 21 and 27 °C, respectively. $K_{m(app)}$, $V_{max(app)}$, standard errors and p values for these estimates, respectively, and residual standard errors of the models were estimated using non-linear regression, applying a Michaelis-Menten function (see materials and methods section "statistics for physiological measurements"). Cell divisions per µmol CH_4 oxidized for different dissolved CH_4 concentrations are shown in **(C)**. The first panel of (C) shows these growth efficiency curves for all temperatures combined. Panel two to five show the models for each temperature. Estimates of specific growth rates and CH_4 oxidation rates at different dissolved CH_4 concentrations were predicted from models in **(A)** and **(B)**. Dividing specific growth rate estimates by CH_4 oxidation rates, we obtained Cell divisions per µmol CH_4 oxidized. Four-parameter logistics curves (dose-response model) were fitted to the quotients. P values for the four parameters are shown for the individual models in panel two to five. In all panels, x-axis is displayed on a log10 scale.

This file is not included in the
print version of the thesis

Supplementary dataset 1: Physiological data.

This file is not included in the
print version of the thesis

Supplementary dataset 2: The processed and normalized transcript counts and statistics for the differential gene expression analyses.